



**UNIVERSIDAD NACIONAL AUTÓNOMA DE MÉXICO**

**PROGRAMA DE DOCTORADO EN CIENCIAS BIOMÉDICAS**

**FACULTAD DE MEDICINA**

**LAS CÉLULAS TRONCALES MESENQUIMALES DERIVADAS DE TEJIDO  
ADIPOSO PROMUEVEN EL FENOTIPO MALIGNO DEL CÁNCER  
CERVICOUTERINO**

**TESIS**

Que para optar por el grado de:

**DOCTORA EN CIENCIAS BIOMÉDICAS**

**PRESENTA:**

**MARIA DEL ROSARIO CASTRO OROPEZA**

**DIRECTOR DE TESIS:**

**DRA. VILMA ARACELI MALDONADO LAGUNAS**  
**INSTITUTO NACIONAL DE MEDICINA GENÓMICA**

**MIEMBROS DEL COMITÉ TUTOR:**

**DRA. LETICIA ROCHA ZAVALA**  
**INSTITUTO DE INVESTIGACIONES BIOMÉDICAS**

**DR. ERNESTO SOTO REYES SOLÍS**  
**UNIVERSIDAD AUTÓNOMA METROPOLITANA,**  
**UNIDAD CUAJIMALPA**

Ciudad Universitaria, CDMX, agosto 2022



Universidad Nacional  
Autónoma de México



**UNAM – Dirección General de Bibliotecas**  
**Tesis Digitales**  
**Restricciones de uso**

**DERECHOS RESERVADOS ©**  
**PROHIBIDA SU REPRODUCCIÓN TOTAL O PARCIAL**

Todo el material contenido en esta tesis esta protegido por la Ley Federal del Derecho de Autor (LFDA) de los Estados Unidos Mexicanos (México).

El uso de imágenes, fragmentos de videos, y demás material que sea objeto de protección de los derechos de autor, será exclusivamente para fines educativos e informativos y deberá citar la fuente donde la obtuvo mencionando el autor o autores. Cualquier uso distinto como el lucro, reproducción, edición o modificación, será perseguido y sancionado por el respectivo titular de los Derechos de Autor.

*Cierto que casi siempre se encuentra algo, si se mira, pero no siempre es lo que uno busca.*

*J. R. R. Tolkien*

*“El saber es el único espacio de libertad del ser”*

*Michael Foucault.*

*“La ciencia no es solo una disciplina de razón, sino también de romance y pasión”*

*Stephen Hawking*

---

## AGRADECIMIENTOS ACADÉMICOS

A mi tutora la Dra. Vilma Maldonado Lagunas

Por permitirme ser parte del Laboratorio de Epigenética. Por su mentoría, dedicación, calidez humana y el gran apoyo que siempre me ha dado para enriquecer mi carrera profesional. Y sobre todo gracias por su disponibilidad, por la confianza puesta en mí y por su incansable compromiso académico.

A la Dra. Karla Vázquez Santillán

Por sus brillantes aportaciones que indudablemente enriquecieron el proyecto. Por la confianza, consejos y ánimos recibidos que me ayudaron en momentos difíciles que se viven durante una tesis Doctoral. Gracias por contagiar el ambiente con el ejemplo, dedicación y responsabilidad con la ciencia. Sobre todo, gracias por su gran amistad.

A la Dra. Leticia Rocha Zavaleta y el Dr. Ernesto Soto Reyes

Quienes formaron parte de mi comité tutorial, siempre mostraron profesionalismo, objetividad y disposición que enriquecieron tanto el proyecto como mi formación profesional.

Al posgrado en Ciencias Biomédicas

Por su infraestructura académica que permite la sólida formación de estudiantes de Doctorado.

Al Consejo Nacional de Ciencia y Tecnología (CONACyT)

Por la beca otorgada con número 329852, que me permitió realizar mis estudios de Doctorado.

Al Instituto Nacional de Medicina Genómica (INMEGEN)

Que, mediante la implementación de cursos, congresos, seminarios de investigación, así como las unidades de alta tecnología y personal científico altamente capacitado, fortaleció el proyecto de investigación desarrollado.





---

## AGRADECIMIENTOS PERSONALES

A mi madre Socorro Oropeza, la persona a quien admiro, gracias por su apoyo incondicional para alcanzar este objetivo en mi vida, por ser un ejemplo de fortaleza, sin importar los obstáculos que se han presentado, gracias por los consejos, paciencia, comprensión y por los valores que me has inculcado. ¡Esta tesis es para ti!

A mi tía Gloria Oropeza, a quien quiero como a una madre, por compartir momentos significativos conmigo y por siempre estar dispuesta a escucharme y ayudarme, por el apoyo tan valioso e incondicional que siempre me ha dado. Gracias por la confianza puesta en mí para lograr esta etapa de mi vida. Esta Tesis no habría existido sin tu apoyo. Gracias por todo tu amor y consejos que me has dado.

A mis hermanos Gabriela y Javier, por el amor, los ánimos y el apoyo que siempre me han dado, gracias por su compañía en esta vida!



## ÍNDICE:

<b>1. RESUMEN</b> .....	1
<b>2. ABSTRACT</b> .....	2
<b>3. INTRODUCCIÓN</b> .....	3
3.1 Cáncer.....	3
3.2 Cáncer Cervicouterino .....	5
3.2.1 Oncogénesis del Virus del Papiloma Humano .....	7
3.2.3 Neoplasia Intraepitelial Cervical.....	9
3.3 Obesidad .....	11
3.4 Cáncer Cervicouterino y Obesidad .....	12
3.5 Células troncales .....	14
3.6 Células troncales derivadas del tejido adiposo (ADSC) y Cáncer .....	17
<b>4. JUSTIFICACIÓN</b> .....	21
<b>5. HIPÓTESIS</b> .....	21
<b>6. OBJETIVO GENERAL</b> .....	22
6.1 Objetivos Particulares .....	22
<b>7. MATERIAL Y MÉTODOS</b> .....	23
7.1 Cultivo celular.....	23
7.2 Aislamiento, cultivo y caracterización de ADSC.....	23
7.3 Ensayos de cocultivo HeLa-ADSC.....	24
7.4 Producción de medio condicionado .....	24
7.5 Secuenciación de RNA.....	25
7.6 Análisis de enriquecimiento de conjunto de genes (GSEA) .....	25
7.7 Análisis vías y procesos biológicos .....	26
7.8 Análisis de supervivencia general .....	26
7.9 RT-PCR .....	26
7.10 Droplet Digital PCR .....	26

7.11 Ensayos de migración e invasión celular (in vitro). .....	27
7.12 Ensayos de proliferación celular .....	28
7.13 Ciclo celular .....	28
7.14 Ensayos de Inmunofluorescencia .....	29
7.15 Ensayos en peces cebra y xenotrasplantes .....	29
7.16 Ensayos de dilución limitante extrema (ELDA). .....	30
7.17 Angiogénesis.....	30
7.18 Análisis estadísticos.....	30
<b>8. ANTECEDENTES.....</b>	<b>31</b>
<b>9. RESULTADOS .....</b>	<b>32</b>
9.1 El cocultivo de HeLa / ADSCs induce cambios en el transcriptoma de las células HeLa .	32
9.2 Transcritos diferencialmente expresados por la presencia de ADSC exhiben importancia clínica en pacientes con cáncer cervical. ....	38
9.3 Efecto de las ADSC en la proliferación de cáncer cervicouterino .....	39
9.4 Las ADSC promueven la migración e invasión del cáncer cervicouterino. ....	42
9.5 Las ADSC promueven el crecimiento tumoral e incrementan la población de CTC del cáncer cervicouterino.....	48
9.6 ADSC induce la activación de la vía NF-kappa B en células de cáncer cervicouterino ...	52
9.7 Las ADSC inducen un fenotipo troncal y TEM en células de cáncer cervicouterino .....	58
9.8 Las ADSC modulan la angiogénesis en tumores de cáncer cervicouterino .....	63
<b>10. DISCUSIÓN .....</b>	<b>65</b>
<b>11. CONCLUSIÓN.....</b>	<b>70</b>
<b>12. REFERENCIAS.....</b>	<b>72</b>
<b>13. ARTÍCULOS.....</b>	<b>78</b>
i. Adipose-derived mesenchymal stem cells promote the malignant phenotype of cervical cancer	
ii. The emerging role of lncRNAs in the regulation of cancer stem cells	

## 1. RESUMEN

Estudios epidemiológicos indican que la obesidad afecta negativamente la progresión y el tratamiento del cáncer cervicouterino. Investigaciones recientes muestran que existe una subpoblación de células troncales derivadas de tejido adiposo (ADSCs) que pueden alterar las propiedades del cáncer. En el presente proyecto, describimos por primera vez el impacto de las ADSC sobre el comportamiento maligno de células de cáncer cervicouterino como HeLa, SiHa y Caski. Las ADSC se obtuvieron a partir de tejido adiposo de pacientes femeninas libres de cáncer sometidas a bypass gástrico, con obesidad mórbida. La identidad celular fue corroborada mediante marcadores de superficie. El transcriptoma de las células cancerosas cultivadas en presencia de las células troncales se analizó utilizando RNA-seq, nuestros resultados muestran que 95 RNAs modificaron su expresión en las células cancerosas como resultado de esta interacción. Los cambios en la expresión génica se validaron mediante PCR digital, entre los genes validados encontramos a ITGA5, IL4R, TIMP1, OASL, IL6, FN1 y PLAC8 que interesantemente están implicados en la supervivencia, migración, invasión o quimiotaxis. Para identificar las principales vías de señalización afectadas en las células cancerosas debido a la presencia de ADSCs se utilizaron diferentes herramientas bioinformáticas como IPA, KPA y GSEA. Los procesos celulares y moleculares alterados se validaron mediante ensayos *in vitro* e *in vivo*. Los ensayos experimentales indican que las células troncales provocan un incremento en la migración de todas las líneas celulares de cáncer cervicouterino de al menos 807% veces más, así como de 549% más invasión; sin embargo, no se encontraron alteraciones en la proliferación. Mediante el modelo de pez cebra se evidenció un incremento en la angiogénesis y la tumorigénesis de las células cancerosas por la presencia de las ADSCs. Los análisis bioinformáticos y experimentales demostraron que la vía de señalización de NF-kappa B se enriquece en las células cancerosas debido a la influencia de las ADSCs. Curiosamente, las células tumorales cambian su morfología epitelial a mesenquimal, que se refleja en el aumento de la expresión de marcadores mesenquimales como de fibronectina, n-cadherina y vimentina. Además, las ADSCs también amplían el grupo de CSCs en las células de cáncer en un 55,6 %, incrementando la malignidad tumoral. En conclusión, nuestros resultados sugieren que las células troncales derivadas del tejido adiposo inducen a las células de cáncer cervicouterino a adquirir características malignas donde NF-kappa B juega un papel clave.

## 2. ABSTRACT

Epidemiological studies indicate that obesity negatively affects the progression and treatment of cervical-uterine cancer. Recent evidence shows that a subpopulation of adipose-derived stem cells (ADSCs) can alter cancer properties. In the present project, we described for the first time the impact of ADSCs over the malignant behavior of cervical cancer cells (HeLa, SiHa, and Caski). ADSCs were obtained from the adipose tissue of morbidly obese, cancer-free female patients undergoing gastric bypass. Cellular identity was corroborated by the expression of cell surface markers. The transcriptome of cancer cells cultured in the presence of ADSCs was analyzed using RNA-seq, our results show that the expression of 95 RNAs was altered in cancer cells as a result of this interaction. Changes in gene expression were validated using digital-PCR, among the validated genes we find ITGA5, IL4R, TIMP1, OASL, IL6, FN1, and PLAC8 that interestingly are involved in survival, migration, invasion, or chemotaxis. Bioinformatics tools such as IPA, KPA, and GSEA were used to identify the main signaling pathways disrupted in cancer cells due to the presence of ADSCs. *In vitro* and *in vivo* assays were conducted to validate cellular and molecular processes altered in cervical cancer cells owing to stem cells. Experimental assays indicate that stem cells provoke an increment in migration (807-1758%) and invasion (549-1080%) of all cervical cancer cell lines; however, no alterations were found in proliferation. Using the zebrafish model, an increase on angiogenesis, and tumorigenesis of cancer cells was evidenced by the presence of ADSCs. Bioinformatics and experimental analyses demonstrated that the NF-kappa B signaling pathway is enriched in cancer cells due to the influence of ADSCs. Interestingly, the tumor cells shift their epithelial to a mesenchymal morphology, which was reflected by the increased expression of specific mesenchymal markers (fibronectin, e-cadherin, and vimentin). In addition, ADSCs also expand the pool of CSCs in cervical cancer cells by 55.6%, increasing tumor malignancy. In conclusion, our results suggest that adipose-derived stem cells induce cervical cancer cells to acquire malignant features where NF-kappa B plays a key role.

## 3. INTRODUCCIÓN

### 3.1 Cáncer

El cáncer es un grupo complejo de enfermedades con ciertas características comunes que se comportan como un sistema evolutivo dinámico, interrelacionado y multidimensional, centrado entre los procesos genómicos y epigenómicos alterados.<sup>1-3</sup>

Existen más de 100 tipos de cáncer que pueden originarse en diferentes órganos, los más comunes son el cáncer de pulmón, mama, colon, próstata, estómago, hígado, cérvix, esófago y vejiga. Independientemente del tejido en el que se desarrolle el tumor, las células cancerosas comparten ciertas características fenotípicas (Hallmarks)<sup>1,3-5</sup>. Los Hallmarks del cáncer, reúnen un conjunto de capacidades funcionales adquiridas por las células humanas que les confiere la capacidad de formar tumores malignos. Estas características incluyen el mantenimiento de la señalización proliferativa, evasión de supresores de crecimiento, evasión de la respuesta inmune, resistencia a muerte celular, inmortalidad replicativa, inducción de angiogénesis, activación de invasión y metástasis. Subyacentes a estas características se encuentran la inestabilidad genómica, la reprogramación del metabolismo energético y la inflamación<sup>4,6</sup> (Figura 1).

Cabe destacar que el conocimiento de los mecanismos del cáncer ha ido progresando y han surgido nuevas facetas de la enfermedad. Actualmente Douglas Hanahan (2022), propone cuatro nuevos sellos distintivos que podrían incorporarse como componentes centrales de los Hallmarks del cáncer. Estas características son desbloqueo de la plasticidad fenotípica, reprogramación epigenética no mutacional, microbiomas polimórficos y células senescentes<sup>5</sup> (Figura 1).

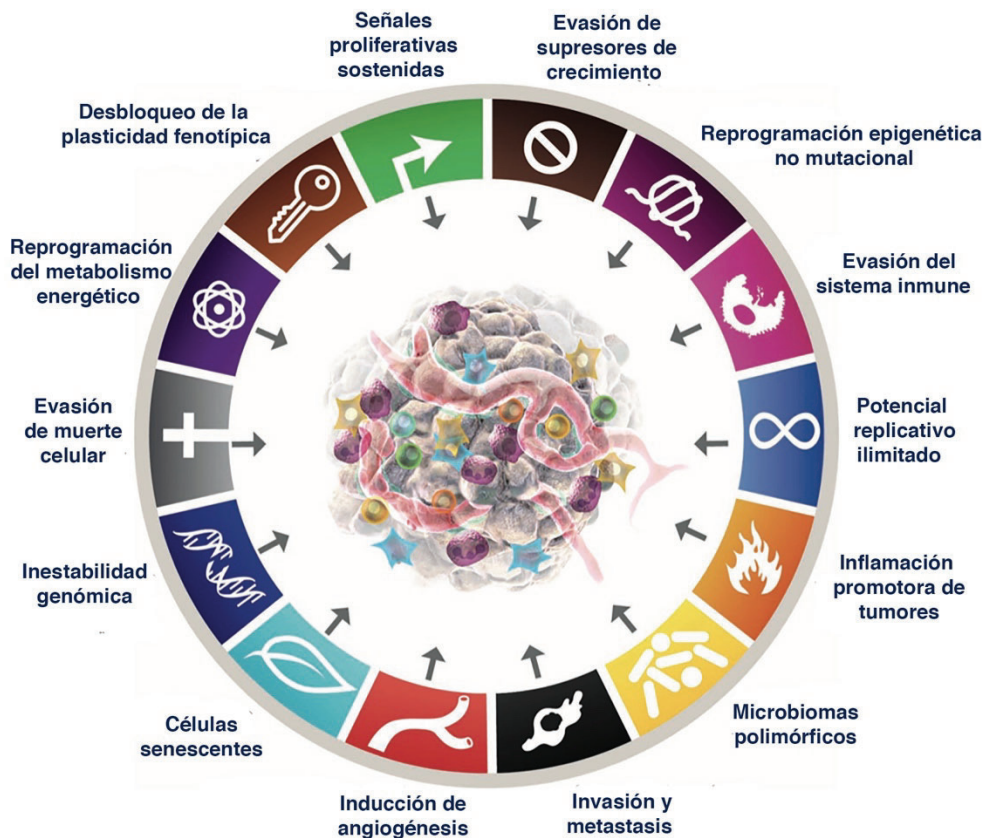


**Figura 1. Características distintivas del cáncer.** Características de las células malignas adquiridas a lo largo del desarrollo tumoral. Imagen tomada y modificada de Douglas Hanahan (2022)<sup>5</sup>

Cabe destacar que un tumor no solo es una colección de células cancerosas relativamente homogéneas, es decir, los tumores reclutan otros tipos de células aparentemente normales que generan el "microambiente tumoral". Tanto el parénquima como el estroma de los tumores contienen distintos tipos celulares que permiten en conjunto el crecimiento y la progresión del tumor.

El microambiente tumoral incluye células estromales multipotentes, fibroblastos, precursores de células endoteliales, células presentadoras de antígeno, linfocitos, etc<sup>7</sup>. Como resultado de esta heterogeneidad, muchos tumores son histopatológicamente diversos y contienen distintos grados de diferenciación, proliferación, vascularización, inflamación, invasividad, etc.

### 3.2 Cáncer Cervicouterino

El cáncer cervicouterino (CC) es el cuarto tipo de cáncer más común en mujeres en todo el mundo y es una de las principales causas de muerte en países en desarrollo. Datos del Globocan 2020, indican que a nivel mundial el CC representa aproximadamente el 12% de todas las neoplasias en la población femenina, con un estimado de 604,127 casos y 341,831 muertes por año<sup>8</sup> (Figura 2).

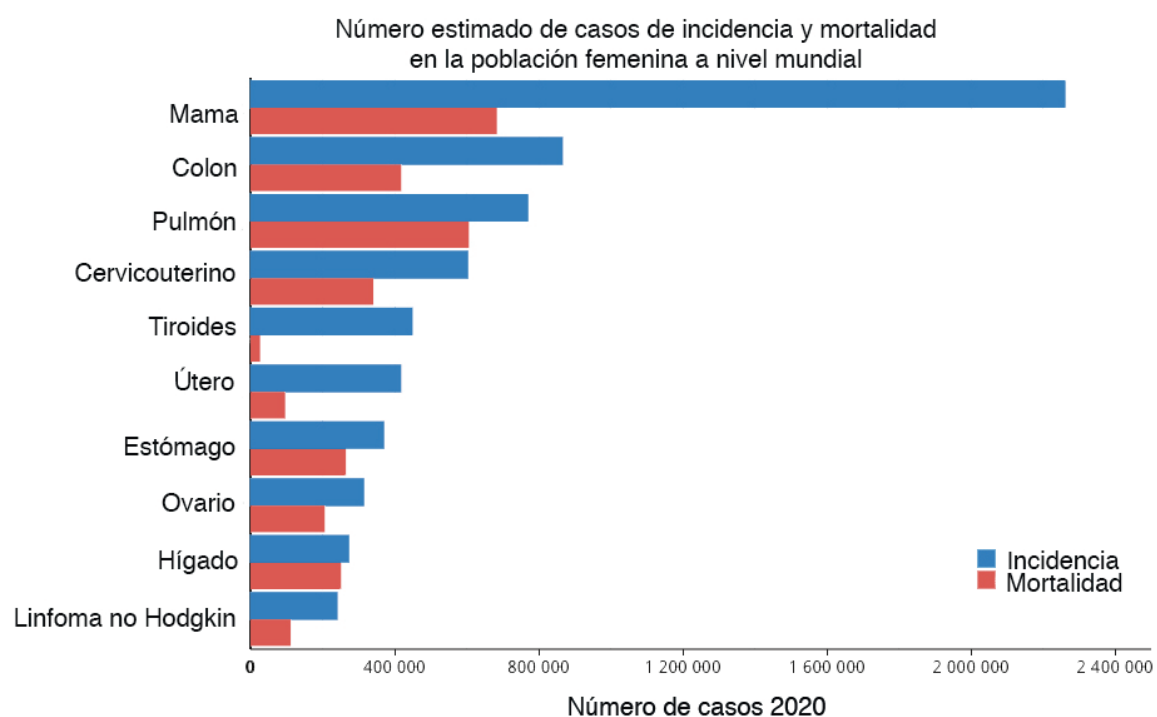


**Figura 2. Incidencia de cáncer y mortalidad en mujeres a nivel mundial.** La gráfica muestra que el cáncer de cervicouterino es el cuarto tipo de cáncer más común. Imagen tomada y modificada *Global Cancer Observatory*( <https://gco.iarc.fr> )

En México, el CC ocupa el segundo lugar por mortalidad e incidencia en la población femenina, con una tasa de 4,335 defunciones de un total de 9,439 casos nuevos en 2020, solo después del cáncer de mama<sup>8</sup>. Esto constituye un importante problema de salud tanto en México como a nivel mundial (Figura 3).



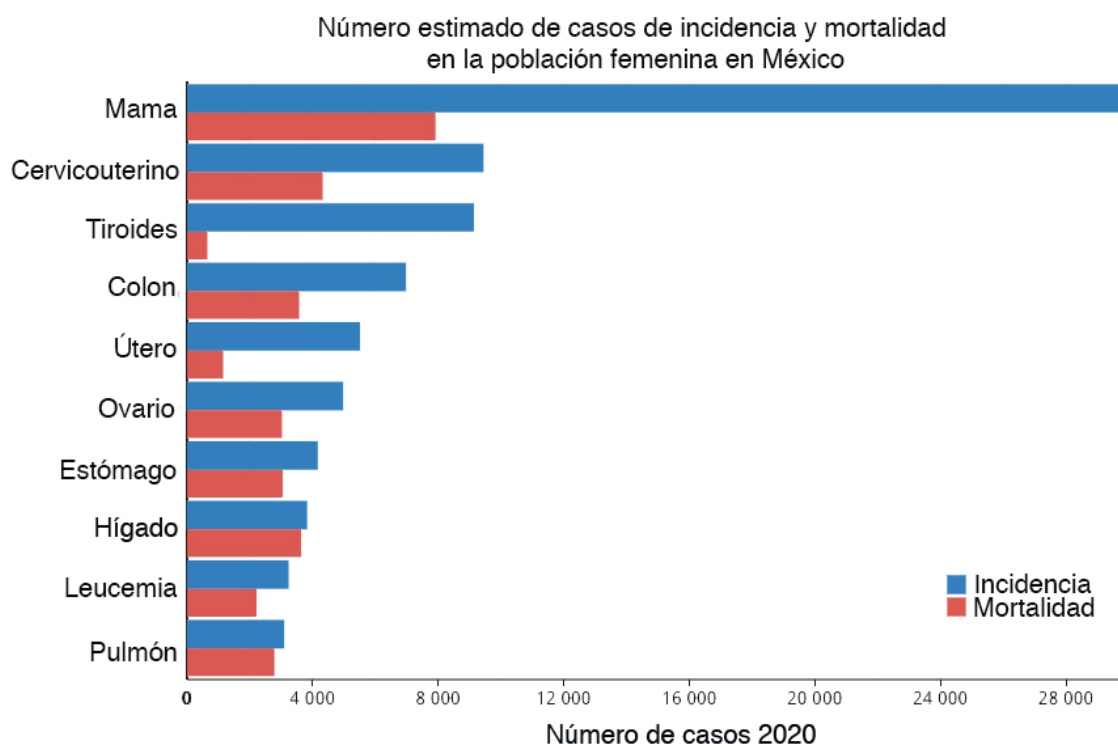


**Figura 3. Incidencia de cáncer y mortalidad en la población femenina en México.** La gráfica muestra que el cáncer de cervicouterino es el segundo tipo de cáncer más común. Imagen tomada y modificada *Global Cancer Observatory*( <https://gco.iarc.fr> )

Dentro de la diversidad de los factores de riesgo relacionados con cáncer destacan las infecciones bacterianas y virales. En este tipo de factores se encuentra con frecuencia a *helicobacter pylori*, hepatitis B y C, epstein-barr, sarcoma de kaposi, el virus linfotrópico de células T humanas 1, entre otros. Sin embargo, la infección por el virus de papiloma humano (VPH) sigue siendo el factor viral con mayor representatividad equivalente a un 31.1 %<sup>9</sup>.

Del 100% de los diferentes tipos de cáncer asociados al VPH en mujeres, encontramos un 14.01 % asociado a orofaringe, 17.64 % con cáncer anal, 3.49 % con vagina, 16.23% con vulva y un 48.63% asociado a cáncer cervicouterino<sup>9</sup>.

Con respecto al desarrollo de CC existen diversos factores de riesgo, incluyendo el número de parejas sexuales, inicio temprano de vida sexual activa, infección con VPH,

inmunosupresión (por ejemplo: después de un trasplante de órgano o trastornos de inmunodeficiencia como el VIH) entre otros<sup>10</sup>.

Casi todos los casos de cáncer cervical están asociados a la persistencia del VPH. El virus del papiloma humano se ha clasificado en genotipos de bajo y alto riesgo según su potencial oncogénico <sup>11</sup>. Entre el 90 % y 99 % de las lesiones pre-cancerosas y carcinomas cervicales están asociadas a la infección de VPH de alto riesgo, el 70% de todos los casos son atribuibles a los genotipos 16 y 18 <sup>9,12</sup>. Cabe destacar que el VPH 16 es responsable del 50% de los carcinomas de células escamosas, mientras que el VPH 18 está relacionado con aproximadamente el 20% de los adenocarcinomas cervicales. Otros genotipos virales oncogénicos incluyen VPH 31, 33, 35, 39, 45, 51, 52, 56, 58, 59 y 68, que en combinación causan el 25% de los carcinomas cervicales <sup>12 13</sup>.

Estudios recientes han mostrado que factores como el consumo de tabaco, la inmunosupresión, el bajo nivel socioeconómico y el uso de anticonceptivos orales a largo plazo, podrían favorecer la persistencia del VPH <sup>14</sup>.

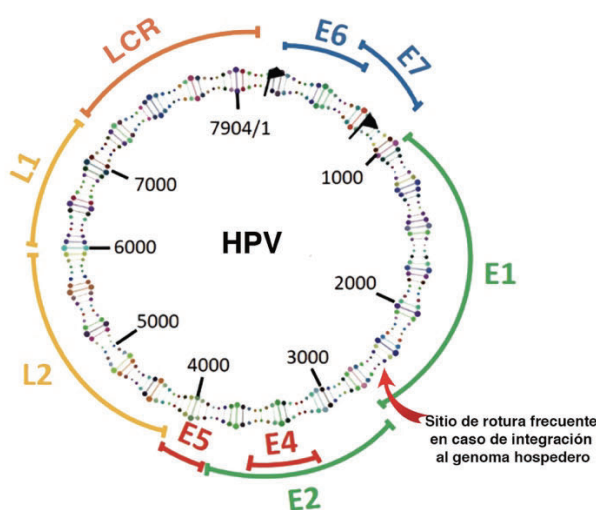
Cabe destacar que la historia natural del cáncer cervicouterino implica la infección por VPH, persistencia de VPH, progresión a displasia e invasión<sup>12</sup>.

### **3.2.1 Oncogénesis del Virus del Papiloma Humano**

El VPH pertenece a la familia *Papillomaviridae*, y es un virus de DNA circular de doble cadena, aproximadamente de 8000pb y tiene una cápside icosaédrica sin envoltura. El genoma de este virus abarca 8 marcos de lectura abiertos (E1, E2, E4, E5, E6, E7, L1 y L2), una región de control (LCR) y 2 sitios de poliadenilación. Los genes virales de transcripción temprana “E” controlan el mantenimiento, replicación y transcripción del DNA viral, mientras que los genes de expresión tardía “L” codifican las proteínas de la cápside <sup>11,15</sup>(Figura 4).

Las proteínas codificadas por E1 y E2 permiten la replicación y transcripción viral dentro de las células cervicales, lo cual conduce a cambios citológicos de bajo grado. La proteína oncoviral E4 ayuda a la liberación del virus a través de la interrupción de la citoqueratina del epitelio superior. La proteína codificada por E5 induce factores de crecimiento en la célula huésped y juega un papel importante en la modulación inmunitaria. Las oncoproteínas virales E6 y E7 son necesarias para la transformación maligna de las células<sup>15</sup>. La proteína E6 se une a la proteína supresora de tumores p53 y, por otro lado, E7 se une a la proteína supresora de tumores de retinoblastoma (Rb); ambos casos conducen a la degradación de las proteínas supresoras, permitiendo así la transformación e inmortalización de las células infectadas<sup>12,16</sup>. La inactivación de genes supresores de tumor, ya sea por mutaciones génicas o por presencia de virus, genera alteraciones en el ciclo celular y conduce a la activación de diversos oncogenes.

Con respecto a los genes tardíos, L1 y L2 codifican las proteínas estructurales mayor y menor que forman la cápside del VPH. La región LCR contiene la mayor variación genética entre un tipo viral y otro. Además, la secuencia LCR contiene el promotor p97 (en VPH 16) ó el promotor p105 (en VPH 18) que permite potenciar o silenciar secuencias que regulan la replicación del DNA viral mediante el control a nivel transcripcional y epigenético. (Figura 4)<sup>17</sup>.



GENES	FUNCIÓN
L1	Proteína estructural de cápside mayor
L2	Proteína estructural de cápside menor
E1	Replicación del genoma
E2	Iniciación de la replicación del ADN viral; regula la transcripción de E6 y E7
E4	Liberación de partículas virales
E5	Mejora las vías de señalización del factor de crecimiento
E6	Degradación de p53 y causa pérdida en la regulación del ciclo celular
E7	Descontrol del ciclo celular por degradación de Rb

**Figura 4. Estructura y función del virus del papiloma humano (VPH).** El genoma del VPH se compone de 8kb y se divide en genes de expresión temprana (E1, E2, E4, E5, E6 y E7) y expresión tardía (L1 y L2). Las oncoproteínas E6 y E7 degradan los supresores tumorales p53 y pRb, respectivamente. La región LCR contiene secuencias regulatorias para el control de la transcripción. Imagen tomada y modificada de Asmita Pal y Rita Kundu (2020)<sup>15</sup>.

La infección inicial requiere que las partículas virales tengan acceso a la capa de células basales del epitelio cervical, esto puede iniciarse a través del rompimiento del epitelio estratificado ó microlesiones de tejido. Ahí, el VPH puede multiplicarse en un estado episomal con un ciclo de replicación relacionado con la diferenciación de la célula infectada<sup>18</sup> En células totalmente diferenciadas, los genes tardíos del VPH producen proteínas de la cápside para empaquetar viriones que se liberarán de las capas epiteliales superficiales<sup>15</sup>.

Alternativamente, durante la infección persistente puede ocurrir la integración del DNA viral al genoma de la célula hospedera. El proceso de integración conduce a la eliminación de diversos genes virales, entre ellos E2, que además de participar en la replicación viral, actúa como un regulador negativo de los oncogenes E6 y E7. La ausencia del gen E2 conduce a la expresión elevada de estas oncoproteínas importantes para la transformación maligna <sup>16</sup>(Figura 4).

### **3.2.3 Neoplasia Intraepitelial Cervical**

El desarrollo del CC está precedido por la aparición de la neoplasia intraepitelial cervical (NIC) la cual se clasifica dependiendo del grado de la lesión del epitelio <sup>10,16</sup> (Figura 5).

Usualmente, se ha descrito que en un tejido sano con infección persistente de VPH se promueve el desarrollo de NIC 1 (grado bajo) y consecutivamente de manera lenta y progresiva se convierte en NIC 2 (grado moderado), seguido de NIC 3 (grado alto) y finalmente cáncer. Sin embargo, estudios recientes sugieren que NIC 1 podría no ser necesario para el desarrollo de NIC 3, ya que NIC 3 podría evolucionar directamente a partir del epitelio normal infectado por VPH. Este modelo (“Molecular Switch”) plantea que la

progresión no lineal podría estar determinada por el grado de metilación de ciertos genes  
12,19.

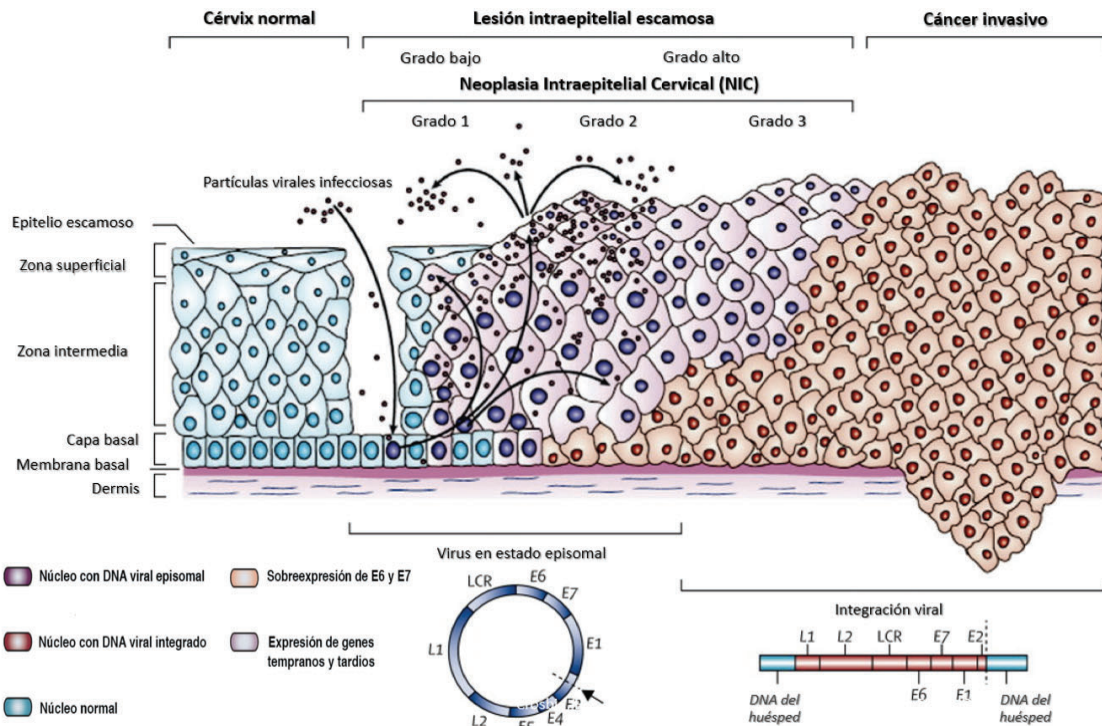


**Figura 5: Ciclo de infección del VPH relacionada a la progresión de la neoplasia intraepitelial cervical.** La imagen muestra que el VPH accede a las células basales a través de microabrasiones en el epitelio cervical. Las lesiones intraepiteliales de bajo grado apoyan la replicación viral (esferas moradas). Un número desconocido de infecciones por el VPH de alto riesgo progresa a neoplasia intraepitelial cervical de alto grado (núcleos morados). La progresión de las lesiones (NIC2 y NIC3) conlleva a cáncer invasivo, lo cual se asocia con la integración del genoma del virus en los cromosomas de las células huésped (núcleos rojos), con la pérdida o interrupción asociada de E2, y la posterior regulación positiva de la expresión de los oncogenes E6 y E7. Imagen tomada y modificada de *Emma J Crosbie (2013)*<sup>16</sup>

Como se ha mencionado, entre un 90 y 99% de los pacientes con cáncer cervicouterino son positivos al VPH, sin embargo, no todos los pacientes infectados con VPH llegan a desarrollar cáncer. Esto significa que el virus no es suficiente para inmortalizar y transformar a las células, por lo que debe haber un conjunto de alteraciones a nivel genético y epigenético que conlleven a desarrollar la enfermedad. En la última década, se han propuesto algunos factores de riesgo adicionales relacionados con el estilo de vida y la salud

nutricional. La baja ingesta de frutas y verduras, el sobrepeso y la obesidad podrían estar relacionados con el desarrollo de la carcinogénesis cervical.

### **3.3 Obesidad**

Es bien sabido que la acumulación de mutaciones en las células, la predisposición de factores genéticos, exposición a agentes ambientales y estilo de vida, juegan un rol importante en el proceso de carcinogénesis. Estudios recientes han mostrado que otro factor que complica el curso clínico del cáncer es la obesidad<sup>20,21</sup>.

La obesidad se ha definido como la acumulación excesiva de tejido adiposo, equivalente a un índice de masa corporal (IMC) igual o superior a 30 Kg/m<sup>2</sup>. El tejido adiposo se puede dividir según la ubicación anatómica en tejido subcutáneo, intramuscular y visceral.

El tejido adiposo subcutáneo está contenido principalmente en los depósitos abdominales, glúteos, femorales y grasa mamaria. Este tejido comprende aproximadamente un 80% de la grasa corporal total. El tejido adiposo visceral rodea los órganos vitales e incluye tejido adiposo omental, mesentérico y epiploico, así como las almohadillas de grasa gonadal, epicárdica y retroperitoneal. Los depósitos viscerales representan aproximadamente del 5% al 20% de la grasa corporal total en individuos con peso normal (sin sobrepeso u obesidad). Finalmente, múltiples depósitos más pequeños, como los intramusculares, intraorbitales y de médula ósea, nutren y protegen los tejidos de todo el cuerpo<sup>22</sup>.

Adicionalmente, el tejido adiposo se puede subclasificar como blanco, marrón o beige, dependiendo del contenido mitocondrial celular, es decir, un mayor número de mitocondrias corresponde a un tono de adipocito más oscuro, esto debido a la presencia de hierro en las mitocondrias<sup>23,24</sup>.

Cabe destacar que el tejido adiposo marrón quema energía y genera calor mediante la oxidación de lípidos. En adultos, el tejido marrón se encuentra en pequeños depósitos en la parte superior de la espalda, el costado del cuello, el área del hombro y a lo largo de la

columna vertebral. Los bebés tienen un mayor porcentaje de grasa marrón que los adultos. El tejido adiposo beige es genéticamente diferente del adiposo marrón y blanco, pero quema calorías para liberar energía como el adiposo marrón.

Por otro lado, el tejido adiposo blanco constituye la mayoría del tejido adiposo del cuerpo, estos depósitos almacenan reservas energéticas en forma de lípidos y ayudan a aislar el cuerpo. El tejido adiposo blanco es un órgano endocrino que secreta numerosos factores con funciones autocrinas, paracrinas y endocrinas. Además, el tejido adiposo blanco está implicado en el desarrollo de la obesidad, así como trastornos metabólicos asociados. Cabe destacar que este tipo de tejido muestra un perfil metabólico diferente con relación a su localización.

### **3.4 Cáncer Cervicouterino y Obesidad**

Se ha reportado que la obesidad aumenta el riesgo de 13 tipos distintos de cáncer, entre los que encontramos mama, ovario, hígado, vesícula biliar, riñón, colon, pancreático, gástrico, esofágico, endometrial, tiroideo, mieloma múltiple y meningioma. Además de un mayor riesgo de desarrollar cáncer, las personas obesas tienen más probabilidades de tener una respuesta reducida a las terapias contra el cáncer.

La obesidad se ha relacionado de manera inconsistente con una mayor incidencia de cáncer cervicouterino; sin embargo, no se ha explorado a fondo el efecto de la obesidad sobre este tipo de cáncer. Actualmente, se sabe que el aumento de la masa corporal podría impedir la detección de lesiones malignas y aumentar el riesgo de cáncer cervical, incluso en mujeres que se someten a pruebas de detección de última generación. Adicionalmente, estudios epidemiológicos indican que la obesidad incrementa tres veces más el riesgo de morir en pacientes con cáncer cervicouterino. (Figura 6).



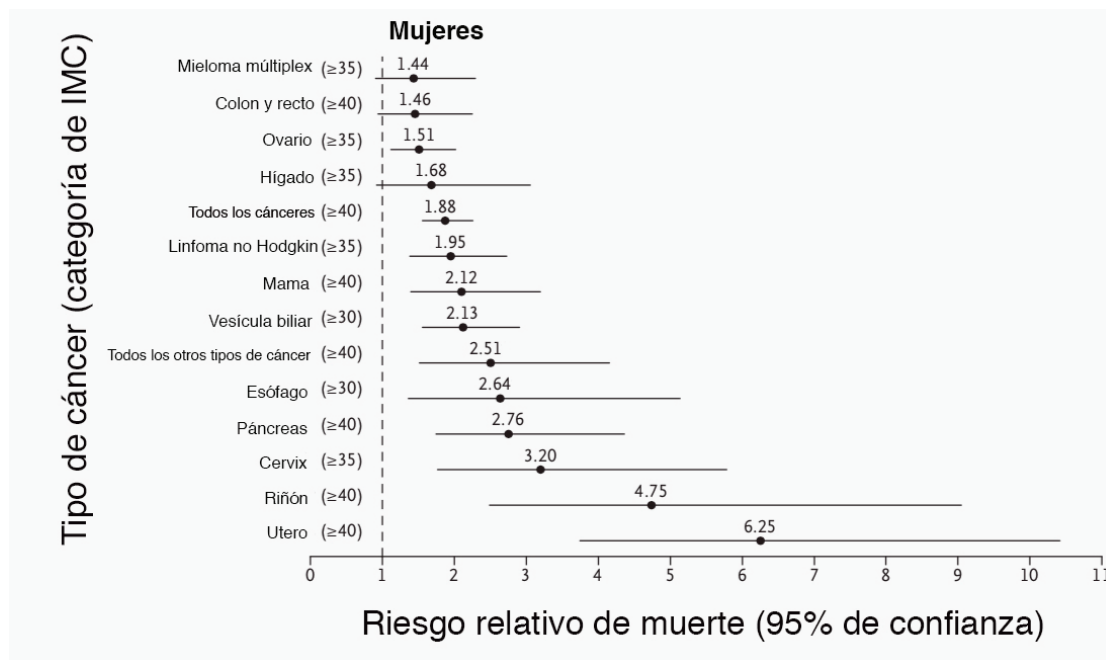


**Figura 6. Resumen de la mortalidad por cáncer en mujeres según el índice de masa corporal.**

La gráfica indica el riesgo relativo a muerte en mujeres por cáncer con relación al índice de masa corporal (IMC), se muestra un incremento de 3.2 para CC. Imagen tomada y modificada de Calle EE. (2003)<sup>25</sup>.

En general, la relación entre obesidad y cáncer puede explicarse por el cambio de la señalización hormonal alterada, inflamación crónica, metabolismo de ácidos grasos, la regulación anormal de insulina y otros compuestos de la dieta implicados en el metabolismo del tejido adiposo. Sin embargo, para el cáncer cervicouterino no se ha dilucidado como es que la obesidad podría incrementar el riesgo a muerte en pacientes con este tipo de cáncer.

Si bien el tipo celular que ha caracterizado al tejido adiposo es el adipocito, este no es el único tipo celular presente en el tejido, ni es el más abundante, es decir, se han descrito otros tipos celulares presentes en el tejido adiposo como: pre-adipocitos, macrófagos, neutrófilos, linfocitos y células endoteliales. No obstante, en los últimos años, se ha demostrado que el tejido adiposo, posee una población de células troncales multipotentes denominadas células troncales derivadas del tejido adiposo. Estas células han destacado por su amplia aplicación en la medicina regenerativa<sup>26</sup>, sin embargo, evidencias recientes sugieren que esta población tiene una participación crucial en cáncer.



### 3.5 Células troncales

Las células troncales no poseen características morfológicas claras que puedan distinguirlas dentro de un tejido celular, por lo que se han definido con relación a su función como células indiferenciadas con alta capacidad de autorrenovación, y diferenciación a múltiples linajes celulares. Existen varios tipos de células troncales que provienen de diferentes nichos celulares ó se forman en diferentes momentos del desarrollo, estas son las células troncales totipotentes, pluripotentes y multipotentes<sup>27,28</sup>.

Las células troncales totipotentes, son capaces de producir todos los linajes celulares de un organismo, por ejemplo, el cigoto (Figura 7). Las células totipotentes también incluyen las estructuras extraembrionarias como las células de la placenta, saco vitelino y cordón umbilical.

A medida que avanza el desarrollo, el embrión alcanza la etapa de blastocisto y cada célula que forma parte de la masa celular interna se denomina célula pluripotente. Estas células son capaces de producir todas las células del embrión, es decir, se pueden diferenciar en cualquiera de las capas embrionarias: ectodermo, mesodermo ó endodermo, pero no pueden generar las estructuras extraembrionarias<sup>28</sup> (Figura 7).

Se ha identificado un tercer grupo de células denominadas células troncales multipotentes (CTM), estas pueden aislarse del estroma de la médula ósea, del sistema nervioso central y prácticamente pueden aislarse de todos los órganos, incluido el tejido adiposo. A diferencia de las células totipotentes o pluripotentes, la capacidad de diferenciación de las células multipotentes se limita a los tipos celulares del órgano o tejido del cual proceden, por lo que también son llamadas células troncales de tejido adulto<sup>29-31</sup>

Las CTM al igual que otras células troncales, se pueden identificar por la expresión combinada de varios marcadores de superficie celular. Estas células no poseen marcadores

exclusivos, pero comparten ciertos marcadores con otras células troncales. Estas células son positivas a los marcadores CD90, CD73, CD105 y negativas al marcador de células hematopoyéticas (CD45)<sup>32</sup>.

El tejido adiposo es una fuente abundante de CTM, las cuales se denominan células troncales derivadas del tejido adiposo (ADSC) y son capaces de autorrenovarse y diferenciarse a linajes celulares como el linaje osteogénico, adipogénico y condrogénico<sup>30</sup>  
<sup>33</sup> (Figura 7).

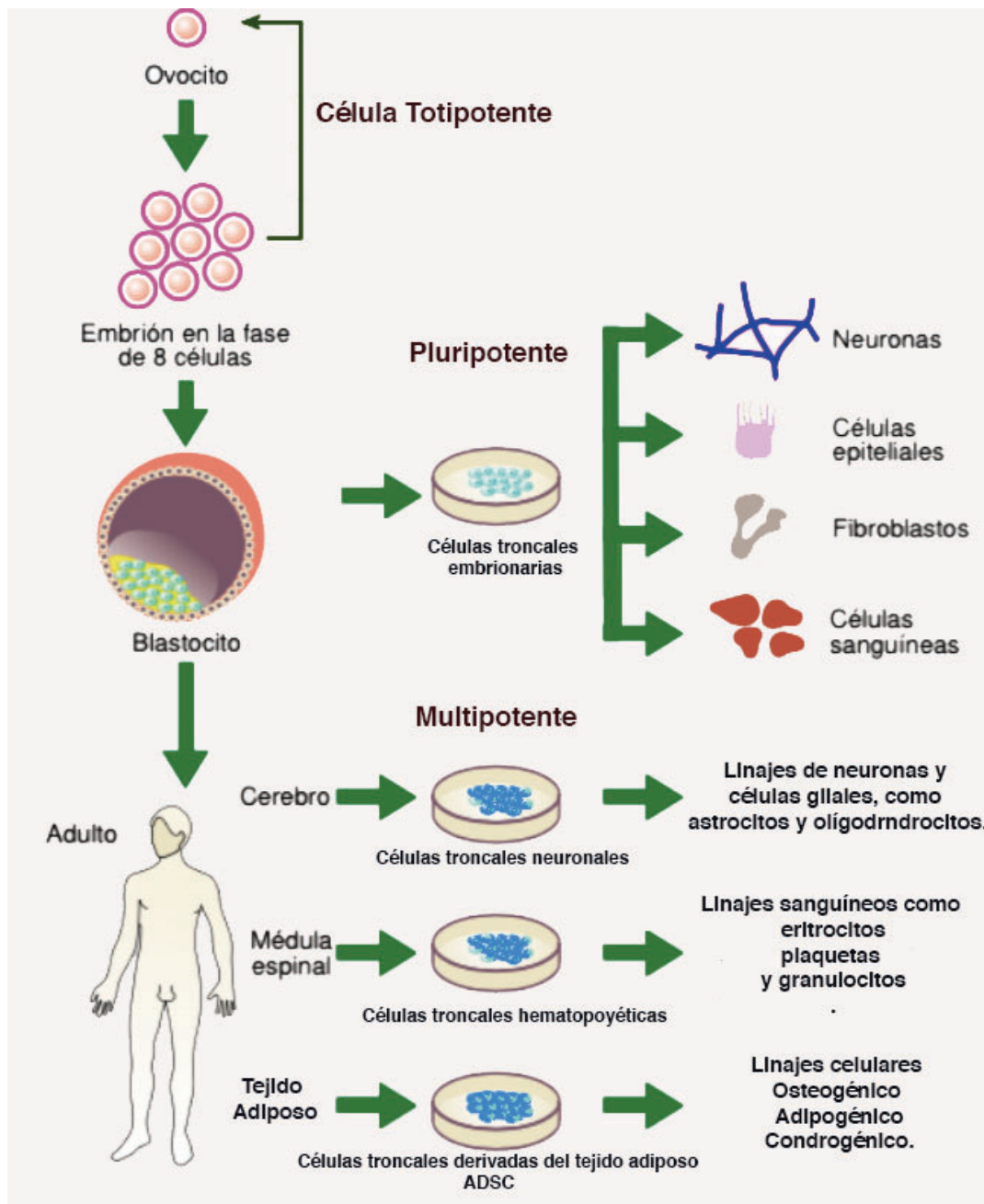


**Figura 7: Origen de los tipos de células troncales.** La figura muestra que las células troncales totipotentes tienen la capacidad de desarrollar un embrión completo; las pluripotentes dan origen a cualquier tipo celular, y las multipotentes dan origen a los distintos tipos celulares del órgano o tejido al que pertenecen, entre las células multipotentes encontramos a las ADSC. Imagen tomada y modificada de *Sandra Torrades (2003)* <sup>34</sup>.

### 3.6 Células troncales derivadas del tejido adiposo (ADSC) y Cáncer

Al igual que las células troncales mesenquimales, las ADSCs existen abundantemente en el tejido adiposo. Las ADSC se encuentran en la fracción vascular estromal (SVF), además de ADSCs (alrededor del 10%), esta fracción contiene macrófagos, células precursoras endoteliales, células endoteliales, células de músculo liso, linfocitos, pericitos y pre-adipocitos, entre otros. Las ADSC se aíslan del tejido adiposo obtenido a partir de mecanismos de liposucción<sup>35 36</sup>.

En cuanto a morfología, las ADSC son similares a los fibroblastos<sup>36</sup>, cabe destacar que el fenotipo exacto de las ADSC aún no es muy preciso, porque los biomarcadores de superficie varían dependiendo del sitio donante ó pase de cultivo, sin embargo, las ADSC se caracterizan principalmente por expresar marcadores de superficie como: CD13, CD29, CD44, CD73, CD90, CD105, CD166 y CD271, y son negativas a los marcadores CD14, CD34 y CD45<sup>37,38</sup>.

Diversos estudios han descrito que las citocinas, exovesículas, exosomas, ácidos nucleicos, lípidos y proteínas son los principales factores a través de los cuales las ADSC ejercen sus efectos biológicos, ya que estos factores son capaces de atravesar las membranas celulares para participar en el intercambio de moléculas que modulan diversos procesos biológicos y vías de señalización<sup>39</sup>. Se ha reportado que la cantidad de citocinas a partir del medio condicionado de ADSC puede variar dependiendo de las condiciones de oxígeno<sup>39</sup>.

Las ADSC han sido de interés debido a su participación en la reparación y regeneración de diversos tejidos dada su plasticidad y alta capacidad proliferativa<sup>30,40</sup>. En comparación a las células troncales mesenquimales derivadas de médula ósea (BM-MSC), las ADSCs son mejores candidatos para su aplicación en medicina regenerativa debido a que estas son más fáciles de aislar y son más abundantes que las BMSC. Esto asegura la disponibilidad de ADSC para aplicaciones de investigación y su futura aplicación, por ejemplo, para solucionar

problemas de daño ortopédico, problemas de fertilidad, pérdida de cabello, insuficiencia hepática, diabetes mellitus, etc<sup>41</sup>.

A pesar del potencial regenerativo de las ADSCs, estudios recientes han demostrado que estas células tienen una función vital en cáncer, ya que podrían contribuir con el microambiente tumoral para modificar la recurrencia y metástasis<sup>42-44</sup>.

Se ha demostrado que al igual que las BM-MSc, las ADSC pueden ser quimio-atraídas hacia los tumores sólidos para así formar parte del microambiente tumoral, un proceso que instala y acompaña la progresión del cáncer<sup>45,46</sup>.

Se ha propuesto que la quimio-atracción de las células ADSC hacia los tumores es debido a que las ADSC reconocen el tumor como una fuente constante de inflamación y migran en respuesta a citocinas secretadas por el microambiente tumoral. El mecanismo por el cual las células ADSC migran a sitios tumorales aún es desconocido; sin embargo, se ha sugerido el eje de señalización CXCR4-CXCL12<sup>45</sup>.

Cabe resaltar que en pacientes con obesidad la movilidad sistémica de ADSC es alta comparada con pacientes sanos y esta movilización sistémica está aún más elevada en pacientes con cáncer<sup>47</sup>, lo que sugiere la posibilidad de su incorporación hacia tumores.

Es importante resaltar que de forma natural, las ADSC no poseen características patógenas por sí mismas<sup>48</sup>, sin embargo, se ha propuesto que una vez que las ADSC se instalan en el tumor contribuyen a un fenotipo más agresivo en las células cancerosas, modificando la viabilidad, proliferación, migración y tumorigenicidad<sup>46,49</sup>.

Se ha propuesto que esta acción podría deberse a que las ADSC secretan tanto factores de crecimiento como factores angiogénicos que le permiten al tumor tener acceso a nutrientes

y oxígeno y de esta manera promover el crecimiento<sup>46</sup>, sin embargo; el mecanismo molecular y celular de la interacción entre células tumorales y ADSC se desconoce a fondo.

Por ejemplo, se ha descrito que la presencia de ADSC provoca un incremento de FGF2 en células tumorales de próstata, sugiriendo un posible incremento de vascularización en este tipo de tumores<sup>45</sup>. Otros estudios han revelado que las ADSC podrían inducir la activación de STAT3 en células de cáncer de endometrio y osteosarcoma para inducir proliferación e invasión celular mediante la regulación positiva de las metaloproteinasas 2 y 9<sup>50,51</sup>. En cáncer de mama se ha propuesto que la presencia de ADSC incrementa el riesgo oncológico y podría favorecer la metástasis, debido a que estas células provocan un incremento de moléculas como CCL2, HGF, y MMPs, que conllevan a un incremento en la migración de las células cancerosas<sup>52</sup>.

Asimismo, Fabian Preisner y colaboradores realizaron estudios in vitro sobre la interacción de ADSC y células de melanoma maligno y concluyeron que las ADSC provocan un incremento en la movilidad de las células cancerosas<sup>53</sup>. En cáncer colorrectal también las ADSC han demostrado favorecer la progresión tumoral. Incluso las ADSC pueden reducir la apoptosis inducida por cisplatino en las células epiteliales de cáncer de ovario, dando como resultado la resistencia a este fármaco<sup>54</sup>. Igualmente Hong-Jian et al. 2015, evidenciaron que las ADSC promueven el inicio tumoral de células cancerosas de mama y colón, además, reportaron que las células cancerosas estimularon la secreción de interleucina-6 (IL-6) en ADSC, y a su vez IL-6 actuó de manera paracrina en las células cancerosas para mejorar sus propiedades malignas<sup>55</sup>.

Sin embargo, la evidencia emergente muestra que hay resultados contradictorios sobre los efectos de las ADSC en la progresión tumoral. Aunque la mayoría de los artículos reportan un incremento en el fenotipo maligno, existen estudios que demuestran un potencial antitumoral de las ADSC. En cáncer de vejiga, por ejemplo, experimentos in vitro mostraron que el medio condicionado de las células ADSC induce apoptosis en las células cancerosas y

este efecto parece estar mediado por la secreción de factores solubles que están involucrados en la vía de señalización PTEN / PI3K / Akt<sup>56</sup>.

Asimismo, en células A549 de cáncer de pulmón se ha reportado que las ADSC podrían disminuir las características tumorigénicas de las células cancerosas<sup>49</sup>, incluso otras células mesenquimales como las BM-MSc también exhibieron un efecto inhibitorio sobre las células tumorales A549 tanto en experimentos *in vivo* como *in vitro*.

En cáncer de páncreas, se han encontrado resultados similares donde las ADSC inhibieron la viabilidad y proliferación de las células cancerosas en modelos *in vitro* e *in vivo*<sup>57</sup>. Igualmente, Takahara et al. 2014, ha descrito que las ADSC inducen apoptosis a células de cáncer de próstata, posiblemente por la vía de señalización TGF-β<sup>58</sup>.

Tomando en cuenta todas las evidencias, es posible que el efecto opuesto que confieren las ADSC pueda depender del tipo de tumor.

A la fecha no existía ninguna información sobre la participación de las ADSC en cáncer cervicouterino, ni se conocían los mecanismos moleculares que podrían alterar el fenotipo de las células de CC.

Por lo que en este proyecto revelamos cuál es el impacto biológico de las ADSC sobre células de cáncer cervicouterino, ya que existe evidencia epidemiológica que es uno de los tipos de cáncer más afectados por la obesidad.

#### **4.- JUSTIFICACIÓN**

En México y en el mundo el cáncer cervicouterino sigue siendo una de los tipos de cáncer con mayor incidencia y mortalidad. A pesar de que actualmente existen tratamientos más eficientes para tratar este tipo de cáncer de forma más oportuna, existen evidencia epidemiológica que indica que la obesidad puede acelerar y complicar el curso clínico de este tipo de cáncer e incrementar el riesgo de muerte. A pesar de la influencia de la obesidad en el deterioro de la salud, el efecto de esta enfermedad sobre el cáncer cervicouterino aún no se ha explorado a fondo.

Recientemente, se ha demostrado que el tejido adiposo, posee una población de células troncales multipotentes denominadas células troncales derivadas del tejido adiposo (ADSC), estas células han destacado por su aplicación en la medicina regenerativa, sin embargo, diversos estudios sugieren que esta población podría presentar una participación crucial en cáncer. La función de las ADSC en cáncer aún es controversial, existen algunos informes que evidencian el comportamiento maligno de las ADSC favoreciendo el crecimiento tumoral, por el contrario, algunos estudios han demostrado que las ADSC tienen un potencial antitumoral. Hoy en día se desconoce el papel de las ADSC en cáncer cervicouterino y el mecanismo por el cual podrían afectar el comportamiento de las células cancerosas; por lo tanto, es necesario determinar el efecto de las ADSC en este tipo de cáncer.

#### **5.- HIPÓTESIS**

Las células troncales derivadas de tejido adiposo podrían inducir la adquisición de múltiples características que contribuyen a la malignidad en células de cáncer cervicouterino.



## **6.- OBJETIVO GENERAL**

Evaluar los cambios fenotípicos en células de cáncer cervicouterino debidos a la influencia de células troncales derivadas de tejido adiposo.

### **6.1.- Objetivos Particulares**

- 1.** Establecer un modelo de cocultivo para el estudio de células de cáncer cervicouterino y ADSC.
- 2.** Analizar el impacto de la presencia de ADSC en el transcriptoma de células de cáncer cervicouterino.
- 3.** Analizar la capacidad de migración, invasión y proliferación en células de cáncer cervicouterino ante la presencia de ADSC.
- 4.** Evaluar la capacidad tumorigénica de células de cáncer cervicouterino en presencia y ausencia de ADSC en un modelo in vivo.
- 5.** Determinar las vías de señalización más afectadas en células de cáncer cervicouterino por la presencia de ADSC y analizar cambios expresión en las moléculas clave de esas vías.
- 6.** Evaluar la capacidad angiogénica de células de cáncer cervicouterino en presencia y ausencia de ADSC en un modelo in vivo.

## **7.- MATERIAL Y METODOS**

### **7.1 Cultivo celular**

Las líneas celulares HeLa, SiHa, Caski, HaCaT y ADSC se obtuvieron de ATCC (Manassas, VA, EE. UU.) y se autentificaron mediante la detección de STRs (Short Tandem Repeats). Las líneas de cáncer cervicouterino (HeLa, SiHa y Caski) y la línea de queratinocitos (HaCaT) se cultivaron en medio DMEM suplementado con suero fetal bovino (SFB) al 5% (ATCC, 30-2020) a 37 °C / 5% CO<sub>2</sub>. Las ADSC se cultivaron en medio basal de células troncales mesenquimales para tejido adiposo (ATCC PCS-500-030), el cual contiene aminoácidos esenciales y no esenciales, vitaminas, otros compuestos orgánicos, minerales traza y sales inorgánicas. Este medio se complementó con un kit de crecimiento específico para ADSC (ATCC PCS-500-040) que contiene los siguientes suplementos de crecimiento: (bajo nivel de suero (2% de FBS), FGF básico, EGF y L-alanina-glutamina).

### **7.2 Aislamiento, cultivo y caracterización de ADSC**

Las muestras de tejido adiposo se obtuvieron de 3 pacientes femeninas libres de cáncer sometidas a bypass gástrico, con obesidad mórbida (IMC > 40) (Tabla 1). Las muestras fueron recolectadas en el Hospital de Especialidades del Centro Médico Nacional Siglo XXI - del Instituto Mexicano del Seguro Social (IMSS). Este estudio se realizó de acuerdo a las pautas institucionales bajo un protocolo aprobado (Número de registro R-2013-3601-34). Todos los donantes dieron su consentimiento informado por escrito.

Los tejidos se lavaron con PBS 1X y se fragmentaron en pequeños trozos. Posteriormente, las muestras se sometieron a digestión con colagenasa tipo I al 0,075% (SCR103, Millipore USA MA) durante 40 minutos a 37 °C con agitación suave. Después, las muestras fueron centrifugadas y se recuperó la fracción estromal que es la que contiene las células ADSC. Posteriormente, las células se cultivaron en placas petri para células adherentes con medio DMEM suplementado con estreptomycin / penicilina 1X (30-2300 ATCC, Virginia, EE. UU.) Las ADSC se expandieron y se congelaron en pases primarios.

La identidad de las ADSC fue analizada mediante citometría de flujo, en donde se analizó la expresión de marcadores de superficie como CD44 (MACS Miltenyi Biotec 130-095-195, CA, EE. UU.), CD90 (Millipore FCMAB211F, MA, EE. UU.), CD31, (CBL468F Millipore, MA, EE. UU.) y CD45 (FCMAB118F Millipore, MA, EE. UU.). Estos marcadores definen a la población de ADSC, CD44 y CD90 son marcadores de troncalidad, CD31 es un marcador hematopoyético y CD45 es un marcador endotelial. Como control de isotipo se usó IgG1-PE de ratón (103.092-212 MACS Miltenyi Biotec) e IgG-FITC de ratón (130-092-213 MACS Miltenyi Biotec).

Una vez identificadas las ADSC se realizó un pool de las muestras de pacientes para los ensayos posteriores, y a partir de este punto las ADSC fueron cultivadas en el medio específico para ADSC y sus correspondientes suplementos.

### **7.3 Ensayos de cocultivo HeLa-ADSC**

Para garantizar el aislamiento de dos líneas celulares a través de una membrana permeable, pero con la finalidad de mantenerlas en el mismo microambiente se usaron ensayos de cocultivo indirecto. Las células HeLa (950,000) se sembraron en el compartimento superior de un sistema Transwell (3420 Corning Costar, NY, EUA) con un tamaño de poro de 3.0µm. Además, en el compartimento inferior se sembraron 450,000 células ADSC obtenidas de pacientes ó de la ATCC. El co-cultivo permaneció durante 24 horas en medio DMEM libre de suero (Figura 11).

### **7.4 Producción de medio condicionado**

Medio condicionado de Cocultivo (Cocultivo-MC). El medio DMEM libre de suero fue recolectado del cocultivo HeLa-ADSC de 24h. (Figura 11). Para obtener el medio condicionado de ADSC (ADSC-MC), se sembraron 450,000 células ADSC y fueron cultivadas con medio DMEM libre de suero por 24h y posteriormente el medio condicionado fue recolectado. (Figura 19). Finalmente, para extraer el medio condicionado de HeLa (HeLa-MC), se sembraron 950,000 células HeLa y se cultivaron con medio DMEM libre de suero

por 24h. (Figura 19). Todos los medios obtenidos se filtraron para eliminar cualquier célula en el medio.

### **7.5 Secuenciación de RNA**

El RNA total se aisló de células HeLa y HeLa cocultivadas con ADSC (N = 3) usando QIAzol (79306, QIAGEN, MD, EE. UU.). La concentración e integridad de RNA se evaluó mediante el uso de un Qubit fluorometer y un Bioanalizador. Las muestras con un número de integridad de RNA (RIN) mayor que 9 se consideraron para análisis posteriores. Las células HeLa cultivadas en presencia o ausencia de ADSC se sometieron a un análisis de RNAseq mediante la plataforma illumina (GAII). Se secuenciaron tres réplicas biológicas de cada condición para un análisis más acertado y se obtuvieron aproximadamente 20 millones de lecturas por réplica. Los datos de secuenciación se analizaron con el banco de trabajo CLC Genomics (7CLC BioCambridge), y se determinó la expresión diferencial entre grupos usando el algoritmo EdgeR. Solo los genes con un cambio de expresión mayor a 2 o menor que -2 y un valor  $p \leq 0.05$  y valores ajustados de  $p$  (FDR) menor a 0.1 se consideraron para su posterior análisis. Para validar los datos de RNAseq, elegimos genes diferencialmente expresados con recuentos de lectura medios a altos. Además se verificaron los valores de expresión de esas transcripciones en las réplicas y elegimos genes con recuentos de lectura constante entre réplicas. Finalmente, utilizamos bases de datos como IPA y Metacore para diseccionar las interpretaciones funcionales de los genes con expresión diferencial y se seleccionaron genes candidatos de acuerdo con su relevancia en el desarrollo y la progresión del cáncer. Los genes seleccionados se analizaron por PCR digital.

### **7.6 Análisis de enriquecimiento de conjunto de genes (GSEA)**

Para realizar este análisis, se importaron los datos obtenidos de RNAseq al software GSEA descargado del sitio web: <http://software.broadinstitute.org/gsea/index.jsp>. Los conjuntos de genes relacionados con diferentes procesos de ontología génica sirvieron como set de genes de referencia para determinar los procesos biológicos enriquecidos en nuestros datos. Solo consideramos el conjunto de datos de enriquecimiento que tuvieron una tasa

de descubrimiento falso (FDR)  $<0.25$  y un puntaje de enriquecimiento normalizado (NES) $>1.2$ .

### **7.7 Análisis de vías y procesos biológicos.**

El software Ingenuity Pathway Analysis (IPA-QIAGEN), el software Metacore y Key Pathway Advisor se utilizaron para identificar los principales procesos biológicos alterados por la presencia de ADSC en HeLa, así como para inferir qué genes están involucrados en la regulación de las rutas celulares esenciales. Todo ello con base a la lista de genes con expresión diferencial del RNAseq.

### **7.8 Análisis de supervivencia general**

La supervivencia general de los pacientes con cáncer cervicouterino se analizó en el sitio web: <http://kmplot.com/analysis/>. El software integra simultáneamente la expresión génica y los datos clínicos. Para analizar la supervivencia de los pacientes con carcinoma de células escamosas cervicales se utilizó la sección Pan-cancer RNA-seq de la plataforma KM plotter, calculándose la relación de riesgo con un intervalo de confianza del 95% y el valor de P de rango logarítmico.

### **7.9 RT-PCR**

El RNA total se extrajo con TRIzol (Cat. 15596026, Thermo, MA USA) de acuerdo a las instrucciones del fabricante. La integridad del RNA fue analizada en geles de agarosa y cada muestra fue cuantificada en el nanodrop para determinar la pureza del RNA mediante la relación 260/280nm. El cDNA se sintetizó con 2 microgramos del RNA Total utilizando el Kit High Capacity cDNA Reverse transcription kit (Cat. 4368813, ThermoFisher, MA, USA).

### **7.10 Droplet Digital PCR**

Todos los ensayos de ddPCR se realizaron utilizando el sistema de PCR digital en gotas QX200 de acuerdo con las instrucciones del fabricante (Bio-Rad). En resumen, cada reacción de EvaGreen ddPCR Supermix (#1864034) con los primers específicos y cDNA diana fue

emulsificada con aceite (#1864006) y fraccionada hasta en 20,000 gotas en el generador QX200. Las gotitas generadas se transfirieron a una placa de 96 pozos (#10023379) para ser sometidas a amplificación por PCR con las siguientes condiciones de reacción: 1× (95°C por 5 min), 40× (95°C por 30 s, T<sub>m</sub>°C por 30 s, 72°C por 30 s), 1× (4°C por 5 min, 90°C por 5 min), 10°C ∞. Las gotas positivas, es decir, que contienen al menos una copia de la molécula de cDNA amplificable, exhibieron un aumento de fluorescencia en comparación con las gotas negativas, por lo que la fluorescencia individual de las gotas fue cuantificada con el detector QX200 Droplet reader. El análisis de los datos se realizó mediante el software QuantaSoft configurado previamente para un análisis de cuantificación absoluta (ABS). Los valores de expresión absolutos en número de copias/μl se calcularon utilizando estadística para una distribución de tipo Poisson. Los resultados de estas mediciones se representan en el número de copias / μl de cDNA amplificable.

#### **7.11 Ensayos de migración e invasión celular (*in vitro*).**

Para evaluar la capacidad de migración celular de las células HeLa y CasKi ante la presencia de los diferentes quimioatrayentes (ADSC, células NH3T3, los diferentes medios condicionados, 5% FBS ó sin FBS), se usaron Transwell permeables de policarbonato con un poro de 8 μm (BD Biosciences). Para estos experimentos, se sembraron en la cámara superior 35,000 células en medio de cultivo desprovisto de FBS y se incubó toda la noche, en seguida se agregaron 600 μl de los diferentes quimioatrayentes según correspondiera. Las células se cultivaron a 37°C y 5% CO<sub>2</sub> durante 24 h. Luego se retiraron los insertos de los pozos, se eliminaron las células en la superficie superior de la membrana del transwell y las células migratorias ubicadas en la superficie inferior se lavaron con PBS y se fijaron con paraformaldehído (PFA) al 4%. Finalmente, se tiñeron con cristal violeta al 0,1%. Las imágenes se capturaron en un estereomicroscopio y el número de células migratorias se cuantificó con el software ImageJ.

Para los experimentos de invasión, también se usaron Transwell permeables de policarbonato con un poro de 8 μm, y se cubrieron con 50 μl de Matrigel. Un total de 35,000

células se sembraron en la cámara superior libres de FBS y posteriormente, se agregaron 600  $\mu$ l de los quimioatrayentes correspondientes en la cámara inferior. Todas las condiciones de incubación, procesamiento y análisis se llevaron a cabo de la misma forma que los ensayos de migración. Se realizaron al menos tres ensayos independientes para cada condición de cultivo con sus respectivas réplicas técnicas cada uno.

### **7.12 Ensayos de proliferación celular**

La proliferación de la línea celular HeLa se evaluó bajo dos condiciones experimentales: A) HeLa vs HeLa co-cultivada con ADSC. B) HeLa ante la presencia de los diferentes medios (DMEM libre de FBS, DMEM suplementado al 5% FBS, medio condicionado de ADSC, HeLa ó medio de co-cultivo HeLa-ADSC) se analizó mediante el método MTS. En resumen, se sembraron 7,000 células por triplicado en placas de 96 pozos y se incubaron a 37 °C en una atmósfera de CO<sub>2</sub> al 5% en medio DMEM libre de FBS para la condición “A” y para la condición “B” según el medio correspondiente. La viabilidad celular fue evaluada a diferentes tiempos. Las células se cuantificaron por triplicado utilizando el kit de ensayo de proliferación de células no radiactivas CellTiter-96 (#G4000, Promega). Las células HeLa se incubaron con el reactivo MTS durante 1 hora. Luego, se midió la absorbancia a una densidad óptica de 590 nm utilizando un lector multidetector (Bekman Coulter).

### **7.13 Ciclo celular**

Los ensayos del ciclo celular se realizaron mediante citometría de flujo utilizando el kit de reactivos Cycletest Plus # 340242, BD, Billerica, MA, siguiendo las recomendaciones del fabricante. El ensayo está basado en el análisis de DNA, el cual es marcado con yoduro de propidio, esta unión es cuantificada mediante un citómetro. En la fase inicial del ciclo celular (G0/G1), las células 2n contienen la mitad de la cantidad de DNA que las células 4n que se están preparando para la mitosis (G2/M).

#### **7.14 Ensayos de Inmunofluorescencia.**

Las células HeLa se cultivaron sobre cubreobjetos de vidrio en placas de 6 pozos y se expusieron a medio condicionado obtenido de ADSC ó medio DMEM libre de FBS durante 24 horas. Después las células se lavaron con PBS 1X y se fijaron con paraformaldehído al 4% (Sigma-Aldrich, St. Louis, MO, EE. UU.). Posteriormente, las células se bloquearon en PBS 1X y 5% de albúmina de suero bovino (Sigma-Aldrich) durante 2 horas y luego se incubaron toda la noche en una cámara húmeda con el anticuerpo primario correspondiente: Rel B, p65, p52, Vincristina, Fibronectina, Ncadherina ó E cadherina (Thermo-Fisher). Las células se lavaron y se incubaron con un anticuerpo secundario correspondiente (#W4028 ó #W4018 Promega) durante 1 h. Finalmente, las células se lavaron con PBS y los portaobjetos se montaron en medio de montaje Everbrite con DAPI (Biotium Inc, Hayward, CA, EE. UU.). Las laminillas se almacenaron a 4°C y el análisis de fluorescencia se realizó en un microscopio confocal (Zeiss LSM 510).

#### **7.15 Ensayos en peces cebra y xenotrasplantes**

El pez cebra (*Danio rerio*) se mantuvo a una temperatura de 28.5 °C a un pH de 7.4 con 14 h. de luz y 10 h. de oscuridad. Se utilizó la cepa Tab Wik (proporcionada por el Dr. Ernesto Maldonado de ICMYL-UNAM y el Dr. Francisco Carmona de IFC-UNAM). Además, se empleó un modelo de pez cebra (Tg (fli1a: EGFP)) que alberga la expresión de GFP en los vasos sanguíneos de forma estable.

Para los experimentos con xenotrasplantes, los huevos fertilizados se obtuvieron de cruces naturales y dos días después de la fertilización (dpf) fueron decorionados y anestesiados con triclaína (MS-222; Sigma), luego, las células fueron microinyectadas en la región del saco vitelino embrionario. Para analizar la capacidad tumorigénica, se inyectaron 300 células SiHa ó Caski en combinación con 50, 100, 150 o 300 células ADSC, NIH3T3 ó HaCaT, cada una de las condiciones se cargó en una aguja de vidrio de borosilicato mediante el uso del extractor Flaminf/Brown micropipette. En cada embrión se implantarán de 5 a 10 nanolitros de la suspensión celular en el saco vitelino de los embriones de pez cebra Tab-wik. El protocolo de microinyección se realizó como se informó anteriormente<sup>59</sup>. Para los ensayos



de migración, las células SiHa se tiñeron con un colorante rojo PKH26-GL (marca de forma general de membranas celulares) o se transfectaron con GFP y los embriones se analizaron a 12 hpi (horas después de la inyección) usando un microscopio de epifluorescencia (Zeiss). Cuatro días después de la inyección (dpi), las larvas se analizaron por estereoscopio para evaluar la formación de tumores.

#### **7.16 Ensayos de dilución limitante extrema (ELDA).**

Los ensayos de dilución limitante in vivo se analizaron usando el software ELDA. Este modelo se centra en la estimación de la frecuencia de células troncales en múltiples conjuntos de datos<sup>60</sup>. El análisis ELDA considera el número de individuos que no lograron formar un tumor cuando se emplean diluciones celulares limitadas. El gráfico generado representa las pendientes de la fracción logarítmica de las células activas con un intervalo de confianza del 95%.

#### **7.17 Angiogénesis.**

Para estos experimentos, se utilizó el modelo de pez cebra Tg (fli1a: EGFP) descrito anteriormente. Las células cancerosas SiHa se marcaron con un colorante rojo PKH26-GL, la migración en el modelo in vivo fue evaluada a las 12hrs post inyección y la formación de nuevos capilares sanguíneos se evaluó a las 12hrs y 3 días posteriores a la inyección.

#### **7.18 Análisis estadísticos**

Se realizaron al menos 3 réplicas biológicas de cada experimento. Los datos fueron analizados con el programa GraphPad Prism 5, en el cual se realizó la prueba T de Student ó ANOVA según correspondiera, considerando un valor de  $p < 0.05$  como estadísticamente significativo. Las gráficas reportadas muestran el promedio de las réplicas y la desviación estándar ( $\pm SD$ ).

## 8. ANTECEDENTES

Las ADSC se obtuvieron del tejido adiposo de 3 pacientes femeninas libres de cáncer con obesidad mórbida (IMC > 40) sometidas a bypass gástrico (Tabla 1). Después de un par de días de cultivo, las ADSC exhibieron una morfología estable en forma alargada tipo fibroblastoide (Figura 9).

Donador	Edad	Peso (kg)	Estatura (m)	IMC (kg/m <sup>2</sup> )
I	26	98	1.55	40.5
II	47	140	1.7	48.5
III	39	130	1.57	52

**Tabla 1. Características de pacientes donantes de ADSC.** Se obtuvieron ADSC de tres pacientes donadores, la tabla resume las características principales de los pacientes que se sometieron a bypass gástrico.

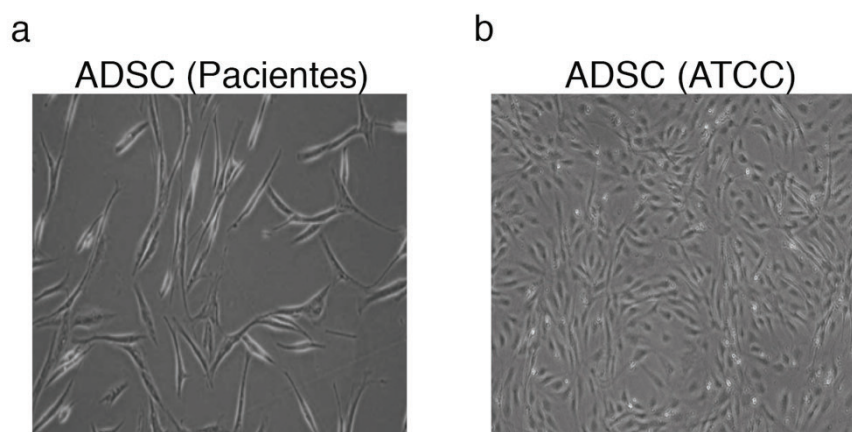


**Figura 9. Aislamiento de ADSC obtenidas de pacientes sometidas a bypass gástrico.** La imagen muestra las ADSC aisladas de tejido adiposo de pacientes mexicanas (a) u obtenidas de ATCC (b).

Para verificar la identidad y la pureza de las ADSC, se analizó la expresión de un panel de marcadores de superficie mediante citometría de flujo en los cultivos de ADSCs de cada paciente. Los resultados indicaron que la mayoría de las células expresaron los marcadores positivos característicos de ADSC (CD44 y CD90) y muy pocas células expresaron marcadores negativos (CD31 y CD45). Estos resultados muestran que los cultivos exhiben el

inmunofenotipo típico de las ADSC con tasas de expresión de CD44 (96%), CD90 (95%), CD31 (0.36%) y CD45 (0.16%) (Figura 10).

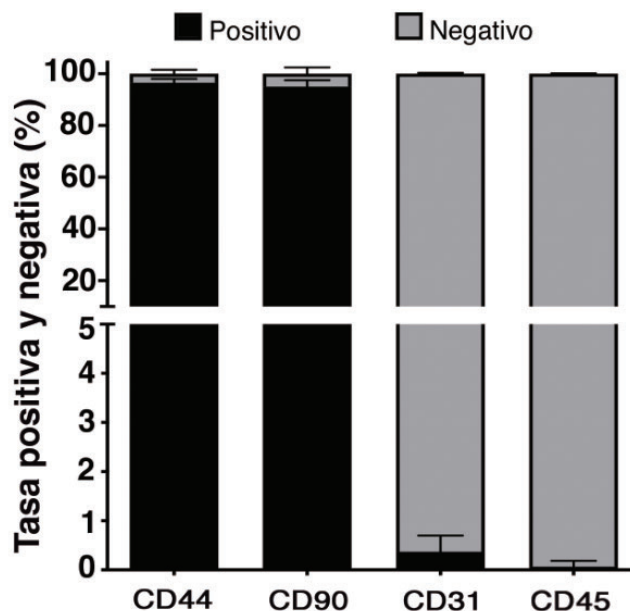


**Figura 10. Identidad de las ADSC.** La pureza de las ADSC se evaluó en cada paciente mediante análisis de citometría de flujo usando marcadores de superficie celular que incluyen CD44, CD90, CD31 y CD45. El gráfico muestra el porcentaje de células positivas y negativas para cada marcador (n = 3 pacientes, 2 réplicas, las barras de error representan la media  $\pm$  desviación estándar (s.d.))

Posteriormente, las células se sometieron a cocultivo indirecto con una línea celular de cáncer cervicouterino y se sometieron a secuenciación masiva de RNA.

## 9. RESULTADOS

### 9.1 El cocultivo de HeLa / ADSCs induce cambios en el transcriptoma de las células HeLa

Es bien sabido que las ADSCs son quimioatraídas a los tumores y ejercen funciones esenciales en la comunicación paracrina de las células. Evidencia acumulada indica que las ADSCs secretan varios factores de crecimiento, citocinas, etc., que pueden influir sobre la proliferación, migración y supervivencia de las células cancerosas de algunos tumores. Para evaluar si las ADSC influyen en el comportamiento de las células de CC, las células HeLa se cocultivaron con las ADSC obtenidas de pacientes, empleando un sistema de cocultivo indirecto. Este sistema permite que las ADSC y las células de CC se cultiven en las mismas

condiciones, pero manteniéndolas físicamente separadas por una membrana permeable, evitando así el contacto directo, pero permitiendo la comunicación celular (Figura 11).

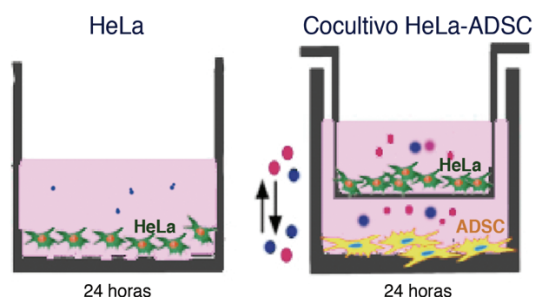
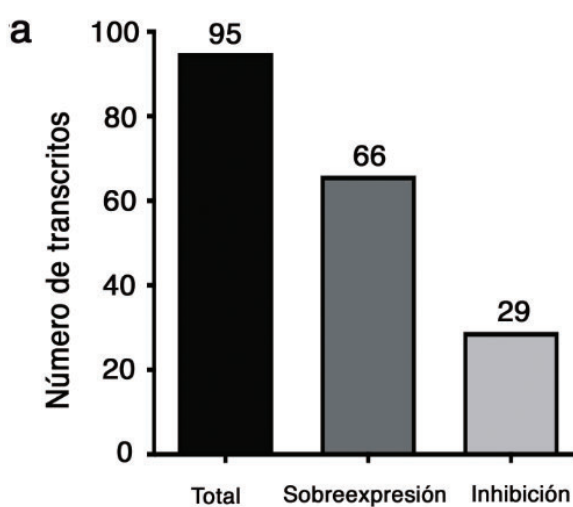


**Figura 11. Ensayos de cocultivo HeLa-ADSC.** Las células HeLa se cultivaron solas o en presencia de ADSC mediante un sistema de cocultivo indirecto. La imagen muestra que ambas líneas celulares se cultivan en el mismo medio, pero están físicamente separadas por una membrana permeable, evitando el contacto directo.

El efecto de las ADSC en el comportamiento de las células de CC, se evaluó mediante el análisis del transcriptoma de las células HeLa co-cultivadas en presencia y ausencia de ADSC con el objetivo de identificar los principales procesos y moléculas afectadas por esta interacción. El análisis del transcriptoma reveló que las células HeLa cocultivadas con ADSC tienen 95 RNAs expresados diferencialmente (ED) (Fold Change > 2 o < -2, un valor de  $p < 0,05$  y  $FDR < 0.1$ ), de los cuales 66 transcritos se regularon positivamente y 29 se regularon negativamente (Figura 12a).



**b**

Procesos de ontología génica	
Nombre	p-value
Regulación de motilidad celular	2.794E-64
Regulación de muerte celular	5.016E-91
Regulación positiva de comunicación celular	2.716E-80
Procesos de desarrollo celular	5.746E-78
Regulación de la proliferación	5.083E-84

**Figura 12. Cambios en el transcriptoma de las células HeLa** (a) La gráfica de barras muestra los RNAm alterados en las células HeLa debido a la presencia de ADSC. (b) La tabla muestra los principales procesos moleculares y celulares alterados durante el cocultivo de HeLa-ADSC.

Para dilucidar los efectos de las ADSC en el comportamiento de las células de cáncer cervicouterino, se realizó un análisis de enriquecimiento de redes utilizando Ingenuity Pathway Analysis (IPA), Metacore y Key pathway Advisor (KPA). Estas plataformas biocomputacionales nos permitieron analizar, integrar y comprender los datos de expresión génica obtenidos por el RNAseq. Como se muestra en la figura 12a-b, la interacción de las ADSC con las células de CC modifican la expresión de genes implicados en procesos celulares, incluida la motilidad celular, muerte celular, comunicación celular, procesos de desarrollo y proliferación.

Además, encontramos redes específicas enriquecidas que incluyen la transición epitelio mesénquima (TEM), la angiogénesis, la inflamación mediada por la señalización de interleucina-6 (IL6) y la adhesión celular (Figura 13).

<b>Redes enriquecidas</b>	
<b>Nombre</b>	<b>p-value</b>
<b>Desarrollo de transición epitelio mesénquima</b>	<b>9.833E-19</b>
<b>Desarrollo y regulación de angiogénesis</b>	<b>1.823E-12</b>
<b>Inflamación mediada por la señalización de interleucina-6</b>	<b>1.371E-9</b>
<b>Adhesión celular</b>	<b>4.853E-7</b>

**Figura 13. Redes enriquecidas durante el cocultivo HeLa-ADSC.** La tabla muestra las principales redes enriquecidas durante el cocultivo de HeLa-ADSC.

Estos resultados sugieren que las ADSCs impactan en procesos que promueven la malignidad de las células de CC. Cabe destacar que la TEM fue el proceso más enriquecido en nuestros datos, esos resultados sugieren que las ADSC pueden influir en las células HeLa para inducir TEM, un proceso biológico que permite que las células epiteliales pierdan su

polaridad y se sometan a cambios bioquímicos para adquirir propiedades migratorias e invasivas.

Asimismo, en presencia de ADSC, las células HeLa exhibieron un enriquecimiento de la vía de señalización IL6, una importante molécula de la familia de las citocinas proinflamatorias. IL6 induce la expresión de una variedad de proteínas responsables de la inflamación aguda y desempeña un papel importante en la progresión tumoral y la metástasis. Para respaldar estos hallazgos, encontramos también cambios de expresión en genes blanco de IL6, por ejemplo: STAT, IGFBP, IGF y CD163 (Figura 14). Cabe resaltar que todas estas moléculas se han propuesto como predictores de malignidad celular en algunos tipos de tumor.

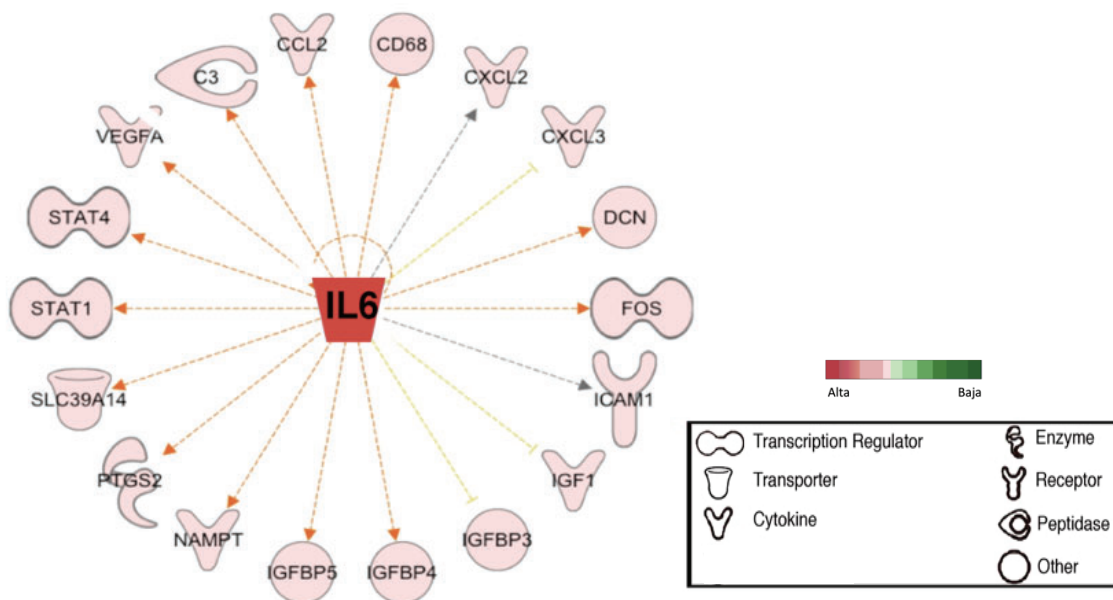


**Figura 14. Señalización de IL6 en células HeLa cocultivadas con ADSC** El análisis de IPA (Ingenuity Pathway Analysis) muestra que la señalización de IL6 se activa en células HeLa expuestas a ADSC, y la red muestra los genes expresados diferencialmente que son regulados por esta vía de señalización. El color rojo indica la sobreexpresión génica.

En la Figura 15, se muestran los mejores 20 RNAs diferencialmente expresados con una mayor tasa de cambio en células HeLa cocultivadas con ADSC. Estos transcritos se asociaron principalmente con la migración, la adhesión celular, la invasión y la metástasis (Figura 15).

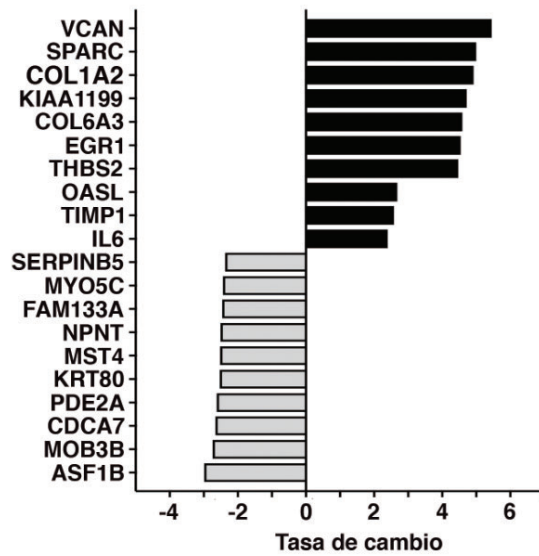


**Figura 15. Top 20 de genes expresados diferencialmente en HeLa durante el cocultivo.** La gráfica muestra la tasa de cambio en la expresión durante el cocultivo HeLa-ADSC.

Además, KPA y Metacore predijeron la activación de la vía de señalización NF-kappa B en las células HeLa cocultivadas con ADSC, indicando que esta vía podría ser un regulador clave esencial que modula los cambios de expresión génica (Figura 16). La vía de NF-kB comprende a una familia de factores de transcripción inducibles que regulan un gran número de genes involucrados en diferentes procesos incluyendo proliferación, metástasis, angiogénesis, respuesta inmune y troncalidad.

Curiosamente, se ha demostrado que NF-kappa B es esencial tanto para la inducción como para el mantenimiento de TEM en muchos tipos de células cancerosas. En conjunto, estos resultados sugieren que las células HeLa pueden adquirir capacidades de migración probablemente asociadas a la inducción de TEM.

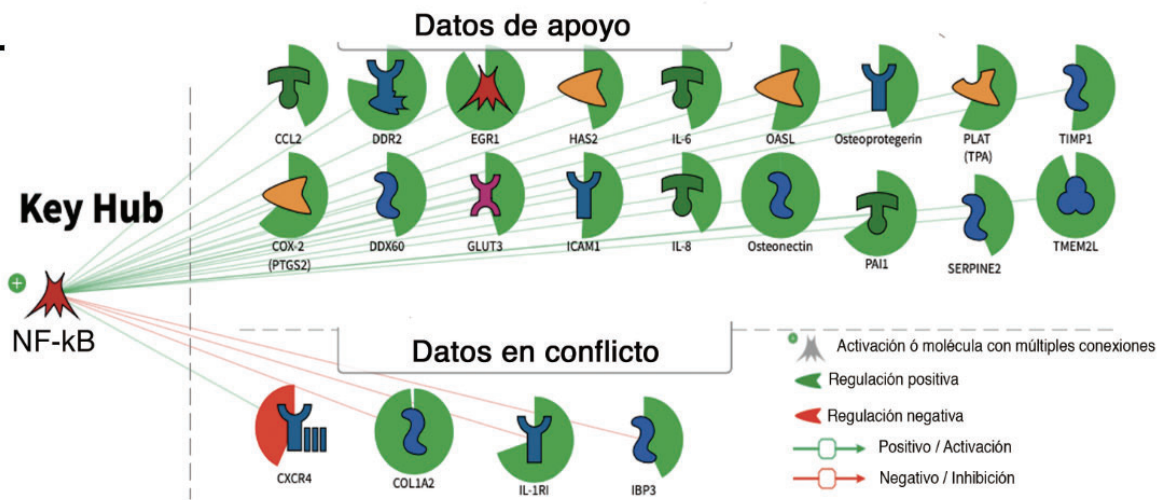


**Figura 16. Vías de señalización alterada en células HeLa cocultivadas con ADSC.** La figura muestra una descripción esquemática de la ruta de señalización de NF-KB, que mediante un análisis de KPA (Key pathway Advisor) se predijo podría estar activa en células HeLa cocultivadas con ADSC.

Posteriormente, para validar los datos de RNAseq, se utilizó la tecnología de PCR digital (ddPCR). Esta técnica ofrece distintas ventajas como la cuantificación absoluta del número de copias de los transcritos, alta precisión y mayor sensibilidad de detección. Esta técnica nos permite cuantificar a partir de muy pequeñas concentraciones de muestra. En estos experimentos se generaron al menos un total de 10,000 nanogotas para cada muestra, y se analizaron mediante el software Quanta-Soft.

Para validar los datos de secuenciación, se usaron las células ADSC derivadas de pacientes mexicanas y una línea celular ADSC obtenida de ATCC. Para cuantificar los niveles de expresión se realizó PCR digital de algunos de los transcritos con expresión diferencial. Los datos mostraron que todos los transcritos analizados (ITGA5, IL4R, TIMP1 y OASL) se validaron con éxito tanto en ADSC obtenidas de pacientes como en ADSC obtenidas de la ATCC. La figura 17 a-b muestra que todos los RNAm cambian sus niveles de expresión en células HeLa debido a la presencia de ADSC. La expresión de otros tres transcritos (IL6, FN1 y PLAC8) fue analizada utilizando ADSC de ATCC. Estos resultados sugieren que los resultados de secuenciación fueron validados exitosamente por ddPCR (Figura 17b).



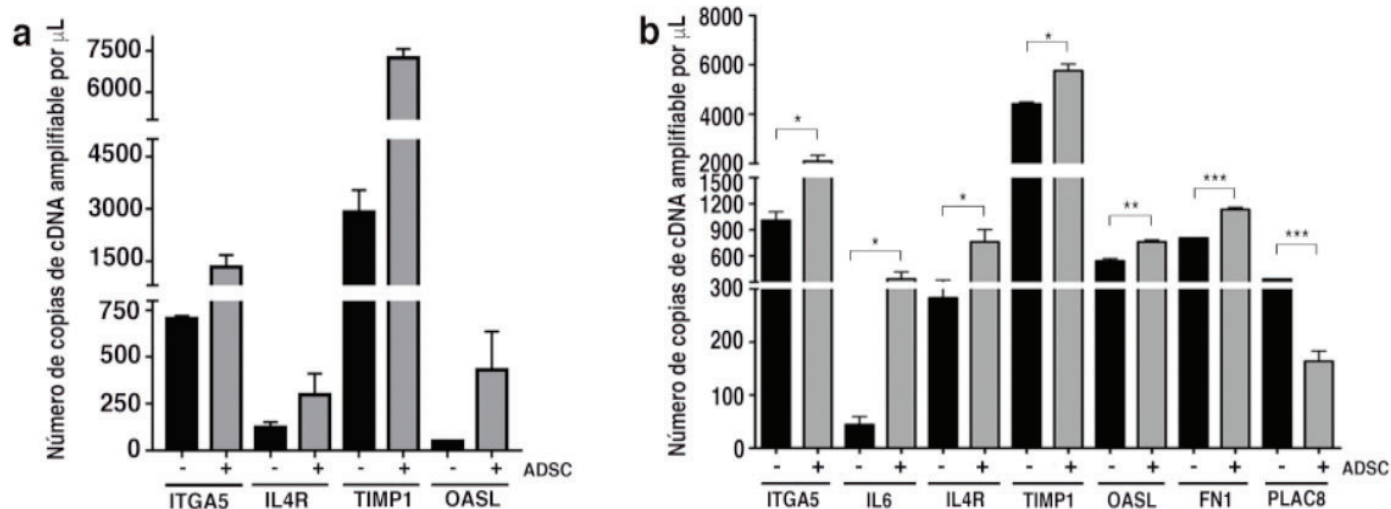


**Figura 17. Validación de cambios en el transcriptoma de células HeLa cocultivadas con ADSC.** (a) La gráfica muestra la cuantificación de la expresión génica fue realizada mediante ddPCR. La gráfica muestra la validación de los transcritos alterados en HeLa por la presencia de ADSC obtenidas de (a) pacientes o (b) ATCC. Los gráficos representan tres réplicas biológicas, y las barras de error representan la media  $\pm$  s.d., \*  $P < 0.05$ .

## 9.2 Transcritos diferencialmente expresados por la presencia de ADSC exhiben importancia clínica en pacientes con cáncer cervical.

Con el objetivo de estimar la supervivencia de pacientes con cáncer cervicouterino tomando en cuenta los cambios de expresión de los genes validados, se realizó un análisis que integra la expresión génica y los datos clínicos simultáneamente. Seis de los genes validados se encontraron anotados en datos de expresión de una cohorte de 304 pacientes con CC. Las curvas de Kaplan-Meier muestran la asociación entre la expresión génica y la supervivencia al cáncer (Figura 18a-f), los datos indican que el aumento de ITGA5 y FN1 están asociados con una menor supervivencia de los pacientes (Figura 18a,d), mientras que la baja expresión de PLAC8 se asocia con una supervivencia más corta (Figura 18e). La sobreexpresión de TIMP1, IL6 y IL4R también se asoció ligeramente con la supervivencia a este tipo de cáncer; sin embargo, este efecto no fue significativo (Figura 18b,c,f). En conjunto, estos datos sugieren que las ADSC podrían aumentar el fenotipo maligno en pacientes con cáncer cervicouterino.

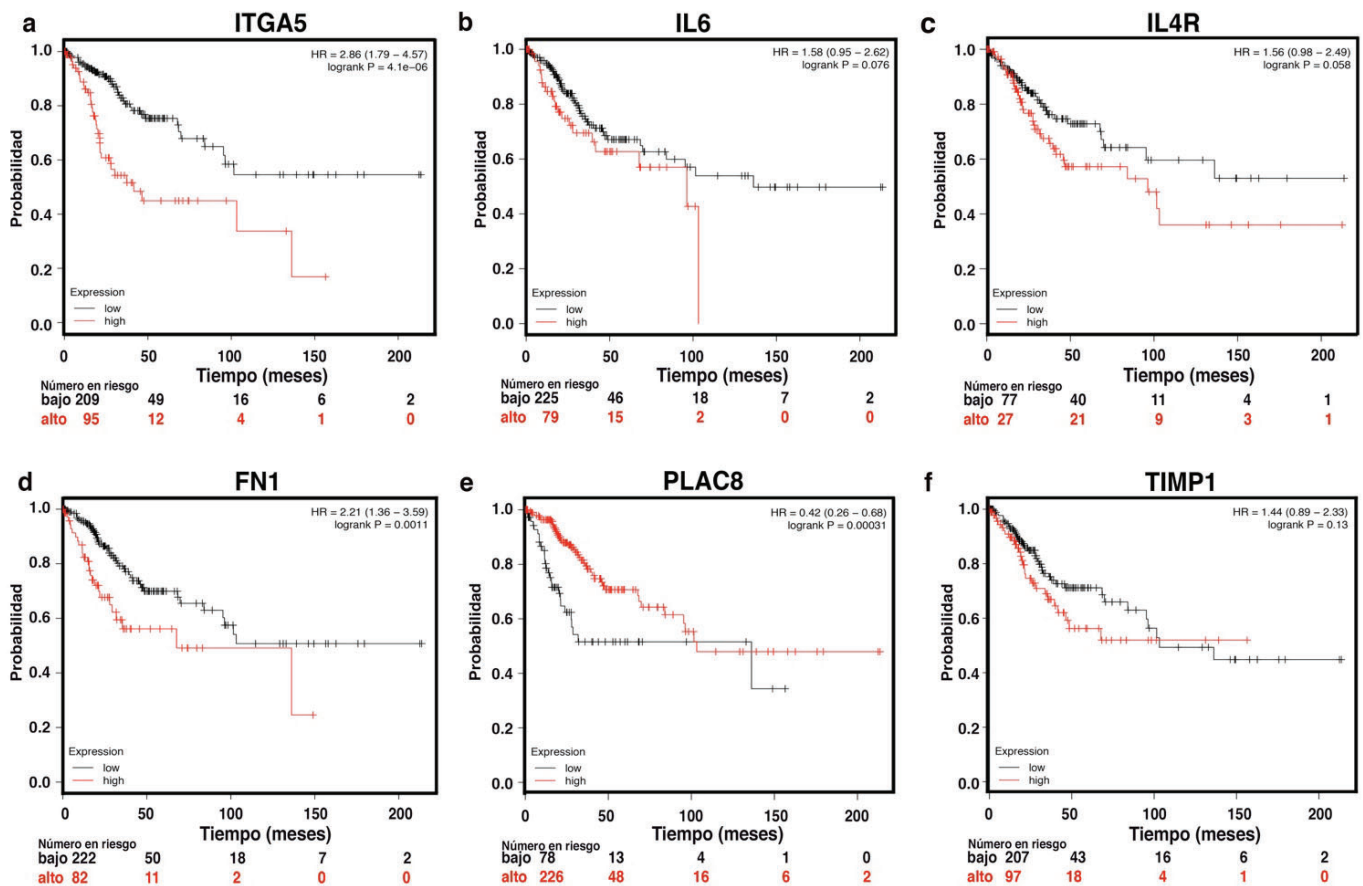


**Figura 18. Genes con expresión diferencial alterados por la presencia de ADSC exhiben importancia clínica en pacientes con cáncer cervical.** (a-f) Se muestran las curvas de Kaplan Meyer que comparan la supervivencia global del carcinoma cervical de células escamosas con la expresión baja ó alta de los genes alterados (ITGA5, IL6, IL4R, FN1, PLAC8, TIMP1). Los datos se obtuvieron de una base de datos pública: KM Plotter. Los valores "p" se muestran en cada uno de los gráficos.

### 9.3 Efecto de las ADSC en la proliferación de cáncer cervicouterino.

De acuerdo al análisis bioinformático, la expresión de genes implicados en la proliferación se alteraron durante el cocultivo de HeLa / ADSC (Figura 12b). Para evaluar el efecto de las ADSCs en la proliferación, estimamos el porcentaje de las células HeLa en las difentes fases del ciclo celular y analizamos la viabilidad de las células co-cultivadas con ADSC o estimuladas con medio condicionado. Los resultados mostraron que las células HeLa cocultivadas con ADSCs se comportan igual que las células HeLa sin ADSCs. Estos resultados muestran que el porcentaje de células en G0/G1, G2, S son muy similares entre ambas

condiciones (Figura 19a). Tampoco encontramos ninguna diferencia en el número de células HeLa con respecto a las células HeLa cocultivadas con ADSC en un ensayo de proliferación con MTS durante 124 horas (Figura 19b).

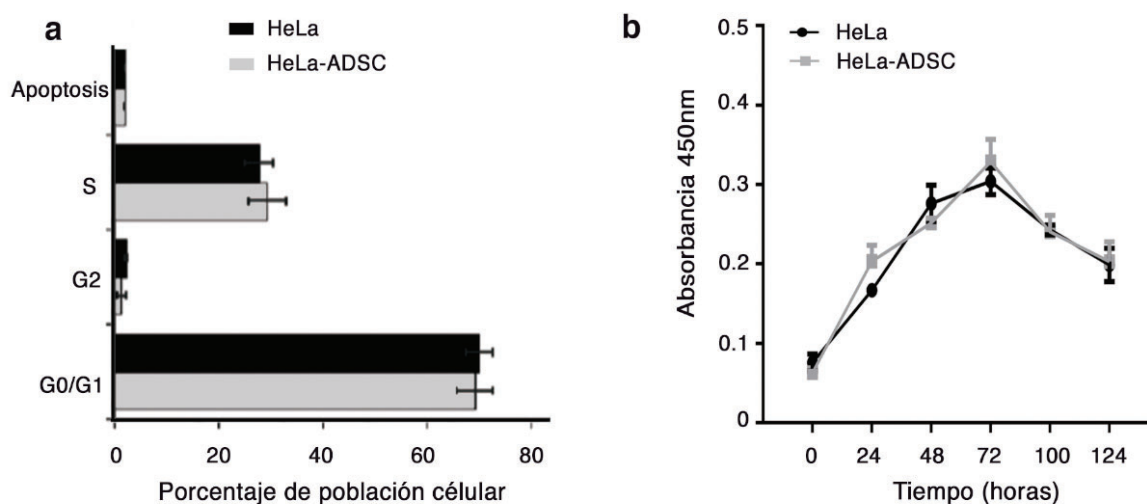


**Figura 19. Efecto de las ADSC en la proliferación de cáncer cervicouterino.** (a) Análisis del ciclo celular de células HeLa cocultivadas con ADSC en comparación con las células HeLa control. El gráfico no muestra cambios significativos en ninguna de las fases del ciclo celular. (b) Ensayo de proliferación a diferentes tiempos de HeLa control frente a células HeLa cocultivadas con ADSC. La gráficas muestran los resultados obtenidos de ensayos independientes (N = 3, las barras de error son la media  $\pm$  s.d., pero no se mostraron cambios significativos).

Además, se probó la capacidad de las células tumorales de proliferar en presencia de diferentes medios condicionados (MC). Los MC se obtuvieron del cultivo de células en medio DMEM libre de suero durante 24h como se describe detalladamente en la metodología. Los MCs que se usaron fueron: ADSC-MC, HeLa-MC ó Cocultivo-MC (Figura 20). Las células HeLa cultivadas con DMEM al 5% de FBS se usaron como control positivo (Figura 21).

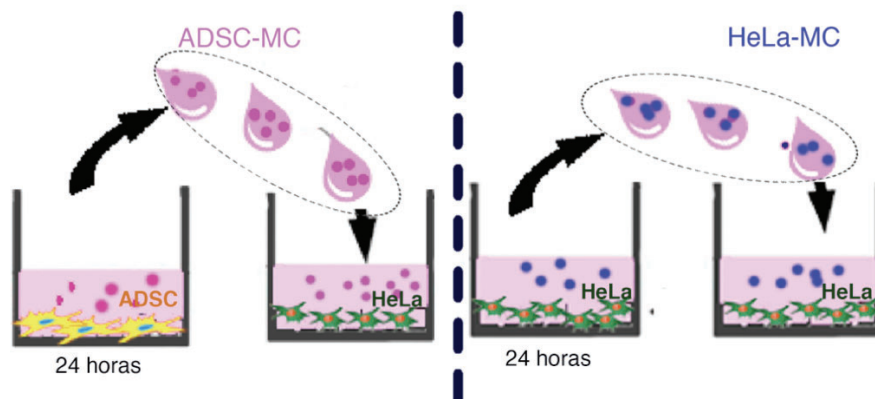


**Figura 20. Producción de medios condicionados.** La imagen muestra el método para obtener el medio condicionado de ADSC (ADSC-MC) o el medio condicionado de células HeLa (HeLa-MC). Las células ADSC o HeLa se cultivaron en DMEM libre de suero durante 24 horas y luego se empleó el medio condicionado para cultivar células de cáncer cervicouterino.

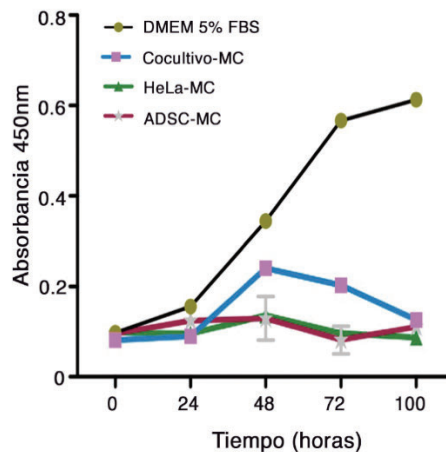


**Figura 21. Efecto de los diferentes MC en la proliferación de cáncer cervicouterino.** Ensayo de proliferación de células HeLa cultivadas con diferentes medios condicionados (MC) en diferentes momentos. ( $n = 3$ , las barras de error representan la media  $\pm$  s.d., pero no se mostraron cambios significativos).

Los resultados muestran que no hubo cambios significativos en la proliferación de las células HeLa tratadas con medio condicionado. En general, estos hallazgos demuestran que las ADSC no tienen influencia en la proliferación y muerte de las células tumorales (Figuras 19 y 21).

#### **9.4 Las ADSC promueven la migración e invasión del cáncer cervicouterino.**

De manera interesante, el análisis bioinformático predijo que el movimiento celular es uno de los procesos más alterados en células HeLa cultivadas en presencia de ADSC (Figura 12b). Para evaluar si las ADSC influyen en las capacidades de migración o invasión de las células de cáncer cervicouterino, se utilizaron transwells para analizar el comportamiento de las células HeLa, CaSki y SiHa cultivadas en presencia de diversos quimioatrayentes como las células ADSC, fibroblastos (NIH3T3), medio condicionado obtenido del cocultivo de HeLa / ADSCs (Cocultivo-MC) y medio condicionado de ADSC (ADSC-MC). Como se mencionó anteriormente, los medios condicionados fueron obtenidos en condiciones libres de suero. Como control positivo de migración, las células fueron estimuladas con DMEM suplementado con FBS al 10% y como control negativo se usó DMEM sin FBS.

Los resultados mostraron que las ADSC promueven un incremento drástico en la capacidad de migración de las células HeLa, CaSki y SiHa en comparación con los demás quimioatrayentes (Figura 22a-c). Sorprendentemente, las ADSC actuaron como un poderoso quimioatrayente, ya que las células HeLa y SiHa incrementaron 807% y 1758% su capacidad de migración en comparación con las células estimuladas con 10% de FBS (Figura 22a,c). Curiosamente, las células HeLa exhiben muy poca capacidad de migración cuando se estimulan con fibroblastos (NIH3T3) (Figura 22a). Estos resultados destacan la importancia biológica de las ADSC para proveer a las células cancerosas con mejores capacidades de migración. Para probar si los factores secretados por las ADSC influyen en la migración de las células CC, probamos la capacidad de migración de las células CC estimuladas con medio condicionado de ADSC. Nuestros resultados mostraron que el medio condicionado de ADSC aumenta la migración de células HeLa (300%), CaSki (245%) y SiHa (1885%) en comparación con las células estimuladas con FBS al 10%. En conjunto estos resultados indican que las líneas celulares de cáncer cervicouterino expuestas a ADSC o al secretoma de ADSC exhiben un incremento dramático en la capacidad de migración de líneas celulares de CC.

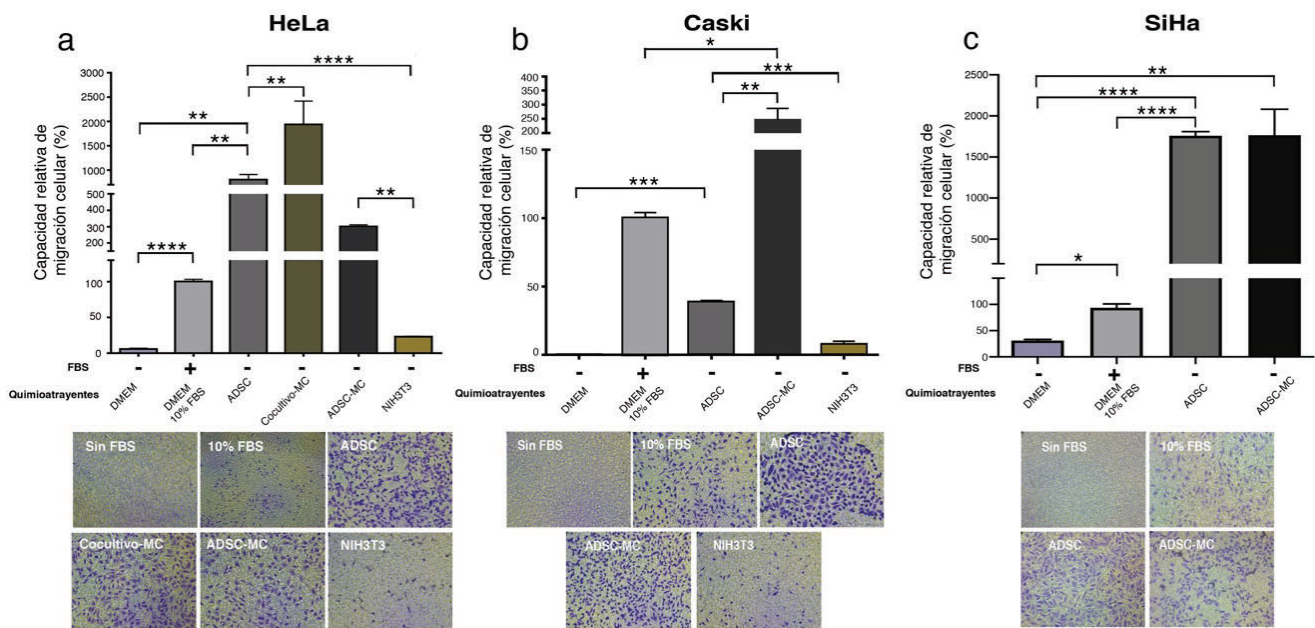


**Figura 22. Las ADSC influyen en la migración de las células de cáncer cervical.** (a-c) El gráfico muestra la capacidad de migración de las células HeLa (a), CaSki (b) y SiHa (c) cultivadas sin suero y expuestas a diferentes quimioatrayentes, incluidos ADSC, medio condicionado de cocultivo (Coculture-MC), medio condicionado de ADSC (ADSC-MC) y las células NIH3T3. Como control, las células CC también se cultivaron con DMEM suplementado con FBS al 10% o sin FBS. El gráfico muestra el porcentaje relativo de la capacidad de migración de las células HeLa, CaSki y SiHa después de 12 h. El gráfico representa tres réplicas biológicas, las barras de error representan la media  $\pm$  s.d y \*  $p < 0.05$ . Las imágenes muestran una imagen representativa de las células CC migratorias en cada condición.

Debido a que la invasión permite que las células tumorales se propaguen hacia sitios distantes y colonicen otros tejidos, determinamos la influencia de las ADSC en la invasión de CC. Los ensayos de invasión se realizaron utilizando cámaras de Boyden previamente recubiertas con Matrigel, como se muestra en la Figura 23a-c. Los resultados muestran que la capacidad de invasión de las células HeLa, CaSki y SiHa aumentó drásticamente 767%, 1080% y 549% respectivamente cuando fueron quimioatraídas por ADSC en contraste con las células estimuladas con 10% de FBS. Consistentemente, el medio condicionado de ADSC también aumentó la invasión de todas las células de CC (Figura 23a-c). En conjunto, todos



estos datos indican que las ADSC inducen fuertes cambios en la migración e invasión celular, lo que confiere ventajas malignas a las células de CC.

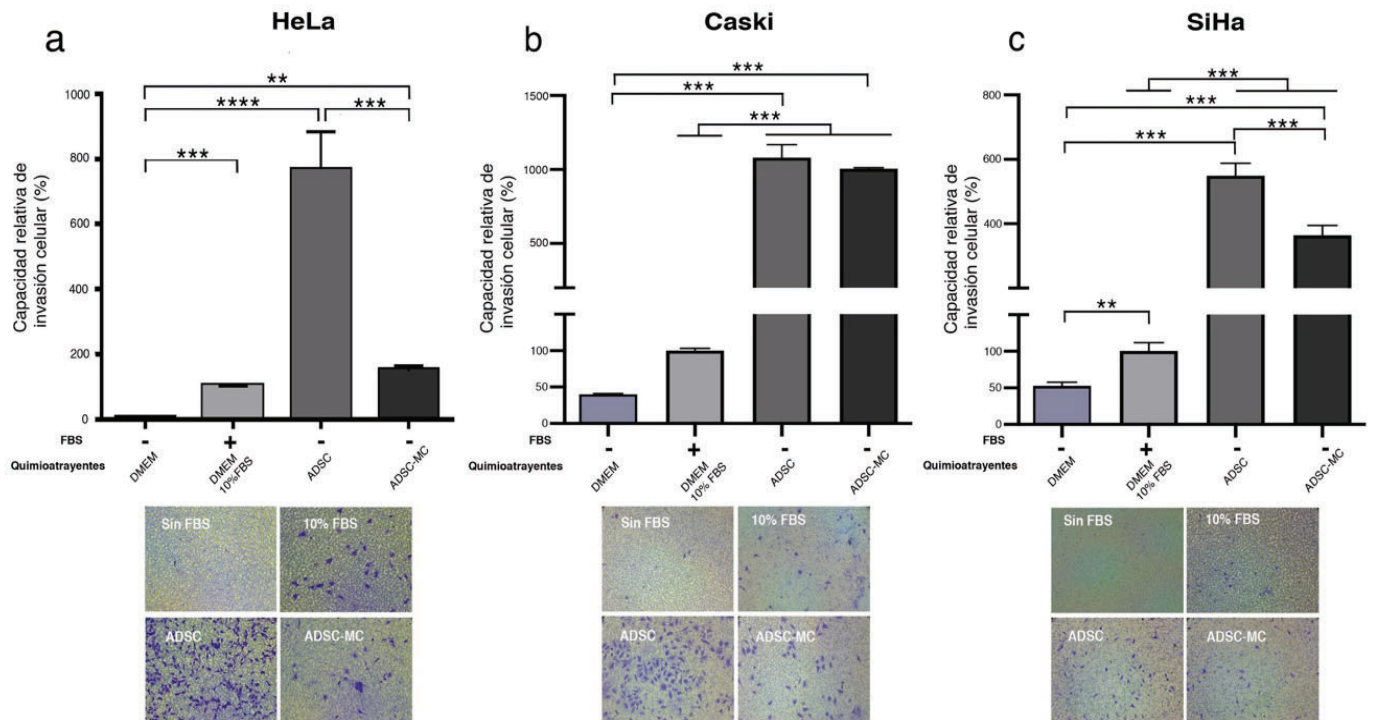


**Figura 23. Las ADSC influyen en la invasión de las células de cáncer cervical.** (a-c) Las figuras muestran el porcentaje relativo de células invasoras HeLa, CaSki y SiHa después de 12 horas de exposición a los quimioatrayentes ADSC ó ADSC-MC. Como control, las células CC también se cultivaron con DMEM suplementado con FBS al 10% o sin FBS. Las figuras muestran una imagen representativa de las células invasoras en cada condición. El gráfico representa el resultado de tres réplicas biológicas, las barras de error representan la media  $\pm$  s.d. y \*  $p < 0.05$ .

Para identificar que transcritos podrían estar asociados a los fuertes cambios de migración e invasión que sufrieron las células cancerosas por la presencia de ADSC, se realizó un análisis de las redes generadas por IPA. Los resultados mostraron a transcritos como: VCAN, SPARC, CXCL12, IL6, MMP14, IL-1 $\beta$ , IL3, IL4R, ICAM y NF-kB (Figura 24a-c).

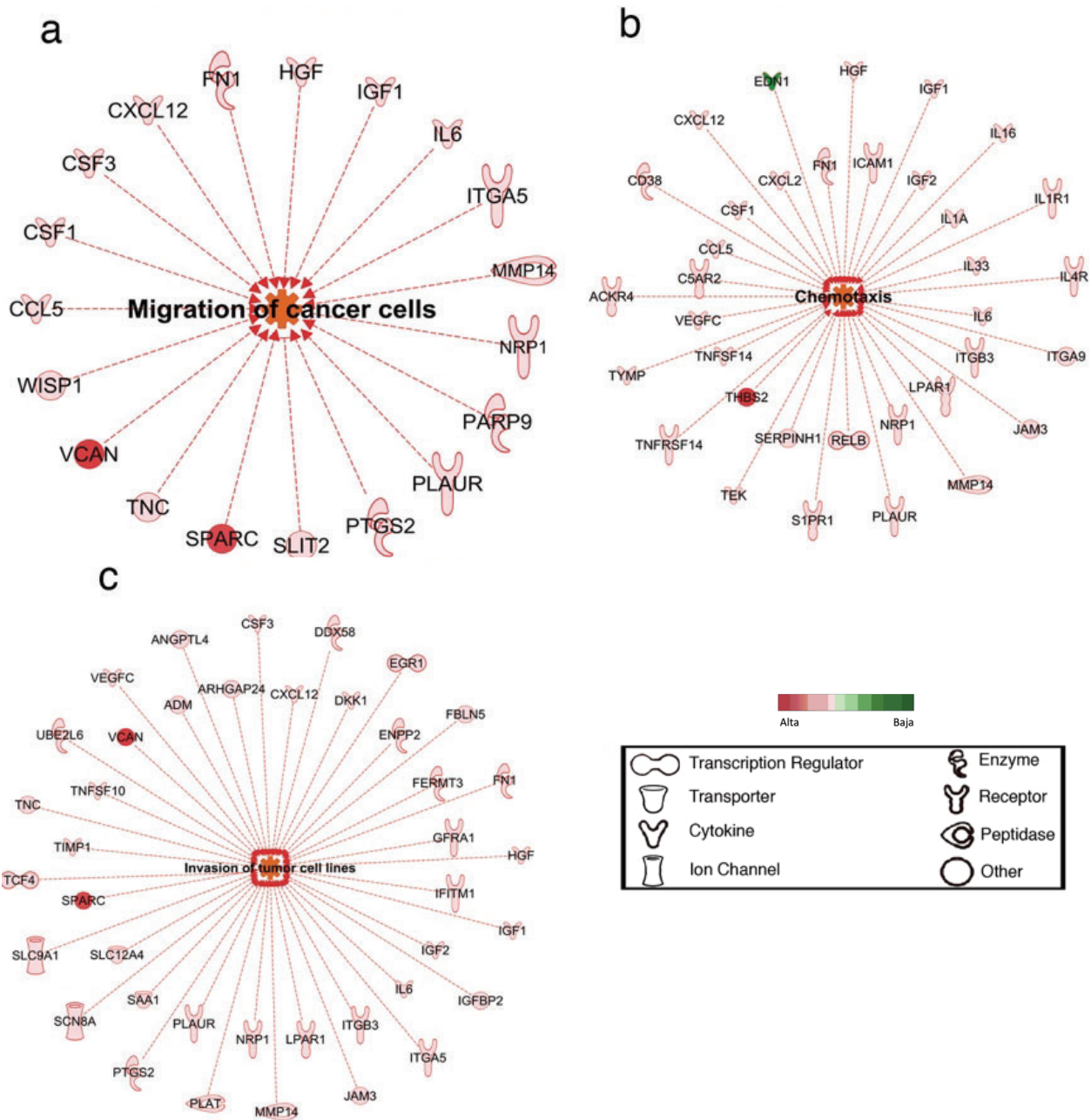


**Figura 24. Redes de transcritos afectadas en el movimiento celular durante el cocultivo HeLa-ADSC.** Análisis de IPA que muestra los principales transcritos afectados en células de cáncer cervicouterino cultivadas con ADSC que están involucradas en (a) la migración, (b) quimiotaxis (c) e invasión. Las redes muestran genes con expresión diferencial regulados por cada vía de señalización. El color rojo indica la sobreexpresión de los transcritos y el color verde su inhibición.



Con la finalidad de confirmar la influencia de las ADSC en la capacidad de migración o invasión de las líneas celulares de CC, realizamos experimentos in vivo utilizando embriones de pez cebra (*Danio rerio*).

Los ensayos de xenotrasplante que se generan mediante la implantación de células tumorales humanas en un huésped animal, permiten el estudio de los mecanismos de señalización involucrados en el inicio y la progresión del cáncer. Nosotros utilizamos el modelo de pez cebra porque este modelo nos permite tener tumores a corto plazo, además de que la transparencia de sus embriones permite realizar seguimiento a la migración e invasión de las células inoculadas<sup>61</sup>.

Los experimentos en embriones de pez cebra se realizaron con la línea celular SiHa, debido a que presentó una mayor capacidad tumorigénica que HeLa (datos no mostrados). Las células SiHa se transfectaron con un plásmido que expresaba la proteína verde fluorescente (GFP) (Figura 25) ó se tiñeron con el colorante PKH26-GL (Figura 26). Un total de 300 células SiHa que expresaban GFP ó células SiHa marcadas previamente con el colorante PKH26-GL se inyectaron en presencia o ausencia de ADSC en el vitelo del embrión de pez cebra a las 48 horas después de la fertilización. Posteriormente, se evaluó la migración y la invasión 12hpi. Los embriones inyectados solo con células SiHa mostraron pocas células esporádicas fluorescentes en todo el embrión; en contraste, las células SiHa inoculadas con ADSC exhibieron una mayor migración que se observó en todo el cuerpo, ojos y cola del embrión. En algunos casos, observamos invasión celular y posterior metástasis a la cola. Las células SiHa teñidas con PKH26 ante la presencia de ADSC también mostraron el mismo comportamiento. Estos datos sugieren que la presencia de ADSC promueve la capacidad de migración e invasión de células de CC (Figuras 25 y 26).

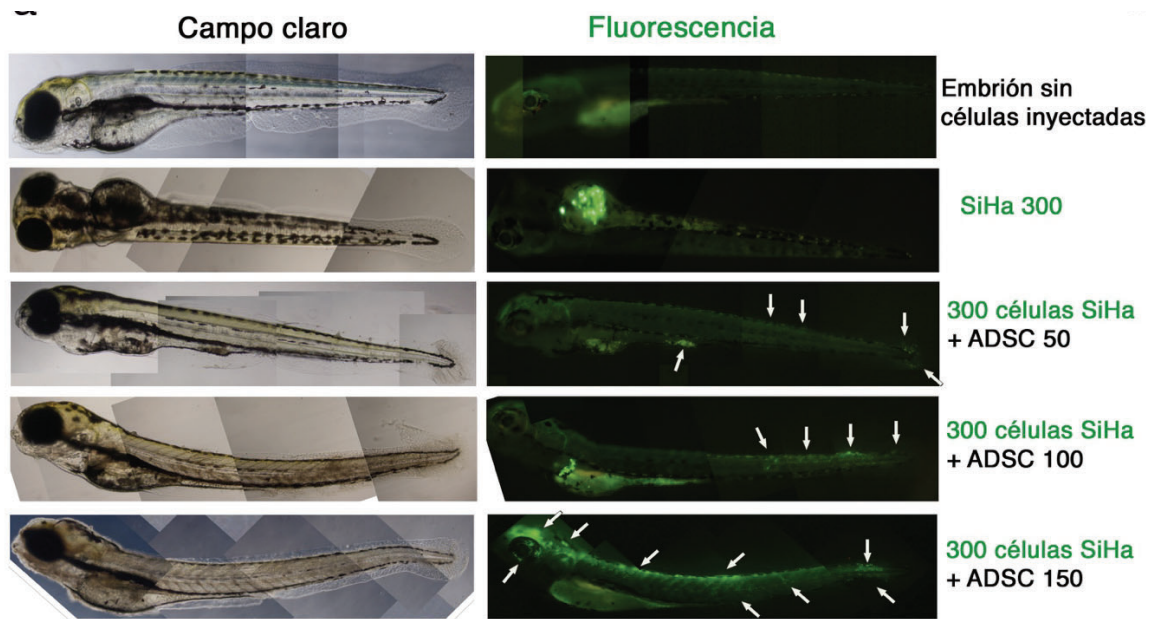


**Figura 25. Las ADSC aumentan la migración e invasión de células de cáncer cervicouterino en un modelo *in vivo*.** Las imágenes muestran que la capacidad de migración de las células SiHa aumenta proporcionalmente con respecto a la cantidad de ADSC inoculadas en embriones de pez cebra después de 12 h. Las células SiHa se muestran en verde debido a que fueron transfectadas con un plásmido que alberga un gen GFP. Las imágenes muestran un aumento gradual en la migración e invasión de las células cancerosas desde el vitelo hasta la cola de los embriones debido a la presencia de ADSC. Las flechas blancas muestran las áreas de migración en el embrión.

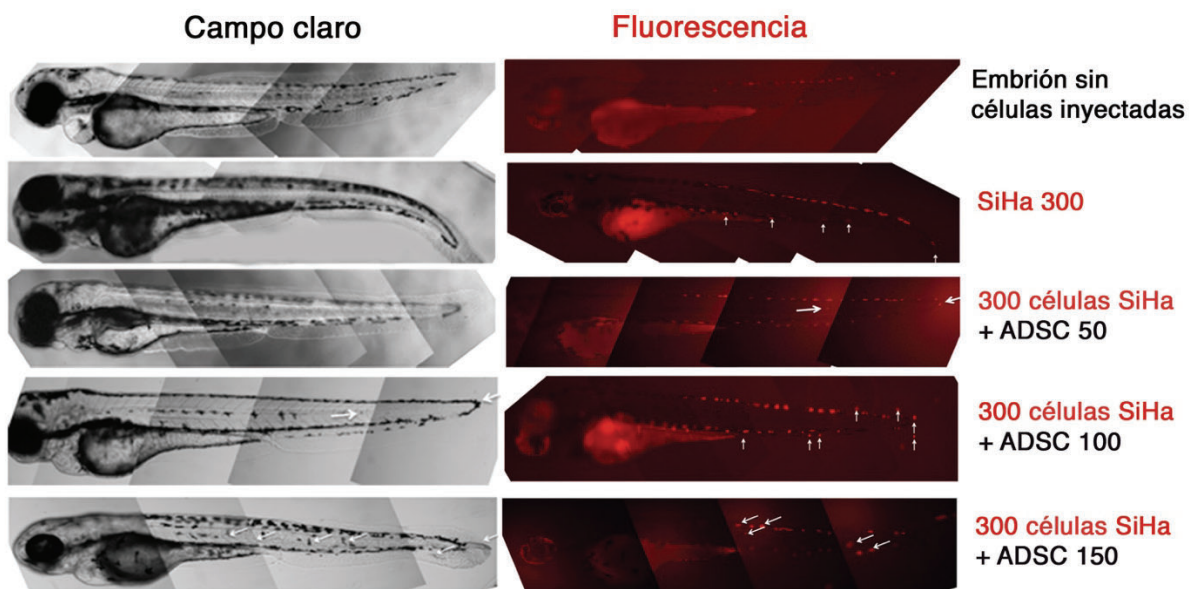


**Figura 26. Las ADSC aumentan la migración e invasión de células de cáncer cervicouterino en un modelo *in vivo*.** (a) Las imágenes muestran que la capacidad de migración de las células SiHa aumenta proporcionalmente con respecto a la cantidad de ADSC inoculadas en embriones de pez cebra después de 12 h. Las células SiHa se muestran en rojo debido a la tinción con el colorante PKH26. Las imágenes muestran un aumento gradual en la migración e invasión de las células

cancerosas desde el vitelo hasta la cola de los embriones debido a la presencia de ADSC. Las flechas blancas muestran las áreas de migración en el embrión.

### 9.5 Las ADSC promueven el crecimiento tumoral e incrementan la población de células troncales de cáncer cervicouterino.

Para evaluar si las ADSCs podrían contribuir a la progresión de CC; realizamos coinyecciones de 300 células SiHa con diferentes diluciones de células ADSC (50, 100 o 150) y se monitoreó el crecimiento tumoral en el modelo de pez cebra durante 5 días. El número de células inoculadas no afectó la viabilidad del embrión durante un ensayo de 7 días (datos no mostrados). La formación de tumores se controló en embriones coinyectados con los siguientes controles: ADSC + HaCaT, SiHa + HaCaT y SiHa + NIH3T3 (Tabla 2). Como se muestra en la Tabla 2, la coinyección de células SiHa con cantidades crecientes de ADSC provocó un aumento en el número de embriones con tumor; notablemente, este aumento fue dependiente del número de ADSC inyectadas. Los resultados muestran que las células SiHa generaron tumores en 35% de embriones, mientras que SiHa + ADSC desarrollaron tumores hasta en el 69% de embriones. Como se esperaba, las ADSC solas no desarrollaron ningún tumor, incluso cuando estas células se inocularon en cantidades más altas. La coinyección de ADSC + HaCaT solo desarrolló tumores en embriones al 10%, mientras que SiHa + HaCaT o SiHa + NIH3T3 exhibieron el mismo potencial tumorigénico que las células SiHa inyectadas solas.

Tratamiento	Células	% Tumor
SiHa	300	35.29
SiHa+ADSC	300+50	<b>47.83*</b>
SiHa+ADSC	300+100	<b>61.90*</b>
SiHa+ADSC	300+150	<b>68.97*</b>
ADSC	300	0.00
HaCaT+ADSC	300+150	10.00
SiHa+HaCaT	300+150	44.44
SiHa+NIH3T3	300+150	36.84

**Tabla 2. La ADSC promueven el crecimiento tumoral de células SiHa.** La tabla muestra el número de células inoculadas en embriones de pez cebra y la proporción de tumores formados en cada condición. SiHa, SiHa + ADSC o células de control: ADSC, HaCaT + ADSC, SiHa + HaCaT y SiHa + NIH3T3 se inocularon en embriones de pez cebra, y los tumores se monitorearon todos los días durante 5 días.

Además, se calculó la frecuencia de células troncales cancerosas (CTCs) en cada condición a través de un análisis de ELDA. La Figura 27 muestra un incremento en la proporción de CTCs observada en tumores formados por SiHa-ADSC con 1 CTC por cada 384 células; estos tumores tienen aproximadamente un 55.6% más de CTCs que en los tumores derivados de SiHa solas. Como se esperaba, los tumores derivados de HaCaT + ADSC, SiHa + HaCaT o SiHa + NIH3T3 exhiben un menor número de CTC que en los tumores derivados de SiHa solas.

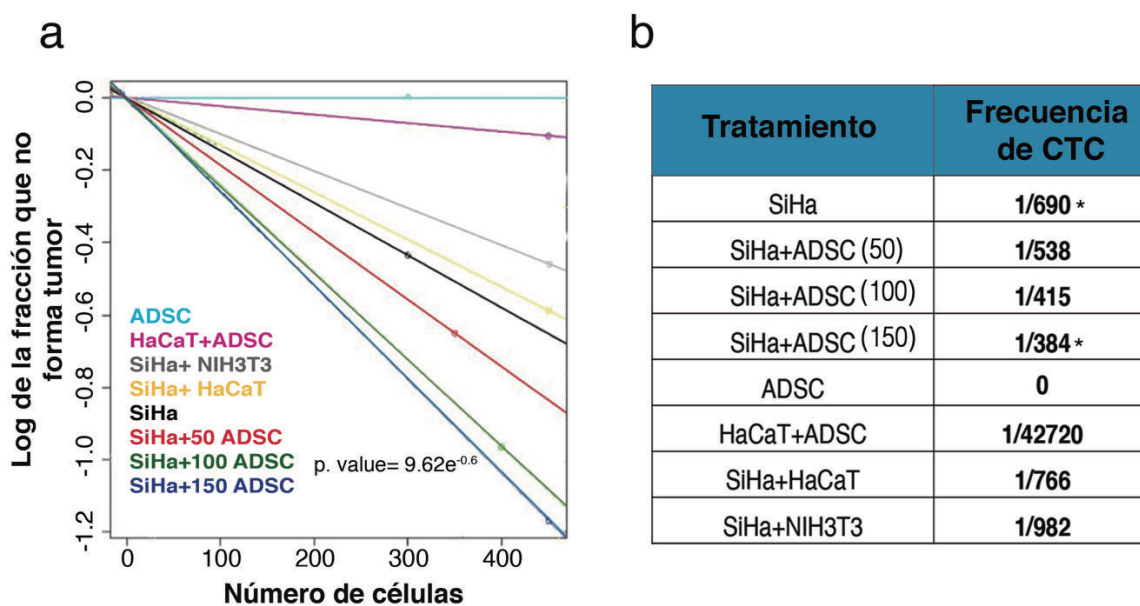


**Figura 27. Las ADSCs aumentan la población de CTCs de células SiHa en un modelo in vivo.** (a) El gráfico muestra la frecuencia de CTCs en cada condición ( SiHa, SiHa + ADSC o células de control: ADSC, HaCaT + ADSC, SiHa + HaCaT y SiHa + NIH3T3 ) que representa el número de células inyectadas con respecto a la fracción logarítmica de animales sin tumor. Cada experimento fue repetido al menos tres veces. (b) La tabla muestra la frecuencia de CSC calculada con base en el software ELDA.

Curiosamente, las células SiHa coinyectadas con ADSC formaron nódulos tumorales más grandes en comparación con los tumores generados solo por células SiHa (Figura 28).

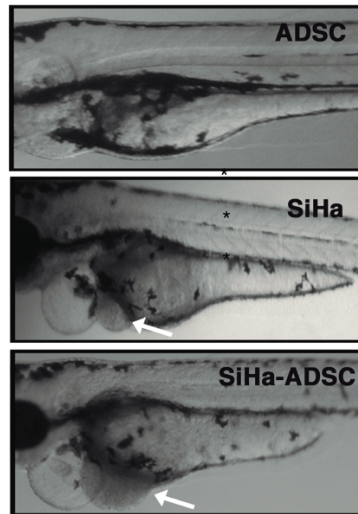


**Figura 28. Las ADSC mejoran la capacidad tumorigenica de células SiHa.** Las imágenes muestran tumores desarrollados durante 5 días en embriones de pez cebra inoculados con células ADSC, SiHa o SiHa + ADSC. Cada experimento fue repetido al menos tres veces.

La relevancia de las ADSC en la tumorigénesis está respaldada por otra línea celular CC, en la que se observó que las células CaSki por sí mismas no pueden formar tumores, mientras que las células inoculadas con ADSC lograron generar el 36% de embriones con tumor (Figura 29a). Además, observamos que el número de CTCs aumentó en las células CaSki inoculadas con mayores cantidades de ADSC (Figura 29b-c). Como se muestra en la figura 4h, las células CaSki inoculadas con mayores cantidades de ADSC tenían 1 CTC por cada 996, mientras que las células inyectadas con una menor cantidad de ADSC solo tenían 1 CTC por 2328 células. Estos resultados indican que la presencia de ADSC mejora el potencial tumorigénico de las células CC y aumenta la frecuencia de las CTCs.



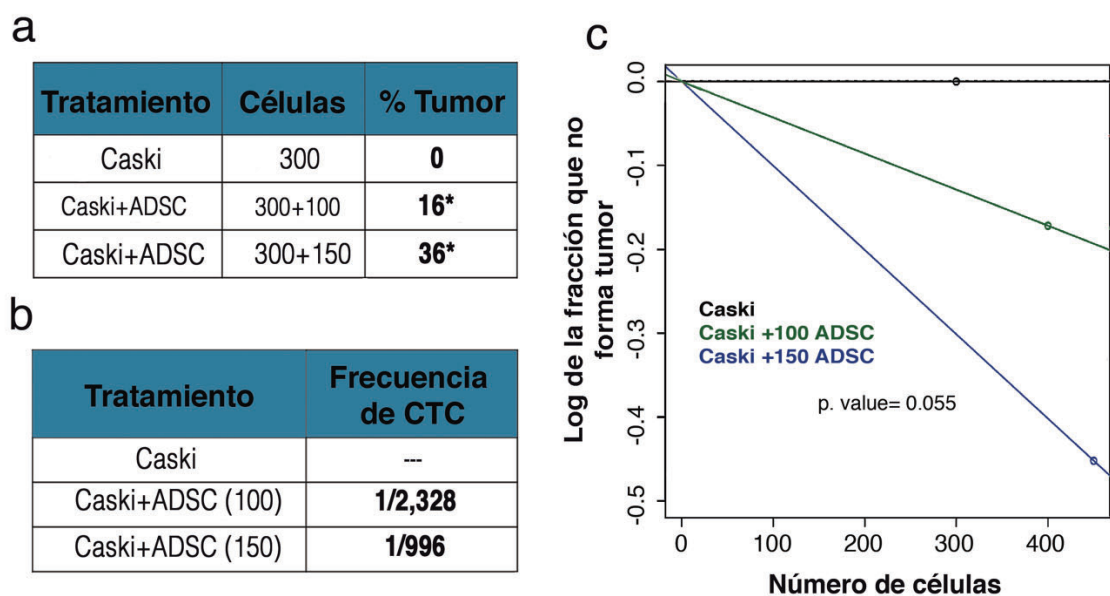


**Figura 29. Las ADSC afectan la capacidad tumorigénica y la frecuencia de CTC en células Caski.** (a) La tabla muestra el número de células inoculadas en embriones de pez cebra y la proporción de tumores formados en embriones inyectados con células CaSki o células CaSki + ADSC. Los tumores fueron monitoreados todos los días durante 5 días. (b) La tabla muestra la frecuencia de CSC en tumores formados a partir de células Caski ó Caski + ADSC calculada en función del software ELDA. (c) El gráfico representa la frecuencia de CSC en cada condición que representa el número de células Caski inyectadas con respecto a la fracción logarítmica de animales sin tumor.

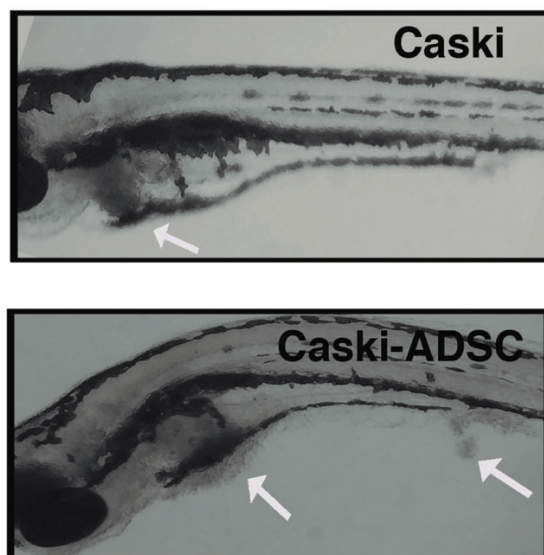


**Figura 30. Las ADSC mejoran la capacidad tumorigénica de células Caski.** Las imágenes muestran tumores desarrollados durante 5 días en embriones de pez cebra inoculados con células CaSki o CaSki + ADSC.

## 9.6 ADSC induce la activación de la vía NF-kappa B en células de cáncer cervicouterino.

Curiosamente, el análisis de datos con el software IPA sugiere que la mayoría de los genes con expresión diferencial durante el cocultivo de HeLa/ADSC culminan en la activación de la vía de señalización NF-kappa B. Además, estos datos fueron respaldados por un análisis de enriquecimiento de conjunto de genes (GSEA) que confirmó que la señalización de NF-kappa B se enriqueció en células HeLa cultivadas en presencia de ADSC con un p-value = 0.049, FDR = 0.00 y NES = 1.61 (Figura 31 b-c).

La figura 31a muestra un mapa de calor que exhibe el top 50 genes expresados diferencialmente. Entre estos genes, encontramos a RelB, un jugador en la señalización no canónica de NF-kB, que se expresa altamente en HeLa/ADSC. El GSEA mostró 23 RNAs con expresión diferencial involucrados en la vía NF-kappa B, que incluye CXCL2, RELB, BCL3, FOS, BCL6, IL1A e IL6 (Figura 31 c-d).

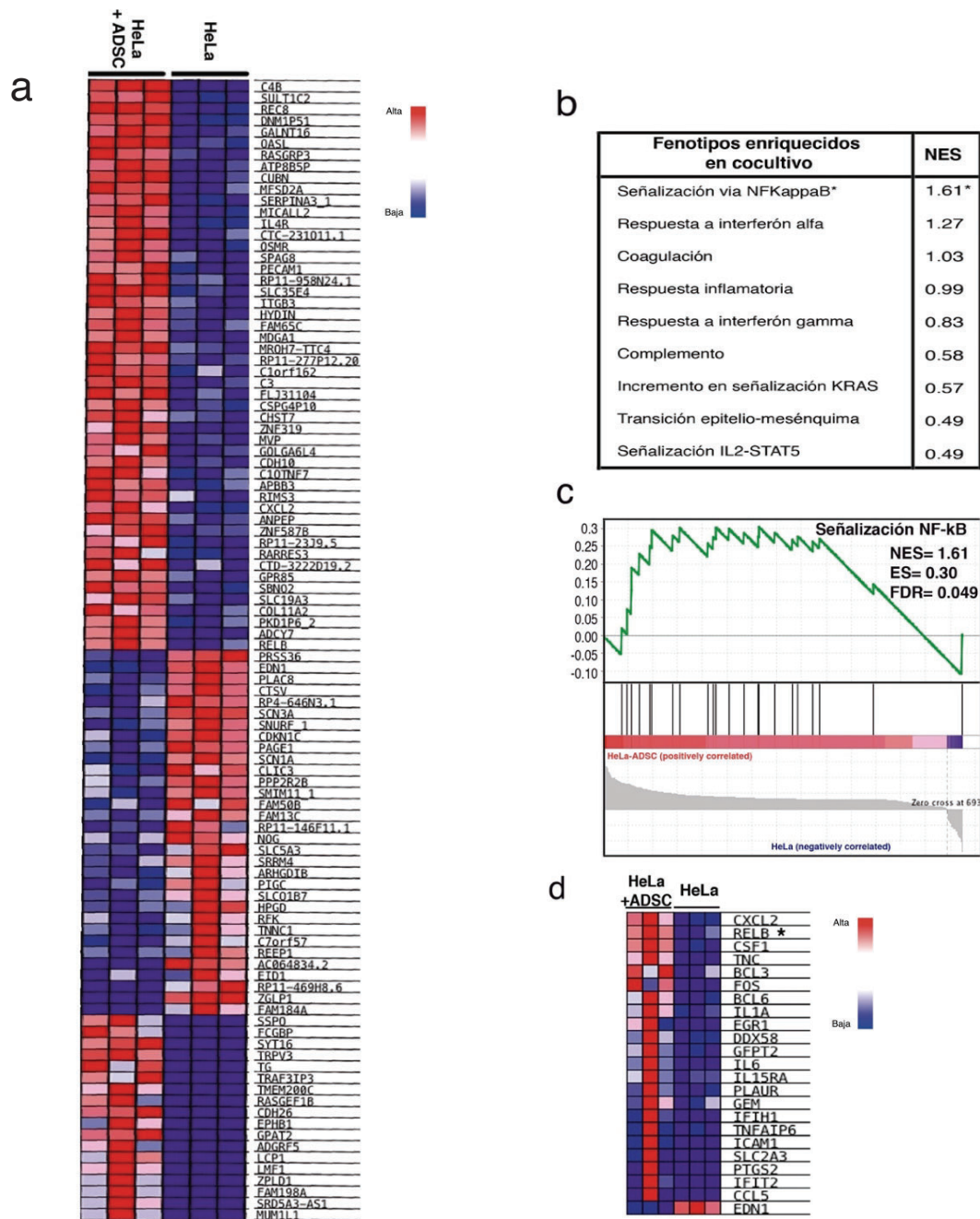


**Figura 31. La señalización de NF-Kappa B es activada durante el cocultivo de HeLa-ADSC.** (a) El mapa de calor muestra los principales genes expresados diferencialmente en la línea celular HeLa cultivada en presencia o ausencia de ADSC. Los valores de expresión se representan en colores, donde el intervalo de colores (rojo, rosa, azul claro, azul oscuro) representa el rango de valores de expresión (muy alto, alto, moderado, bajo, más bajo). (b) La tabla muestra los fenotipos principales enriquecidos en células HeLa debido a la presencia de ADSC obtenidas de un análisis de enriquecimiento de genes (GSEA). Para cada uno de los fenotipos, se indica el puntaje de enriquecimiento normalizado (NES). (c) Análisis de GSEA que muestra un enriquecimiento significativo (NES = 1.61 y un FDR = 0.049) de la vía de señalización NF-kappa B en células de cáncer cervical debido a la presencia de ADSC. (d) El mapa de calor muestra el subconjunto de genes enriquecidos involucrados en la vía de NF-kappa B, donde la mayoría de los genes alterados están involucrados en la señalización no canónica de NF-Kappa B, como RELB.



Para validar y determinar qué moléculas de NF-kappa B están involucradas en la regulación de CC mediada por ADSC, realizamos un análisis de inmunofluorescencia para determinar la expresión y localización parcial de las proteínas clave de NF-kappa B (Figura 32).

Como se muestra en la Figura 32a-b, los análisis de inmunofluorescencia mostraron que el medio condicionado de ADSC indujo un aumento en la expresión de RelB, así como su translocación nuclear en las células HeLa. Además, observamos un ligero aumento en la fosforilación de p52 en células HeLa cultivadas con el medio condicionado de ADSC. Curiosamente, los niveles de p65, un jugador canónico de NF-kappa B, también aumentaron, lo que implica una diafonía entre la señalización canónica y no canónica de NF-kappa B (Figura 32 c-f). De hecho, evidencia acumulada sugiere que RelB puede regular la expresión de subunidades de la vía canónica NF-kappa B.

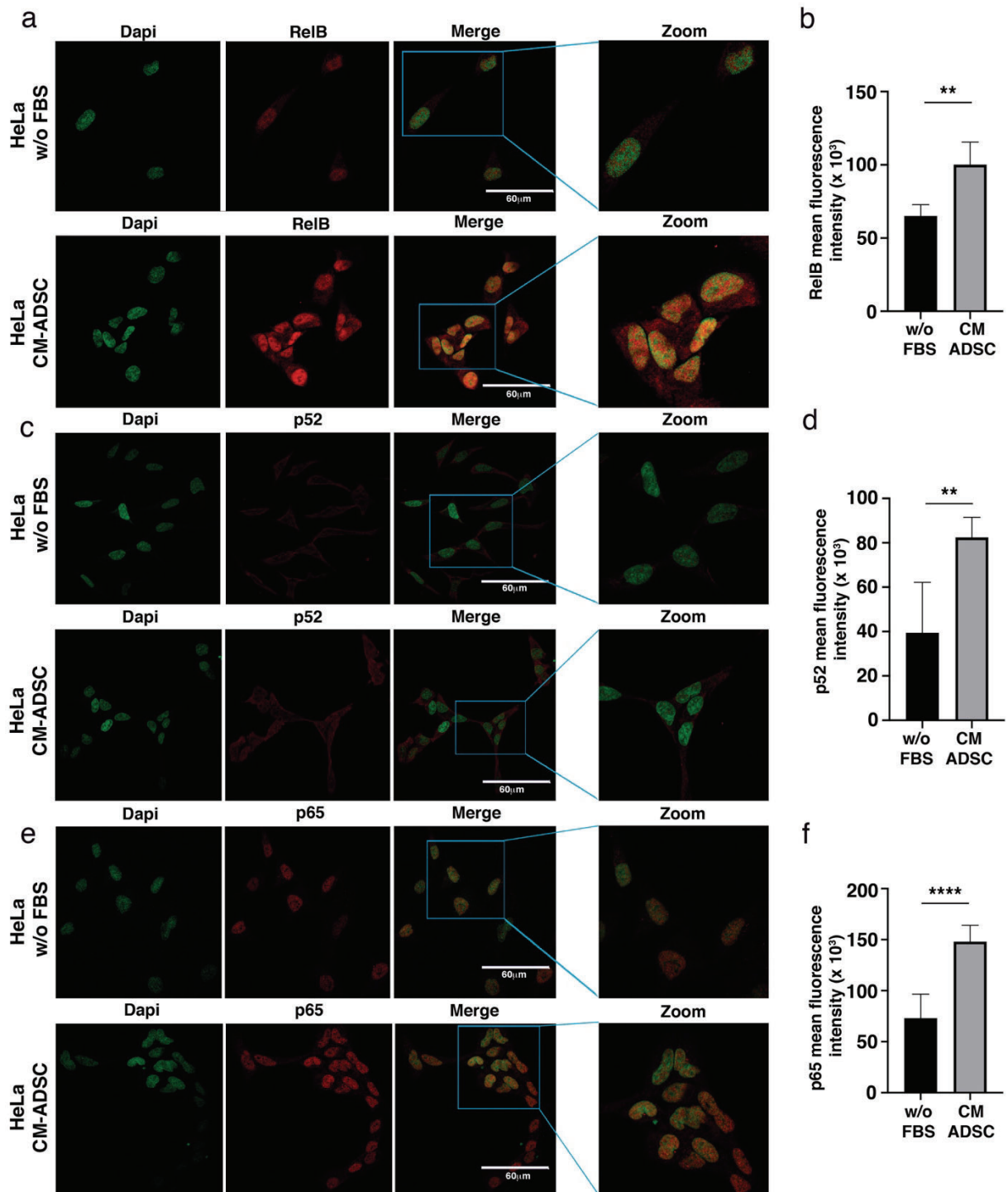


**Figura 32. Las ADSC inducen la expresión de los factores de transcripción de NF-kappa B en células de cáncer cervicouterino.** (a, c, e) Las fotografías muestran la expresión de factores de transcripción de la familia NF-Kappa B (RelB, p52 y p65) obtenidas por inmunofluorescencia de células HeLa cultivadas con medio DMEM sin suero o ADSC-CM (sin suero) durante 24 horas. Las imágenes fueron tomadas en un microscopio confocal. La barra de escala equivale a 60  $\mu$ m. Los núcleos celulares se contrastaron con DAPI. Cada experimento fue repetido al menos tres veces. Para

cuantificar los niveles de expresión de RelB (b), p52 (d) y p65 (f), la intensidad de fluorescencia fue cuantificada usando ImageJ. Las gráficas representan tres réplicas biológicas, las barras de error representan la media  $\pm$  s.d. y \*\* $p < 0.01$  and \*\*\* $p < 0.001$ .

Para verificar la participación de las ADSC en la regulación de los factores de transcripción de NF-kappa B no canónicos, también analizamos la expresión de p52 y RelB en las células SiHa o CaSki cocultivadas con medio condicionado de ADSC (Figura 33 y 34). Observamos que el medio condicionado de ADSC indujo un notable incremento en la expresión de RelB (Figura 33a-b) y p52 (Figura 33b-c) en las células SiHa. También observamos que algunas células CaSki exhiben un incremento en la expresión de RelB cuando se cultivan con medio condicionado de ADSC (Figura 34a-b). Apoyando resultados anteriores, también demostramos que el medio condicionado de ADSC induce un incremento en la fosforilación de p52 en las células CaSki (Figura 34b-c). En conjunto, estos resultados sugieren que las ADSC podrían inducir la activación de la vía B NF-kappa B no canónica.

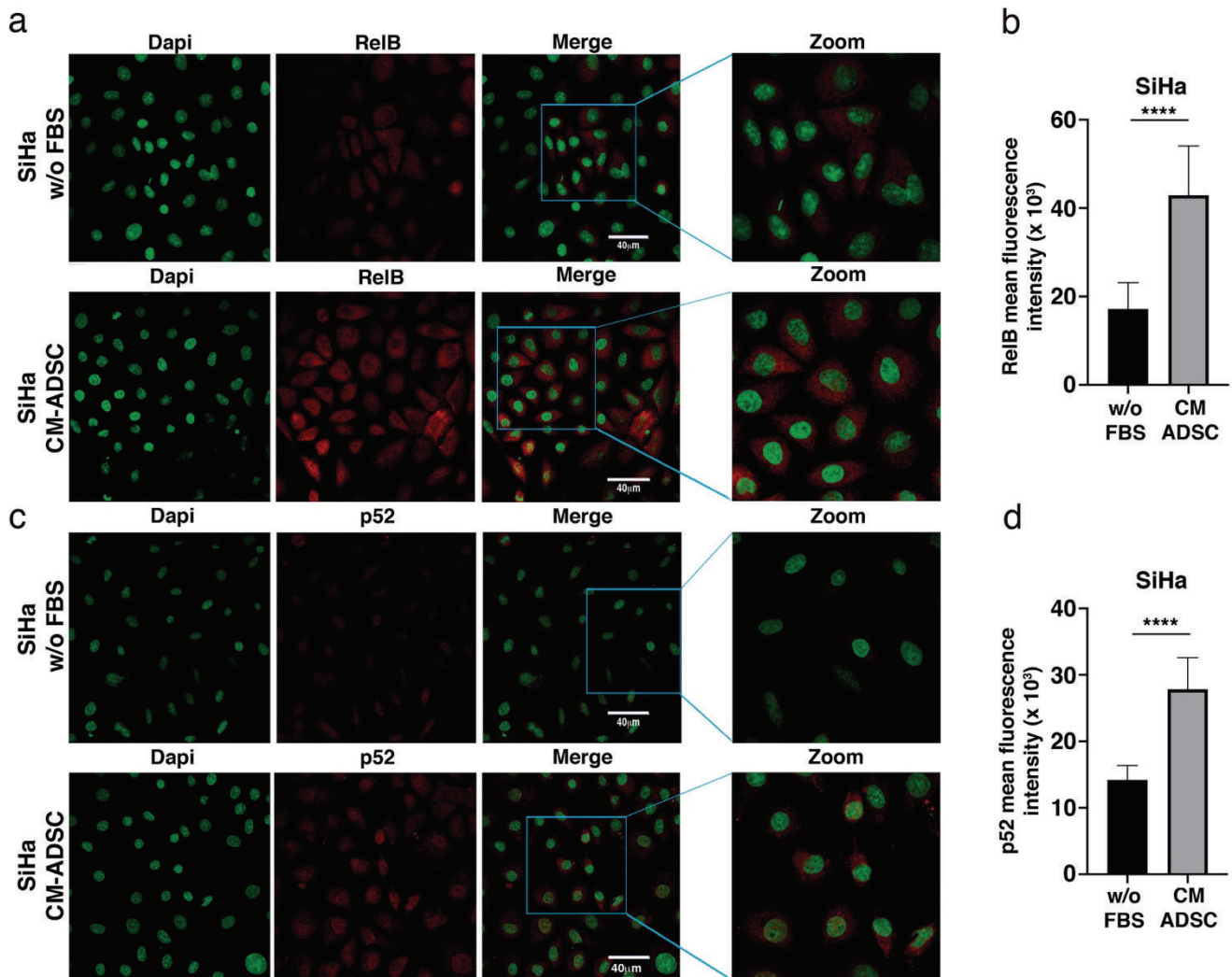


**Figura 33. ADSC induce la activación de la vía NF-kappa B en células SiHa.** (a,c) Las fotografías muestran la expresión de RelB y p52 obtenidas por inmunofluorescencia de células SiHa cultivadas con DMEM libre de suero o ADSC-CM (libre de suero) durante 24 horas. Las imágenes fueron tomadas bajo un microscopio confocal. La barra de escala equivale a 40  $\mu$ m. Los núcleos celulares se contrastaron con DAPI. Para cuantificar los niveles de expresión de RelB (b) y p52 (d), la intensidad de fluorescencia fue cuantificada usando ImageJ. Cada experimento fue repetido al menos tres veces, las barras de error representan la media  $\pm$  s.d. y \*\*\*\*  $p < 0.0001$ .

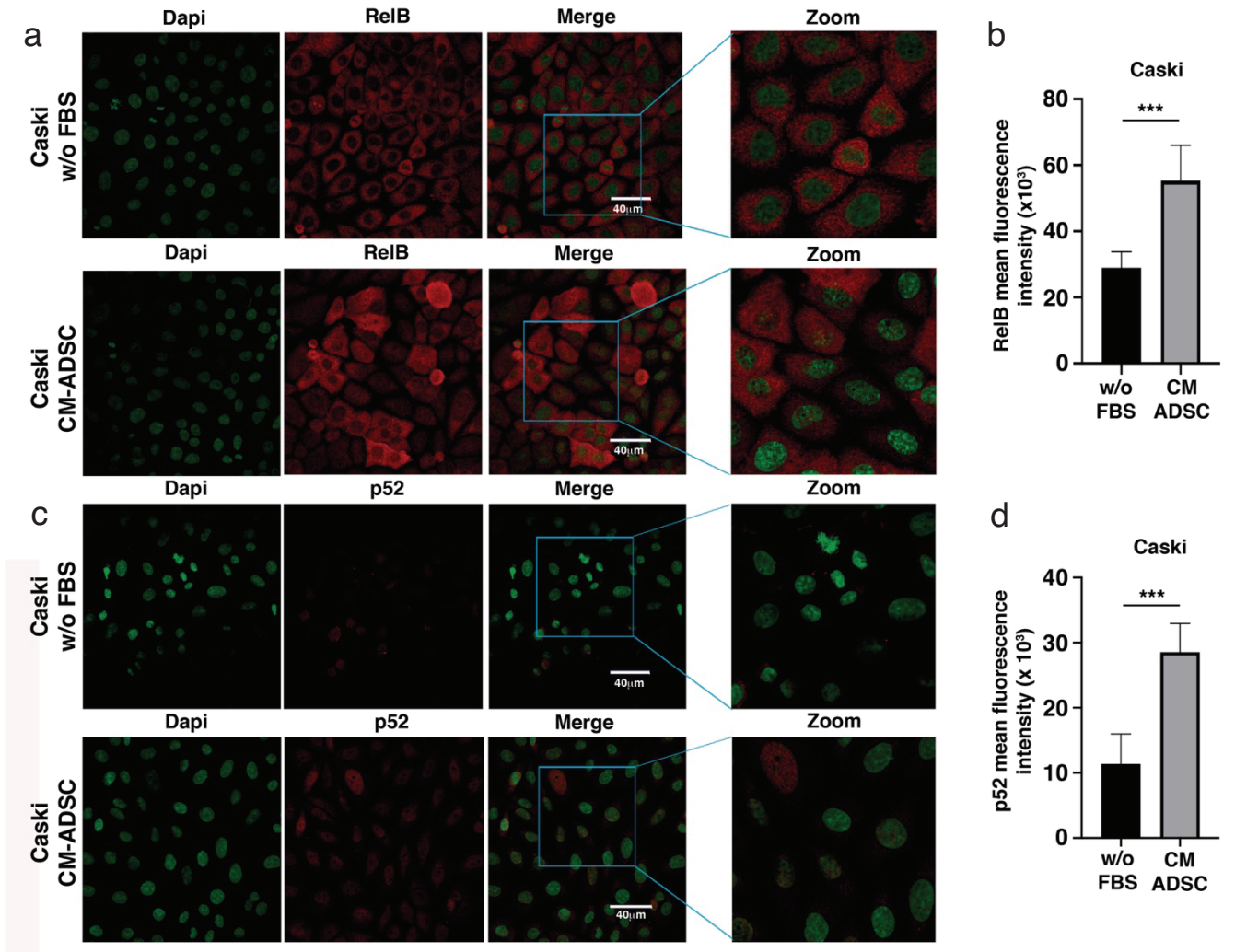


**Figura 34. ADSC induce la activación de la vía NF-kappa B en células CaSki.** (a,c) Las fotografías muestran la expresión de RelB y p52 obtenidas por inmunofluorescencia de células CaSki cultivadas con DMEM libre de suero o ADSC-CM (libre de suero) durante 24 horas. Las imágenes fueron tomadas bajo un microscopio confocal. La barra de escala equivale a 40  $\mu$ m. Los núcleos celulares se contrastaron con DAPI. Para cuantificar los niveles de expresión de RelB (b) y p52 (d), la intensidad de fluorescencia fue cuantificada usando ImageJ. Cada experimento fue repetido al menos tres veces, las barras de error representan la media  $\pm$  s.d. y \*\*\*  $p < 0.001$ .

### 9.7 Las ADSC inducen un fenotipo troncal y transición epitelio mesénquima en células de cáncer cervicouterino.

Evidencia convincente sugiere que la señalización de NF-kappa B participa en la regulación de genes asociados a fenotipos de células troncales. En particular, RelB se sobreexpresa en la fracción mesenquimal de algunos tipos de tumores, por lo que se analizó si las ADSC podrían aumentar el fenotipo troncal en las células HeLa. Los resultados mostraron que las células HeLa cultivadas en presencia de ADSC exhiben una mayor expresión de marcadores de células troncales, como OCT4, KLF4 y ABCG (Figura 35a-c). Estos resultados van de acuerdo con el análisis de ELDA, que calculó una mayor frecuencia de CTC en los tumores generados por células SiHa ó CaSki inoculados en presencia de ADSC (Figuras 26a-b y 28bc).

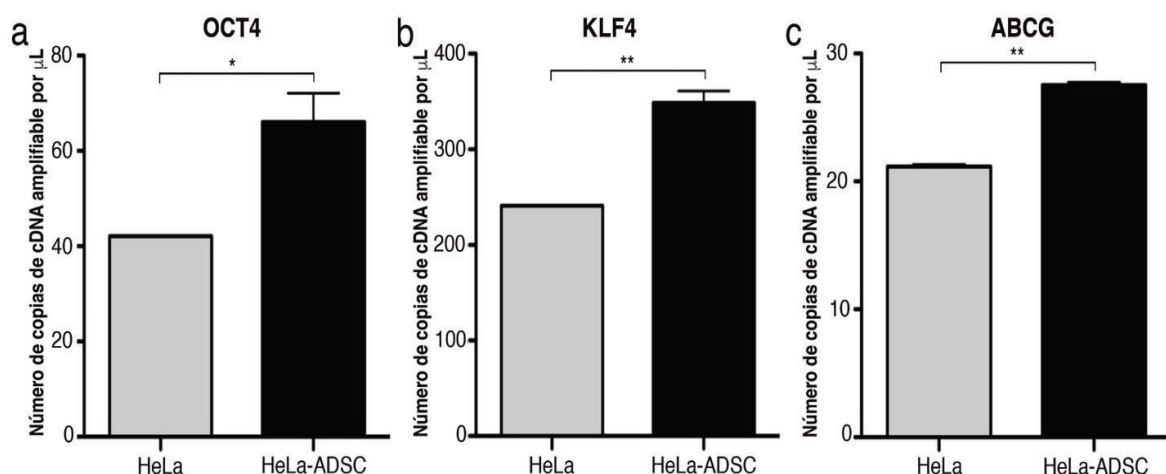


**Figura 35. Las ADSCs incrementan la expresión de marcadores de troncalidad en células de cáncer cervicouterino.** (a-c) Los gráficos muestran el nivel de expresión de los genes de pluripotencia evaluados por ddPCR en HeLa frente a células HeLa cocultivadas con ADSC. Los genes de pluripotencia incluyen OCT4 (a), KLF4 (b) y ABCG (c). Las barras de error representan la media  $\pm$  s.d..Las gráficas representan tres réplicas independientes \* $p < 0.05$ , \*\* $p < 0.01$ .

Sorprendentemente, se observó que las células HeLa cultivadas en el medio condicionado de ADSC exhiben una morfología distintiva similar a un fenotipo mesenquimal con forma alargada y pérdida de contacto celular (Figura 36). Estas características fueron consistentes con el análisis bioinformático que infiere que el proceso biológico de TEM está alterado en HeLa/ADSC.



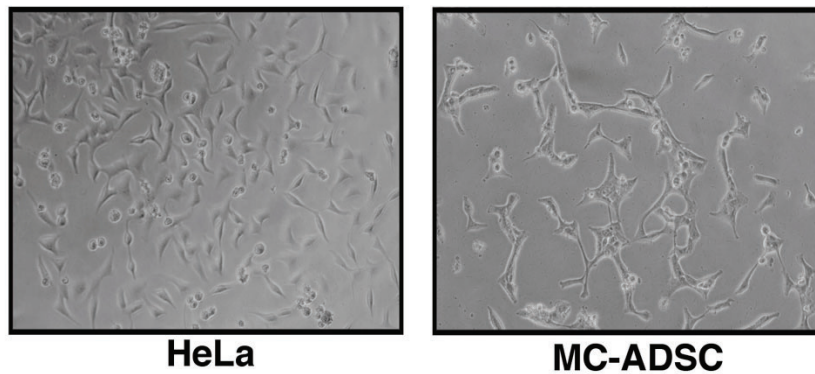
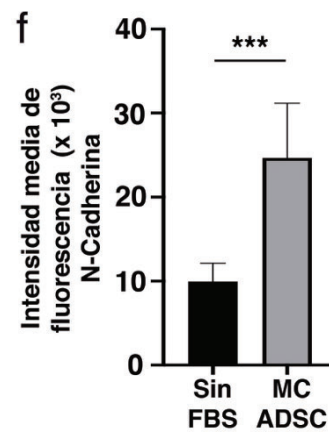
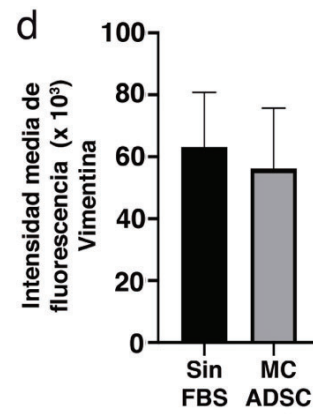
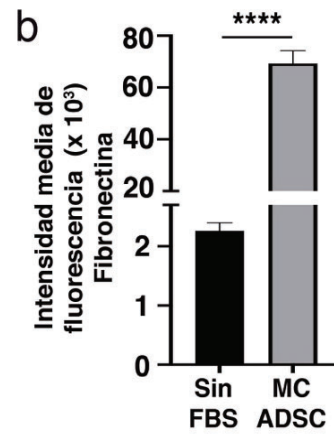
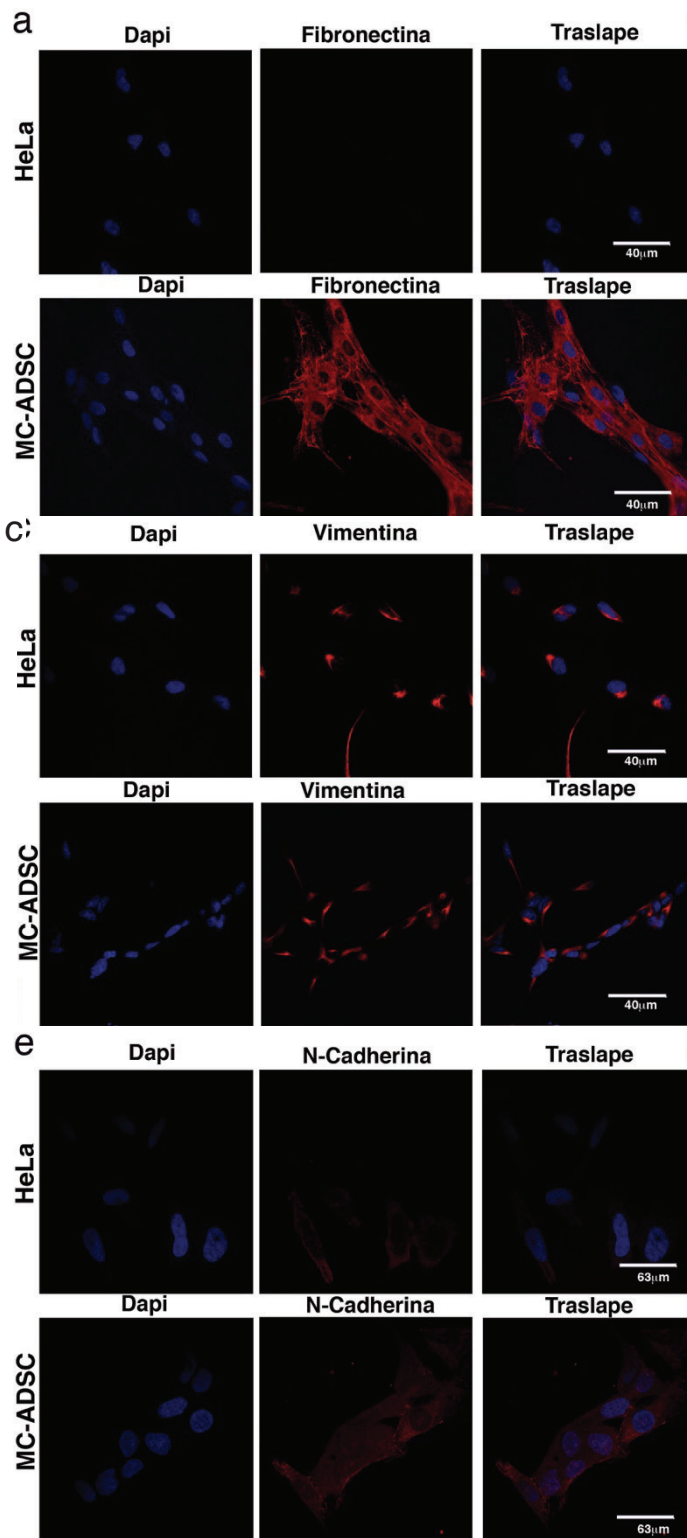


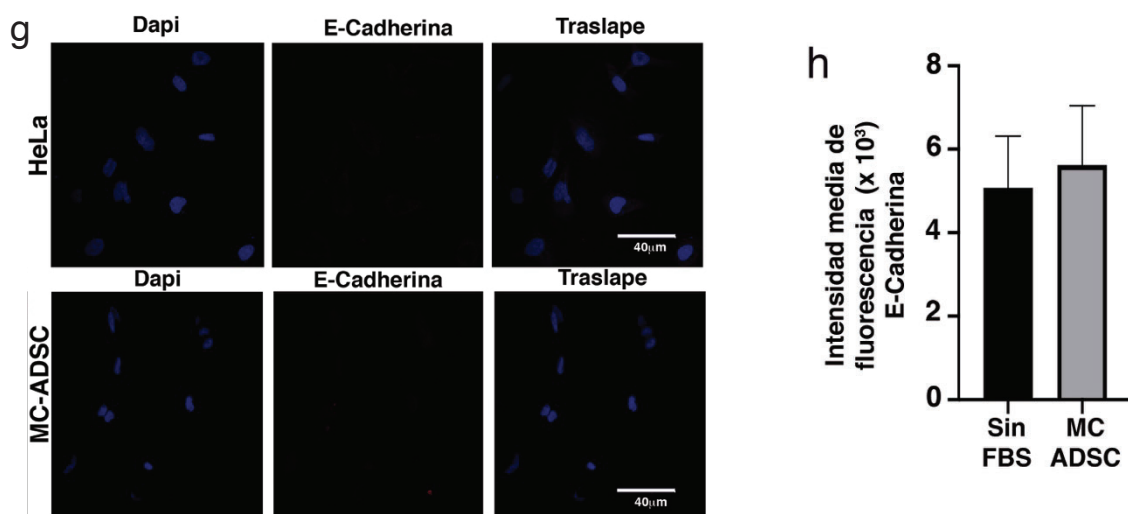
**Figura 36. Las ADSCs inducen cambios morfológicos a las células de cáncer cervicouterino.** La representación esquemática muestra que las células de cáncer cervical exhiben un fenotipo similar a EMT inducido por el medio condicionado de ADSC.

Durante el proceso TEM, las células experimentan una serie de reacciones bioquímicas que eventualmente conducen a alteraciones en la morfología de las células, especialmente la pérdida de polaridad celular. La TEM permite la adquisición de propiedades de células iniciadoras de tumor (TIC), lo que iría de la mano con los datos encontrados anteriormente. Esto es de gran importancia con respecto al avance del CC, ya que la inducción de TEM en células cancerosas, junto con el desarrollo de otras características malignas adquiridas por la presencia de ADSC, podrían acelerar la progresión tumoral.

Para evaluar el papel de las ADSC en la regulación de los marcadores característicos de TEM, se evaluaron los niveles de proteína de fibronectina, N-cadherina, Vimentina y E-cadherina en las líneas celulares HeLa y SiHa.

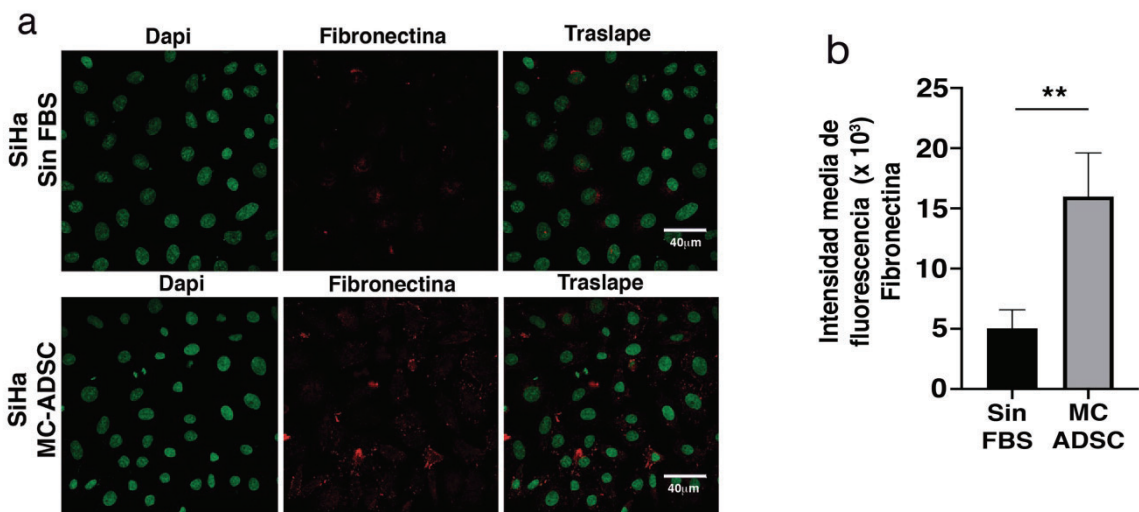
Los resultados mostraron un incremento evidente en los marcadores mesenquimales, las células HeLa expuestas al medio condicionado de ADSC tenían niveles más altos de fibronectina (Figura 36a), Vimentina (Figura 36b) y N-cadherina (Figura 36c), sin embargo, no se encontró ningún cambio en la expresión del marcador epitelial E-cadherina (Figura 36d), quizá debido a su baja expresión en esta línea celular.





**Figura 37. Las ADSC promueven transición epitelio mesénquima en células HeLa.** Análisis por inmunofluorescencia de la expresión de marcadores característicos de TEM que incluye fibronectina (a,b), Vimentina (c,d), N-cadherina (e,f) y E-cadherina (g,h) en células HeLa cultivadas con o sin medio condicionado de ADSC. Las proteínas de TEM se marcaron usando un anticuerpo secundario conjugado con Cy3 y los núcleos se tiñeron con 4'-6-Diamidino-2-fenolindol (DAPI). Las imágenes fueron tomadas en un microscopio confocal utilizando el objetivo de 40x. Las fotografías son representativas de tres experimentos independientes. Para cuantificar los niveles de expresión de fibronectina (b), Vimentina (d), N-cadherina (f) y E-cadherina (h), la intensidad de fluorescencia fue cuantificada usando ImageJ. Las gráficas representan tres réplicas biológicas, las barras de error representan la media  $\pm$  d.s. y \*\*\*  $p < 0.001$ , \*\*\*\*  $p < 0.0001$ .

Corroborando estos resultados, encontramos que las células SiHa expuestas al medio condicionado de ADSC exhibieron un incremento drástico de Fibronectina (Figura 37a) y N-cadherina (Figura 37c), dos moléculas distintivas clave de TEM. También encontramos una ligera disminución en E-cadherina (Figura 37d), un marcador epitelial bien conocido. Colectivamente, estos hallazgos respaldan el papel de las ADSC en la metástasis de CC al promover la migración e invasión de las células cancerosas a través de la inducción de un programa TEM.





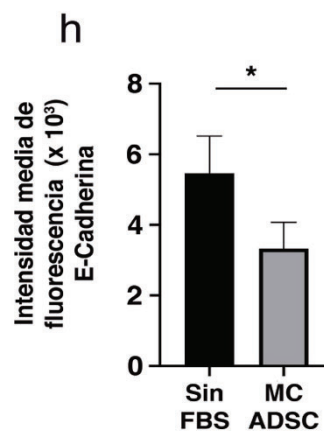
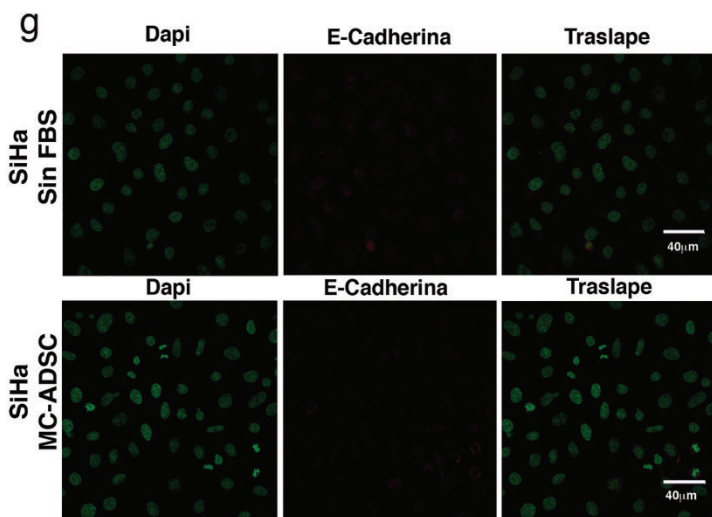
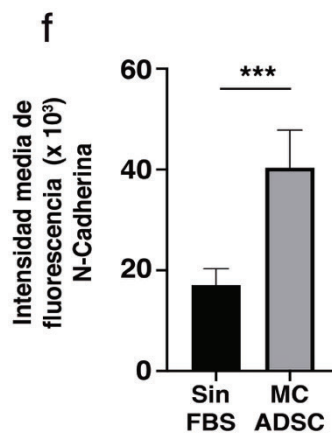
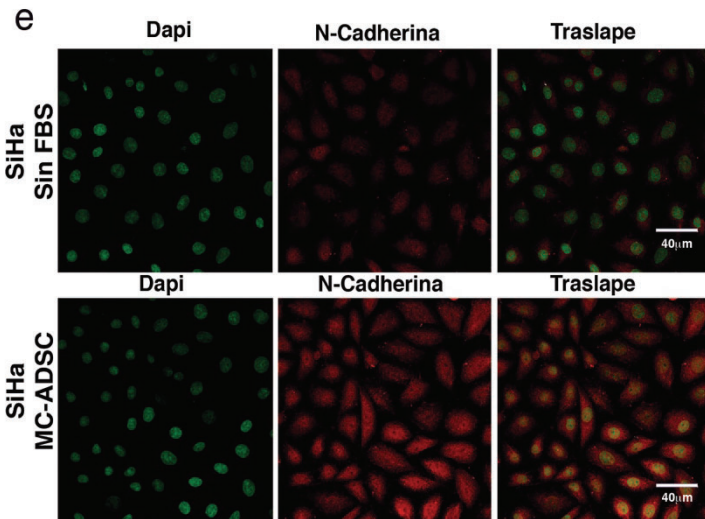
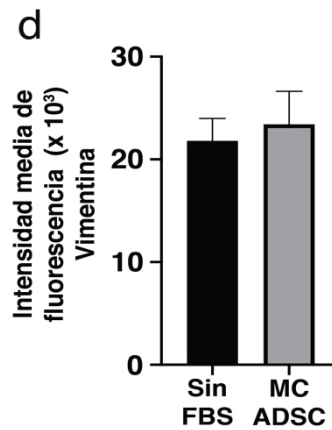
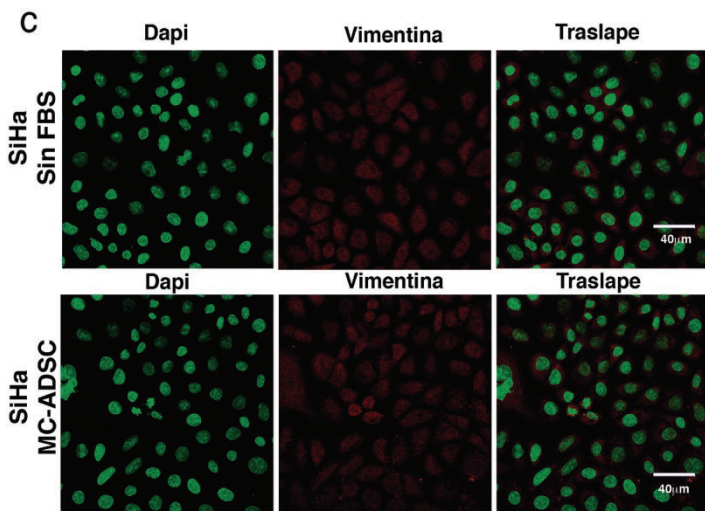


**Figura 38. Las ADSC promueven transición epitelio mesénquima en células SiHa.** Análisis por inmunofluorescencia de la expresión de marcadores característicos de TEM que incluye fibronectina (a,b), Vimentina (c,d), N-cadherina (e,f) y E-cadherina (g,h) en células SiHa cultivadas con o sin medio condicionado de ADSC. Las proteínas de TEM se marcaron usando un anticuerpo secundario conjugado con Cy3 y los núcleos se tiñeron con 4'-6-Diamidino-2-fenolindol (DAPI). Las imágenes fueron tomadas en un microscopio confocal usando el objetivo de 40x. Las fotografías son representativas de tres experimentos independientes. Para cuantificar los niveles de expresión de fibronectina (b), Vimentina (d), N-cadherina (f) y E-cadherina (h), la intensidad de fluorescencia fue cuantificada usando ImageJ. Las gráficas representan tres réplicas biológicas, las barras representan la media  $\pm$  d.s. y \* $p < 0.05$ , \*\* $p < 0.01$  y \*\*\*  $p < 0.001$ .

### **9.8 Las ADSC modulan la angiogénesis en tumores de cáncer cervicouterino.**

La angiogénesis es un proceso en el que se producen nuevos vasos sanguíneos a partir de los vasos preexistentes dentro de un tumor. Aunque la angiogénesis se produce de forma natural, diversos estudios han mostrado que la angiogénesis tiene un papel importante en el desarrollo y la progresión tumoral<sup>62</sup>.

Las células tumorales que secretan altos niveles de factores proangiogénicos contribuyen al desarrollo de una red vascular caracterizada por vasos sanguíneos desorganizados, inmaduros y permeables, lo que puede generar un microambiente ideal para promover la selección de células tumorales más invasivas y agresivas<sup>63</sup>.

Interesantemente, el análisis de secuenciación mostró un aumento en las moléculas con actividades mitogénicas y pro-angiogénicas durante el cocultivo HeLa-ADSC. Estas moléculas incluían quimiocinas CXCL1 y CXCL2, así como el factor de crecimiento endotelial vascular C (VEGF-C), un factor proangiogénico liberado activamente por las células tumorales para la formación de nuevos vasos sanguíneos (Fig. 39a). Los estudios han demostrado que estos factores están regulados por la vía NF-Kappa B. El análisis bioinformático predijo que, en comparación con las células HeLa, las HeLa-ADSC poseen un mayor potencial angiogénico. A través de un análisis de KPA, validamos que la ruta NF-Kappa B promueve la activación de VEGF-C y que esta proteína puede unirse y activar a ligandos como el factor de crecimiento para fibroblastos (FGF2) y factor de crecimiento

epidérmico (EGF), así como al receptor 3 del factor de crecimiento endotelial vascular (VEGFR-3), que activa a su vez a fibronectina (Fig. 39b).

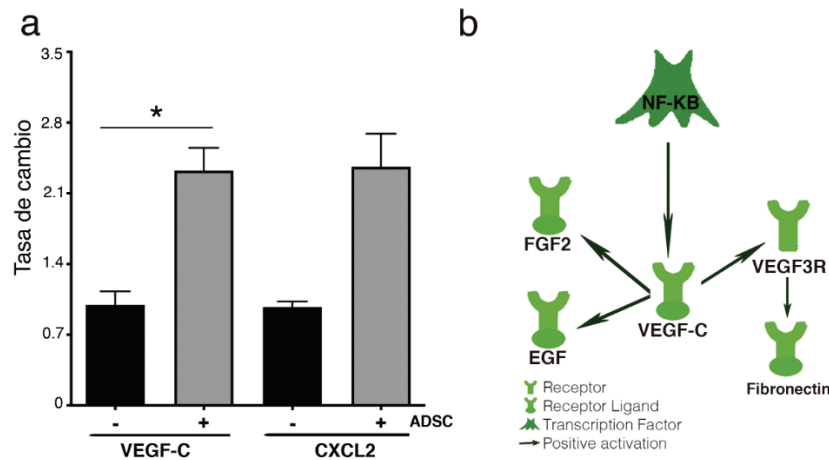


**Figura 39. RNAs relacionados a angiogénesis.** (a) La gráfica muestra el incremento de RNAm involucrados en angiogénesis obtenidos de los datos de RNAseq HeLa-ADSC. (b) Red de KPA que muestra que VEGF-C, puede ser regulado por NFKB en las células HeLa cocultivadas con ADSC.

Para evaluar si las ADSC influyen en la capacidad de los tumores cervicales para establecer la angiogénesis, evaluamos los efectos in vivo de las ADSC en el desarrollo de la vasculatura de embriones de pez cebra transgénicos (fli1a: EGFP) inoculados con células SiHa/ADSC o SiHa únicamente. Estos embriones expresan EGFP específicamente en los capilares vasculares, lo que permite el monitoreo de nuevos vasos sanguíneos. Para respaldar los resultados anteriores, también observamos una clara migración de células SiHa al torrente sanguíneo, principalmente en embriones inyectados con SiHa/ADSC (Fig. 40).

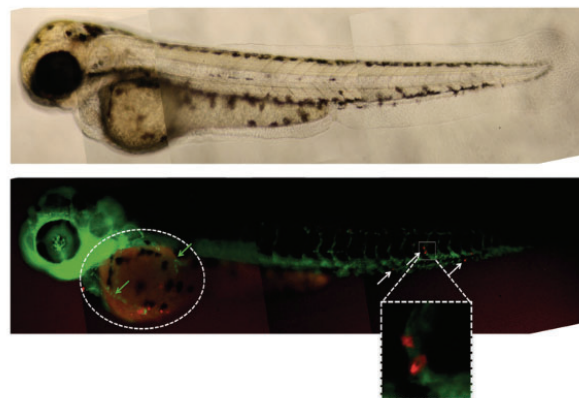


**Figura 40. Infiltración de células SiHa en los vasos sanguíneos del pez cebra.** Fotografía que representa la infiltración de células SiHa en los vasos sanguíneos del embrión *fli1a:EGFP* después de 12hrs. pi. Las células SiHa se observan en color rojo y los vasos sanguíneos en color verde.

Monitoreamos la vascularización de 1 a 3 días y observamos que las células SiHa no lograron formar nuevos vasos sanguíneos; sin embargo, las células SiHa inoculadas en presencia de ADSC formaron tumores vascularizados (Fig. 41).

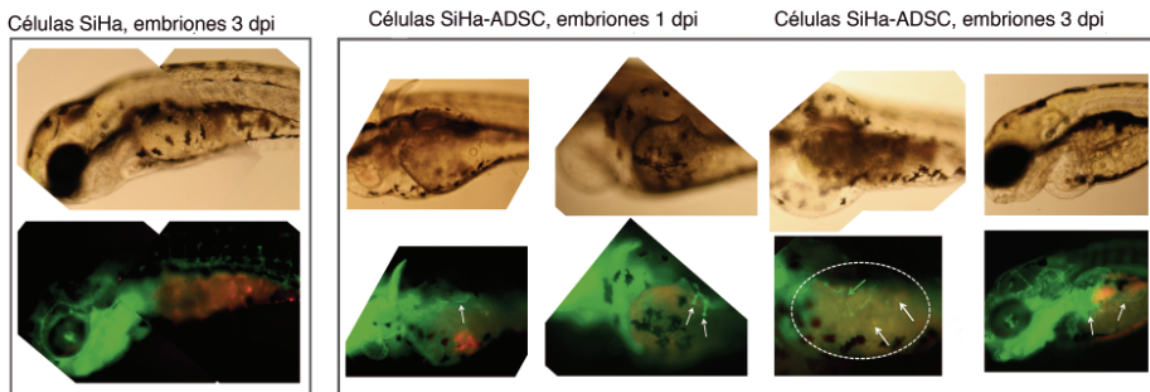


**Figura 41. Las ADSC modulan la angiogénesis en tumores de cáncer cervicouterino.** Figuras representativas que muestran la formación de nuevos vasos sanguíneos en embriones *fli1a:EGFP* de 1 dpi y 3dpi de células SiHa vs SiHa-ADSC.

## 10. DISCUSIÓN

El cáncer, las enfermedades cardiovasculares y la diabetes mellitus representan más del 70% de las muertes en todo el mundo. Además, el cáncer cervicouterino sigue siendo la cuarta causa de incidencia de cáncer y muerte por cáncer en mujeres de todo el mundo.

La obesidad es un factor de riesgo importante para el cáncer, y se ha asociado con una disminución de 5 a 20 años en la supervivencia de los pacientes con cáncer. Según datos de la OCED, México ocupa el segundo lugar en la prevalencia mundial de obesidad (IMC  $\geq 30$  kg / m<sup>2</sup>). Cada vez es más claro que las mujeres obesas tienen un mayor riesgo de desarrollar CC en comparación con las mujeres con un IMC normal<sup>64-66</sup>.

Aunque la célula característica del tejido adiposo es el adipocito, este no es el único tipo de célula presente en este tejido, otras células como preadipocitos, macrófagos, neutrófilos, linfocitos y células endoteliales se albergan en el tejido adiposo y también se han relacionado con obesidad y cáncer.

Los estudios que vinculan la obesidad y el cáncer se han centrado en las repercusiones endocrinas y metabólicas que promueven un proceso inflamatorio generalizado<sup>20,21,67</sup>; sin embargo, se sabe poco sobre el mecanismo molecular específico por el cual la obesidad aumenta el riesgo de cáncer.

En este proyecto, estudiamos a las ADSC que también se encuentran en el tejido adiposo y son jugadores esenciales en el desarrollo y la regeneración de los tejidos<sup>68</sup>. Las ADSC se encuentran en cantidades abundantes en el tejido adiposo, estudios han informado que las ADSC representan hasta el 30% del total de células contenidas en este tejido<sup>69</sup>. En particular, estudios recientes han proporcionado evidencia de que el número de ADSC excede la frecuencia de células troncales mesenquimales derivadas de médula (BMSC) encontradas en el estroma medular<sup>70</sup>. Aproximadamente, 1 ml de tejido adiposo obtenido por liposucción contiene aproximadamente  $6 \times 10^5$  a  $2 \times 10^6$  ADSC<sup>71</sup>, esto representa al menos 500 veces más que el número de células troncales obtenidas de la médula ósea<sup>72-74</sup>. En conjunto, estos datos destacan al tejido adiposo como la fuente más rica de células troncales multipotentes, posiblemente superando a cualquier otra fuente en el cuerpo.

Sorprendentemente, evidencia reciente ha demostrado que los pacientes con obesidad exhiben una mayor movilidad sistémica de ADSC que los pacientes sanos y, curiosamente, esta movilización es aún mayor en pacientes con cáncer<sup>47</sup>, lo que apoya la incorporación de ADSC a los tumores. Evidencias acumuladas han demostrado que las ADSC poseen la capacidad de migrar hacia los tumores mediante quimioatracción<sup>45,75</sup>.

El papel de las ADSC en cáncer aún no es claro, existen algunos informes que evidencian el comportamiento maligno de las ADSC permitiendo el crecimiento de los tumores. Por el

contrario, algunos estudios han demostrado que las ADSC exhiben un potencial antitumoral. Aún se desconoce el papel de las ADSC en el cáncer cervical; por lo tanto, es necesario determinar el efecto de las ADSC en CC<sup>76,77</sup>. En este estudio, demostramos por primera vez que las ADSC aumentan el fenotipo maligno de líneas celulares de cáncer cervicouterino, como las células HeLa, SiHa y CaSki.

Se utilizó un sistema de cocultivo indirecto en el que tanto las células tumorales como las ADSC se separaron físicamente a través de una membrana permeable y se cultivaron en el mismo microambiente, permitiendo así la señalización paracrina. Este método se ha utilizado para estudiar el efecto de las ADSC en otros tumores, como el carcinoma de células escamosas<sup>78</sup>, el cáncer de mama<sup>52</sup>, el melanoma<sup>53</sup>, el cáncer de pulmón y colorrectal<sup>49</sup>.

Nuestros resultados muestran que la presencia de ADSC (CD90<sup>+</sup> / CD44<sup>+</sup> / CD31<sup>-</sup> / CD45<sup>-</sup>) altera el transcriptoma de las células de CC. Los datos obtenidos de RNA-seq revelaron que 95 RNAs se expresaron diferencialmente en células HeLa cocultivadas en presencia de ADSC derivadas de pacientes. Los cambios en la expresión génica se validaron mediante PCR digital, y encontramos que ambas ADSC obtenidas de pacientes o de ATCC exhiben patrones de expresión génica similares, corroborando este fenómeno. Curiosamente, la mayoría de los genes con expresión diferencial, como IL6, RelB, RelA, Plac8, ITGA5, CXCL12 y FN1, entre otras citocinas y factores de crecimiento, han estado involucrados en el crecimiento y la progresión tumoral. Preisner y sus colegas utilizaron qRT-PCR para analizar la expresión de genes promotores de tumores en células de melanoma cocultivadas con ADSC y encontraron citocinas y factores de crecimiento similares<sup>53</sup>, como IL6, CXCL12, VEGF y HGF 69.

Curiosamente, los genes validados (ITGA5, IL6, IL4R, FN1, TIMP1 y PLAC8) son muy relevantes en CC porque su nivel de expresión está directamente relacionado con la supervivencia del paciente con CC. Estos genes también han sido relevantes en otros tipos de tumores. Por ejemplo, ITGA5, una integrina que promueve la invasión tumoral<sup>79</sup>, se ha correlacionado con una menor supervivencia de los pacientes con cáncer de pulmón<sup>80</sup>, y



funciona como un receptor para FN1<sup>81,82</sup>, el cual también se reguló en nuestro cocultivo. IL4R induce un fenotipo prometastásico en tumores epiteliales.

El análisis integral con IPA, KPA y GSEA sugiere que las ADSC modificaron diversos procesos celulares, como la migración, la invasión, la angiogénesis y la proliferación. La evidencia acumulada ha demostrado que las ADSC también pueden influir en la proliferación de células cancerosas; sin embargo, no pudimos observar ninguna influencia de las ADSC en la capacidad de proliferación de las células HeLa. La migración, la invasión y la angiogénesis se corroboraron utilizando estrategias in vitro e in vivo. Para respaldar nuestros resultados, varios estudios han demostrado el efecto de las ADSC en la migración e invasión de melanoma, cáncer de mama, próstata y cáncer pancreático. Sorprendentemente, encontramos una gran cantidad de RNAs diferencialmente expresados relacionados con la migración y la invasión, como VCAN, SPARC, MMP14, ITGA5, PLAUR, NRP1, IL-6, CXCL2 y HGF. Notablemente, también observamos cambios morfológicos drásticos en células HeLa y SiHa cocultivadas con ADSC, lo que confiere capacidades migratorias, tal vez al inducir la transición epitelial a mesenquimal.

Los resultados también muestran que las ADSC modifican el comportamiento de las células de CC, lo que induce un rápido crecimiento tumoral y metástasis. Mecánicamente, se sabe poco acerca de cómo las ADSC facilitan el desarrollo del tumor. Evidencia reciente ha demostrado que ADCS provoca un aumento en los niveles de IL6, induciendo la fosforilación de JAK2 / STAT3<sup>51</sup>, lo que resulta en la proliferación, invasión y crecimiento tumoral en algunos tipos de cáncer como de próstata y endometrio. Sorprendentemente, también encontramos que las ADSC inducen un aumento dramático en IL6 / STAT y un aumento en la señalización no canónica de NF-kappa B en células HeLa y SiHa. Estos resultados son consistentes con un estudio reciente que muestra que las células troncales mesenquimales promueven la progresión del cáncer colorrectal a través de la activación de NF-kappa B<sup>83</sup>. Nuestros resultados muestran por primera vez que la vía de NF-kappa B en CC se activa debido a la presencia de ADSC. El análisis bioinformático detectó 23 genes relacionados con

NF-kappa B y sugiere que RelB, un miembro de la vía no canónica de NF-kappa B, es el principal factor de crecimiento involucrado en la regulación de la señalización de NF-kappa B. También encontramos que la expresión de p52 y p65 es inducida por ADSC, lo que sugiere que ambas vías de señalización canónica y no canónica se activan en CC.

En particular, las ADSC indujeron una rápida expansión de las CTCs en el modelo de pez cebra inoculado con células SiHa y CaSki en presencia de ADSC. Está bien establecido que la expansión de CTCs induce rápidamente el crecimiento y desarrollo de tumores, lo que sugiere que un aumento en el número de CTCs podrían ser responsables de las capacidades altamente invasivas y metastásicas conferidas por ADSC. Una forma por la cual las células de CC pueden adquirir la troncalidad es debido a la activación constitutiva de NF-Kappa B. Estudios recientes han establecido que NF-kappa B contribuye a la drástica expansión del número de células troncales y aumenta la capacidad clonogénica y de autorrenovación de las CTCs<sup>84,85</sup>. Nuestros resultados indican que las ADSC inducen la sobreexpresión de marcadores de células troncales como OCT4, KLF4 y ABCG en las células HeLa. Además, encontramos que las ADSC promueven TEM en células HeLa y SiHa, adquiriendo características mesenquimales verificadas por la alta expresión de fibronectina, n-cadherina y vimentina. Asimismo, cada vez es más claro que el proceso de TEM induce la adquisición y el mantenimiento de características similares a las células troncales.

Estos resultados están de acuerdo con investigaciones recientes que muestran que las células tumorales gliales y las células de cáncer de pulmón pueden someterse a TEM y adquirir características mesenquimales cuando se cultivan en presencia de medio condicionado obtenido de ADSC.

Finalmente, también observamos que los RNAs con expresión diferencial, incluidos VEGFC, CXCL2, VEGF3R, FGF2 y EGF, también están involucrados en angiogénesis. Realizamos ensayos in vivo y observamos constantemente que las ADSC pueden inducir el crecimiento y la formación de nuevos vasos sanguíneos que podrían suministrar nutrientes y oxígeno a



los tumores. Curiosamente, Guiting Lin et al. 2010, demostraron que las ADSC migran hacia tumores de próstata y aumentan la vascularización tumoral mediada por FGF2<sup>45</sup>. Además, Eva, Koellensperger et al. 2014, demostraron que el medio condicionado del cocultivo de ADSC y carcinoma de células escamosas induce la formación de tubos en células endoteliales de la vena umbilical humana (HUVEC), corroborando así el papel proangiogénico de las ADSC<sup>78</sup>.

## **11. CONCLUSIÓN**

En conclusión, nuestros resultados demuestran que las ADSC afectan múltiples características que contribuyen a la malignidad de las células de cáncer cervicouterino, como la expresión génica, la migración, la invasión, la angiogénesis y la troncalidad. A pesar de la contribución de las ADSC en la promoción de estas características, las ADSC no tienen ningún efecto en la proliferación de las células de cáncer cervicouterino (Figura 42). Curiosamente, los efectos de las ADSC encontrados en las ADSC derivados del paciente también se validaron en una línea celular ADSC obtenida de ATCC.

Es importante decir que las ADSC podrían promover características que contribuyen a la malignidad del cáncer cervicouterino a través de la vía de señalización NF- $\kappa$ B y la inducción de TEM (Figura 42). Además, observamos que los RNAm alterados por la presencia de ADSC exhiben significancia clínica, ya que están asociados con una supervivencia más corta de pacientes con cáncer cervicouterino. Aunque la relevancia clínica de las células ADSC sigue siendo incompleta, nuestros resultados brindan pautas para la búsqueda de nuevas moléculas que puedan reducir las tasas de mortalidad de pacientes obesos con cáncer cervicouterino. Creemos que se debe hacer mucho trabajo para dilucidar completamente el mecanismo exacto involucrado en la contribución de las ADSC en el fenotipo maligno de las células cancerosas.

Además, debido al papel maligno de las ADSC en el cáncer, es necesario evaluar la seguridad de las terapias basadas en ADSC para evitar la ubicación conjunta de esas células con células cancerosas que podrían promover el crecimiento tumoral.

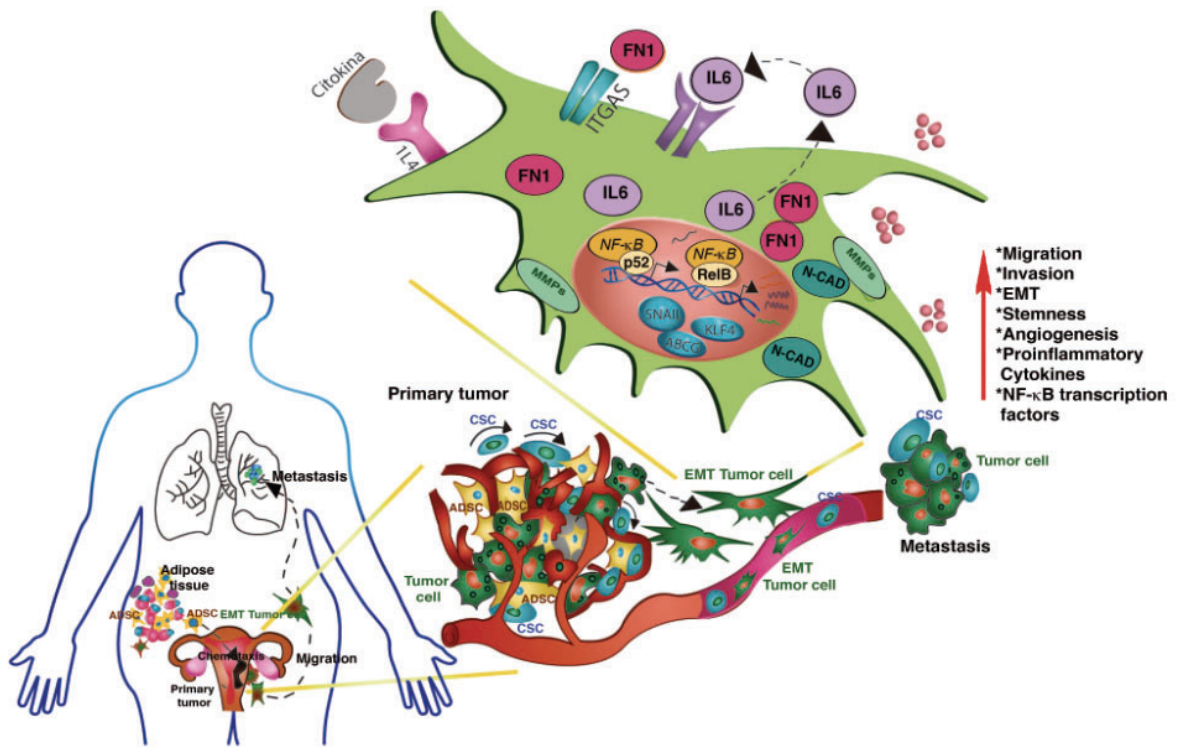


**Figura 42.** La ilustración fue construida a partir de los datos experimentales obtenidos en este proyecto. La figura representa que las ADSC migran desde el tejido adiposo hacia el tumor de CC, y una vez que las ADSC están instaladas en el tumor, incrementan el fenotipo maligno de CC por incremento de la señalización de NF-KappaB causando un incremento en la expresión de quimiocinas, factores de transcripción, integrinas y metaloproteínas, las cuales contribuyen con el incremento de migración e invasión en las células cancerosas. Además, las ADSC activan la TEM y finalmente inducen angiogénesis que juega un roll importante en la progresión tumoral.

## 12. REFERENCIAS

- 1 Floor, S. L., Dumont, J. E., Maenhaut, C. & Raspe, E. Hallmarks of cancer: of all cancer cells, all the time? *Trends Mol Med* **18**, 509-515, doi:10.1016/j.molmed.2012.06.005 (2012).
- 2 Castro-Oropeza, R., Melendez-Zajgla, J., Maldonado, V. & Vazquez-Santillan, K. The emerging role of lncRNAs in the regulation of cancer stem cells. *Cell Oncol (Dordr)* **41**, 585-603, doi:10.1007/s13402-018-0406-4 (2018).
- 3 Weinberg, D. H. a. R. A. The Hallmarks of Cancer. *Cell Press* **100**, 57-70 (2000).
- 4 Hanahan, D. & Weinberg, R. A. Hallmarks of cancer: the next generation. *Cell* **144**, 646-674, doi:10.1016/j.cell.2011.02.013 (2011).
- 5 Hanahan, D. Hallmarks of Cancer: New Dimensions. *Cancer Discov* **12**, 31-46, doi:10.1158/2159-8290.CD-21-1059 (2022).
- 6 Menyhart, O. *et al.* Guidelines for the selection of functional assays to evaluate the hallmarks of cancer. *Biochim Biophys Acta* **1866**, 300-319, doi:10.1016/j.bbcan.2016.10.002 (2016).
- 7 Casey, S. C. *et al.* The effect of environmental chemicals on the tumor microenvironment. *Carcinogenesis* **36 Suppl 1**, S160-183, doi:10.1093/carcin/bgv035 (2015).
- 8 Bray, F. *et al.* Global cancer statistics 2018: Globocan estimates of incidence and mortality worldwide for 36 cancers in 185 countries. *CA Cancer J Clin* **68**, 394-424, doi:10.3322/caac.21492 (2018).
- 9 Szymonowicz, K. A. & Chen, J. Biological and clinical aspects of HPV-related cancers. *Cancer Biol Med* **17**, 864-878, doi:10.20892/j.issn.2095-3941.2020.0370 (2020).
- 10 Cohen, P. A., Jhingran, A., Oaknin, A. & Denny, L. Cervical cancer. *The Lancet* **393**, 169-182, doi:10.1016/s0140-6736(18)32470-x (2019).
- 11 Stanley, M. Pathology and epidemiology of HPV infection in females. *Gynecol Oncol* **117**, S5-10, doi:10.1016/j.ygyno.2010.01.024 (2010).
- 12 Bedell, S. L., Goldstein, L. S., Goldstein, A. R. & Goldstein, A. T. Cervical Cancer Screening: Past, Present, and Future. *Sex Med Rev* **8**, 28-37, doi:10.1016/j.sxmr.2019.09.005 (2020).
- 13 Arezzo, F. *et al.* HPV-Negative Cervical Cancer: A Narrative Review. *Diagnostics (Basel)* **11**, doi:10.3390/diagnostics11060952 (2021).
- 14 Olusola, P., Banerjee, H. N., Phillely, J. V. & Dasgupta, S. Human Papilloma Virus-Associated Cervical Cancer and Health Disparities. *Cells* **8**, doi:10.3390/cells8060622 (2019).
- 15 Pal, A. & Kundu, R. Human Papillomavirus E6 and E7: The Cervical Cancer Hallmarks and Targets for Therapy. *Front Microbiol* **10**, 3116, doi:10.3389/fmicb.2019.03116 (2019).
- 16 Crosbie, E. J., Einstein, M. H., Franceschi, S. & Kitchener, H. C. Human papillomavirus and cervical cancer. *The Lancet* **382**, 889-899, doi:10.1016/s0140-6736(13)60022-7 (2013).

- 17 Lee, S. J., Yang, A., Wu, T. C. & Hung, C. F. Immunotherapy for human papillomavirus-associated disease and cervical cancer: review of clinical and translational research. *J Gynecol Oncol* **27**, e51, doi:10.3802/jgo.2016.27.e51 (2016).
- 18 Wooldridge, T. R. & Laimins, L. A. Regulation of human papillomavirus type 31 gene expression during the differentiation-dependent life cycle through histone modifications and transcription factor binding. *Virology* **374**, 371-380, doi:10.1016/j.virol.2007.12.011 (2008).
- 19 L. Stewart Massad *et al.* 2012 Updated Consensus Guidelines for the Management of Abnormal Cervical Cancer Screening Tests and Cancer Precursors. *Journal of Genital Tract Disease* **17**, S1-S27 (2013).
- 20 Cozzo, A. J., Fuller, A. M. & Makowski, L. Contribution of Adipose Tissue to Development of Cancer. *Compr Physiol* **8**, 237-282, doi:10.1002/cphy.c170008 (2017).
- 21 Khandekar, M. J., Cohen, P. & Spiegelman, B. M. Molecular mechanisms of cancer development in obesity. *Nat Rev Cancer* **11**, 886-895, doi:10.1038/nrc3174 (2011).
- 22 Choe, S. S., Huh, J. Y., Hwang, I. J., Kim, J. I. & Kim, J. B. Adipose Tissue Remodeling: Its Role in Energy Metabolism and Metabolic Disorders. *Front Endocrinol (Lausanne)* **7**, 30, doi:10.3389/fendo.2016.00030 (2016).
- 23 Lee, J. H. *et al.* The Role of Adipose Tissue Mitochondria: Regulation of Mitochondrial Function for the Treatment of Metabolic Diseases. *Int J Mol Sci* **20**, doi:10.3390/ijms20194924 (2019).
- 24 Frigolet, M. E. & Gutierrez-Aguilar, R. The colors of adipose tissue. *Gac Med Mex* **156**, 142-149, doi:10.24875/GMM.M20000356 (2020).
- 25 Eugenia E. Calle, C. R., Kimberly Walker-Thurmond, B.A., and Michael J. Thun. Overweight, Obesity, and Mortality from Cancer in a Prospectively Studied Cohort of U.S. Adults. *The new england journal of medicine* **348** (2003).
- 26 Si, Z. *et al.* Adipose-derived stem cells: Sources, potency, and implications for regenerative therapies. *Biomed Pharmacother* **114**, 108765, doi:10.1016/j.biopha.2019.108765 (2019).
- 27 Levi, B. *et al.* Stem cells: update and impact on craniofacial surgery. *J Craniofac Surg* **23**, 319-322, doi:10.1097/SCS.0b013e318241dbaf (2012).
- 28 Mayani, H. c. A Glance into Somatic Stem Cell Biology: Basic Principles, New Concepts, and Clinical Relevance. *Archives of Medical Research* **34**, 3-15 (2003).
- 29 Mushahary, D., Spittler, A., Kasper, C., Weber, V. & Charwat, V. Isolation, cultivation, and characterization of human mesenchymal stem cells. *Cytometry A* **93**, 19-31, doi:10.1002/cyto.a.23242 (2018).
- 30 Estrov, M. K. r. a. Z. Adult Stem Cells for Tissue Repair — A New Therapeutic Concept? *The new england journal of medicine* **349**, 570-582 (2003).
- 31 Roberts, I. Mesenchymal stem cells. *Vox Sang* **87 Suppl 2**, 38-41, doi:10.1111/j.1741-6892.2004.00452.x (2004).
- 32 Kuntin, D. & Genever, P. Mesenchymal stem cells from biology to therapy. *Emerg Top Life Sci* **5**, 539-548, doi:10.1042/ETLS20200303 (2021).

- 33 Minter, D., Marra, K. G. & Rubin, J. P. Adipose-derived mesenchymal stem cells: biology and potential applications. *Adv Biochem Eng Biotechnol* **129**, 59-71, doi:10.1007/10\_2012\_146 (2013).
- 34 TORRADES, S. La investigación con células madre. *OFFARM* **22** (2003).
- 35 Bora, P. & Majumdar, A. S. Adipose tissue-derived stromal vascular fraction in regenerative medicine: a brief review on biology and translation. *Stem Cell Res Ther* **8**, 145, doi:10.1186/s13287-017-0598-y (2017).
- 36 Fang, J., Chen, F., Liu, D., Gu, F. & Wang, Y. Adipose tissue-derived stem cells in breast reconstruction: a brief review on biology and translation. *Stem Cell Res Ther* **12**, 8, doi:10.1186/s13287-020-01955-6 (2021).
- 37 Wu, Y. C. *et al.* Transplantation of 3D adipose-derived stem cell/hepatocyte spheroids alleviates chronic hepatic damage in a rat model of thioacetamide-induced liver cirrhosis. *Sci Rep* **12**, 1227, doi:10.1038/s41598-022-05174-2 (2022).
- 38 Bourin, P. *et al.* Stromal cells from the adipose tissue-derived stromal vascular fraction and culture expanded adipose tissue-derived stromal/stem cells: a joint statement of the International Federation for Adipose Therapeutics and Science (IFATS) and the International Society for Cellular Therapy (ISCT). *Cytotherapy* **15**, 641-648, doi:10.1016/j.jcyt.2013.02.006 (2013).
- 39 Cai, Y., Li, J., Jia, C., He, Y. & Deng, C. Therapeutic applications of adipose cell-free derivatives: a review. *Stem Cell Res Ther* **11**, 312, doi:10.1186/s13287-020-01831-3 (2020).
- 40 He, L. *et al.* ADSC-Exos containing MALAT1 promotes wound healing by targeting miR-124 through activating Wnt/beta-catenin pathway. *Biosci Rep* **40**, doi:10.1042/BSR20192549 (2020).
- 41 Tabatabaei Qomi, R. & Sheykhasan, M. Adipose-derived stromal cell in regenerative medicine: A review. *World J Stem Cells* **9**, 107-117, doi:10.4252/wjsc.v9.i8.107 (2017).
- 42 Scioli, M. G. *et al.* Adipose-Derived Stem Cells in Cancer Progression: New Perspectives and Opportunities. *Int J Mol Sci* **20**, doi:10.3390/ijms20133296 (2019).
- 43 Lou, G. *et al.* MiR-199a-modified exosomes from adipose tissue-derived mesenchymal stem cells improve hepatocellular carcinoma chemosensitivity through mTOR pathway. *J Exp Clin Cancer Res* **39**, 4, doi:10.1186/s13046-019-1512-5 (2020).
- 44 Zakaria, N. & Yahaya, B. H. Adipose-Derived Mesenchymal Stem Cells Promote Growth and Migration of Lung Adenocarcinoma Cancer Cells. *Adv Exp Med Biol* **1292**, 83-95, doi:10.1007/5584\_2019\_464 (2020).
- 45 Lin, G. *et al.* Effects of transplantation of adipose tissue-derived stem cells on prostate tumor. *Prostate* **70**, 1066-1073, doi:10.1002/pros.21140 (2010).
- 46 Bertolini, F., Petit, J. Y. & Kolonin, M. G. Stem cells from adipose tissue and breast cancer: hype, risks and hope. *Br J Cancer* **112**, 419-423, doi:10.1038/bjc.2014.657 (2015).
- 47 Bellows, C. F., Zhang, Y., Chen, J., Frazier, M. L. & Kolonin, M. G. Circulation of progenitor cells in obese and lean colorectal cancer patients. *Cancer Epidemiol Biomarkers Prev* **20**, 2461-2468, doi:10.1158/1055-9965.EPI-11-0556 (2011).

- 48 Maclsaac, Z. M. *et al.* Long-term in-vivo tumorigenic assessment of human culture-expanded adipose stromal/stem cells. *Exp Cell Res* **318**, 416-423, doi:10.1016/j.yexcr.2011.12.002 (2012).
- 49 Rhyu, J. J., Yun, J. W., Kwon, E., Che, J. H. & Kang, B. C. Dual effects of human adipose tissue-derived mesenchymal stem cells in human lung adenocarcinoma A549 xenografts and colorectal adenocarcinoma HT-29 xenografts in mice. *Oncol Rep* **34**, 1733-1744, doi:10.3892/or.2015.4185 (2015).
- 50 Yan Wang, Y. C., Bin Yue, Xuexiao Ma, Guoqing Zhang, Hongfei Xiang, Yong Liu, Tianrui Wang, Xiaolin Wu, Bohua Chen. Adipose-derived mesenchymal stem cells promote osteosarcoma proliferation and metastasis by activating the STAT3 pathway. *Oncotarget* **8**, 23803-23816 (2017).
- 51 Chu, Y. *et al.* STAT3 activation by IL-6 from adipose-derived stem cells promotes endometrial carcinoma proliferation and metastasis. *Biochem Biophys Res Commun* **500**, 626-631, doi:10.1016/j.bbrc.2018.04.121 (2018).
- 52 Koellensperger, E. *et al.* The impact of human adipose tissue-derived stem cells on breast cancer cells: implications for cell-assisted lipotransfers in breast reconstruction. *Stem Cell Res Ther* **8**, 121, doi:10.1186/s13287-017-0579-1 (2017).
- 53 Preisner, F. *et al.* Impact of Human Adipose Tissue-Derived Stem Cells on Malignant Melanoma Cells in An In Vitro Co-culture Model. *Stem Cell Rev* **14**, 125-140, doi:10.1007/s12015-017-9772-y (2018).
- 54 Wen, Y., Guo, Y., Huang, Z., Cai, J. & Wang, Z. Adiposederived mesenchymal stem cells attenuate cisplatininduced apoptosis in epithelial ovarian cancer cells. *Mol Med Rep* **16**, 9587-9592, doi:10.3892/mmr.2017.7783 (2017).
- 55 Hong-Jian Wei *et al.* Adipose-derived stem cells promote tumor initiation and accelerate tumor growth by interleukin-6 production. *Oncotarget* **6**, 7713-7726 (2015).
- 56 Yu, X. *et al.* Human adipose derived stem cells induced cell apoptosis and s phase arrest in bladder tumor. *Stem Cells Int* **2015**, 619290, doi:10.1155/2015/619290 (2015).
- 57 Cousin, B. *et al.* Adult stromal cells derived from human adipose tissue provoke pancreatic cancer cell death both in vitro and in vivo. *PLoS One* **4**, e6278, doi:10.1371/journal.pone.0006278 (2009).
- 58 Takahara, K. *et al.* Adipose-derived stromal cells inhibit prostate cancer cell proliferation inducing apoptosis. *Biochem Biophys Res Commun* **446**, 1102-1107, doi:10.1016/j.bbrc.2014.03.080 (2014).
- 59 M, W. *The zebrafish book. A guide for the laboratory use of zebrafish (Danio rerio).* (2000).
- 60 Hu, Y. & Smyth, G. K. ELDA: extreme limiting dilution analysis for comparing depleted and enriched populations in stem cell and other assays. *J Immunol Methods* **347**, 70-78, doi:10.1016/j.jim.2009.06.008 (2009).
- 61 Zampedri, C., Martinez-Flores, W. A. & Melendez-Zajgla, J. The Use of Zebrafish Xenotransplant Assays to Analyze the Role of lncRNAs in Breast Cancer. *Front Oncol* **11**, 687594, doi:10.3389/fonc.2021.687594 (2021).



- 62 Rahimian, N. *et al.* Non-coding RNAs related to angiogenesis in gynecological cancer. *Gynecol Oncol* **161**, 896-912, doi:10.1016/j.ygyno.2021.03.020 (2021).
- 63 Viillard, C. & Larrivee, B. Tumor angiogenesis and vascular normalization: alternative therapeutic targets. *Angiogenesis* **20**, 409-426, doi:10.1007/s10456-017-9562-9 (2017).
- 64 Calle, E. E. & Thun, M. J. Obesity and cancer. *Oncogene* **23**, 6365-6378, doi:10.1038/sj.onc.1207751 (2004).
- 65 Choi, Y. J. *et al.* Adult height in relation to risk of cancer in a cohort of 22,809,722 Korean adults. *Br J Cancer* **120**, 668-674, doi:10.1038/s41416-018-0371-8 (2019).
- 66 Ryan, D. Obesity in women: a life cycle of medical risk. *Int J Obes (Lond)* **31 Suppl 2**, S3-7; discussion S31-32, doi:10.1038/sj.ijo.0803729 (2007).
- 67 Brahmkhatri, V. P., Prasanna, C. & Atreya, H. S. Insulin-like growth factor system in cancer: novel targeted therapies. *Biomed Res Int* **2015**, 538019, doi:10.1155/2015/538019 (2015).
- 68 Joo, H. J., Kim, J. H. & Hong, S. J. Adipose Tissue-Derived Stem Cells for Myocardial Regeneration. *Korean Circ J* **47**, 151-159, doi:10.4070/kcj.2016.0207 (2017).
- 69 Mazini, L., Rochette, L., Amine, M. & Malka, G. Regenerative Capacity of Adipose Derived Stem Cells (ADSCs), Comparison with Mesenchymal Stem Cells (MSCs). *Int J Mol Sci* **20**, doi:10.3390/ijms20102523 (2019).
- 70 Van Pham, P. Adipose stem cells in the clinic. *Biomedical Research and Therapy* **1**, doi:10.7603/s40730-014-0011-8 (2014).
- 71 Okamoto, S. Y. a. O. K. Human adipose-derived stem cells: current challenges and clinical perspectives. *Anais Brasileiros de Dermatologia* **85**, 647-656 (2010).
- 72 Fraser, J. K., Wulur, I., Alfonso, Z. & Hedrick, M. H. Fat tissue: an underappreciated source of stem cells for biotechnology. *Trends Biotechnol* **24**, 150-154, doi:10.1016/j.tibtech.2006.01.010 (2006).
- 73 Rojas, M. M. a. M. Células Troncales Derivadas del Tejido Adiposo. *International Journal of Morphology* **28**, 879-889 (2010).
- 74 Alonso-Goulart, V. *et al.* Mesenchymal stem cells from human adipose tissue and bone repair: a literature review. *Biotechnology Research and Innovation* **2**, 74-80, doi:10.1016/j.biori.2017.10.005 (2018).
- 75 Zhang, Y. *et al.* White adipose tissue cells are recruited by experimental tumors and promote cancer progression in mouse models. *Cancer Res* **69**, 5259-5266, doi:10.1158/0008-5472.CAN-08-3444 (2009).
- 76 Hassan, M., Latif, N. & Yacoub, M. Adipose tissue: friend or foe? *Nat Rev Cardiol* **9**, 689-702, doi:10.1038/nrcardio.2012.148 (2012).
- 77 Mishra, P. J., Mishra, P. J., Glod, J. W. & Banerjee, D. Mesenchymal stem cells: flip side of the coin. *Cancer Res* **69**, 1255-1258, doi:10.1158/0008-5472.CAN-08-3562 (2009).
- 78 Koellensperger, E. *et al.* Alterations of gene expression and protein synthesis in co-cultured adipose tissue-derived stem cells and squamous cell-carcinoma cells: consequences for clinical applications. *Stem Cell Res Ther* **5**, 65, doi:10.1186/scrt454 (2014).

- 79 Deng, Y., Wan, Q. & Yan, W. Integrin alpha5/ITGA5 Promotes The Proliferation, Migration, Invasion And Progression Of Oral Squamous Carcinoma By Epithelial-Mesenchymal Transition. *Cancer Manag Res* **11**, 9609-9620, doi:10.2147/CMAR.S223201 (2019).
- 80 Zheng, W., Jiang, C. & Li, R. Integrin and gene network analysis reveals that ITGA5 and ITGB1 are prognostic in non-small-cell lung cancer. *Onco Targets Ther* **9**, 2317-2327, doi:10.2147/OTT.S91796 (2016).
- 81 Mittal, A., Pulina, M., Hou, S. Y. & Astrof, S. Fibronectin and integrin alpha 5 play requisite roles in cardiac morphogenesis. *Dev Biol* **381**, 73-82, doi:10.1016/j.ydbio.2013.06.010 (2013).
- 82 Chen, D. *et al.* Fibronectin signals through integrin alpha5beta1 to regulate cardiovascular development in a cell type-specific manner. *Dev Biol* **407**, 195-210, doi:10.1016/j.ydbio.2015.09.016 (2015).
- 83 Wu, X. B. *et al.* Mesenchymal stem cells promote colorectal cancer progression through AMPK/mTOR-mediated NF-kappaB activation. *Sci Rep* **6**, 21420, doi:10.1038/srep21420 (2016).
- 84 Yang, L. *et al.* Targeting cancer stem cell pathways for cancer therapy. *Signal Transduct Target Ther* **5**, 8, doi:10.1038/s41392-020-01110-5 (2020).
- 85 Liu, W. *et al.* TNF-alpha increases breast cancer stem-like cells through up-regulating TAZ expression via the non-canonical NF-kappaB pathway. *Sci Rep* **10**, 1804, doi:10.1038/s41598-020-58642-y (2020).





OPEN

# Adipose-derived mesenchymal stem cells promote the malignant phenotype of cervical cancer

Rosario Castro-Oropeza<sup>1</sup>, Karla Vazquez-Santillan<sup>1</sup>, Claudia Díaz-Gastelum<sup>1</sup>, Jorge Melendez-Zajgla<sup>2</sup>, Cecilia Zampedri<sup>2</sup>, Eduardo Ferat-Orsorio<sup>3</sup>, Arturo Rodríguez-González<sup>3</sup>, Lourdes Arriaga-Pizano<sup>4</sup> & Vilma Maldonado<sup>1</sup>✉

Epidemiological studies indicate that obesity negatively affects the progression and treatment of cervical-uterine cancer. Recent evidence shows that a subpopulation of adipose-derived stem cells can alter cancer properties. In the present project, we described for the first time the impact of adipose-derived stem cells over the malignant behavior of cervical cancer cells. The transcriptome of cancer cells cultured in the presence of stem cells was analyzed using RNA-seq. Changes in gene expression were validated using digital-PCR. Bioinformatics tools were used to identify the main transduction pathways disrupted in cancer cells due to the presence of stem cells. In vitro and in vivo assays were conducted to validate cellular and molecular processes altered in cervical cancer cells owing to stem cells. Our results show that the expression of 95 RNAs was altered in cancer cells as a result of adipose-derived stem cells. Experimental assays indicate that stem cells provoke an increment in migration, invasion, angiogenesis, and tumorigenesis of cancer cells; however, no alterations were found in proliferation. Bioinformatics and experimental analyses demonstrated that the NF-kappa B signaling pathway is enriched in cancer cells due to the influence of adipose-derived stem cells. Interestingly, the tumor cells shift their epithelial to a mesenchymal morphology, which was reflected by the increased expression of specific mesenchymal markers. In addition, stem cells also promote a stemness phenotype in the cervical cancer cells. In conclusion, our results suggest that adipose-derived stem cells induce cervical cancer cells to acquire malignant features where NF-kappa B plays a key role.

The accumulation of mutations, genetic predisposition of some factors, exposure to environmental agents, and lifestyle all play important roles in the carcinogenic process. Recent studies have revealed that obesity complicates the clinical course of cancer<sup>1-3</sup>. Obesity is defined as body mass index (BMI) over 30 kg/m<sup>2</sup> and is characterized by excessive accumulation of adipose tissue in the body. Interestingly, the International Agency for Research on Cancer (IARC) reported that body fatness increases cancer risk in 13 cancer types denominated obesity-related cancers (ORC), among them, cervical cancer (CC)<sup>4,5</sup>. Further supporting this association, Calle et al. studied approximately 90,000 women and reported that excess BMI is associated with an increased risk of invasive cancer<sup>6</sup>, with cervical cancer being one of the most affected by obesity, thus increasing the relative risk of death 3.2 times more in patients with BMI > 35<sup>6-8</sup>. The relationship between obesity and cancer may be explained by many factors, including altered hormonal signaling, chronic inflammation, fatty acid metabolism, abnormal regulation of insulin and other diet compounds involved in adipose tissue metabolism<sup>9-11</sup>.

Adipose tissue contains multipotent stem cells that are able to self-renew and differentiate into multiple cell lineages<sup>12</sup>. This cell population, referred to as ADSCs (adipose tissue-derived stem cells), has a crucial role in cancer<sup>13-15</sup>. ADSCs can be chemoattracted to solid tumors and secrete cytokines, including IL6 and vascular endothelial growth factor (VEGF), which promote the inflammatory microenvironment and influence tumorigenesis<sup>16-20</sup>. ADSCs could transform the behavior of tumor cells to make them more aggressive<sup>21,22</sup>, able

<sup>1</sup>Epigenetics Laboratories, National Institute of Genomic Medicine (INMEGEN), 14610 Mexico City, Mexico. <sup>2</sup>Functional Genomics Laboratories, National Institute of Genomic Medicine (INMEGEN), 14610 Mexico City, Mexico. <sup>3</sup>Gastrosurgery Service, UMAE, National Medical Center "Siglo XXI", Mexican Institute of Social Security (IMSS), Mexico City, Mexico. <sup>4</sup>Medical Research Unit on Immunochemistry, National Medical Center "Siglo XXI", Mexican Institute of Social Security (IMSS), Mexico City, Mexico. ✉email: vmaldonado@inmegen.gob.mx

to survive, proliferate<sup>23,24</sup>, migrate and seed new tumors. Recently, it has been proposed that the angiogenic and growth factors secreted by ADSCs greatly contribute to facilitating the access of nutrients and oxygen, allowing rapid tumor growth<sup>18</sup>. The molecular mechanism of the interaction between tumor cells and ADSCs is still unknown, so increased efforts are needed to understand how ADSCs contribute to tumor malignancy.

NF-kappa B is a family of transcription factors that regulate multiple genes involved in immune response, cell survival, proliferation, angiogenesis, and metastasis<sup>25–27</sup>. NF-kappa B signaling can be activated by the canonical pathway mainly characterized by the translocation of p50: p65 dimer or by the noncanonical pathway characterized by the translocation of p52: RelB dimer<sup>28,29</sup>. Notably, the NF-kappa B pathway is altered in obesity<sup>30,31</sup> and cancer pathologies<sup>26,27,32–35</sup>. In this study, we analyzed the biological impact and molecular mechanisms of ADSCs in CC cells that are still unknown. We cocultured HeLa cells with ADSCs, evaluated their transcriptome and performed in vitro and in vivo assays to reveal the influence of ADSCs and the molecular mechanisms that alter the phenotype of CC cells.

Our results showed that ADSCs promote cell movement, angiogenesis, migration, and the epithelial–mesenchymal transition (EMT) and increase the malignant properties of CC cells through the positive regulation of NF-kappa B signaling, a pathway involved in initiation, progression and resistance to treatment in various types of cancer.

## Materials and methods

**Cell culture.** HeLa, SiHa, CaSki, HaCaT and ADSC were obtained from ATCC (Manassas, VA, USA) and cultured in DMEM medium supplied with 5% fetal bovine serum (FBS) (ATCC, 30-2020) at 37 °C/5% CO<sub>2</sub>. To grow and expand ADSCs we used a commercially available medium (Mesenchymal Stem Cell Basal Medium, ATCC PCS 500030) containing essential and non-essential amino acids, vitamins, other organic compounds, trace minerals, and inorganic salts. This medium was supplemented with a specific growth kit for ADSC (ATCC No. PCS500040) containing the following growth supplements: (low serum (2% FBS), FGF basic, EGF and L-alanyl-L-glutamine).

**Isolation, culture and characterization of ADSCs.** Adipose tissue samples were obtained from 3 female cancer-free patients undergoing gastric bypass, with BMI > 40. The samples were collected from Specialty Hospital, XXI Century National Medical Center of the Mexican Social Security Institute (IMSS). This study was conducted according to institutional guidelines under an approved protocol by the ethics committee of Comité Local de Investigación del Hospital de Especialidades “Dr. Bernardo Sepúlveda Gutiérrez” del Centro Médico Nacional Siglo XXI del Instituto Mexicano del Seguro Social. All donors provided written informed consent.

The enriched ADSC population was isolated from excised human adipose tissue as previously published<sup>36,37</sup>. Briefly, freshly tissues were washed with PBS and minced into small pieces and samples were incubated with collagenase I at 0.075% (SCR103, Millipore USA MA) for 40 min at 37 °C with gently shaker. After centrifugation, the stromal fraction containing the ADSC was collected and seeded with DMEM medium supplemented with streptomycin/penicillin 1X (30-2300 ATCC, Virginia, USA) and 5% FBS. ADSCs were expanded in DMEM-5% FBS.

The identity of the ADSCs, the expression of stromal markers (CD44 (MACS Miltenyi Biotec 130-095-195, CA, USA), (CD90 Millipore FCMAB211F, MA, USA) were analyzed by Flow Cytometry. Also, we analyzed the absence of hematopoietic marker (CD31, CBL468F Millipore, MA, USA), and endothelial marker (CD45 FCMAB118F Millipore, MA, USA). The mouse IgG1-PE (103.092-212 MACS Miltenyi Biotec) and Mouse IgG-FIT (130-092-213 MACS Miltenyi Biotec) were used how isotype control antibodies.

**HeLa-ADSC coculture assays.** Indirect coculture assays were used in order to guaranty the isolation of the two cell lines through a permeable membrane, but also to kept them in the same microenvironment. HeLa cells (950,000) were seeded in the upper compartment of a Transwell system (#3420 Corning Costar, NY, USA) with a pore size of 3.0 µm. Subsequently, 450,000 ADSCs obtained from patients or from the ATCC were seeded onto the lower compartment. The coculture remained for 24 h in serum-free DMEM.

**Production of conditioned medium.** *Coculture conditioned medium (Coculture-CM).* Serum-free DMEM was harvested from the 24 h HeLa-ADSC coculture. *ADSC conditioned medium (ADSC-CM)* ADSCs (450,000) were seeded and cultured with serum-free DMEM for 24 h. *HeLa conditioned medium (HeLa-CM)* HeLa cells (950,000) were seeded and cultured with serum-free DMEM for 24 h. All generated media were filtered to eliminate any cells.

**RNA sequencing.** Total RNA was isolated from HeLa and HeLa cells co-cultured with ADSC (N = 3) using QIAzol (79306, QIAGEN, MD, USA). RNA concentration and integrity were evaluated using a Bioanalyzer, only samples with an RNA integrity number (RIN) greater than 9 were considered for subsequent analysis. HeLa cells cultured in the presence or absence of ADSC was subjected to RNAseq analysis by Illumin platform (GAII). Three biological replicates were used for the analysis and 20 millions of “reads” per replicate were obtained approximately. Sequencing data were analyzed with CLC Genomics workbench (7CLC BioCambridge), and differential expression was determined between groups using the EdgeR algorithm. Only genes with a fold change increment higher than 2 or less than - 2, a p-value ≤ 0.05, and adjusted p-values (FDR) ≤ 0.1 were further considered for subsequent analysis. In order to validate RNAseq data we elected DE genes with mid to high read counts since the variance in those data is less and the differences are more reliable. We also check the expression values of those transcripts across replicates and we choose genes with constant read counts between replicates. Finally, we use databases such as IPA and Metacore to dissect the functional interpretations of DE genes and

select candidate genes according to its relevance in cancer development and progression. Elected genes were analyzed by Digital PCR.

**Gene set enrichment analysis (GSEA).** We imported the data obtained from our RNAseq to the GSEA software downloaded from the website: <https://software.broadinstitute.org/gsea/index.jsp>. The sets of genes related to different gene ontology processes served as reference genes to determine the biological processes enriched in our data. We only consider gene set enrichment dataset having a false discovery rate (FDR) < 0.25 and a normalized enrichment score (NES) > 1.2.

**Key pathway analysis.** Ingenuity Pathway Analysis software (IPA-QIAGEN), Metacore software and Key Pathway Advisor were used to identify the main biological processes altered by the presence of ADSC in HeLa, as well as to infer which genes are involved in the regulation of essential cellular pathways. Those tools use the list of differentially expressed.

**Overall survival analysis.** Overall survival of CC patients was analyzed in the website: <https://kmplo.t.com/analysis/>. The software simultaneously integrates gene expression and clinical data. We used the Pan-cancer RNA-seq section and analyze only cervical squamous cell carcinoma to generate each Kaplan–Meier survival graph, then, we calculated the risk ratio with a 95% confidence interval and the p value of logarithmic range.

**Droplet digital PCR.** All ddPCR assays were performed using the QX200 digital drop PCR system according to the manufacturer's instructions (Bio-Rad)<sup>38</sup>.

Briefly, each reaction of EvaGreen ddPCR Supermix (#1864034) including the specific primers and cDNA was emulsified with oil (#1864006) and fractionated up to 20,000 drops in the QX200 generator. The droplets were transferred to a 96-well plate (#10023379) to carry out a PCR amplification following these conditions: 1 × (95 °C for 5 min), 40 × (95 °C for 30 s, T<sub>m</sub> °C for 30 s, 72 °C for 30 s), 1 × (4 °C for 5 min, 90 °C for 5 min), 10 °C ∞. The positive drops containing at least one copy of amplifiable cDNA, exhibited an increase in fluorescence compared to negative drops. Fluorescent drops were quantified with the QX200 Droplet reader detector. Data analysis was performed in the QuantaSoft software and absolute expression values in copy number per μl were calculated using statistics for a Poisson distribution. Results are represented in copy number per μl of amplifiable cDNA.

**In vitro cell migration and invasion assays.** To evaluate cell migration and invasion capacity of CC cells cultured in the presence of different chemoattractants (ADSC, NH3T3 cells, different CM, 5% FBS or serum free medium).

Cells (35,000) were seeded in the upper chamber and cultured in serum free medium, subsequently, 600 μl of medium with different chemoattractants were added. Cells were cultured at 37 °C and 5% CO<sub>2</sub> for 24 h. The inserts were then removed from wells and cells on the upper surface of the transwell membrane were removed. Migrating cells located on the lower surface were rinsed with PBS and fixed with 4% paraformaldehyde (PFA). Finally, cells were stained with 0.1% crystal violet and images captured in a stereomicroscope were used to calculate migrating cells using the ImageJ software.

For the invasion assays, transwells covered with 50 μl of Matrigel were used. A total of 35,000 cells were seeded with serum-free medium in the upper chamber and subsequently, 600 μl of the corresponding chemoattractants were placed in the lower chamber. All conditions were carried out in the same way as the migration assays. At least three independent replicates and three technical replicates were carried out for each culture condition.

**Cell proliferation assays.** Cell proliferation of HeLa cells was evaluated by the MTS method under two experimental conditions: (A) HeLa vs. HeLa co-cultured with ADSC. (B) HeLa in the presence of different medium (serum-free DMEM, DMEM supplemented with 5% FBS, conditioned medium of ADSC, conditioned medium of HeLa and medium obtained from HeLa-ADSC co-culture).

Briefly, 7,000 cells were seeded in triplicates in 96-well plates and incubated at 37 °C in a 5% CO<sub>2</sub> atmosphere in serum-free DMEM for condition "A" and in the correspondent medium for condition "B". Cell proliferation was evaluated at 0, 24 h, 48 h, 72 h, 100 h and 124 h and cells were incubated with the MTS reagent for 1 h. Late, cell proliferation was quantified using the CellTiter-96 non-radioactive cell proliferation assay kit (#G4000, Promega). Absorbance was measured at an optical density of 590 nm using a multidetector reader (Bekman Coulter).

**Cell cycle.** Cell cycle assays were performed by flow cytometry using the DNA Reagent Kit (Cycletest Plus #340242, BD, Billerica, MA) following the manufacturer's recommendations.

**Immunofluorescence assays.** HeLa cells were grown on glass coverslips in 6-well plates and exposed to conditioned medium obtained from ADSC or serum-free medium during 24 h. Cells were then rinsed with 1X PBS and fixed with 4% paraformaldehyde (Sigma-Aldrich, St. Louis, MO, USA) for 30 min. Subsequently, cells were blocked with PBS and 5% bovine serum albumin (Sigma-Aldrich) for 2 h and then cells were incubated overnight in a humid chamber with the corresponding primary antibody: RelB, p65, p52, Vimentin, Fibronectin, N-cadherin or E-cadherin (Thermo-Fisher). The cells were washed and incubated with a corresponding secondary antibody (#W4028 or #W4018 Promega) for 1 h. Finally, cells were washed with PBS and the slides were mounted in Everbrite mounting medium with DAPI (Biotium Inc., Hayward, CA, USA) and stored at 4 °C. The fluorescence analysis was performed in a confocal microscope (Zeiss LSM 510).

**Zebrafish husbandry and xenotransplant assays.** Zebrafish (*Danio rerio*) were maintained at a temperature of 28.5 °C on a pH of 7.4 with a 14 h. on and 10 h. off light cycle. We use a Tab Wik genetic background (provided by Dr. Ernesto Maldonado from ICMYL-UNAM and Dr. Francisco Carmona from IFC-UNAM), and we also use a zebrafish model (Tg(*fli1a:EGFP*)) harboring GFP expression in blood vessels (donated by Dr. Fernando López-Casillas from IFC-UNAM).

Zebrafish xenotransplants assays were approved by ethic Committee of INMEGEN. Animal care and husbandry followed international ethics standards.

For xenotransplant experiments, two days post-fertilization (dpf) zebrafish embryos were dechorionated and anesthetized with tricaine (MS-222; Sigma), then, cells were microinjected into the embryonic yolk sac region. To analyze the tumorigenic ability, 300 SiHa cells were injected in combination with 50, 100, 150 or 300 either ADSC, NIH3T3 or HaCaT cells into the yolk of Tab-wik zebrafish embryos. The microinjection protocol was carried out as previously reported<sup>39</sup>. For the migration assays, SiHa cells were transfected using Xfect (Clontech) and 5 µg of plasmid pGFP-R-VS or stained with a red PKH26-GL dye. Embryos were analyzed at 12 hpi (hours post injection) using an epifluorescence microscope (Zeiss). Four dpi (days post injection), larvae were analyzed by stereoscope to evaluate tumor formation.

**Extreme limiting dilution assays (ELDA).** In vivo limiting dilution assays were analyzed using the ELDA software. This model is focused on the estimation of the stem cell frequency across multiple data sets<sup>40</sup>. ELDA analysis considers the number of individuals who failed to form a tumor when limited cell dilutions are employed. The generated graph represents the slopes of the active cells logarithmic fraction with a 95% confidence interval.

**Angiogenesis.** The zebrafish model Tg (*fli1a: EGFP*) was employed to inoculate SiHa cancer cells marked with a red PKH26-GL dye. The migration was evaluated at 12 hpi, and the formation of new blood cells was evaluated at 12 h and 3 days after the injection.

**Statistical analysis.** At least 3 biological replicates of each experiment were made. Data were analyzed with the GraphPad Prism 5 program, in which Student's t test or ANOVA was performed as appropriate, considering a p value of <0.05 as statistically significant. The graphs show the average of the three replicates and the standard deviation (± SD).

## Results

**Isolation and characterization of ADSCs.** ADSCs were derived successfully from adipose tissue of 3 female cancer-free patients with morbid obesity (Fig. 1a). After a couple days of culture, ADSCs exhibited a stable spindle-shaped morphology (Supplementary Fig. 1). To further verify the identity and purity of ADSCs, we employed flow cytometry to examine the cell surface markers of three different cultures. We confirm that most of the cells express the appropriate positive ADSCs markers (CD44 and CD90) and very few cells express negative markers (CD31 and CD45). These results show that ADSCs exhibit the typical immunophenotype of ADSCs with expression rates of CD44 (96%), CD90 (95%), CD31 (0.36%) and CD45 (0.16%) (Fig. 1b). Taking together those results we verify that primary cultures are constituted by an enriched population of ADSCs.

**Coculture of HeLa/ADSCs induce changes in the transcriptome of HeLa cells.** To assess whether ADSCs influence the behavior of CC cells, we cocultured HeLa cells with ADSCs obtained from patients. We employed an indirect coculture system where both ADSCs and CC cells are cultured under the same conditions but are physically separated by a permeable membrane thus avoiding direct contact but allowing cell communication (Fig. 1c). To evaluate the effect of ADSCs on the behavior of CC cells, we first evaluated the transcriptome of HeLa cells with the aim to identify the main processes and molecules affected by the presence or absence of ADSCs.

Transcriptome analysis revealed that HeLa cells cocultured with ADSCs have a total of 95 differential expressed (DE) RNAs (fold change > 2 or < - 2, p-value < 0.05 and FDR < 0.1) of which 66 transcripts were consistently upregulated and 29 were downregulated (Fig. 1d).

To elucidate the effects of ADSCs on the behavior of cervical cancer cells, we performed a network enrichment analysis using Ingenuity Pathway Analysis (IPA), Metacore and Key pathway Advisor (KPA). As shown in Fig. 1e, the interaction of ADSCs with HeLa cells disrupts the expression of genes involved in cellular processes, including cell motility, cell death, cell communication, developmental process, and proliferation. In addition, we found specific processes networks enriched in our data, these include the epithelial-mesenchymal transition, angiogenesis, inflammation mediated by interleukin-6 (IL6) signaling and cell adhesion (Fig. 1f), these networks represent a recognized larger group of interactions and/or pathways. Remarkably, EMT was the most enriched process in our data, those results suggest that ADSCs may influence HeLa cells to induce EMT, a biological process that allows epithelial cells to lose their polarity and undergo biochemical changes to acquire migratory and invasive properties. Besides, the most deregulated top genes are mainly associated with migration, cell adhesion, invasion, and metastasis (Fig. 1h).

In addition, KPA and Metacore predict that the activity of NF-kappa B is altered in HeLa cells cocultured with ADSCs and could be an essential regulatory hub, which drives differential expression changes (Fig. 1g). Interestingly, it has been shown that NF- kappa B is essential for both the induction and maintenance of EMT



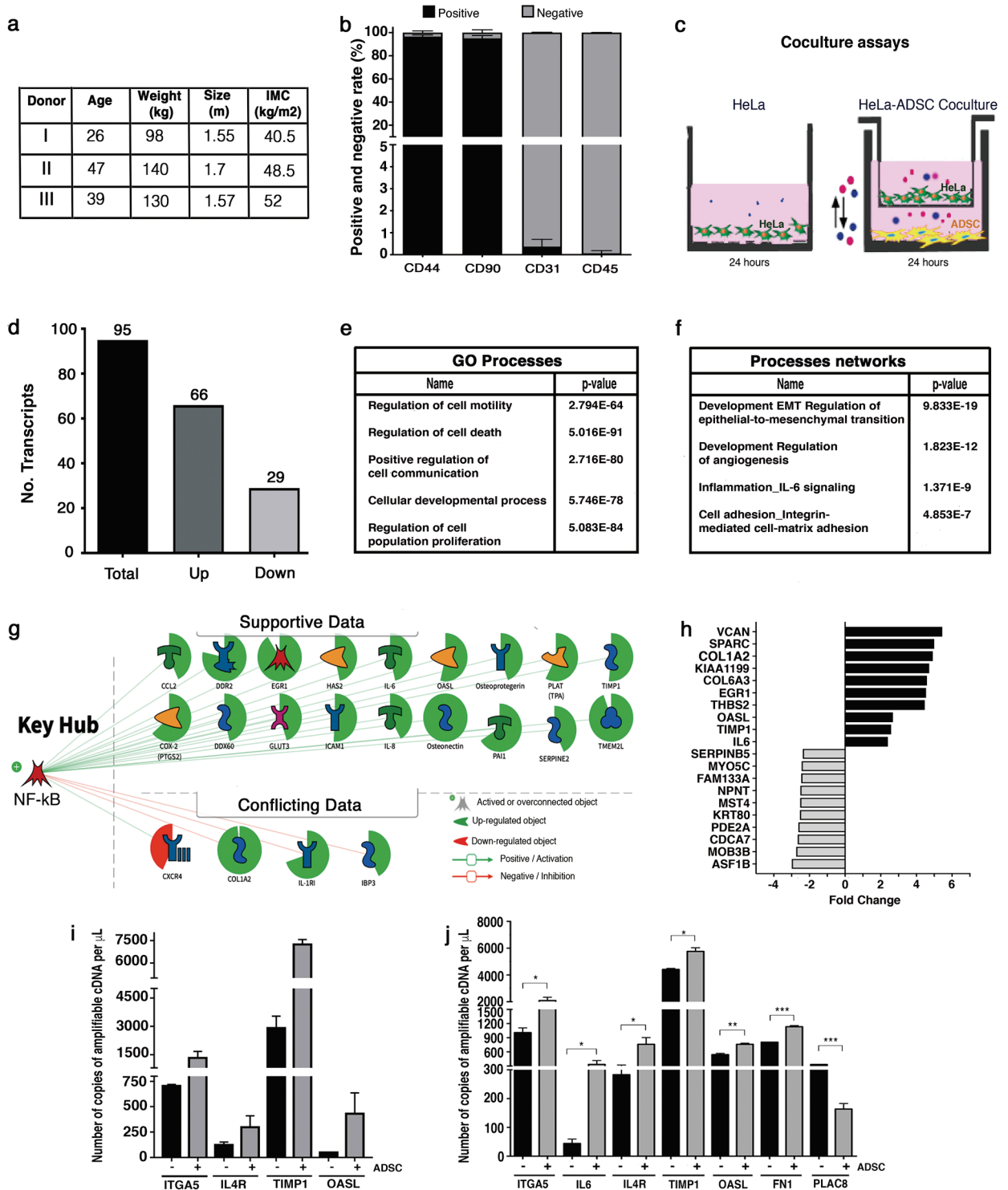


**Figure 1.** The coculture of HeLa/ADSC induces changes in the transcriptome of HeLa cells. (a) ADSCs were obtained from three donor patients. The table summarizes the main characteristics of the donor patients who underwent gastric bypass. (b) The purity of ADSCs in each patient was evaluated by flow cytometry analysis of cell surface markers including CD44, CD90, CD31 and CD45. The graph shows the percentage of positive and negative cells to each marker ( $n=3$  patients, 2 replicates, error bars = s.d.). (c) HeLa cells were cultured alone or in the presence of ADSCs by an indirect coculture system. The picture show that both cells lines are cultured in the same medium, but they are physically separated by a permeable membrane avoiding direct contact. (d) Bar chart shows the mRNAs altered in HeLa cells due to the presence of ADSCs. (e) The table shows the main molecular and cellular processes altered during coculture in HeLa. (f) The table shows the processes networks enriched during coculture in HeLa. (g) Schematic overview showing NF-kappa B as essential key hub driving gene expression, which was predicted to be activated in HeLa cells cocultured with ADSCs. (h) Top 20 differentially expressed genes in HeLa during coculture with ADSCs. (i–j). Quantification of gene expression by ddPCR showing the validation of mRNAs altered in HeLa by the presence of ADSCs obtained from patients (j) or ATCC (k). Graphs represent three biological replicates, and the error bars are s.d., \* $p < 0.05$ ).

in many kinds of cancer cells<sup>41–44</sup>. Taken together those results suggest that HeLa cells may acquire migration abilities probably associated to the induction of EMT.

To validate sequencing data we employed both ADSC-derived from Mexican patients and an ADSC cell line obtained from ATCC. We performed Digital PCR to quantify the expression levels of differentially expressed mRNAs. Our data showed that all transcripts analyzed (ITGA5, IL4R, TIMP1 and OASL) were successfully validated in both ADSCs obtained from Mexican patients and ADSCs provided from ATCC. Figure 1i–j shows that all mRNAs shift its expression levels in HeLa cells due to the presence of both patient-derived ADSCs or ADSC obtained from ATCC. We further analyze the expression of three more transcripts (IL6, FN1, and PLAC8) using ADSC obtained from ATCC and observed that all mRNAs were well validated (Fig. 1j).

We performed a survival analysis with six DE RNAs using expression data from 304 patients with CC. Kaplan–Meier curves show the association between gene expression and cancer survival (Fig. 2a–f), data indicate that patients with high expression of ITGA5 and FN1 exhibit lower survival (Fig. 2a,d), while the low expression of PLAC8 is associated with shorter survival (Fig. 2e). However, the expression of IL6, IL4R, TIMP1 was not significantly associated with cancer survival and may possibly be associated with another biological process altered by ADSC (Fig. 2b,c,f). Taken together, these data suggest that ADSCs could increase the malignant phenotype of CC.

**Effect of ADSCs on the proliferation of CC.** The expression of genes involved in proliferation was altered during the coculture of HeLa/ADSCs; however, the cell cycle analysis showed no changes (Fig. 2g). We also did not find any difference in the number of HeLa cells respect to HeLa cells cocultured with ADSCs in a proliferation assay with MTS during 124 h (Fig. 2h). In addition, we tested the ability of tumor cells to proliferate in the presence of different conditioned media obtained from ADSCs, HeLa cells or HeLa-ADSCs (Fig. 2i–j). HeLa cells cultured with DMEM at 5% FBS were used as a positive control (Fig. 2j). There was no significant change in the proliferation of HeLa cells treated with conditioned medium. Overall, these findings demonstrate that ADSCs have no influence on the proliferation and death of tumor cells.

**ADSCs promote the migration and invasion of CC.** Bioinformatic analysis predicts cell migration to be altered in HeLa cells cultured in the presence of ADSCs (Fig. 1e). To assess whether ADSCs influence the migration or invasion abilities of CC, we used transwells and evaluated the behavior of HeLa, CaSki and SiHa cells cultured in the presence of some chemoattractants, including ADSCs, conditioned medium obtained from the coculture of HeLa/ADSCs, conditioned medium of ADSCs and fibroblasts (NIH3T3). Conditioned mediums were obtained under serum free conditions after 24 hr of the coculture of CC cells in the presence of ADSCs (Coculture CM) or the culture of ADSCs alone (ADSCs CM). As a positive control of migration, cells were stimulated with DMEM supplemented with 10% FBS and as a negative control we employed DMEM without FBS.

Our results showed that ADSCs promote a drastic increment in the migration ability of HeLa, CaSki and SiHa cells compared to unstimulated cells (Fig. 3a–c). Strikingly, ADSCs acted as a powerful chemoattractant since HeLa and SiHa cells reached 807% and 1758% more migration abilities compared to cells stimulated with 10% FBS (Fig. 3a,c). Interestingly, HeLa cells exhibit very little migration ability when stimulated with fibroblast (NIH3T3) (Fig. 3a). These results highlight the biological significance of ADSCs in improving the migration of cancer cells. To test whether the factors secreted by ADSCs influence the migration of CC cells, we test the migration ability of CC cells stimulated with conditioned medium of ADSCs. Our results showed that conditioned medium of ADSCs increase the migration of HeLa (300%), CaSki (245%) and SiHa (1885%) cells when compared with cells stimulated with 10% FBS. These results indicate that CC cell lines expose to the ADSCs or the conditioned medium of ADSCs exhibit a dramatic increment in the migration ability of CC.

Because invasion allows cells to spread toward distant sites and colonize tissues, we determined the influence of ADSCs on the invasion of CC. We performed invasion assays using Matrigel-coated Boyden chambers, as shown in Fig. 3d–f, the invasion capacity of HeLa, CaSki and SiHa cells drastically increases 767%, 1,080% and 549% respectively when they are chemoattracted by ADSCs in contrast to cells stimulated with 10% FBS. Consistently, the conditioned medium of ADSCs also increase the invasion of all CC cells (Fig. 3d–f).

Taken together, these data indicate that ADSCs induce profound changes in cell migration and invasion, thus conferring advantages to CC. Interestingly, an IPA analysis showed that different regulated genes were positively associated with the invasion and migration process in cancer cells: VCAN, SPARC, IL6, MMP14, IL4R, ICAM, TIMP1 and IGF2 (Fig. 3g–i).

To confirm the influence of ADSCs on the migration or invasion ability of CC cell lines, we conducted in vivo experiments using zebrafish embryos (*Danio rerio*). Those experiments were performed in SiHa cell line, due to it has a higher tumorigenic ability than HeLa (data not shown). SiHa cells were transfected with a plasmid carrying a GFP gen (Fig. 4a) or were stained with the PKH26-GL dye (Supplementary Fig. 2). A total of 300 SiHa cells expressing GFP or labeled with a dye in the presence or absence of ADSCs were injected into the zebrafish embryonic yolk sacs at 48 hpf. The number of inoculated cells did not affect embryo viability during a 7-day trial (data not shown). Migration and invasion were evaluated at 12 h after the injection. Embryos injected only with SiHa displayed few fluorescent sporadic cells throughout the embryo; in contrast, SiHa cells inoculated with ADSCs exhibited higher migration observed throughout the body, eyes and tail of the embryo. In some cases, we observed cell invasion and subsequent tail metastasis. These data suggest that the presence of ADSCs promotes the migration and invasion ability of CC cells (Fig. 4a and Supplementary Fig. 2).

**ADSCs promote tumor growth.** Subsequently, we evaluated whether ADSC could contribute to CC progression; thus, we performed coinjections of 300 SiHa cells with different dilutions of ADSC cells (50, 100 or 150) and monitored tumor growth. In addition, tumor formation was also monitored in coinjected embryos

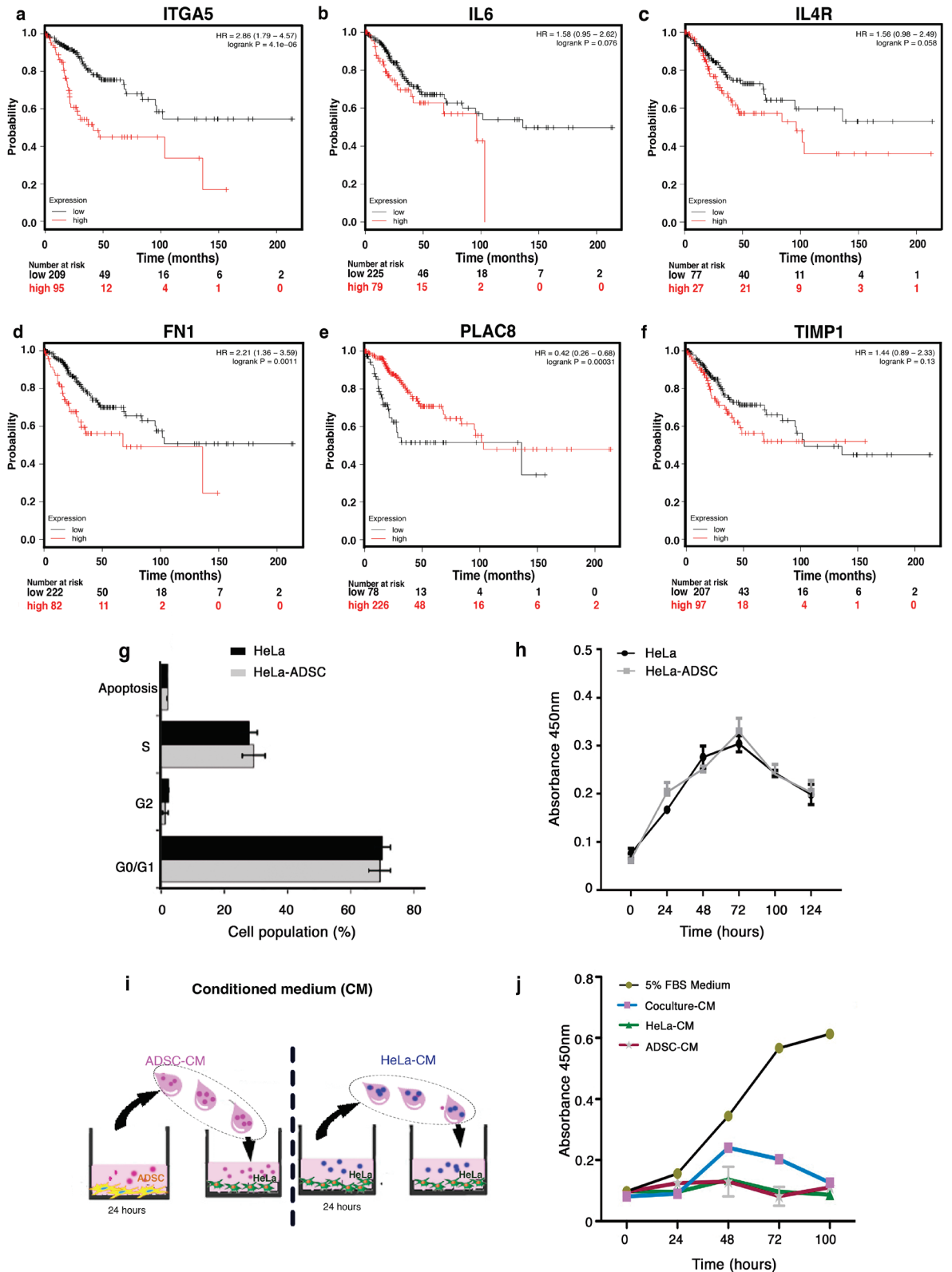


**Figure 2.** Deregulated genes altered by the presence of ADSC exhibit clinical significance in cervical cancer patients. (a–f) Kaplan Meyer curves comparing the overall survival of 304 cervical squamous cell carcinomas with low versus high expression of altered genes (ITGA5, IL6, IL4R, FN1, PLAC8, TIMP1). Data were obtained from a public database: KM Plotter. The “p” values are shown in each of the graphs. ADSCs do not alter the proliferative capacity of HeLa cells. (g) Cell cycle analysis of HeLa cells cocultured in the presence of ADSCs compared to HeLa control cells. (n = 3, the error bars are s.e.m) The graph shows no significant changes in any of the phases of the cell cycle. (h) Proliferation assay of HeLa control vs HeLa cells cocultured at different times. (i) The picture shows the method to obtain the conditioned medium of ADSCs (ADSC-CM) or the conditioned medium of HeLa cells (HeLa CM). ADSCs or HeLa cells were cultured in serum-free DMEM for 24 h and then the conditioned medium was employed to culture CC cells. (j) Proliferation assay of HeLa cells cultured with different conditioned media (CM) at different times. (n = 3, the error bars are S.D., but no significant changes were shown).

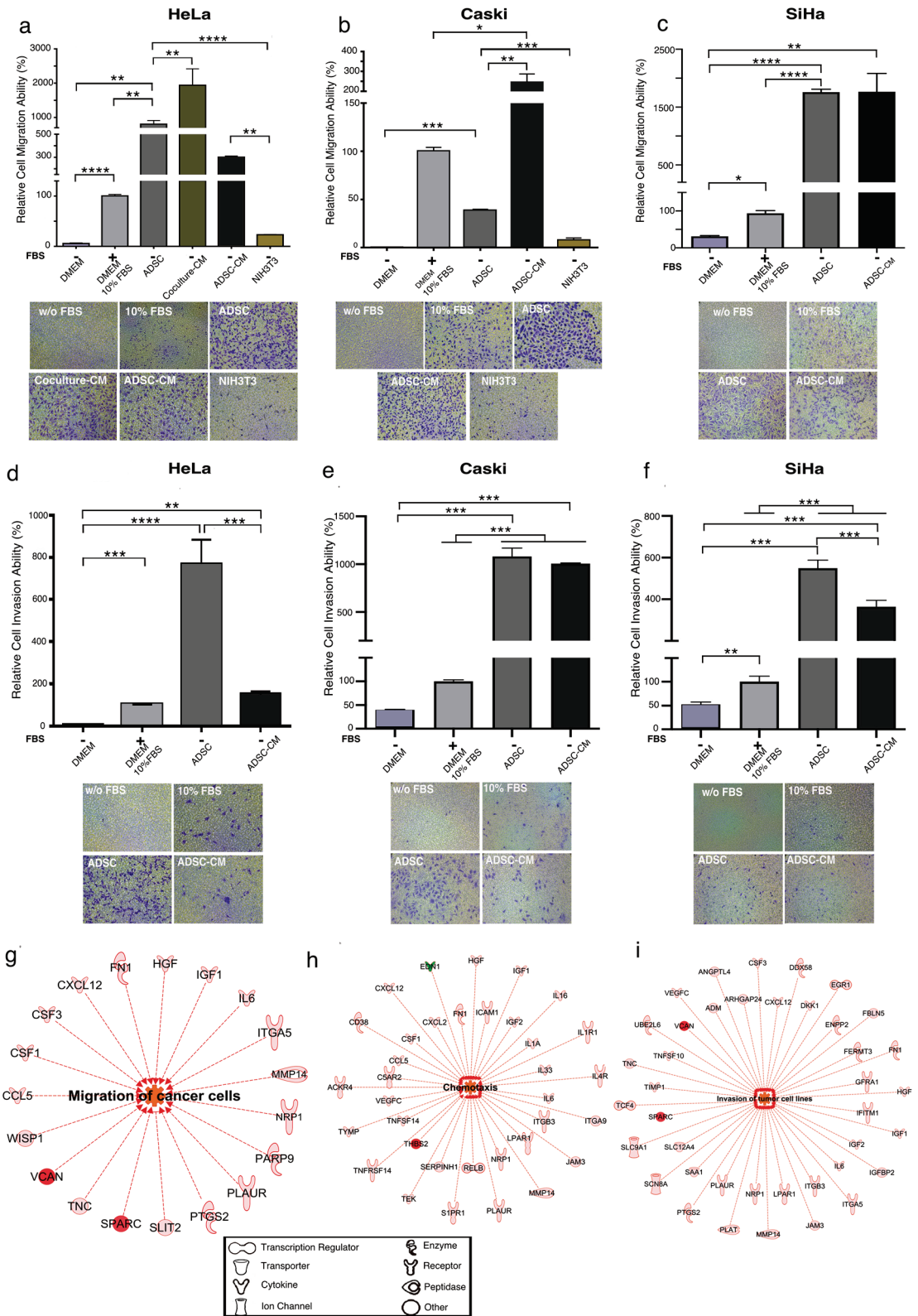


**Figure 3.** ADSCs influence the migration and invasion of cervical cancer cells. Graph shows the migration ability of HeLa (a), CaSki (b) and SiHa (c) cells cultured without serum and exposed to different chemoattractants including ADSCs, conditioned medium of coculture (Coculture-CM), conditioned medium of ADSCs (ADSC-CM) and NIH3T3 cells. As a control, CC cells were also cultured with DMEM supplemented with 10% FBS or without FBS. The graph shows the relative percentage of the migration capacity of HeLa, CaSki and SiHa cells after 12 h (a–c). The graph represents three biological replicates, error bars are s.d and \*p < 0.05. Pictures show a representative image of the migratory CC cells in each condition. (d–f) Figures show the relative percentage of invading HeLa, CaSki and SiHa cells after 12 h of exposure to various chemoattractants. Figures show a representative image of invading cells in each condition. The graph represents three biological replicates, error bars are s.d and \*p < 0.05. IPA analysis showing that the main altered transcripts in HeLa cells cultured in presence of ADSCs are involved in migration (g), chemotaxis (h), and invasion (i). The networks show differentially expressed genes regulated by each signaling pathway. The red color indicates the overexpression of the transcripts.



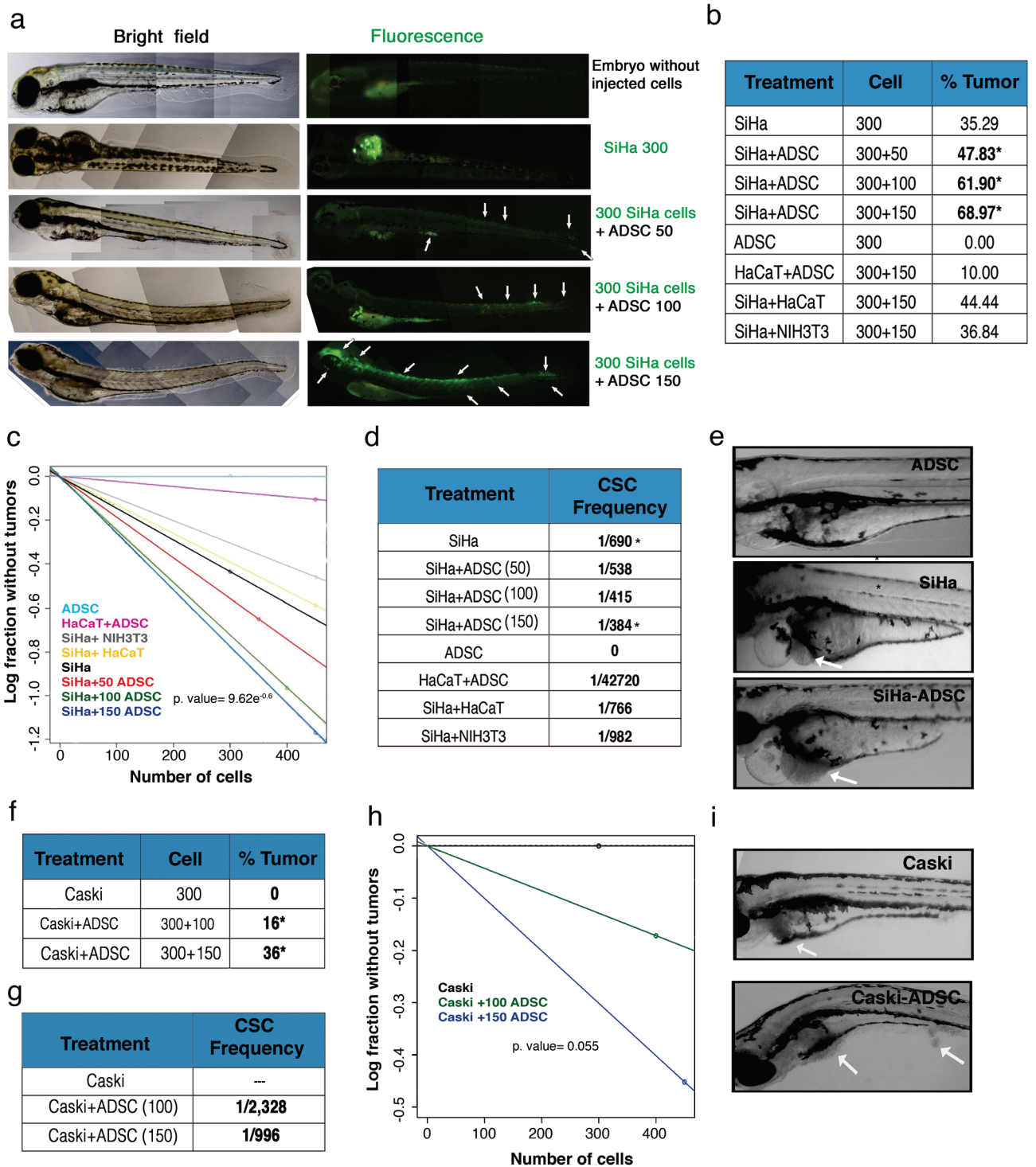


**Figure 4.** ADSC increases the CSC population, migration and invasion in an in vivo model. (a) Images show that the migration capacity of SiHa cells increases proportionally with respect to the amount of ADSCs inoculated in zebrafish embryos after 12 h. SiHa cells are shown in green due to they were transfected with a plasmid harboring a GFP gene. The images show a gradual increase in the migration and invasion of cancer cells from the yolk to the tail of embryos due to the presence of ADSCs. The white arrows show the migration areas in the embryo. (b) The table shows the number of cells inoculated in zebrafish embryos and the proportion of tumors formed in each condition. SiHa, SiHa + ADSC, or control cells: ADSC, HaCaT + ADSC, SiHa + HaCaT and SiHa + NIH3T3 were inoculated into zebrafish embryos, and the tumors were monitored every day for 5 days. (c) The graph depicts the frequency of CSC in each condition representing the number of cells injected with respect to the logarithmic fraction of animals without tumors. (d) The table shows the frequency of CSC calculated based on the ELDA software. (e) The images show tumors developed during 5 days in zebrafish embryos inoculated with ADSC, SiHa or SiHa + ADSC cells. Each experiment was repeated at least three times. (f) The table shows the number of cells inoculated in zebrafish embryos and the proportion of tumors formed in embryos injected with CaSki cells or CaSki + ADSCs cells. (g) The table shows the frequency of CSC calculated based on the ELDA software. (h) The graph depicts the frequency of CSC in each condition representing the number of Caski cells injected with respect to the logarithmic fraction of animals without tumors. (i) The images show tumors developed during 5 days in zebrafish embryos inoculated with CaSki or CaSki + ADSC cells.

with the following controls: ADSC + HaCaT, SiHa + HaCaT and SiHa + NIH3T3 (Fig. 4b). As shown in Fig. 4b, the coinjection of SiHa cells with different numbers of ADSCs promoted an increase in the number of embryos with a tumor; notably, this increase was dependent on the number of ADSCs injected. The results show that SiHa cells produced tumors in 35% embryos, while SiHa-ADSCs could develop tumors in 69% embryos. As expected, ADSCs alone did not develop any tumor, even when these cells were inoculated in higher amounts. The coinjection of ADSC/HaCaT only developed tumors in 10% embryos, while SiHa/HaCaT or SiHa/NIH3T3 exhibited the same tumorigenic potential as SiHa cells injected alone.

In addition, we calculated the frequency of cancer stem cells (CSCs) in each condition through an ELDA analysis. Figure 4c and d shows an increment in the CSC proportion observed in tumors formed by SiHa-ADSC with 1 CSC per every 384 cells; these tumors have approximately 55.6% more CSCs than in the tumors derived from SiHa alone. As expected, tumors derived from HaCaT + ADSC, SiHa + HaCaT or SiHa + NIH3T3 exhibit lower numbers of CSCs than in the tumors derived from SiHa. Interestingly, SiHa cells coinjected with ADSC produced larger tumor nodules compared with tumors generated only by SiHa cells (Fig. 4e).

The relevance of ADSCs in the tumorigenesis, is further supported by another CC cell line, in which we observed that CaSki cells by themselves are unable to form tumors while cells inoculated with ADSCs can produce tumors in 36% embryos (Fig. 4f,i). Furthermore, we observed that the number of CSCs increased in CaSki cells inoculated with higher amounts of ADSCs (Fig. 4g). As shown in Fig. 4h, CaSki cells inoculated with bigger amounts of ADSCs had 1 CSC per every 996, while cells injected with lower quantity of ADSCs only had 1 CSC per 2,328 cells. These results indicate that the presence of ADSCs improves the tumorigenic potential of CC cells and increases the frequency of CSCs.

**ADSC induces the activation of the NF-kappa B pathway in CC cells.** Interestingly, the data analysis with IPA software suggests that most deregulated genes culminate in NF-kappa B pathway activation during the coculture of HeLa/ADSCs. A Gene Set Enrichment Analysis (GSEA) confirmed that NF-kappa B signaling was enriched (p-value = 0, FDR = 0.049 and NES = 1.61) in HeLa cells cultured in the presence of ADSCs (Fig. 5b and c). Figure 5a shows a heat Map exhibiting differentially expressed genes with high significance. Among these genes, we found RelB, a player in noncanonical NF-kB signaling, which is highly expressed in HeLa/ADSCs. The GSEA showed 23 DE RNAs associated with the NF-kappa B pathway, including CXCL2, RELB, BCL3, FOS, BCL6, IL1A, and IL6 (Fig. 5c,d).

To validate and determine which NF-kappa B molecules are involved in the CC regulation mediated by ADSC, we performed immunofluorescence analysis of key NF-kappa B proteins (Fig. 6). As shown in Fig. 6a, immunofluorescence analyses showed that the conditioned medium of ADSCs induced an increase in RelB expression (Fig. 6a,b) as well as its nuclear translocation in HeLa cells. In addition, we observed a slight increase in p52 phosphorylation in HeLa cells cultured with the conditioned medium of ADSCs (Fig. 6c,d). Interestingly, the levels of p65, a canonical NF-kappa B player, were also increased, thus implying crosstalk between canonical and noncanonical NF-kappa B signaling (Fig. 6e-f). In fact, accumulating evidence suggests that RelB can regulate the expression of subunits of the canonical NF-kappa B pathway.

To verify the involvement of ADSCs in the regulation of non-canonical NF-kappa B molecules, we also analyze the expression of p52 and RelB in SiHa or CaSki cells cocultured with conditioned medium of ADSCs (Fig. 7a-h). We observe that the conditioned medium of ADSCs induced a notorious increment in the expression of both RelB (Fig. 7a,b) and p52 (Fig. 7c,d) in the SiHa cells. We also observed that some CaSki cells exhibit an increment in the expression of RelB when they are cultured with conditioned medium of ADSCs (Fig. 7e,f). Supporting previous results, we also demonstrated that the conditioned medium of ADSCs induces an increment in the phosphorylation of p52 in the CaSki cells (Fig. 7g,h). Taking together these results suggest that ADSCs could induce the activation of the noncanonical NF-kappa B pathway.

**ADSC induces a stem cell phenotype and EMT in CC cells.** Compelling evidence suggests that NF-kappa B signaling participates in the regulation of stem cell-associated genes. Notably, RelB is overexpressed in the mesenchymal fraction of some tumor types, so we assessed whether ADSCs could increase stemness in HeLa cells. Our results showed that HeLa cells cultured in the presence of ADSCs exhibit increased expression of stem cell markers, such as OCT4, KLF4 and ABCG (Fig. 8a-c). These results are in agreement with the ELDA analysis, which calculated a higher frequency of CSCs in tumors grown by SiHa and CaSki cells inoculated in the presence of ADSCs (Fig. 4d,h). Remarkably, we observed that HeLa cells cultured in the conditioned medium of ADSCs exhibit a distinctive morphonology similar to a mesenchymal phenotype with elongated shape and loss of cell contact (Fig. 8d). This feature is consistent with the bioinformatic analysis inferring that the EMT program is altered in HeLa/ADSCs. To assess the role of ADSCs in the regulation of EMT markers, we evaluated the protein levels of fibronectin, N-cadherin, Vimentin and E-cadherin in HeLa and SiHa cell lines. The results showed an evident increment in the mesenchymal markers, HeLa cells exposed to conditioned medium of ADSCs had higher levels of Fibronectin (Fig. 8e,i) and N-cadherin (Fig. 8g,k), however, we could not find any significant change in the mesenchymal marker Vimentin (Fig. 8f,j) and E-cadherin (Fig. 8h,l), a well-known epithelial marker, perhaps due to its low expression in this cell line. Corroborating these results, we found that SiHa cells exposed to conditioned medium of ADSCs exhibited a drastic increment in Fibronectin (Fig. 9a,e) and N-cadherin (Fig. 9c,g), two key hallmark molecules of EMT. We also find a slight decrement in E-cadherin (Fig. 9d,h), a well-known epithelial marker. Collectively, these findings support the role of ADSCs in the metastasis of CC by promoting the migration and invasion of cancer cells through the induction of an EMT program.

**ADSC modulates angiogenesis in CC tumors.** Our analysis of sequencing showed an increase in molecules with mitogenic and pro-angiogenic activities during HeLa-ADSC coculture. These molecules included a

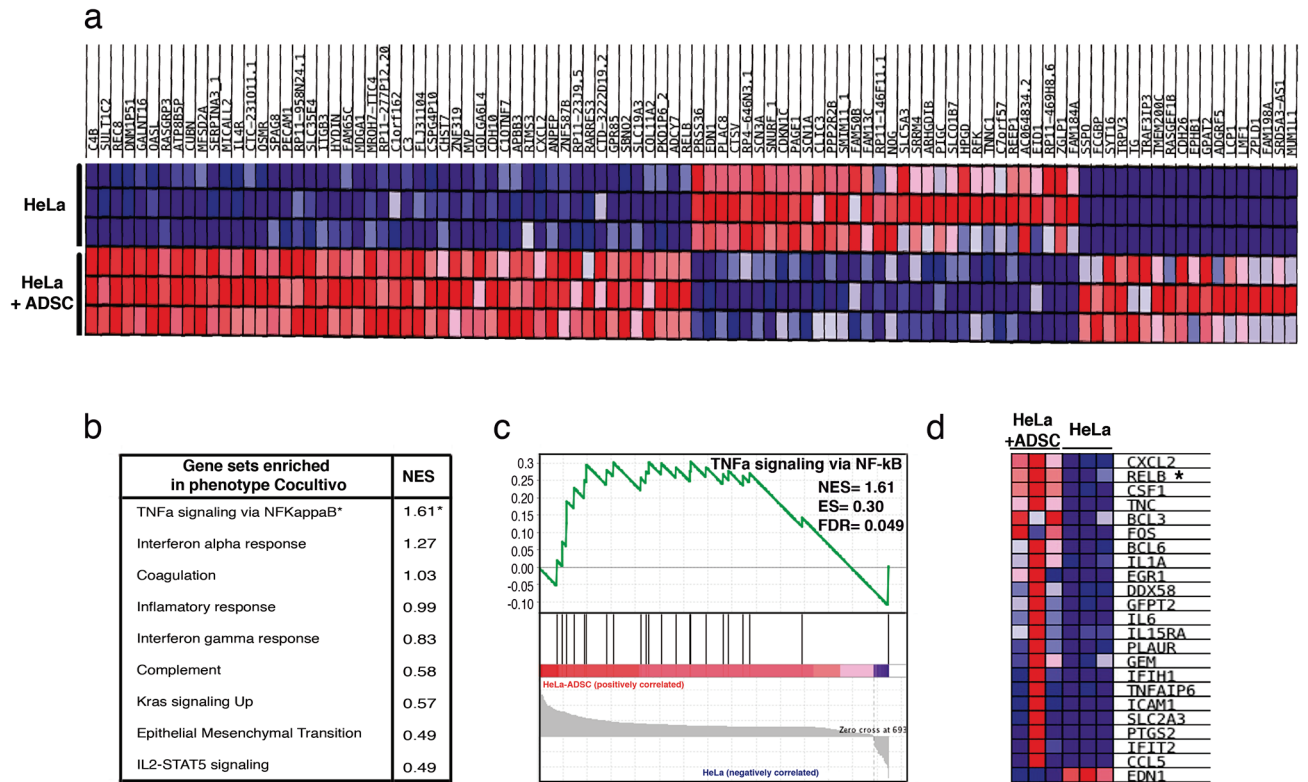


**Figure 5.** The NF-Kappa B pathway is the most activated pathway during the coculture of HeLa-ADSC. **(a)** Heat map shows the main differentially expressed genes in the HeLa cell line cultured in the presence or absence of ADSC. The expression values are represented as colors, where the range of colors (red, pink, light blue, dark blue) represents the range of expression values (high, moderate, low, lowest). **(b)** Table shows the main phenotypes enriched in HeLa cells due to the presence of ADSCs obtained from a gene set enrichment analysis (GSEA). For each of the phenotypes, the normalized enrichment score (NES) is indicated. **(c)** Analysis of GSEA showing significant enrichment (NES = 1.61 and an FDR = 0.049) of the TNF $\alpha$ -NF-kappa B signaling pathway in cervical cancer cells due to the presence of ADSCs. **(d)** The heat map shows the subset of enriched genes involved in the TNF $\alpha$ -NF-kappa B pathway, where most deregulated genes are involved in the noncanonical NF-Kappa B pathway, such as RELB.

chemokine CXCL2 as well as the ligand VEGF-C, a proangiogenic factor actively released by the tumor cells for the formation of new vessels (Fig. 10a). Studies have shown that these factors are regulated by the NF-Kappa B pathway<sup>45,46</sup>. Bioinformatics analysis predicted that compared to HeLa cells, HeLa-ADSCs possess a higher angiogenic potential. Through a KPA analysis, we validate that the NF-Kappa B pathway promotes the activation of VEGF-C and that this protein can bind and activate to FGF2 and EGF ligands as well as VEGFR-3 receptor, which activates fibronectin (Fig. 10b).

To test whether ADSCs influence the ability of cervical tumors to establish angiogenesis, we evaluated the in vivo effects of ADSCs in the vasculature development of transgenic zebrafish embryos (fli1a: EGFP) inoculated with SiHa/ADSC or SiHa cells only. These embryos express EGFP specifically in the vascular vessels, thus allowing the monitoring of new blood vessels. Supporting the above results, we also observed a clear migration of SiHa cells into the bloodstream mainly in embryos injected with SiHa/ADSCs (Fig. 10c). We monitored vascularization from 1 up to 3 days and observed that SiHa cells failed to form new blood vessels; however, SiHa cells inoculated in the presence of ADSCs formed vascularized tumors (Fig. 10d).

### Discussion

Cancer, cardiovascular diseases and diabetes mellitus account for more than 70% of deaths worldwide<sup>47</sup>. In addition, cervical cancer remains the fourth cause of cancer incidence (13.1) and cancer death (6.9) in women worldwide<sup>48</sup>.

Obesity is an important risk factor for cancer, and it has been associated with a decrease of 5 to 20 years in the survival of cancer patients. According to data from the OCED, Mexico ranks second in the worldwide prevalence of obesity (BMI  $\geq 30$  kg/m<sup>2</sup>)<sup>47,49,50</sup>. It is increasingly clear that obese women exhibit a higher risk of developing CC compared to women with normal BMI<sup>51-53</sup>. Although the characteristic cell of adipose tissue is the adipocyte, this is not the only cell type present in this tissue, other cells such as preadipocytes, macrophages, neutrophils, lymphocytes and endothelial cells are harbored in the adipose tissue and have also been linked to obesity and cancer.



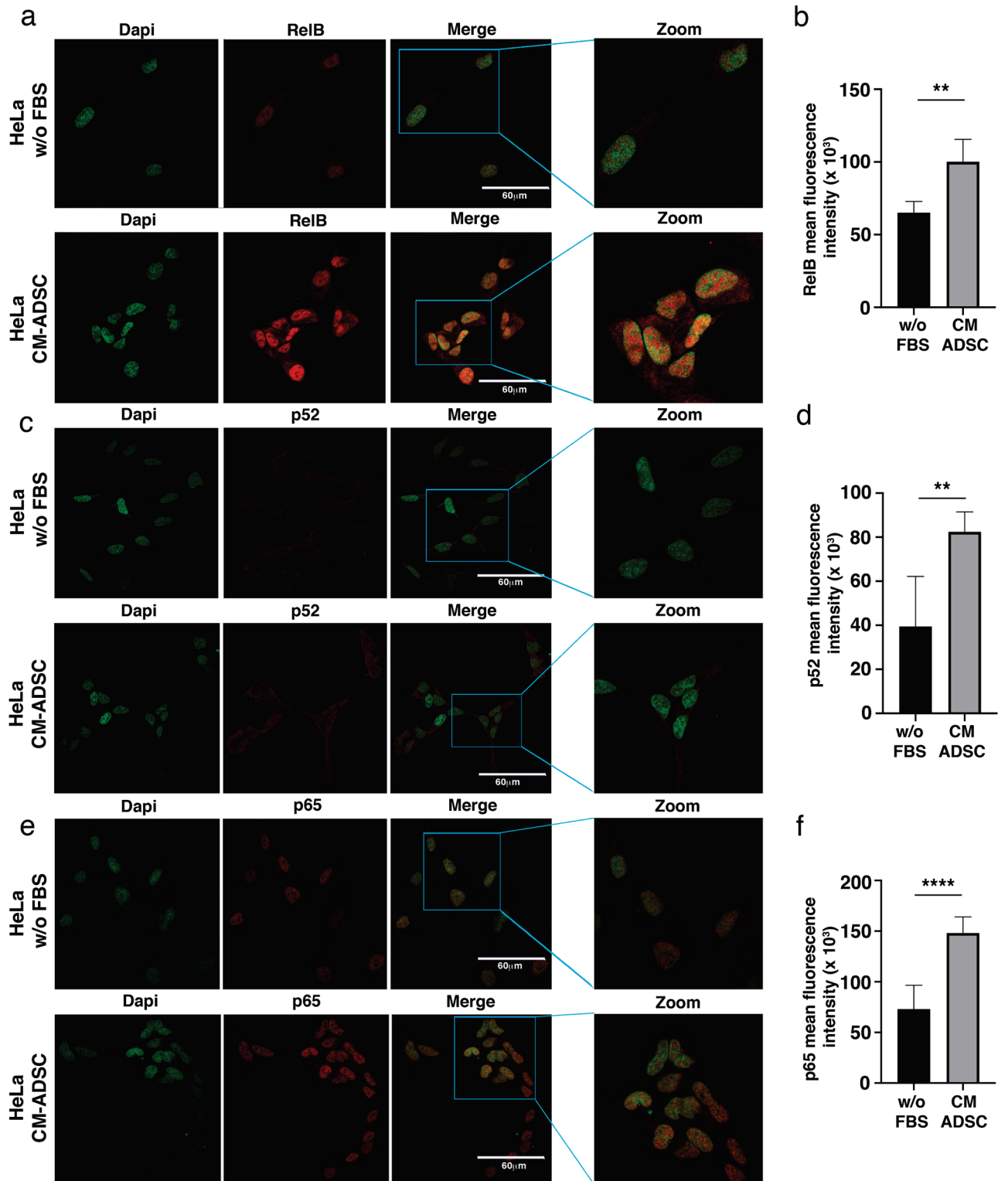


**Figure 6.** ADSCs induce the expression of the NF-kappa B molecules in CC cells. (a–f) The photographs show the expression of transcription factors of the NF-Kappa B family including RelB (a), p52 (c) and p65 (e) obtained by immunofluorescence of HeLa cells cultured with serum-free DMEM medium or ADSC-CM (free of serum) for 24 h. The images were taken under a confocal microscope. The scale bar = 60  $\mu$ m. The cell nuclei were contrasted with DAPI. Each experiment was repeated at least three times and to quantify the expression levels of Relb (b), p52 (d), and p65 (f), the intensity of fluorescence was quantified using ImageJ. Graph represents three biological replicates, error bars are s.d. and \*\*\*\* $p < 0.0001$  and \*\* $p < 0.01$ .

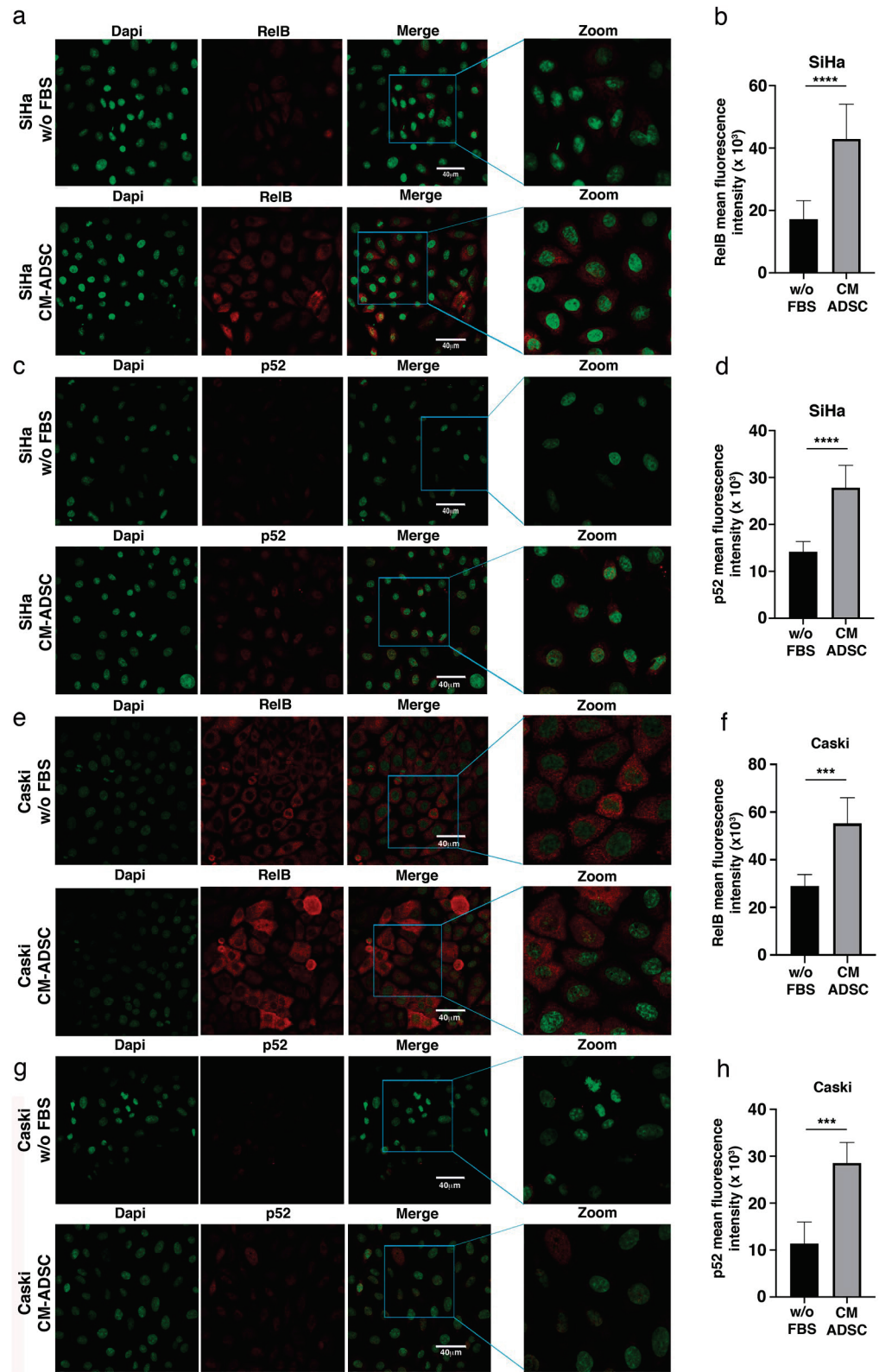


**Figure 7.** ADSC induces the activation of the NF-kappa B pathway in SiHa and CaSki cells. (a–h) The photographs show the expression of RelB and p52 obtained by immunofluorescence of SiHa (a–c) or CaSki (e–g) cells cultured with serum-free DMEM or ADSC-CM (free of serum) for 24 h. The images were taken under a confocal microscope. The scale bar = 40  $\mu$ m. The cell nuclei were contrasted with DAPI. Each experiment was repeated at least three times. To quantify the expression levels, the intensity of fluorescence was quantified using Image J. Graphs show the mean fluorescence intensity of RelB (b), p52 (d) in SiHa and RelB (f) and p52 (h) in CaSki cells. Graph represents three biological replicates, error bars are s.d. and \*\*\*\* $p < 0.0001$  and \*\*\* $p < 0.001$ .

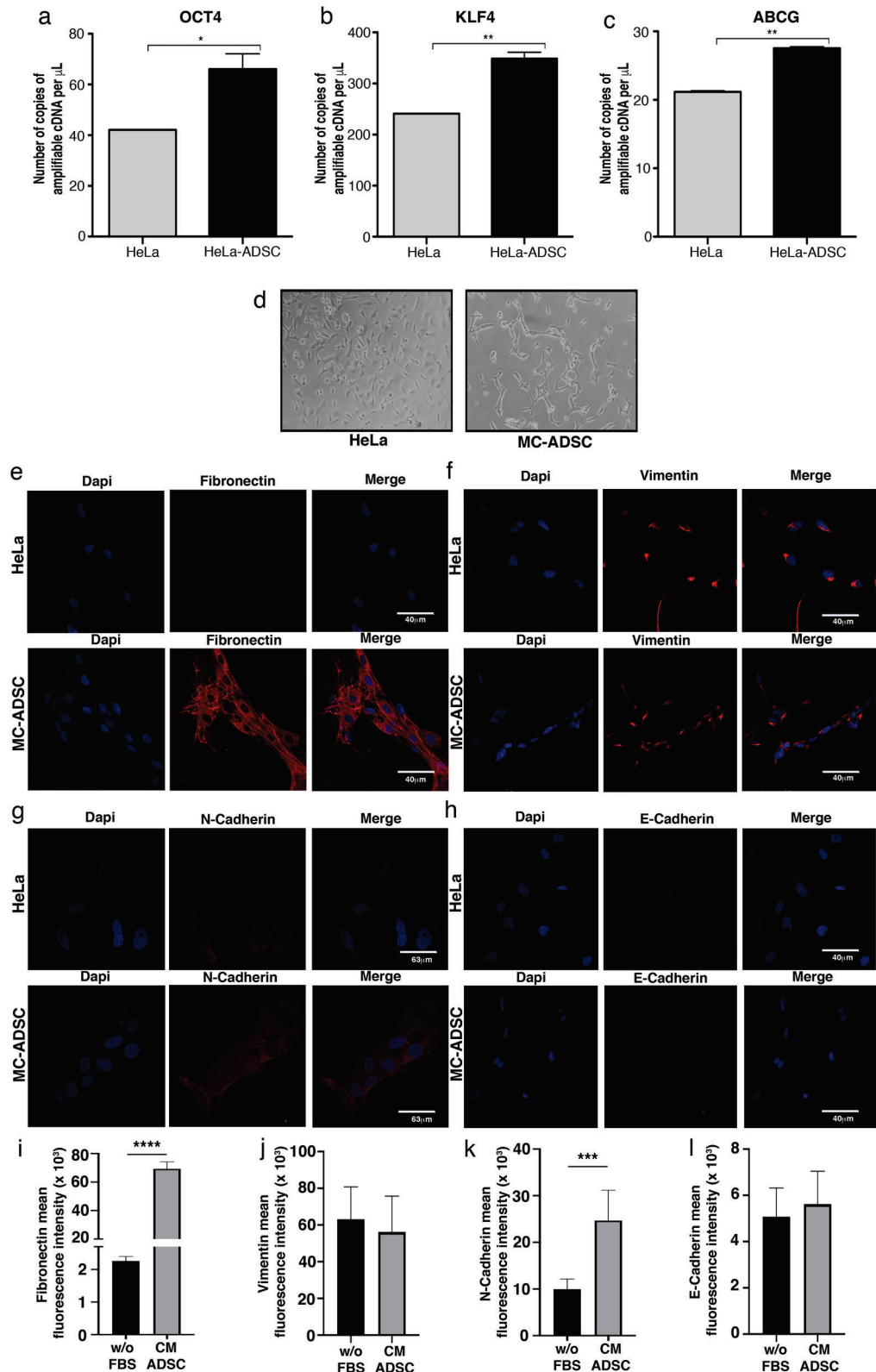


**Figure 8.** ADSC promotes a stem cell and EMT phenotype in HeLa cells. (a–c) Graphs show the expression level of pluripotency genes evaluated by ddPCR in HeLa control vs HeLa cells cocultured with ADSC. Pluripotency genes include OCT4 (a), KLF4 (b) and ABCG (c). The error bars represent the means  $\pm$  standard deviation (SD). (d) Schematic representation shows that cervical cancer cells exhibit an EMT-like phenotype induced by the conditioned medium of ADSC. Expression of EMT markers including fibronectin (e), Vimentin (f), N-cadherin (g) and E-cadherin (h) analyzed by immunofluorescence of HeLa cells cultured with or without conditioned ADSC. EMT proteins were stained with Cy3-conjugated secondary antibody and nuclei were stained with 4'-6-Diamidino-2-phenolindole (DAPI). Images were taken in a confocal microscope using an  $\times 40$  oil lens. Photographs are representative of three independent experiments. (i–j) To quantify the expression levels of fibronectin (i), vimentin (j), N-cadherin (k) and E-cadherin (l), the intensity of fluorescence was quantified using Image J. Graph represents three biological replicates, error bars are s.d and \*\*\*\* $p < 0.0001$  and \*\*\* $p < 0.001$ .

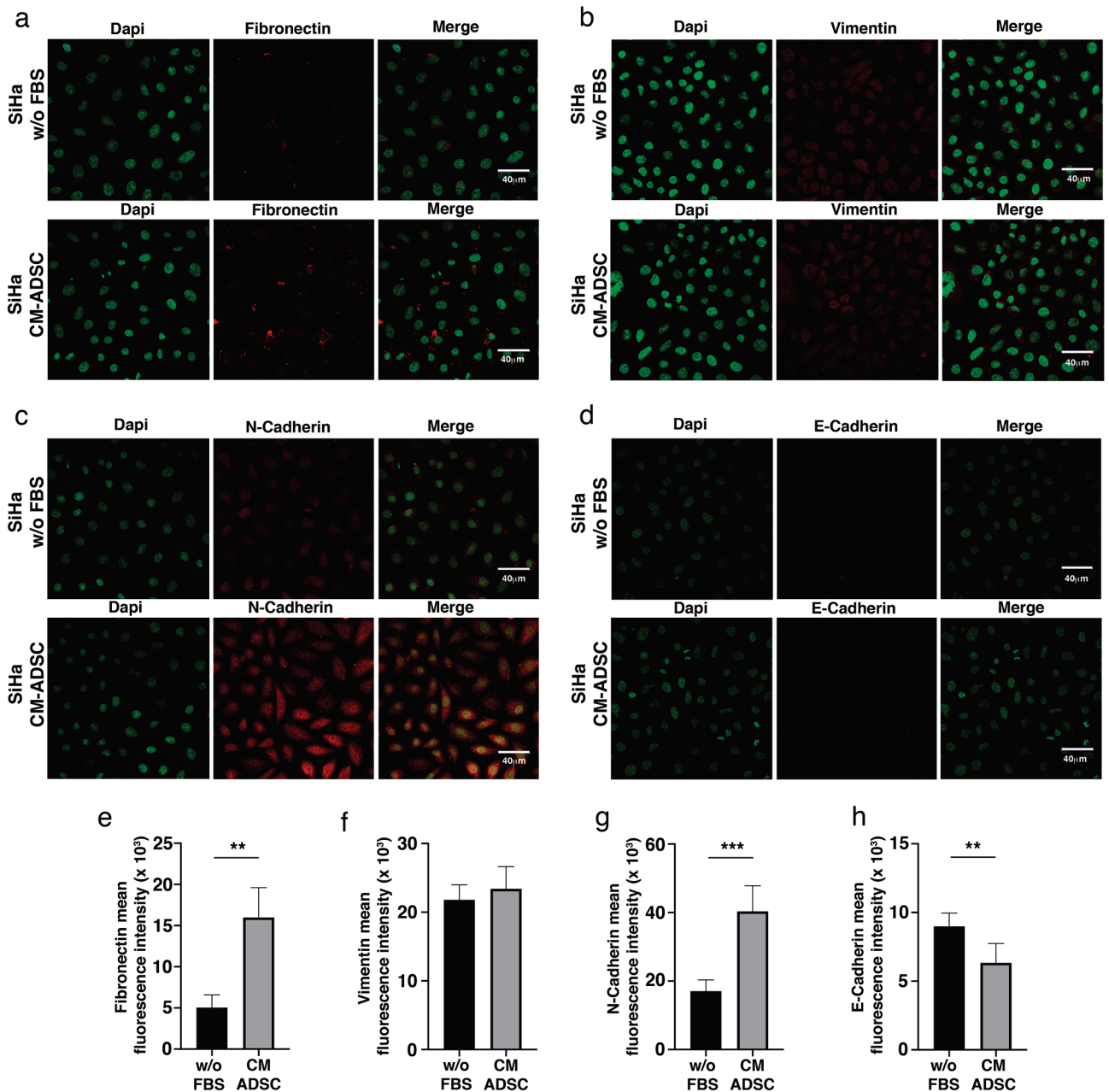
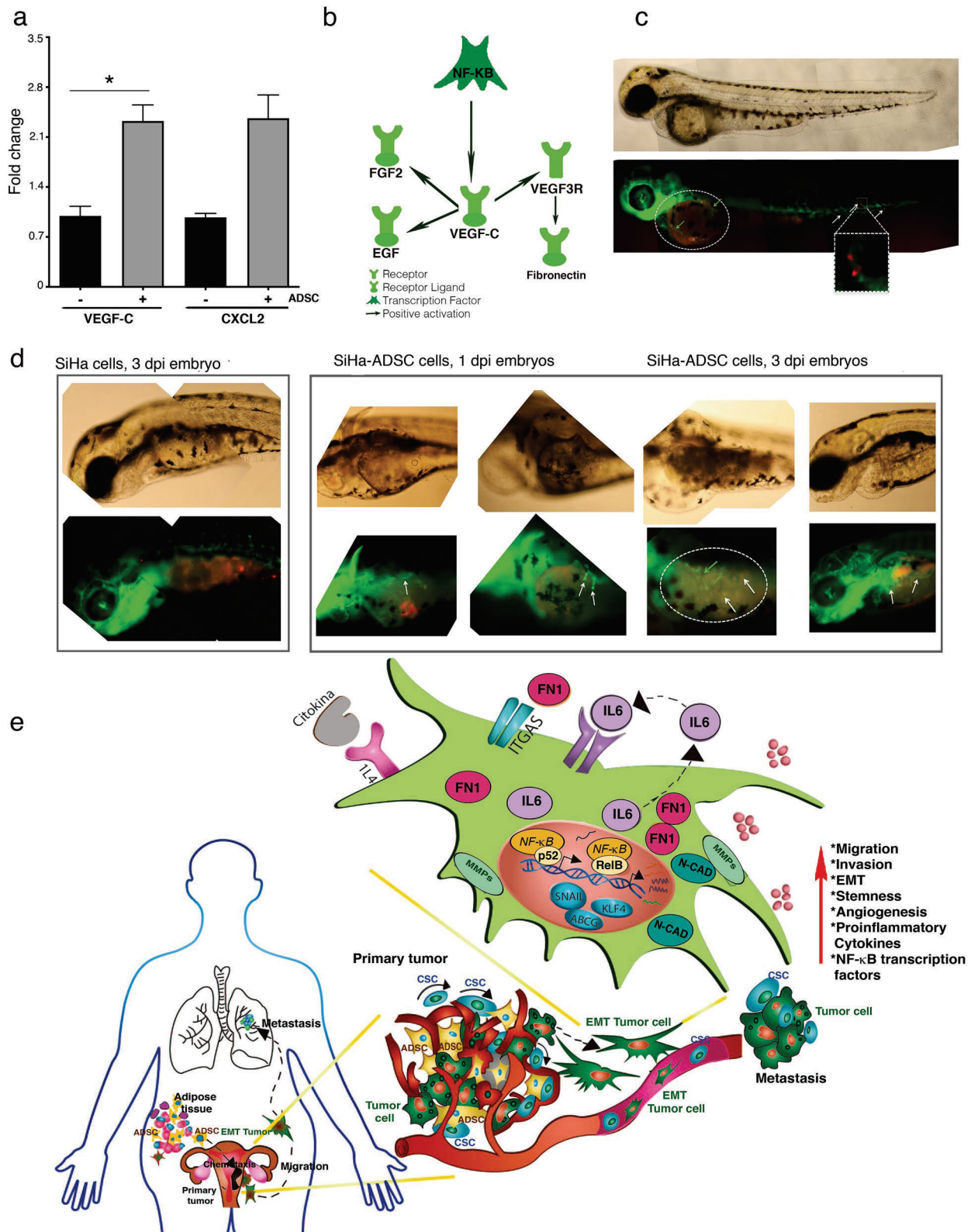


**Figure 9.** ADSC induce an EMT phenotype in SiHa cells. (a–d) Immunofluorescence analysis of EMT markers including fibronectin (a), Vimentin (b), N-cadherin (c) and E-cadherin (d) in SiHa cells cultured with or without conditioned medium of ADSC. EMT proteins were stained with Cy3-conjugated secondary antibody and nuclei were stained with 4'-6-Diamidino-2-phenylindole (DAPI). Images were taken in a confocal microscope using an  $\times 40$  oil lens. Photographs are representative of three independent experiments. To quantify the expression levels of fibronectin (e), vimentin (f), N-cadherin (g) and E-cadherin (h), the intensity of fluorescence was quantified using Image J. Graph represents three biological replicates, error bars are s.d. and \*\* $p < 0.01$  and \*\*\* $p < 0.001$ .

Studies linking obesity and cancer have focused on endocrine and metabolic repercussions that promote a generalized inflammatory process<sup>54–56</sup>, however, little is known about the specific molecular mechanism by which obesity increases the risk of cancer.

In this project, we studied ADSCs which are also harbored in the adipose tissue and are essential players in tissue development and regeneration<sup>57</sup>. ADSCs are found in abundant quantities in the adipose tissue, it has been reported that ADSCs represents up to 30% of total cells contained in this tissue<sup>58,59</sup>. Notably, recent studies have provided evidence that the number of ADSCs exceeds the frequency of marrow-derived mesenchymal stem cells (BMSC) found in the medullary stroma<sup>60</sup>. Approximately, 1 ml of adipose tissue obtained by liposuction contains about  $6 \times 10^5$  to  $2 \times 10^6$  ADSCs<sup>61</sup>, this represents at least 500 times more cells than the number of stem





cells obtained from bone marrow<sup>62–64</sup>. Taken together these data highlight adipose tissue as the richest source of multipotent stem cells, possibly outperforming any other source in the body.

Remarkably, recent evidence has shown that patients with obesity exhibit higher systemic mobility of ADSC than healthy patients and interestingly, this mobilization is even higher in cancer patients<sup>65</sup>, which supports the incorporation of ADSCs into tumors.

Accumulating evidence has demonstrated that these cells possess the ability to migrate toward tumor sites by chemoattraction<sup>11,19</sup>. The role of ADSCs in cancer has not been clearly elucidated, and there are some reports

**◀Figure 10.** ADSC modulate angiogenesis in CC tumors. **(a)** Graph shows the fold increase of DE mRNAs involved in angiogenesis obtained from HeLa/ADSC RNAseq data. Angiogenesis-related mRNAs shown are VEGF-C, and CXCL2. **(b)** Representative network of KPA analysis showing that NF-Kappa B/VEGF-C activates the signaling of angiogenic factors in HeLa cells cocultured in the presence of ADSC. **(c)** Representative photograph of the infiltration of SiHa cells in the blood vessels of *fli1a* embryos: EGFP after 12 h post-injection is shown. The SiHa cells are observed in red color and blood vessels in green. **(d)** Representative figure showing the formation of new blood vessels in the yolk of embryos from day 1 dpi and 3 dpi of SiHa cells vs SiHa-ADSC. **(e)** The illustration built with the experimental data obtained, indicates that the ADSCs migrate from the adipose tissue to CC tumor and there, they increase the malignant phenotype of the CC cells and promoting metastasis. The ADSC potentiate the malignant phenotype of cervical cancer cells by increasing the non-canonical NF-Kappa B pathway, causing an increase in the expression of chemokines, transcription factors, metalloproteases, integrins, etc., which contribute to the increased migration and invasion capacity of cancer cells. In addition, ADSC activate the EMT process mainly due to the increase of Fibronectin in CC cells. Finally, ADSCs induce the angiogenic potential that plays an important role in tumor progression. It should be mentioned that all these phenotypic changes could be given by the activation of the NF-Kappa B pathway.

that evidence the malignant behavior of ADSCs allowing rapid growth of tumors. In contrast, some studies have shown that ADSCs exhibit antitumoral potential. The role of ADSCs in cervical cancer is still unknown, thus, it is necessary to determine the effect of ADSCs on CC<sup>66,67</sup>. In this study, we demonstrated for the first time that ADSCs increase the malignant phenotype of cervical cancer cell lines, such as HeLa, SiHa and CaSki cells.

We used an indirect coculture system in which both tumor cells and ADSCs were physically separated through a permeable membrane and cultured in the same microenvironment, thus allowing paracrine signaling. This method has been used to study the effect of ADSCs on other tumors, such as squamous cell carcinoma<sup>21</sup>, breast cancer<sup>17,68</sup>, melanoma<sup>69</sup>, lung and colorectal cancer<sup>22</sup>.

Our results show that the presence of ADSCs (CD90<sup>+</sup>/CD44<sup>+</sup>/CD31<sup>-</sup>/CD45<sup>-</sup>) alters the transcriptome of CC cells. Data obtained from RNA-seq revealed that 95 RNAs were differentially expressed in HeLa cells cocultured in the presence of ADSCs derived from patients. Gene expression changes were validated by digital PCR, and we found that both ADSCs obtained from patients or from ATCC exhibit similar gene expression patterns, thus corroborating this phenomenon. Interestingly, most deregulated genes, such as IL6, RelB, RelA, Plac8, ITGA5, CXCL12 and FN1, among other cytokines and growth factors, have been involved in tumor growth and progression. Preisner and colleagues used qRT-PCR to analyze the expression of 229 tumor-promoting genes in melanoma cells cocultured with ADSCs and found similar cytokines and growth factors, such as IL6, CXCL12, VEGF, and HGF<sup>69</sup>.

Interestingly, validated genes (ITGA5, IL6, IL4R, FN1, TIMP1, and PLAC8) are highly relevant in CC because their expression level is directly related to CC patient survival. These genes have also been relevant in other tumor types. For example, ITGA5, an integrin that promotes tumor invasion<sup>70</sup>, has been correlated with lower survival of lung cancer patients<sup>71</sup>, and it also functions as a receptor for FN1<sup>72,73</sup>, which was also upregulated in our coculture. IL4R induces a prometastatic phenotype in epithelial tumors.

Integral analysis with IPA, KPA, and GSEA suggests that ADSCs modified cellular processes, such as migration, invasion, angiogenesis and proliferation. Accumulating evidence has demonstrated that ADSCs can also influence the proliferation of cancer cells; however, we could not observe any influence of ADSCs on the proliferation ability of HeLa cells. The migration, invasion, and angiogenesis were corroborated using *in vitro* and *in vivo* strategies. Supporting our results, various studies have demonstrated the effect of ADSCs on the migration and invasion of melanoma, breast, prostate and pancreatic cancer. Strikingly, we found many DE RNAs related to migration and invasion, such as VCAN, SPARC, MMP14, ITGA5, PLAUR, NRPI, IL-6, CXCL2, and HGF. Notably, we also observed drastic morphological changes in HeLa and SiHa cells cocultured with ADSCs, thus conferring migratory abilities perhaps by inducing epithelial to mesenchymal transition.

Our results also show that ADSCs modify the behavior of CC cells, thus inducing rapid tumor growth and metastasis. Mechanistically, little is known about how ADSCs facilitate tumor development. Recent evidence has shown that ADSCs provoke an increase in IL6 levels, which induces the phosphorylation of JAK2/STAT3<sup>16</sup>, resulting in proliferation, invasion and tumor growth in prostate and endometrial cancers. Strikingly, we also found that ADSCs induce a dramatic increase in IL6/STATs and an increase in noncanonical NF-kappa B signaling in HeLa and SiHa cells. These results are consistent with a recent study showing that mesenchymal stem cells promote colorectal cancer progression through NF-kappa B activation<sup>74</sup>. Our results show for the first time that the NF-kappa B pathway in CC is activated due to the presence of ADSCs. The bioinformatic analysis detects 23 NF-kappa B-related genes and suggests that RelB, a member of the noncanonical NF-kappa B pathway, is the main growth factor involved in the regulation of NF-kappa B signaling. We also found that the expression of p52 and p65 is induced by ADSCs, suggesting that both canonical and noncanonical signaling pathways are activated in CC.

Notably, ADSCs induced a rapid expansion of CSCs in zebrafish inoculated with SiHa and CaSki in the presence of ADSCs. It is well established that CSC expansion rapidly induces tumor growth and development, which further suggests that an increase in the number of CSCs is responsible for the highly invasive and metastatic abilities conferred by ADSCs. One way by which CC cells may acquire stemness is due to the constitutive activation of NF-Kappa B. Recent evidence has clearly established that NF-kappa B dramatically expands the number of stem cells and increases the clonogenicity and self-renewal abilities of CSCs<sup>25,75,76</sup>. Our results indicate that ADSCs induce the overexpression of stem cell markers such as OCT4, KLF4, and ABCG in HeLa cells. In addition, we found that ADSCs promote HeLa and SiHa cells to undergo EMT, thereby acquiring mesenchymal

features verified by the high expression of fibronectin, n-cadherin, and vimentin. In addition, it is increasingly clear that EMT induces the acquisition and maintenance of stem cell-like features. These results are in accordance with recent research showing that glial tumor and lung cancer cells are able to undergo EMT and acquire mesenchymal features when they are cultured in the presence of conditioned medium obtained from ADSCs.

Finally, we also observed that DE RNAs, including VEGFC, CXCL2, VEGF3R, FGF2 and EGF, are also involved in angiogenesis. We performed in vivo assays and consistently observed that ADSCs are able to induce the growth and formation of new blood vessels that could supply nutrients and oxygen to the tumors. Interestingly, Lin CS et al. demonstrated that ADSCs migrate toward prostatic tumor sites and increase tumor vascularity mediated by FGF2<sup>19</sup>. In addition, Dexheimer et al. demonstrated that the conditioned medium of the coculture of ADSCs and squamous cell carcinoma induces tube formation in human umbilical vein endothelial cells (HUVECs), thus corroborating the proangiogenic role of ADSCs<sup>21</sup>.

In conclusion, our results demonstrate that ADSCs affect multiple features that contribute to malignancy of cervical cancer cells such as gene expression, migration, invasion, angiogenesis, and stemness. In spite of the contribution of ADSCs into the promotion of those features, ADSCs have no effect in the proliferation of cervical cancer cells (Fig. 10e). Interestingly, the effects of ADSCs found in patient-derived ADSCs were also validated in an ADSC cell line obtained from ATCC.

It is important to say that ADSCs could promote features that contribute to malignancy of cervical cancer through the NF- $\kappa$ B signaling pathway and the induction of EMT (Fig. 10e). In addition, we observed that mRNAs altered by the presence of ADSCs exhibit clinical significance since they are associated with shorter survival of cervical cancer patients. Although the clinical relevance of the ADSC cells remains incomplete, our results give guidelines to the search for new molecules that can reduce the mortality rates of cervical cancer obese patients. We believe that much work needs to be done to fully elucidate the exact mechanism involved in the contribution of ADSCs in the malignant phenotype of cancer cells.

Furthermore, due to the malignant role of ADSCs in cancer, it is necessary to evaluate the safety of ADSC-based therapies in order to avoid the co-localization of those cells with cancer cells which could promote tumor growth.

Received: 4 September 2019; Accepted: 27 May 2020

Published online: 26 August 2020

## References

- Mackenzie, H. *et al.* Obesity surgery and risk of cancer. *Br. J. Surg.* **105**, 1650–1657. <https://doi.org/10.1002/bjs.10914> (2018).
- Onstad, M. A., Schmandt, R. E. & Lu, K. H. Addressing the role of obesity in endometrial cancer risk, prevention, and treatment. *J. Clin. Oncol.* **34**, 4225–4230. <https://doi.org/10.1200/JCO.2016.69.4638> (2016).
- Amling, C. L. The association between obesity and the progression of prostate and renal cell carcinoma. *Urol. Oncol.* **22**, 478–484. <https://doi.org/10.1016/j.urolonc.2004.10.004> (2004).
- Lauby-Secretan, B., Dana-Loomis, C. S., Grosse, Y., Bianchini, F. & Straif, K. Body fatness and cancer—viewpoint of the IARC working group. *N. Engl. J. Med.* **375**, 794–798 (2016).
- Smith, L. A., O’Flanagan, C. H., Bowers, L. W., Allott, E. H. & Hursting, S. D. Translating mechanism-based strategies to break the obesity-cancer link: a narrative review. *J. Acad. Nutr. Diet.* **118**, 652–667. <https://doi.org/10.1016/j.jand.2017.08.112> (2018).
- Calle, E. E., Walker-Thurmond, K. & Thun, M. J. Overweight, obesity, and mortality from cancer in a prospectively studied cohort of U.S. adults. *N. Engl. J. Med.* **348**, 1–10 (2003).
- Clarke, M. A. *et al.* Epidemiologic evidence that excess body weight increases risk of cervical cancer by decreased detection of precancer. *J. Clin. Oncol.* **36**, 1184–1191. <https://doi.org/10.1200/JCO.2017.2017> (2018).
- Poorolajal, J. & Jenabi, E. The association between BMI and cervical cancer risk: a meta-analysis. *Eur. J. Cancer Prev.* **25**, 232–238. <https://doi.org/10.1097/CEJ.0000000000000164> (2016).
- Pischon, T. & Nimpf, K. Obesity and risk of cancer: an introductory overview. *Recent Results Cancer Res.* **208**, 1–15. [https://doi.org/10.1007/978-3-319-42542-9\\_1](https://doi.org/10.1007/978-3-319-42542-9_1) (2016).
- Spyrou, N., Avgerinos, K. I., Mantzoros, C. S. & Dalamaga, M. Classic and novel adipocytokines at the intersection of obesity and cancer: diagnostic and therapeutic strategies. *Curr. Obes. Rep.* **7**, 260–275. <https://doi.org/10.1007/s13679-018-0318-7> (2018).
- Zhang, Y. *et al.* White adipose tissue cells are recruited by experimental tumors and promote cancer progression in mouse models. *Cancer Res.* **69**, 5259–5266. <https://doi.org/10.1158/0008-5472.CAN-08-3444> (2009).
- Motohara, T. *et al.* An evolving story of the metastatic voyage of ovarian cancer cells: cellular and molecular orchestration of the adipose-rich metastatic microenvironment. *Oncogene* **38**, 2885–2898. <https://doi.org/10.1038/s41388-018-0637-x> (2018).
- Berry, R., Rodeheffer, M. S., Rosen, C. J. & Horowitz, M. C. Adipose tissue residing progenitors (adipocyte lineage progenitors and adipose derived stem cells (ADSC)). *Curr. Mol. Biol. Rep.* **1**, 101–109. <https://doi.org/10.1007/s40610-015-0018-y> (2015).
- Bertolini, F., Petit, J. Y. & Kolonin, M. G. Stem cells from adipose tissue and breast cancer: hype, risks and hope. *Br. J. Cancer* **112**, 419–423. <https://doi.org/10.1038/bjc.2014.657> (2015).
- Lazennec, G. & Lam, P. Y. Recent discoveries concerning the tumor: mesenchymal stem cell interactions. *Biochim. Biophys. Acta* **290–299**, 2016. <https://doi.org/10.1016/j.bbcan.2016.10.004> (1866).
- Chu, Y. *et al.* STAT3 activation by IL-6 from adipose-derived stem cells promotes endometrial carcinoma proliferation and metastasis. *Biochem. Biophys. Res. Commun.* **500**, 626–631. <https://doi.org/10.1016/j.bbrc.2018.04.121> (2018).
- Dwyer, R. M. *et al.* Monocyte chemoattractant protein-1 secreted by primary breast tumors stimulates migration of mesenchymal stem cells. *Clin. Cancer Res.* **13**, 5020–5027. <https://doi.org/10.1158/1078-0432.CCR-07-0731> (2007).
- Freese, K. E. *et al.* Adipose-derived stem cells and their role in human cancer development, growth, progression, and metastasis: a systematic review. *Cancer Res.* **75**, 1161–1168. <https://doi.org/10.1158/0008-5472.CAN-14-2744> (2015).
- Lin, G. *et al.* Effects of transplantation of adipose tissue-derived stem cells on prostate tumor. *Prostate* **70**, 1066–1073. <https://doi.org/10.1002/pros.21140> (2010).
- Wels, J., Kaplan, R. N., Rafii, S. & Lyden, D. Migratory neighbors and distant invaders: tumor-associated niche cells. *Genes Dev.* **22**, 559–574. <https://doi.org/10.1101/gad.1636908> (2008).
- Koellensperger, E. *et al.* Alterations of gene expression and protein synthesis in co-cultured adipose tissue-derived stem cells and squamous cell-carcinoma cells: consequences for clinical applications. *Stem Cell Res. Ther.* **5**, 65. <https://doi.org/10.1186/scrt454> (2014).



22. Rhyu, J. J., Yun, J. W., Kwon, E., Che, J. H. & Kang, B. C. Dual effects of human adipose tissue-derived mesenchymal stem cells in human lung adenocarcinoma A549 xenografts and colorectal adenocarcinoma HT-29 xenografts in mice. *Oncol. Rep.* **34**, 1733–1744. <https://doi.org/10.3892/or.2015.4185> (2015).
23. Li, M. *et al.* Human omental adipose-derived stem cells from donors with different body mass index had similar effects on proliferation and migration of endometrial cancer cells in vitro. *J. Obstet. Gynaecol. Res.* **45**, 417–427. <https://doi.org/10.1111/jog.13820> (2019).
24. Yan Wang, Y. C. *et al.* Adipose-derived mesenchymal stem cells promote osteosarcoma proliferation and metastasis by activating the STAT3 pathway. *Oncotarget* **8**, 23803–23816 (2017).
25. Vazquez-Santillan, K., Melendez-Zajgla, J., Jimenez-Hernandez, L., Martinez-Ruiz, G. & Maldonado, V. NF-kappaB signaling in cancer stem cells: a promising therapeutic target?. *Cell Oncol.* **38**, 327–339. <https://doi.org/10.1007/s13402-015-0236-6> (2015).
26. Vazquez-Santillan, K. *et al.* NF-kappaBeta-inducing kinase regulates stem cell phenotype in breast cancer. *Sci. Rep.* **6**, 37340. <https://doi.org/10.1038/srep37340> (2016).
27. Xia, Y., Shen, S. & Verma, I. M. NF-kappaB, an active player in human cancers. *Cancer Immunol Res* **2**, 823–830. <https://doi.org/10.1158/2326-6066.CIR-14-0112> (2014).
28. Taniguchi, K. & Karin, M. NF-kappaB, inflammation, immunity and cancer: coming of age. *Nat. Rev. Immunol.* **18**, 309–324. <https://doi.org/10.1038/nri.2017.142> (2018).
29. Xia, L. *et al.* Role of the NFkappaB-signaling pathway in cancer. *Oncol. Targets Ther.* **11**, 2063–2073. <https://doi.org/10.2147/OTT.S161109> (2018).
30. Dranse, H. J., Muruganandan, S., Fawcett, J. P. & Sinal, C. J. Adipocyte-secreted chemerin is processed to a variety of isoforms and influences MMP3 and chemokine secretion through an NFkB-dependent mechanism. *Mol. Cell Endocrinol.* **436**, 114–129. <https://doi.org/10.1016/j.mce.2016.07.017> (2016).
31. Zhou, H., Urso, C. J. & Jadeja, V. Saturated fatty acids in obesity-associated inflammation. *J. Inflamm. Res.* **13**, 1–14. <https://doi.org/10.2147/JIR.S229691> (2020).
32. Staudt, L. M. Oncogenic activation of NF-kappaB. *Cold Spring Harb. Perspect. Biol.* **2**, a000109. <https://doi.org/10.1101/cshperspect.a000109> (2010).
33. Cildir, G., Low, K. C. & Tergaonkar, V. Noncanonical NF-kappaB signaling in health and disease. *Trends Mol. Med.* **22**, 414–429. <https://doi.org/10.1016/j.molmed.2016.03.002> (2016).
34. Teng, H., Xue, L., Wang, Y., Ding, X. & Li, J. Nuclear factor kappaB-inducing kinase is a diagnostic marker of gastric cancer. *Medicine* **99**, e18864. <https://doi.org/10.1097/MD.00000000000018864> (2020).
35. Tilborghs, S. *et al.* The role of nuclear factor-kappa B signaling in human cervical cancer. *Crit. Rev. Oncol. Hematol.* **120**, 141–150. <https://doi.org/10.1016/j.critrevonc.2017.11.001> (2017).
36. Ning, H., Lin, G., Lue, T. F. & Lin, C. S. Neuron-like differentiation of adipose tissue-derived stromal cells and vascular smooth muscle cells. *Differentiation* **74**, 510–518. <https://doi.org/10.1111/j.1432-0436.2006.00081.x> (2006).
37. Lin, G. *et al.* Defining stem and progenitor cells within adipose tissue. *Stem Cells Dev.* **17**, 1053–1063. <https://doi.org/10.1089/scd.2008.0117> (2008).
38. Bio-Rad Laboratories. *Droplet Digital™ PCR. Applications Guide*, [https://www.bio-rad.com/webroot/web/pdf/lsr/literature/Bulletin\\_6407.pdf](https://www.bio-rad.com/webroot/web/pdf/lsr/literature/Bulletin_6407.pdf)
39. Westerfield, M. *The Zebrafish Book: A Guide for the Laboratory Use of Zebrafish (Danio rerio)* (University of Oregon Press, Eugene, 2000).
40. Hu, Y. & Smyth, G. K. ELDA: extreme limiting dilution analysis for comparing depleted and enriched populations in stem cell and other assays. *J. Immunol. Methods* **347**, 70–78. <https://doi.org/10.1016/j.jim.2009.06.008> (2009).
41. Li, C. W. *et al.* Epithelial-mesenchymal transition induced by TNF-alpha requires NF-kappaB-mediated transcriptional upregulation of Twist1. *Cancer Res.* **72**, 1290–1300. <https://doi.org/10.1158/0008-5472.CAN-11-3123> (2012).
42. Huber, M. A. *et al.* NF-kB is essential for epithelial-mesenchymal transition and metastasis in a model of breast cancer progression. *J. Clin. Invest.* **114**, 569–581. <https://doi.org/10.1172/jci200421358> (2004).
43. Pires, B. R. *et al.* NF-kappaB is involved in the regulation of EMT genes in breast cancer cells. *PLoS ONE* **12**, e0169622. <https://doi.org/10.1371/journal.pone.0169622> (2017).
44. Chua, H. L. *et al.* NF-kappaB represses E-cadherin expression and enhances epithelial to mesenchymal transition of mammary epithelial cells: potential involvement of ZEB-1 and ZEB-2. *Oncogene* **26**, 711–724. <https://doi.org/10.1038/sj.onc.1209808> (2007).
45. Hernandez, L. *et al.* Activation of NF-kappaB signaling by inhibitor of NF-kappaB kinase beta increases aggressiveness of ovarian cancer. *Cancer Res.* **70**, 4005–4014. <https://doi.org/10.1158/0008-5472.CAN-09-3912> (2010).
46. Zhang, Z. *et al.* GNA13 promotes tumor growth and angiogenesis by upregulating CXCL chemokines via the NF-kappaB signaling pathway in colorectal cancer cells. *Cancer Med.* **7**, 5611–5620. <https://doi.org/10.1002/cam4.1783> (2018).
47. Bluher, M. Obesity: global epidemiology and pathogenesis. *Nat. Rev. Endocrinol.* <https://doi.org/10.1038/s41574-019-0176-8> (2019).
48. Bray, F. *et al.* Global cancer statistics 2018: globocan estimates of incidence and mortality worldwide for 36 cancers in 185 countries. *CA Cancer J. Clin.* **68**, 394–424. <https://doi.org/10.3322/caac.21492> (2018).
49. O'Sullivan, J., Lysaght, J., Donohoe, C. L. & Reynolds, J. V. Obesity and gastrointestinal cancer: the interrelationship of adipose and tumour microenvironments. *Nat. Rev. Gastroenterol. Hepatol.* **15**, 699–714. <https://doi.org/10.1038/s41575-018-0069-7> (2018).
50. OECD. *Organization for Economic Co-operation and Development. Obesity Update 2017. OECD*. <https://www.oecd.org/els/health-systems/Obesity-Update-2017.pdf> (2017).
51. Calle, E. E. & Thun, M. J. Obesity and cancer. *Oncogene* **23**, 6365–6378. <https://doi.org/10.1038/sj.onc.1207751> (2004).
52. Choi, Y. J. *et al.* Adult height in relation to risk of cancer in a cohort of 22,809,722 Korean adults. *Br. J. Cancer* **120**, 668–674. <https://doi.org/10.1038/s41416-018-0371-8> (2019).
53. Ryan, D. Obesity in women: a life cycle of medical risk. *Int. J. Obes.* **31**(Suppl 2), S3–7. <https://doi.org/10.1038/sj.ijo.0803729> (2007) (Discussion S31–S32).
54. Brahmkhatri, V. P., Prasanna, C. & Atreya, H. S. Insulin-like growth factor system in cancer: novel targeted therapies. *Biomed. Res. Int.* **2015**, 538019. <https://doi.org/10.1155/2015/538019> (2015).
55. Cozzo, A. J., Fuller, A. M. & Makowski, L. Contribution of adipose tissue to development of cancer. *Comp. Physiol.* **8**, 237–282. <https://doi.org/10.1002/cphy.c170008> (2017).
56. Khandekar, M. J., Cohen, P. & Spiegelman, B. M. Molecular mechanisms of cancer development in obesity. *Nat. Rev. Cancer* **11**, 886–895. <https://doi.org/10.1038/nrc3174> (2011).
57. Joo, H. J., Kim, J. H. & Hong, S. J. Adipose tissue-derived stem cells for myocardial regeneration. *Korean Circ. J.* **47**, 151–159. <https://doi.org/10.4070/kcj.2016.0207> (2017).
58. Mazini, L., Rochette, L., Amine, M. & Malka, G. Regenerative capacity of adipose derived stem cells (ADSCs), comparison with mesenchymal stem cells (MSCs). *Int. J. Mol. Sci.* <https://doi.org/10.3390/ijms20102523> (2019).
59. Lenz, M., Arts, I. C. W., Peeters, R. L. M., de Kok, T. M. & Ertaylan, G. Adipose tissue in health and disease through the lens of its building blocks. *bioRxiv* <https://doi.org/10.1101/316083> (2018).
60. Van Pham, P. Adipose stem cells in the clinic. *Biomed. Res. Ther.* <https://doi.org/10.7603/s40730-014-0011-8> (2014).
61. Yarak, S. & Okamoto, O. K. Human adipose-derived stem cells: current challenges and clinical perspectives. *An. Bras. Dermatol.* **5**, 647–656 (2010).

62. Fraser, J. K., Wulur, I., Alfonso, Z. & Hedrick, M. H. Fat tissue: an underappreciated source of stem cells for biotechnology. *Trends Biotechnol.* **24**, 150–154. <https://doi.org/10.1016/j.tibtech.2006.01.010> (2006).
63. Meruane, M. & Rojas, M. Células troncales derivadas del tejido adiposo. *Int. J. Morphol.* **3**, 879–889 (2010).
64. Alonso-Goulart, V. *et al.* Mesenchymal stem cells from human adipose tissue and bone repair: a literature review. *Biotechnol. Res. Innov.* **2**, 74–80. <https://doi.org/10.1016/j.biori.2017.10.005> (2018).
65. Bellows, C. F., Zhang, Y., Chen, J., Frazier, M. L. & Kolonin, M. G. Circulation of progenitor cells in obese and lean colorectal cancer patients. *Cancer Epidemiol. Biomark. Prev.* **20**, 2461–2468. <https://doi.org/10.1158/1055-9965.EPI-11-0556> (2011).
66. Hassan, M., Latif, N. & Yacoub, M. Adipose tissue: friend or foe?. *Nat. Rev. Cardiol.* **9**, 689–702. <https://doi.org/10.1038/nrcardio.2012.148> (2012).
67. Mishra, P. J., Mishra, P. J., Glod, J. W. & Banerjee, D. Mesenchymal stem cells: flip side of the coin. *Cancer Res.* **69**, 1255–1258. <https://doi.org/10.1158/0008-5472.CAN-08-3562> (2009).
68. Koellensperger, E. *et al.* The impact of human adipose tissue-derived stem cells on breast cancer cells: implications for cell-assisted lipotransfers in breast reconstruction. *Stem Cell Res. Ther.* **8**, 121. <https://doi.org/10.1186/s13287-017-0579-1> (2017).
69. Preisner, F. *et al.* Impact of human adipose tissue-derived stem cells on malignant melanoma cells in an in vitro co-culture model. *Stem Cell Rev.* **14**, 125–140. <https://doi.org/10.1007/s12015-017-9772-y> (2018).
70. Deng, Y., Wan, Q. & Yan, W. Integrin  $\alpha 5$ /ITGA5 promotes the proliferation, migration, invasion and progression of oral squamous carcinoma by epithelial–mesenchymal transition. *Cancer Manag. Res.* **11**, 9609–9620 (2019).
71. Zheng, W., Jiang, C. & Li, R. Integrin and gene network analysis reveals that ITGA5 and ITGB1 are prognostic in non-small-cell lung cancer. *Onco Targ. Ther.* **9**, 2317–2327. <https://doi.org/10.2147/OTT.S91796> (2016).
72. Mittal, A., Pulina, M., Hou, S. Y. & Astrof, S. Fibronectin and integrin alpha 5 play requisite roles in cardiac morphogenesis. *Dev. Biol.* **381**, 73–82. <https://doi.org/10.1016/j.ydbio.2013.06.010> (2013).
73. Chen, D. *et al.* Fibronectin signals through integrin alpha5beta1 to regulate cardiovascular development in a cell type-specific manner. *Dev. Biol.* **407**, 195–210. <https://doi.org/10.1016/j.ydbio.2015.09.016> (2015).
74. Wu, X. B. *et al.* Mesenchymal stem cells promote colorectal cancer progression through AMPK/mTOR-mediated NF- $\kappa$ B activation. *Sci. Rep.* **6**, 21420. <https://doi.org/10.1038/srep21420> (2016).
75. Yang, L. *et al.* Targeting cancer stem cell pathways for cancer therapy. *Signal Trans. Targ. Ther.* <https://doi.org/10.1038/s41392-020-0110-5> (2020).
76. Liu, W. *et al.* TNF- $\alpha$  increases breast cancer stem-like cells through up-regulating TAZ expression via the non-canonical NF- $\kappa$ B pathway. *Sci. Rep.* **10**, 1804. <https://doi.org/10.1038/s41598-020-58642-y> (2020).

## Acknowledgements

Castro Oropeza Maria Del Rosario was supported by a fellowship from Consejo Nacional de Ciencia y Tecnología (CONACYT), number 329852 (CVU 299366); this study is part of her Doctoral Thesis from the Programa de Doctorado en Ciencias Biomédicas, Facultad de Medicina from the Universidad Nacional Autónoma de México (UNAM). This work was supported by Grant A1-S-33543 CONACYT (CB2017-2018). We thank to MC. Alfredo Mendoza for the processing of RNAseq (High Technology Unit, National Institute of Genomic Medicine, Mexico).

## Author contributions

R.C.O.: Conducted most of the experiments, analyzed the results, K.V.S.: Performed immunohistochemical assays and bioinformatic analysis, C.D.G.: Conducted experiments, J.M.: Analyzed the results, C.Z.: Performed the in vivo assays, E.F.O., A.R.G. and L.A.P.: Provided samples of patients, V.M.: Analyzed the results and wrote most of the paper.

## Competing interests

The authors declare no competing interests.

## Additional information

**Supplementary information** is available for this paper at <https://doi.org/10.1038/s41598-020-69907-x>.

**Correspondence** and requests for materials should be addressed to V.M.

**Reprints and permissions information** is available at [www.nature.com/reprints](http://www.nature.com/reprints).

**Publisher's note** Springer Nature remains neutral with regard to jurisdictional claims in published maps and institutional affiliations.




**Open Access** This article is licensed under a Creative Commons Attribution 4.0 International License, which permits use, sharing, adaptation, distribution and reproduction in any medium or format, as long as you give appropriate credit to the original author(s) and the source, provide a link to the Creative Commons license, and indicate if changes were made. The images or other third party material in this article are included in the article's Creative Commons license, unless indicated otherwise in a credit line to the material. If material is not included in the article's Creative Commons license and your intended use is not permitted by statutory regulation or exceeds the permitted use, you will need to obtain permission directly from the copyright holder. To view a copy of this license, visit <http://creativecommons.org/licenses/by/4.0/>.

© The Author(s) 2020



# The emerging role of lncRNAs in the regulation of cancer stem cells

Rosario Castro-Oropeza<sup>1</sup> · Jorge Melendez-Zajgla<sup>2</sup> · Vilma Maldonado<sup>1</sup> · Karla Vazquez-Santillan<sup>1,3</sup> 

Accepted: 29 August 2018  
© International Society for Cellular Oncology 2018

## Abstract

**Background** Tumors contain a functional subpopulation of cells that exhibit stem cell properties. These cells, named cancer stem cells (CSCs), play significant roles in the initiation and progression of cancer. Long non-coding RNAs (lncRNAs) can act at the transcriptional, posttranscriptional and translational level. As such, they may be involved in various biological processes such as DNA damage repair, inflammation, metabolism, cell survival, cell signaling, cell growth and differentiation. Accumulating evidence indicates that lncRNAs are key regulators of the CSC subpopulation, thereby contributing to cancer progression. The aim of this review is to overview current knowledge about the functional role and the mechanisms of action of lncRNAs in the initiation, maintenance and regulation of CSCs derived from different neoplasms. These lncRNAs include CTCF7, ROR, DILC, HOTAIR, H19, HOTTIP, ATB, HIF2PUT, SOX2OT, MALAT-1, CUDR, Lnc34a, Linc00617, DYNC2H1-4, PVT1, SOX4 and ARSR Uc.283-plus. Furthermore, we will illustrate how lncRNAs may regulate asymmetric CSC division and contribute to self-renewal, drug resistance and EMT, thus affecting the metastasis and recurrence of different cancers. In addition, we will highlight the implications of targeting lncRNAs to improve the efficacy of conventional drug therapies and to hamper CSC survival and proliferation.

**Conclusions** lncRNAs are valuable tools in the search for new targets to selectively eliminate CSCs and improve clinical outcomes. lncRNAs may serve as excellent therapeutic targets because they are stable, easily detectable and expressed in tissue-specific contexts.

**Keywords** Non-coding RNAs · lncRNAs · Cancer stem cells · Self-renewal · Differentiation · Stemness

## 1 Introduction

Although it has been assumed that the vast majority of the human genome (85%) is transcribed, only ~2% of the transcripts are translated into proteins [1]. Since it has become evident that the remaining transcripts are not translated into

proteins they are, concordantly, called non-coding RNAs (ncRNAs) [2]. Long non-coding RNAs (lncRNAs) represent a very interesting subgroup of ncRNAs that have recently come into light as powerful players in various diseases, including cancer. Up to date, the GENCODE database [3], which has the largest compilation of transcripts, reports a total of 7258 small ncRNAs and 15,767 annotated lncRNAs (<http://www.genencodegenes.org/stats/current.html>).

lncRNAs represent a heterogeneous mix of transcripts, most of them with unknown function. These RNAs have been grouped into 5 categories based on their location relative to the nearest protein-coding genes: 1) sense lncRNAs that overlap with coding mRNAs on the coding strand of a gene, 2) anti-sense lncRNAs that overlap with coding mRNAs on the non-coding strand of a gene, 3) bidirectional lncRNAs that share its transcription start site with a coding gene on the opposite strand, 4) intronic lncRNAs that are transcribed from an intronic region of a coding gene and 5) intergenic lncRNAs that are located between coding genes [4].

✉ Karla Vazquez-Santillan  
kivazquez@inmegen.gob.mx

Rosario Castro-Oropeza  
genomicsmile@hotmail.es

<sup>1</sup> Epigenetics, Instituto Nacional de Medicina Genómica, Periférico Sur No.4809, Col Arenal Tepepan, Tlalpan, 14610 Mexico City, Mexico

<sup>2</sup> Functional Genomics Laboratories, Instituto Nacional de Medicina Genómica, Periférico Sur No.4809, Col Arenal Tepepan, Tlalpan, 14610 Mexico City, Mexico

<sup>3</sup> National Institute of Genomic Medicine, Mexico City, Mexico

## 2 Molecular mechanisms involving lncRNAs

In humans, lncRNAs are mainly transcribed by RNA Polymerase (Pol) II or III, but they can also be transcribed by polymerase V in other eukaryotic organisms [5]. It has been found that lncRNAs that are transcribed by different RNA polymerases may exhibit distinct epigenetic marks. lncRNAs transcribed by RNA polymerase II usually exhibit, for instance, histone H3 trimethylation of lysine 4 (H3K4me3) and histone H3 trimethylation of lysine 36 (H3K36me3). RNA polymerase III-transcribed genes on the other hand usually exhibit mono-, bi- or trimethylation of histone H3 lysine 4 (H3K4me1/2/3) or acetylation of histone H3 lysine 4 (H3K4ac) as long as H3K36me3 and bi-methylation of histone H3 lysine 27 (H3K27me2) are absent [6]. Furthermore, Pol II-transcribed lncRNAs are processed as mRNAs, i.e., 5' caps and 3' poly-A tails are added, while Pol III-transcribed lncRNAs are not polyadenylated. Mature lncRNAs can interact with an array of diverse molecules, creating supramolecular structures such as RNA:RNA, RNA:DNA (double or triple chains), RNA:Protein, DNA:RNA:Protein or DNA:RNA:RNA complexes [7].

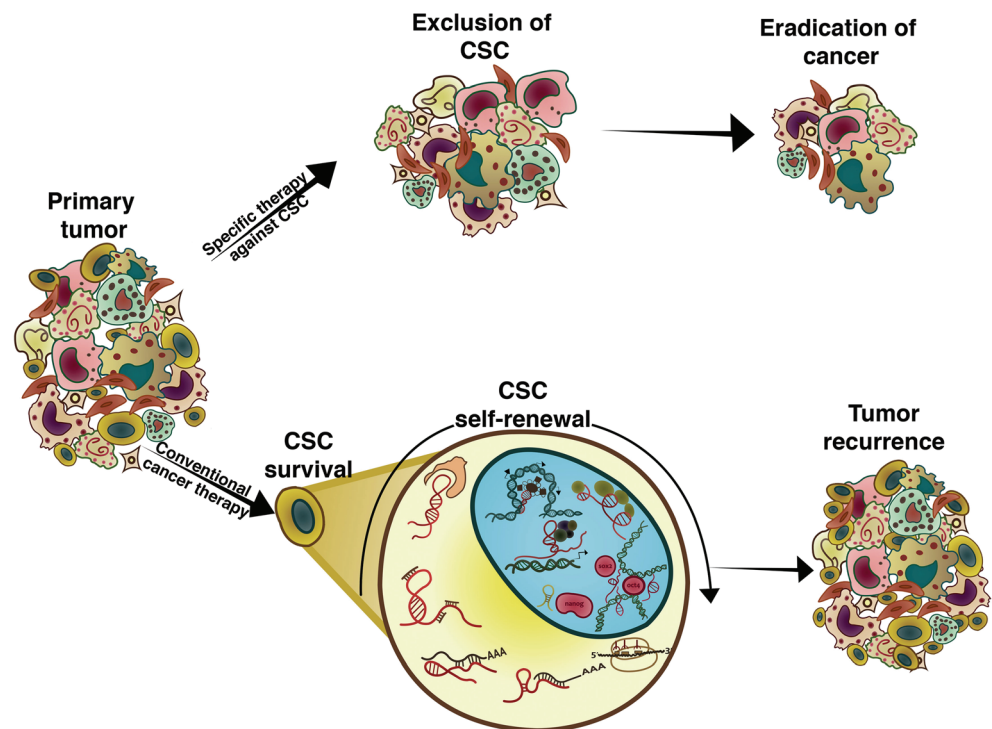
lncRNAs may exhibit distinct subcellular localization patterns including nuclear, cytoplasmic or both. Inside the nucleus, lncRNAs may stay close to the site of transcription anchored to the chromatin or accumulate away from the transcription site. Once transcribed, lncRNAs may act *in cis* (controlling local gene expression) or *in trans* (controlling distant gene expression) resulting in the silencing or activation of tissue-specific genes [8]. Cytoplasmic lncRNAs have been found to play essential roles in multiple molecular

mechanisms, including mRNA stability and translation regulation, protein modification mediation, serving as microRNA precursors or as competing endogenous RNAs. In general, lncRNAs are thought to act as master regulators of transcription, since they can remodel chromatin and create binding domains for the transcriptional machinery, as well as interact with several repressor complexes to block transcription start sites [9].

lncRNAs have been found to be involved in a broad range of biological processes and to exhibit multiple modes of action [10, 11]. Based on this, lncRNAs can be classified by function as 1) decoy lncRNAs that can bind and sequester proteins to modify their catalytic activity or avoid their interaction with targets, 2) guide lncRNAs that can recruit chromatin modifiers to specific genomic loci, 3) scaffold lncRNAs that can function as adaptors to bring together two or more proteins into a complex, 4) lncRNA sponges that can interact with miRNAs to avoid their effect on mRNA targets, 5) competitive endogenous lncRNAs that can provide stability to mRNAs for correct translation and 6) enhancers that function by stabilizing chromosomal loops between gene enhancers and promoters [12–15].

lncRNAs are differentially expressed during normal physiological processes such as development, differentiation and imprinting, as well as during pathological processes such as cancer [16]. Interestingly, abnormal modulation of specific lncRNAs has been reported in cancer stem cell (CSC) subpopulations [9, 17, 18]. Here, we will summarize recent advances on the involvement of specific lncRNAs in the regulation of CSCs (Fig. 1).

**Fig. 1 Role of CSCs in the relapse of solid tumors.** Since CSCs are resistant to chemotherapeutic agents, current cancer treatments fail to eradicate them. This failure eventually allows CSCs to self-renew and provoke tumor relapse. Therefore, it is essential to identify specific targets to eliminate the CSC fraction and, thereby, to ensure the eradication of cancer. Recent work has shown that various lncRNAs may play crucial roles in both the nucleus and the cytoplasm of CSCs, thereby allowing them to self-renew and to promote tumor growth





### 3 Cancer stem cells

Cancer represents a group of diseases with certain commonalities ('hallmarks') that behave as dynamic, interrelated and multidimensional evolutionary systems, centered around deregulated genomic and epigenomic processes [19–21]. In recent years, it has been suggested that tumors harbor functional cell subpopulations with stem cell features, i.e., the ability to self-renew and to produce a phenotypically diverse progeny [22, 23]. These cells, named cancer stem cells (CSCs), are able to divide either asymmetrically or symmetrically, possess a limitless proliferative capacity, have a high tumorigenic, invasive and metastatic potential and are resistant to commonly used chemotherapeutic agents [24–26]. CSCs achieve self-renewal through asymmetric cell division, in which one daughter cell retains the self-renewal capacity and the other undergoes differentiation. The mechanisms that regulate asymmetric versus symmetric division are key to cancer progression, since the deregulation of this process is intrinsically associated with neoplastic transformation and tumor growth.

CSCs can be identified using specific cell surface markers such as CD44, CD24, CD133, EpCAM and CD117 [27, 28]. CSCs express high levels of transcription factors that are associated with pluripotency and epithelial-mesenchymal transition (EMT), and they exhibit an increased potential to form new tumors in e.g. immunodeficient mice or other animal models [25, 29]. Since strong evidence indicates that CSCs are responsible for local and/or distant recurrences (Fig. 1), it is imperative to understand the molecular mechanisms that govern CSCs in order to design specific therapeutic strategies directed against CSCs.

### 4 The function of lncRNAs in CSCs

Until recently, most research has focused on the role of coding genes in cancer development, providing a basis for most of the knowledge that we have to date. It has, however, become clear that also lncRNAs may participate in cancer development and progression. Since lncRNAs are emerging as master regulators of transcription and as possible oncogenes or tumor suppressors, their role in the establishment of CSC phenotypes has recently been explored. It has for example been shown that the overexpression, deficiency or mutation of lncRNAs may have functional implications for the self-renewal capacity of CSCs (Fig. 1). The role of various lncRNAs in the regulation of CSCs has been studied in several cancers including colon, breast, prostate, esophagus, lung, liver, kidney, stomach, bone and liver cancers. In the next section, we will describe the functions and regulatory roles of lncRNAs in CSCs in different cancers (Table 1).

### 5 lncRNAs associated with CSCs

**LncHPVT1** LncHPVT1 is a nuclear lncRNA that has been found to be significantly upregulated in hepatocellular carcinomas (HCC) and to be associated with hepatitis B virus (HBV) infection [30]. LncHPVT1 has recently been linked to the expansion of CSCs [31, 32]. Notably, LncHPVT1 has been found to be regulated by the TGF- $\beta$  pathway, which can be activated by HBV in HCC tissues. Gain and loss of function experiments have been used to demonstrate that LncHPVT1 can enhance liver cancer stem cell abilities both in vitro and in vivo. Specifically, it has been found that this lncRNA can mediate the acquisition of stem cell-like properties in HCC cells by stabilizing the nucleolar protein NOP2 [31]. Remarkably, a high LncHPVT1 expression has been found to be associated with a poor clinical outcome.

**Linc00617** Linc00617 is a chromosome 14 associated long intergenic non-coding RNA (lincRNA) with a size of 2937 nt. This lincRNA has been found to be highly expressed in advanced breast cancer tissues and its associated lymph node metastases. Gain of function studies have demonstrated that this lincRNA can promote the migration and invasion of breast cancer cells. Notably, overexpression of linc00617 has been found to induce EMT by reducing the level of E-cadherin and increasing that of N-cadherin and Vimentin [33]. This lincRNA is not only associated with EMT, but also with the self-renewal and expansion of breast CSCs. Overexpression of this lincRNA has been found to increase the mammosphere forming and tumorigenic abilities of breast cancer cell populations due to an enrichment of the CSC fraction. Interestingly, in vivo assays have shown that linc00617 deficiency may lead to a dramatic reduction in the number of metastatic nodules.

The molecular mechanism underlying stemness control by linc00617 has recently been elucidated. Linc00617 has been identified as a nuclear RNA that binds to the promoter of the *Sox2* gene and activates its transcription through the recruitment of hnRNP-K (Fig. 2a). SOX2 regulation by linc00617 has been verified through loss and gain of function experiments showing a positive strong correlation between the expression levels of linc00617 and SOX2. It was concluded that linc00617 probably exhibits oncogenic activity through the regulation of SOX2, which stimulates EMT and enhances the self-renewal ability of CSCs.

**HIF2PUT** The hypoxia-inducible factor-2 $\alpha$  promoter upstream transcript (HIF2PUT) is a novel lncRNA with key regulatory functions in osteosarcoma and colon cancer stem cells [34–36]. HIF2PUT is an antisense lncRNA located in the promoter upstream region of the hypoxia-inducible factor-2 $\alpha$  (*HIF-2 $\alpha$* ) gene. HIF2PUT regulates the transcriptional activity of its host gene *HIF-2 $\alpha$*  in bone and colon tissues.

**Table 1** LncRNAs involved in CSC regulation

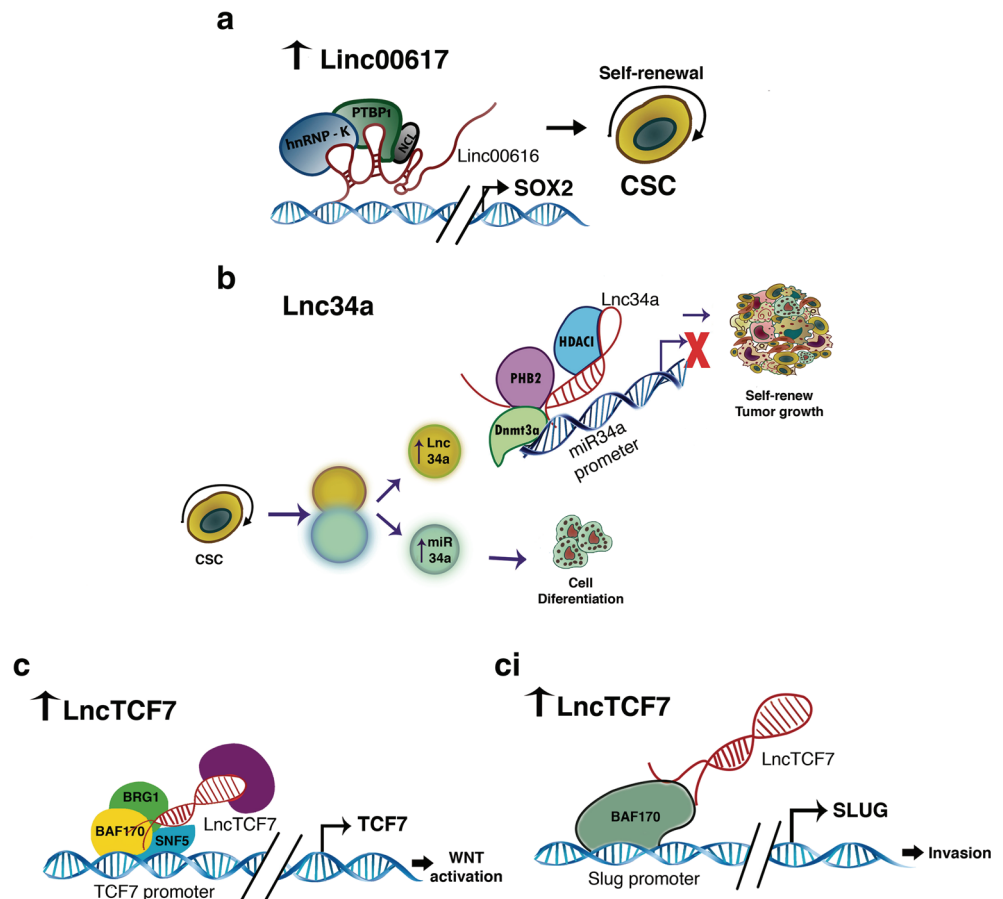
LncRNA	Chr	Cancer stem cell type	Regulated by	Expression status	Diagnosis patients	Subcellular detection	Functions in cancer stem cells	Molecular mechanisms	Ref.
LncPVT1	8	Liver	TGF-B	Overexpressed	Poor prognosis	Nucleus	CSC trait acquisition	Stabilize NOP2	[25–27]
Linc00617	14	Breast	NA	Overexpressed	Poor prognosis	Nucleus	Self-renew of CSCs	RNA binds to the Sox2 promoter and activates its transcription through the recruitment of hnRNP-K.	[28]
HIF2PUT	2	Osteosarcoma Colon	NA	Overexpressed	Poor prognosis	Nucleus	Acts as an inhibitor of self-renewal of osteosarcoma CSC. Participates in the enrichment of stem phenotype in colon cancer	NA	[29–31]
LncSOX2OT	3	Embryonic tissues Breast Esophageal squamous Glioblastoma	SOX3 in glioblastoma	Overexpressed	Poor prognosis	Nucleus / Cytoplasm	Regulates pluripotency, and increase proliferation, migration and invasion of CSC.	SOX2OT capture the miR-194-5p / miR-122 to allow the transcription of TDGF-1 by SOX3.	[32–35]
HOTAIR	12	Breast Oral, Glioma Colon	NA	Overexpressed	Poor prognosis	Nucleus / Cytoplasm	Promotes growth, migration, invasion, self-renewal of CSC, and induces the expression of pluripotent induced genes.	Transcriptional regulation by binding to the PRC2 complex. Additionally, HOTAIR reduces the binding of p53 to the p21 promoter region. Also, promotes growth through negative regulation of SETD2. HOTAIR regulates pluripotency genes by capturing miR-34a.	[9, 10, 37–40]
LncRNA uc.283-plus	10	Glioma Prostate	NA	Overexpressed	Poor prognosis	NA	Enrichment of stem phenotype. The expression of this lncRNA distinguishes between embryonic stem cells or adult tissues.	Uc.283-plus could work as a sponge to recruit miRNAs such as miR-455-5p, miR-640 and miR-1909-3p.	[45, 46]
Lnc34a	1	Colon	NA	Overexpressed	Poor prognosis	Nucleus	Lnc34a generates the epigenetic silencing of miR-34, triggering proliferation of Colon CSC through symmetric self-renewal.	Lnc34a binds to the miR-34a promoter to recruit PHB2 / Dnmt3a and HDAC1 to methylate and deacetylate the miR-34a promoter.	[50]
LncTCF7	5	Liver Lung Prostate	IL6/STAT3 pathway	Overexpressed	Poor prognosis	Nucleus / Cytoplasm	LncTCF7 promotes invasion and self-renewal of CSC in different ways, in order to increase tumor formation.	Interacts with the SWI/SNF complex, to regulate the transcription of TCF7 and Slug. It also works as a sponge of miR-200c to avoid EpCAM degradation.	[51, 53–56]
lncH19	11	Breast Prostate Glioblastoma	NA	Overexpressed	Poor prognosis	Cytoplasm	Maintenance and self-renewal of CSC, resulting in an increment in cell migration and tumor growth.	H19 functions as sponge of miRNA let-7 to increase the expression of LIN28.	[58–61]
LncATB	14	Colon Gastric Stomach Liver	TFG-B	Overexpressed	Poor prognosis	Cytoplasm	LncATB promotes the acquisition and maintenance of stem cell phenotype, inducing vascular invasion and metastasis. It also generates resistance to drugs.	LncATB functions as a sponge of mir200 to allow the transcription of ZEB1 and ZEB2. It also stabilizes IL-11 to activate the STAT3 signaling.	[72, 73]
Linc-DYNC2H1–4	11	Pancreas	NA	Overexpressed	Poor prognosis	Cytoplasm	DYNC2H1–4 promotes the progression of EMT and enrichment of the CSC fraction	Acts as a sponge of miR-145 to allow the transcription of Oct4,	[78, 79]

**Table 1** (continued)

lncRNA	Chr	Cancer stem cell type	Regulated by	Expression status	Diagnosis patients	Subcellular detection	Functions in cancer stem cells	Molecular mechanisms	Ref.
HOTTIP	7	Pancreas	NA	Overexpressed	Poor prognosis	Nucleus	through the gemcitabine resistance. HOTTIP promotes EMT, invasion, drug resistance and improves the properties of CSC through the Wnt/ $\beta$ -catenin pathways.	Lin28, Nanog, Sox2, MMP3 and ZEB1. HOTTIP is assembled to WDR5 / MLL complex to the HOXA and HOXA9 loci to activate transcription.	[80–82]
lncRNA-HH	9	Breast	Twist	Overexpressed	Poor prognosis	NA	Regulates self-renewal of CSC by activating the Hedgehog pathway	The lncRNA-Hh directly targets GAS1 to activate the hedgehog signaling and increases the SOX2 and OCT4 expression.	[83, 84]
lncARSR	9	Kidney Liver	YAP	Overexpressed	Poor prognosis	Cytoplasm	It is essential for the maintenance of the stem cell phenotype and the metastatic potential of renal CSC. In addition, ARSR is packaged in exosomes and confers pharmacological resistance to sensitive cells by modulating the STAT3, AKT and ERK signaling.	Promotes drug resistance by direct binding of miR-34 / miR-449 to allow the expression of AXL / c-Met. It also prevents the LATSYP interaction to facilitate the nuclear translocation of YAP.	[85–87]
lincROR	18	Gastric Pancreas Lung Endometrium	OCT4	Overexpressed	Poor prognosis	Cytoplasm	lincROR is an important regulator of tumor suppressor miRNAs that control the maintenance and self-renewal of cancer stem cells	Acts as a sponge of miR-145, miR-205, miR-34a and let7 to increase the capabilities of CSCs	[88, 90–96]
MALAT	11	Pancreas Breast Liver	NA	Overexpressed	Poor prognosis	Nucleus / Cytoplasm	MALAT regulates the EMT, proliferation, migration and self-renewal of CSC. It also plays an important role in the telomere lengthening of liver cancer stem cells.	MALAT acts as a sponge to capture miR200c and miR145, to stimulate the expression of pluripotency factors.	[97–100]
CUDR	19	Liver	NA	Overexpressed	Poor prognosis	Nucleus / Cytoplasm	CUDR induces the malignant transformation of stem cells by cooperating with SEAT1 through TRF2 and thus modulating the NF- $\kappa$ B and STAT3 pathways. CUDR also promotes the growth of CSC through the positive regulation of TERT and c-Myc. This lncRNA also regulates other lncRNAs, miRNAs and proteins to protect telomere length, disrupt genomic stability and induce stem cell malignant transformation and proliferation	CUDR induces the expression of SUV39h1 to promote the expression and phosphorylation of NF- $\kappa$ B and the subsequent phosphorylation of STAT3.	[102, 104–108]
DILC	13	Liver	NA	Underexpressed	Poor prognosis	Nucleus	The lack of expression of DILC allows the expansion of CSC through the IL-6 / STAT3 axis	DILC binds to the IL6 promoter and inhibits its transcription.	[110]

**Fig. 2 Mechanisms of action of lncRNAs in CSC nuclei. a**

Lnc00617 may act as a scaffold of hnRNP-K and promote the self-renewal of CSCs. **b** Lnc34a may act as a scaffold of Dnmt3a, PHB2 and HDAC1 to avoid the transcription of miR34a, thus activating the NOTCH and WNT signaling pathways. **c** LncTCF7 may act as a scaffold to recruit the chromatin remodeling complex SWI/SNF to the promoter of TCF7, thereby activating the WNT signaling pathway. **ci** LncTCF7 may promote invasion through the induction of SLUG expression



Overexpression of this lncRNA leads to HIF-2 $\alpha$  upregulation whereas HIF2PUT deficiency has been found to result in reduced levels of HIF-2 $\alpha$  in both osteosarcoma and colon cancer-derived cell lines. Notably, HIF-2 $\alpha$  has been associated with the presence of CSCs in various types of cancer, where it exerts a role in CSC regulation. Interestingly, HIF-2 $\alpha$  and HIF2PUT upregulation has been found to be a common feature of aggressive osteosarcomas and a high expression of HIF2PUT has been found to predict a poor prognosis in osteosarcoma patients [35].

HIF2PUT exerts different regulatory roles in osteosarcoma and colon cancer CSCs. In osteosarcoma, HIF2PUT acts as a potent inhibitor of CSC self-renewal. Inhibition of HIF2PUT has been found to enhance the proliferation, migration and self-renewal of CSCs while its overexpression has been found to inhibit these features [36]. Conversely, in colon cancer HIF2PUT expression has been found to be associated with enrichment of the population of cells with a CSC phenotype [34], whereas HIF2PUT deficiency has been found to impair CSC properties, including proliferation, self-renewal, migration and invasion. In addition, HIF2PUT inhibition has been found to result in a reduction in CSC markers such as Oct4, Sox2 and CD44. Together, these data indicate that this lncRNA may exert opposite roles in the regulation of CSCs derived from different

tissues types. We believe that functional characterization of lncRNAs in different tissue lineages is crucial for the development of tissue-specific therapies. The communication between lncRNAs and components of the microenvironment, such as stromal cells and extracellular components, may have additional implications for cancer progression and therapy development.

**LncSOX2OT** SOX2 overlapping transcript (SOX2OT) is a lncRNA deduced from human chromosome 3q26.3. This lncRNA is transcribed in the same orientation as SOX2, one of the major regulators of pluripotency, which is embedded within the intronic region of SOX2OT. Several studies have shown that there is a positive correlation between SOX2OT and SOX2 expression [37–40]. SOX2OT has been found to be co-upregulated with SOX2 in embryonic stem cells, in breast CSCs and in esophageal squamous carcinoma cells. SOX2OT and SOX2 have also both been found to be highly expressed in estrogen receptor-positive breast cancer and to be associated with tamoxifen sensitivity [38]. Interestingly, in esophageal squamous cell carcinoma, SOX2OT has been found to be co-upregulated with Oct4, another master regulator of pluripotency [37].

SOX2OT is spliced into at least 8 distinct transcripts, and their expression patterns play an emerging role in stem cell biology and tumorigenesis [37, 41]. It has, for example, been found that

SOX2OT variant 7 and 8 are highly expressed in human embryonal carcinoma NT2 cells that exhibit stem cell-like properties. During neuronal differentiation of these cells the SOX2OT-7 variant is dramatically downregulated [41].

**HOTAIR** Hox transcript antisense intergenic RNA (HOTAIR) is an oncogenic lncRNA of which the expression has been found to be altered in various types of cancer, including breast, ovary, colon, pancreas and cervix cancer [42, 43]. This lncRNA is able to induce activation or silencing of its target genes. HOTAIR can recruit the MLL1 methyltransferase and induce histone H3 trimethylation of lysine 4 (H3K4me3), thereby relaxing chromatin and allowing binding of the transcription machinery. HOTAIR can also recruit the PRC2 (Polycomb Repressive Complex 2) complex, induce H3K27me3 and, ultimately, provoke gene silencing [12, 13].

Elevated HOTAIR expression has recently been reported in CSCs derived from breast, oral and colon carcinomas, and from gliomas [44–46]. The expression of this lncRNA has been associated with the acquisition of stem cell characteristic resulting in an increased tumor growth and metastatic potential [44, 47, 48]. HOTAIR induces stemness mainly through triggering EMT in a TGF- $\beta$  dependent way [44, 45]. Exogenous expression of HOTAIR has been found to result in upregulation of the EMT inducers Zeb1, SNAIL, TWIST and CTNNA1, as well as in induction of the mesenchymal markers Vimentin and Fibronectin. Accordingly, also epithelial markers such as E-cadherin, BMP7 and ERBB3 were found to be downregulated by HOTAIR. Interestingly, it was found that the genes downregulated during EMT by HOTAIR exhibit increased PRC2 occupancies [45]. The stem cell features induced by HOTAIR have been validated by the occurrence of increased colony formation, migration and self-renewal capacities [46]. It has also been shown that HOTAIR may regulate colony formation through a reduced p53 binding to the p21 promoter. In addition, it has been shown that HOTAIR may promote CSC growth through downregulation of SETD2 [47]. Several studies have established that HOTAIR may also induce the expression of stem cell markers such as SOX1, SOX2, OCT4 and CD44 [45, 46]. Additionally, it has been found that HOTAIR can regulate SOX2 expression through attenuation of the function of miR-34a. HOTAIR has been positively associated with an advanced clinical tumor stage, the occurrence of metastasis and a worse prognosis [49]. The therapeutic significance of this lncRNA has been established using HOTAIR inhibitors that suppress the proliferation, migration, invasion and self-renewal of CSCs. Thus, HOTAIR may serve as a target to attenuate the progression and invasion/metastasis of cancer [48, 50].

**LncRNA uc.283-plus** LncRNA uc.283-plus is a RNA of 277 nt deduced from an ultra-conserved region (UCR) on chromosome 10. This lncRNA is expressed only in pluripotent stem cells and in some solid neoplasms such as glioma and prostate

adenocarcinoma, but it is absent in normal adult tissues [51]. It has been found that the expression of lncRNA uc.283-plus can discriminate between adult tissues and embryonic stem cells. Although very little is known about this lncRNA, it has been proposed by using bioinformatics tools that it may act as a sponge RNA to recruit miRNAs [52] such as miR-455-5p, miR-640 and miR-1909-3p and, by doing so, allow the expression of target genes such as DICER1, SOX2 and NOTCH1 [51, 53]. Another transcribed RNA called “uc.283-minus” has been found to be deduced from the strand opposite to the uc.283-plus genomic region. The expression of this lncRNA has been found to be regulated by hypermethylation in its CpG islands. Although its function is still unknown, it has been suggested that it may act in the process of tumorigenesis [54].

**Lnc34a** Lnc34a is a novel lncRNA that binds to the miR-34a encoding gene and regulates its silencing by recruiting DNA methyltransferase 3a (DNMT3a) and histone deacetylase 1 (HDAC1) to the miR-34a promoter. Previous studies have shown that miR-34a may act as a negative regulator of the Notch and Wnt signaling pathways, which are essential for the self-renewal of CSCs [55–57]. Interestingly, Wang et al. [58] showed that lnc34a is highly expressed in colon CSCs where it promotes self-renewal (Fig. 2b). Lnc34a is the first lncRNA identified that exhibits an asymmetric distribution during CSC division, thus producing asymmetric daughter cells with different cell fates (Fig. 2b). Lnc34a suppression leads to CSC differentiation via asymmetric cell division, whereas lnc34a overexpression leads to CSC proliferation via symmetric cell division. We consider that further research is warranted to unravel the mechanisms by which this and other lncRNAs regulate asymmetric CSC division. The discovery of the miR-34a - lnc34a axis highlights the importance of ncRNAs in this process and their potential to orchestrate the CSC self-renewal process.

**LncTCF7** LncTCF7 has a length of 3.6 kb and is composed of three exons. This lncRNA can be located in the nucleus as well as in the cytoplasm where it performs different functions depending on the specific cell types or tissues involved. Previous studies have shown that the expression of this lncRNA is regulated through the IL6/STAT3 pathway [59], a key pathway involved in cancer progression [60, 61]. LncTCF7 has been found to interact with three nuclear subunits of the SWI/SNF chromatin remodeling complex (BRG1, BAF170 and SNF5), allowing their recruitment to the *TCF7* gene promoter, thus regulating the transcription of *TCF7* and activating the Wnt signaling cascade, which is involved in stem cell self-renewal (Fig. 2c) [59, 62] LncTCF7 has been found to regulate 2491 genes, many of which belong to the Wnt signaling pathway (Fig. 2c).

LncTCF7 is highly expressed in nuclei of CSCs derived from hepatocellular carcinomas and it has been reported that



inhibition of this lncRNA significantly disrupts the expression of the pluripotency markers Sox2, Nanog and Oct4 and decreases the tumorigenic ability of liver CSCs. Conversely, lncTCF7 overexpression has been found to enhance the tumor-forming ability of liver CSCs [62]. lncTCF7 has also been found to be involved in the regulation of CSCs derived from non-small cell lung cancer (NSCLC) [63]. Together with the SWI/SNF complex, this lncRNA can increase the expression of Slug to promote invasion. Slug is a transcriptional repressor that binds to E-box motifs and represses E-Cadherin transcription (Fig. 2ci). In addition, lncTCF7 increases the expression of the stem cell marker EpCAM to promote self-renewal. This latter effect is not mediated by the SWI/SNF complex, but by competing with EpCAM for binding of the microRNA miR-200c and, thereby, avoiding EpCAM degradation (Fig. 3e) [64]. This sponge effect has been demonstrated in prostate cancer cells as well, thus supporting a more generalized function of this lncRNA. Together, these results show that lncRNAs like lncTCF7 may carry out several molecular functions in the same cells, thereby expanding the possible roles of these RNAs. We consider that this lncRNA depicts a clear example of the multifunctionality of lncRNAs, since some of them may affect the same biological process by acting in different ways according to cellular needs. As we mentioned earlier, lncRNAs can interact directly with DNA, mRNA or proteins to regulate a variety of physiological and pathological processes.

**lncH19** H19 is one of the first ncRNAs identified as a cancer-related lncRNA. Hitherto, this lncRNA has been found to be involved in the development and progression of many different cancer types. *H19* is an imprinting gene located in the 11p15.5 region and encodes a 2.3 kb lncRNA that is expressed exclusively from the maternal allele [65]. H19 is highly expressed during vertebrate embryonic development, but is downregulated in most tissues after birth. Loss of imprinting and, consequently, strong H19 expression has been extensively documented in several types of cancer. Recent studies have shown that H19 is overexpressed in stem-like cells of breast [66] and prostate [67] cancers and glioblastomas [68].

In breast cancer, it has been found that ectopic overexpression of H19 significantly promotes migration, as well as clone and sphere forming capacities. On the contrary, inhibition of H19 has been found to disrupt the growth and tumor forming capacities of breast cancer cells. H19 is mostly found in the cytoplasm of breast cancer cells where it functions to sponge miRNA let-7, which leads to an increase in the expression of LIN28, a well-known let-7 target (Fig. 3a). H19 can also be repressed by let-7 via a negative feedback loop. Notably, H19 and LIN28 are co-expressed in primary breast carcinomas and both have been found to play a critical role in the maintenance of breast CSCs [66]. LIN28 can also block mature let-7 production, thereby avoiding the repression of H19 and reversing

the suppression of breast CSC properties mediated by the loss of H19 [66, 69]. Collectively, these results suggest that H19/let-7/LIN28 forms a double negative feedback loop to promote breast CSC maintenance (Fig. 3b).

In prostate cancer, H19 upregulation has been found to correlate with the expression of stem cell markers such as Sox2, Oct4, Notch1, Klf4, c-Myc and Abcg2. Remarkably, lncH19 level modulations also affect the clonogenic ability of prostate cancer cells [67]. H19 also plays a role in the self-renewal of CSCs in glioblastoma [68]. Interestingly, H19 expression has been found to be mainly restricted to the CSC fraction and exogenous expression has been found to result in an increased migration, as well as neurosphere and tumor formation capacity of this fraction.

Furthermore, H19 is the primary precursor of the proliferation-suppressing miR-675 [70], which has been found to be involved in both neuronal [71, 72] and muscle differentiation [73]. MiR-675 is embedded into the first exon of H19 and its expression is barely detectable in fetal tissues, despite abundant H19 expression [74]. The processing of miR-675 from H19 in embryonic tissues is inhibited by an RNA-binding protein, HuR. MiR-675 is only released in response to cellular stress or oncogenic signals [74]. H19 and miR-675 are both expressed in undifferentiated bone marrow mesenchymal stem cells, but their expression decreases during differentiation of these cells into a neural phenotype. The down-regulation of miR-675 is concomitant with the up-regulation of its target IGF-1R during the differentiation of neural cells [72]. H19 also has an essential function in skeletal muscle differentiation mediated by the microRNAs embedded within it. Strikingly, both miR-675-3p and miR-675-5p promote myogenic differentiation by repressing Smad1, Smad5 and Cdc6. Smad1 and Smad5 are involved in the BMP pathway and Cdc6 is a DNA replication factor that needs to be downregulated during myoblast differentiation [73]. These results support the idea that miR-675 may confer functionality to H19 to control stem cell populations and that disruption of the H19/miR-675 axis may alter the stem cell phenotype.

H19 also functions as a competing endogenous RNA for miR-138, miR-200a and miR-141, which are involved in the regulation of CSCs [75–77]. Notably, H19 interferes with miR-138 and miR-200a, thereby avoiding the repression of Vimentin, Zeb1, and Zeb2 and, concomitantly, inducing EMT. Up-regulation of H19 has been found to result in the modulation of multiple genes involved in EMT, which may promote stemness features [78].

**lncATB** lncRNA-ATB has been recognized as an onco-lncRNA commonly overexpressed in human neoplasms such as colon, gastric, stomach and liver cancer. This lncRNA is a non-polyadenylated RNA mainly located in the cytoplasm. Recent studies have shown that lncATB is associated with EMT. lncATB modulates TFG- $\beta$  which, in turn, regulates

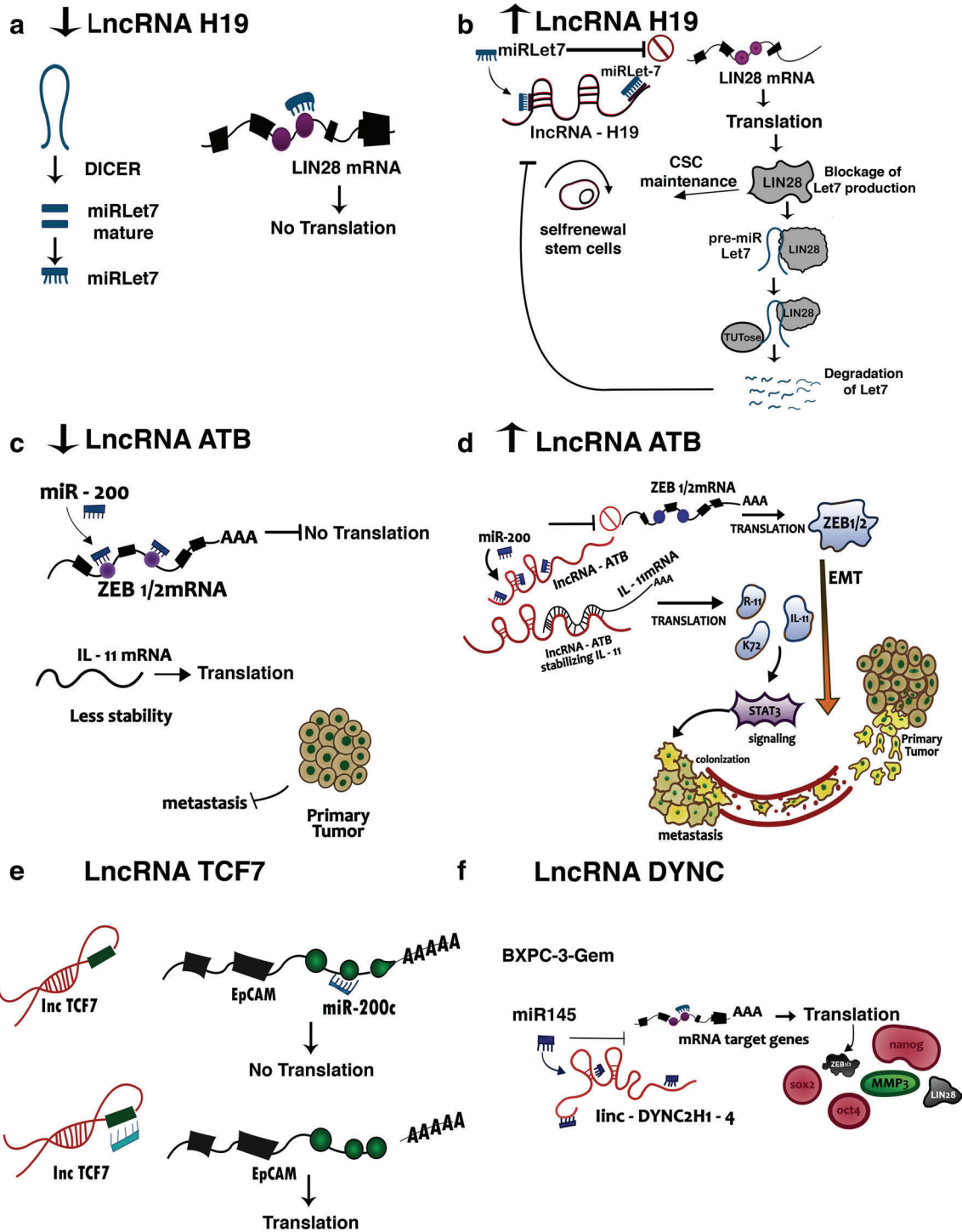


**Fig. 3** Mechanisms of action of lncRNAs in the cytoplasm of CSCs. **a** Absence of lncRNA H19 may inhibit the translation of LIN28 through miRlet-7. **b** LncRNA H19 may act as a sponge RNA for miRlet-7 and allow the translation of LIN28. In addition, H19, let-7 and LIN28 may form a negative feedback loop favoring CSC self-renewal. **c** Decreases in lncRNA ATB levels may allow miR-200 to inhibit ZEB1/2 mRNAs. In addition, the stability of the IL-11 mRNA may be decreased. **d** LncRNA

ATB may act as a sponge RNA for miR-200 to promote the translation of ZEB1/2 and, thus, to promote EMT. LncRNA ATB may also interact directly with IL-11 mRNA and regulate its stability, thereby contributing to cell colonization. **e** LncRNA TCF7 may act as a sponge for miR-200c and, thereby, inhibit the repression of EpCAM. **f** LncDYNC2H1-4 may act as a sponge for miR-145 in the presence of gemcitabine, thereby leading to an increment in stem cell markers

several master regulators of EMT such as Snail, Slug, Zeb1 and Zeb2 [79]. Yuan et al. [80] have found that lncATB

harbors binding sites for miR-200, which prevents EMT through targeting of the Zeb1 and Zeb2 mRNAs. Several



studies have reported that lncATB may induce mesenchymal features and promote cell invasion and metastasis. LncATB binds and stabilizes IL-11, leading to activation of STAT3 signaling and the promotion of cell invasion and metastasis (Fig. 3c) [80, 81]. LncATB has been found to be upregulated in HCC metastases and to be correlated with vascular invasion and a poor patient survival. Recent studies using orthotopic xenografts have demonstrated that lncATB may promote HCC cell intravasation and organ colonization [81]. LncATB may affect metastasis by independent transcription-related mechanisms, first by sponging miR-200 and second by stabilizing IL-11 mRNA (Fig. 3a, b). Both mechanisms lead to the induction of EMT [82, 83]. LncATB has also been found to be involved in trastuzumab resistance in patients with breast cancer [84].

**Linc-DYNC2H1-4** Linc-DYNC2H1-4 is an intergenic lncRNA, transcribed from the same sense strand as its nearby gene *MMP3*, which encodes an important protein for the development of pancreatic cancer [85]. Yuran Gao and colleagues [86] established a gemcitabine-resistant pancreatic ductal adenocarcinoma cell line (BxPC-3-Gem) and found that linc-DYNC2H1-4 was upregulated in these cells. Using in vitro and in vivo assays, it was shown that the resistance to gemcitabine resulted in an enrichment in the CSC fraction. The association of this lincRNA with drug resistance and the CSC phenotype has recently been addressed. It was found that linc-DYNC2H1-4 increases the expression of stemness markers such as Lin28, Nanog, Sox2 and Oct4, as well as that of Zeb1, an EMT regulator. The involvement of this lncRNA in regulating the CSC phenotype was further substantiated by in vitro experiments showing that knockdown of linc-DYNC2H1-4 reduced the colony and spheroid forming abilities, as also the invasive behavior of the gemcitabine-resistant cells. In addition, it was found that exogenous expression of this lincRNA promoted the acquisition of EMT and stemness features in the parental gemcitabine sensitive cells.

Linc-DYNC2H1-4 is mainly located in the cytoplasm, where it acts as a sponge for miR-145, thereby upregulating the expression of its targets Oct4, Lin28, Nanog, Sox2, MMP3 and Zeb1, resulting in EMT progression and CSC enrichment in pancreatic cancer cell populations (Fig. 3f) [86, 87].

**HOTTIP** LncRNA HOTTIP is transcribed from the 5' tip of the HOXA locus and acts *in cis* to regulate the expression of several HOXA genes. HOTTIP binds the adaptor protein WDR5 and targets the WDR5/MLL complex to the HOXA locus, resulting in trimethylation of histone H3 lysine 4. HOXA members play essential roles in the pluripotency, differentiation and self-renewal of stem cells.

HOTTIP is overexpressed in pancreatic ductal adenocarcinoma (PDAC) and promotes its progression, invasion and

drug resistance [88]. This lncRNA also promotes EMT and regulates pancreatic CSCs [88]. Zhiqiang Fu et al. [89] found that HOTTIP is highly expressed in the nucleus of pancreatic CSCs and enhances CSC properties through the Wnt/ $\beta$ -catenin pathway. The role of HOTTIP in the regulation of CSCs is based on the induction of HOXA9 and the subsequent activation of the Wnt pathway. The HOTTIP/HOXA9/WNT axis contributes to stemness by controlling CSC maintenance and self-renewal. HOTTIP and HOXA9 may serve as potential therapeutic targets and molecular biomarkers for PDAC, since their expression may predict survival and prognosis [88, 90].

**LncRNA-Hh** LncRNA-Hh was first identified in breast CSCs expressing high levels of Twist. This lncRNA is transcriptionally regulated by Twist to enrich the CSC population. LncRNA-Hh directly targets GAS1 to stimulate the Sonic Hedgehog-Patched-Gli pathway and to upregulate the expression of SOX2 and OCT4. Notably, Hedgehog signaling is essential for CSC self-renewal and cell fate determination [91]. LncRNA-Hh overexpression leads to EMT and CSC self-renewal, and promotes tumorigenic abilities, while its silencing reverses these effects [92].

**LncARSR** Activated in renal cell carcinoma with sunitinib resistance (ARSR) is a recently identified lncRNA that enhances sunitinib and doxorubicin resistance in renal [93] and hepatocellular [94] carcinomas, respectively. Strikingly, this lncRNA is packaged into exosomes and transmitted to sensitive cells, thereby inducing drug resistance [93]. This lncRNA promotes drug resistance via direct binding to miR-34/miR-449, thereby leading to AXL/c-Met expression and reactivation of STAT3, AKT and ERK signaling [93]. It is worth mentioning that this lncRNA is highly expressed in renal CSCs and is essential for maintenance of their stem cell phenotype. Loss of function analysis of LncARSR has shown that this lncRNA is essential for promoting the self-renewal, tumorigenic and metastatic capacities of renal CSCs. A high LncARSR level has been found to serve as an independent predictor for a poor prognosis of clear cell renal cell carcinoma patients. Mechanistically, this lncRNA binds to Yes-associated protein (YAP) and facilitates its nuclear translocation by blocking the interaction of YAP with the large tumor suppressor kinase-1 (LATS1) [95]. YAP is highly expressed in CSC nuclei where it acts as a transcription co-activator in Hippo signaling, which has been reported to play a critical role in CSC expansion. LncARSR not only plays a role in CSC regulation by inducing Hippo signaling, but also acts on cancer cells with defective Hippo signaling, possibly through other mechanisms [95].

It is well-known that CSC populations do not only emerge from pre-existing CSCs, but also from reprogrammed differentiated cells, possibly through exosomal transfer of lncRNAs. We believe that lncRNA transfer to neighboring cells may play an important role in cancer cell behavior. We

consider that the use of extracellular vesicles as delivery vehicles of lncRNAs may serve as an attractive approach to eliminate CSC populations in tumors.

**lincROR** The lincRNA regulator of reprogramming (lincROR) was first identified in induced pluripotent stem cells (iPSCs). This lincROR acts as an oncogene and plays essential roles in the maintenance of embryonic stem cells (ESCs) and the reprogramming of differentiated cells into iPSCs [96]. Accumulating evidence indicates that lincROR is associated with EMT and tumorigenesis in many malignancies including breast, liver, lung, pancreatic and colon cancer [97]. LincROR appears to play a role in induction of the EMT program, promoting stem cell-like characteristics, drug resistance and metastasis in ovarian, lung and breast cancer [98–100]. Recent studies have revealed that this lncRNA is located in the cytoplasm and acts as a sponge of miR-145 [99, 101], miR-205, miR-34a and let-7 [98]. MiR-205 targets the Zeb1, Zeb2, ErbB3 and VEGF mRNAs and, by doing so, negatively regulates stem cell features [98]. MiR-34a and let-7 also play a role in suppressing breast CSC features [98, 102]. Collectively, these studies indicate that lincROR may be an important regulator of tumor suppressor miRNAs that control stem cell characteristics. LincROR is highly expressed in gastric [103], pancreatic [102] and lung CSCs [101], and its expression has been found to lead to upregulation of several stemness transcription factors such as OCT4, SOX2, NANOG and CD133 [101, 103]. LincROR has been found to act as a miR-145 sponge, resulting in increased expression of the miR-145 targets OCT4, SOX2 and NANOG, allowing the acquisition of lung and endometrial CSC properties [101, 104]. Upregulation of this lincRNA inhibits the differentiation of endometrial CSCs [104]. Accumulating evidence also indicates that lincROR promotes the proliferation and invasion of CSCs [101], inhibits the apoptosis of CSCs [103] and contributes to the acquisition of stem cell properties by acting as a microRNA sponge to regulate gene transcription [101, 102].

**MALAT-1** The metastasis-associated lung adenocarcinoma transcript 1 (MALAT-1) is a highly conserved lncRNA. MALAT-1 has been found to be overexpressed in several human neoplasms and to promote tumor cell invasion and metastasis [105]. Recent studies have shown that MALAT-1 is overexpressed in CSCs derived from pancreas and breast tumors [106, 107]. Through in vitro and in vivo analyses, it has been shown that MALAT-1 enhances CSC phenotypes and regulates their proliferation, colony formation and migration, as well as their self-renewal capacity [106–109]. This stemness regulating role of MALAT-1 is mainly based on the triggering of EMT through Snail, Slug, E-cadherin, N-cadherin and Vimentin regulation [110]. It has also been shown that downregulation of MALAT-1 may reduce the expression of stem cell markers such as Bmi1, Nanog, SOX2

and Nestin in gliomas and pancreatic cancers [106, 108, 109]. MALAT-1 harbors sites complementary to miR-200c and miR-145 and may, therefore, act as an endogenous sponge for these miRNAs resulting in upregulation of the expression of SOX2 [106, 107].

A more recent study has shown that MALAT-1 can cooperate with lncRNA HULC to increase the expression, phosphorylation and sumoylation of telomere repeat-binding factor 2 (TRF2) and to accelerate liver CSC proliferation, resulting in tumor progression (Fig. 4). Additionally, it has been found that TRF2 depletion may abrogate the oncogenic functions of MALAT-1 and HULC. MALAT-1 combined with HULC may also enhance telomerase activity and promote interactions between TERT and TERC, thereby prolonging the telomere length and, thus, lifespan of liver CSCs (Fig. 4) [109].

**CUDR** Cancer up-regulated drug resistance (CUDR) is a lncRNA that plays a role in cancer progression by affecting cell cycle progression and proliferation. CUDR has been found to be involved in drug resistance of several types of cancer through the induction of WNT expression, which turns CUDR into an attractive target to overcome such resistance [111–113]. Since *CUDR* is an oncofetal gene, its upregulation may be relevant for cancer development. Recent evidence has indicated that CUDR expression may lead to disruption of stem cell populations and induce malignant transformation of normal stem cells. Zheng and colleagues [114] have shown that excessive CUDR cooperates with IL6 to triggering the malignant transformation of human embryonic stem cell-derived hepatocyte-like stem cells through the NF- $\kappa$ B/STAT3 pathway. CUDR and IL6 induce the expression of SUV39h1, a histone methyltransferase that induces trimethylation of histone H3 at lysine 9 (H3K9me3) to promote the expression and phosphorylation of NF- $\kappa$ B and, subsequently, STAT3 phosphorylation. STAT3 can, in turn, bind to the promoter regions of several miRNAs and lncRNAs such as miR-21, miR-155, miR-17, CUDR, HOTAIR, MALAT-1 and HULC. Abnormal expression of these ncRNAs results in increased telomere length and increased microsatellite instability. Gui et al. [115] have also found that excessive CUDR may trigger the malignant transformation of hepatocyte stem cells. CUDR induces HULC expression by inhibiting its promoter methylation and induces  $\beta$ -catenin expression by promoting promoter-enhancer chromatin loop formation. Both HULC and  $\beta$ -catenin are crucial for the oncogenic activity of CUDR.

Li et al. [116] found that SET1A, a histone methyltransferase complex component, cooperates with CUDR to trigger the malignant transformation of hepatocyte stem cells through TRF2. CUDR enhances the phosphorylation of RB and the interplay between SET1A and pRB, thereby producing an activated pRB-SET1A complex (Fig. 4). This complex induces tri-methylation of histone H3 (H3K4me3) and loads onto the TRF2 promoter region provoking TRF2 overexpression (Fig. 4). TRF2 is a component of the shelterin complex

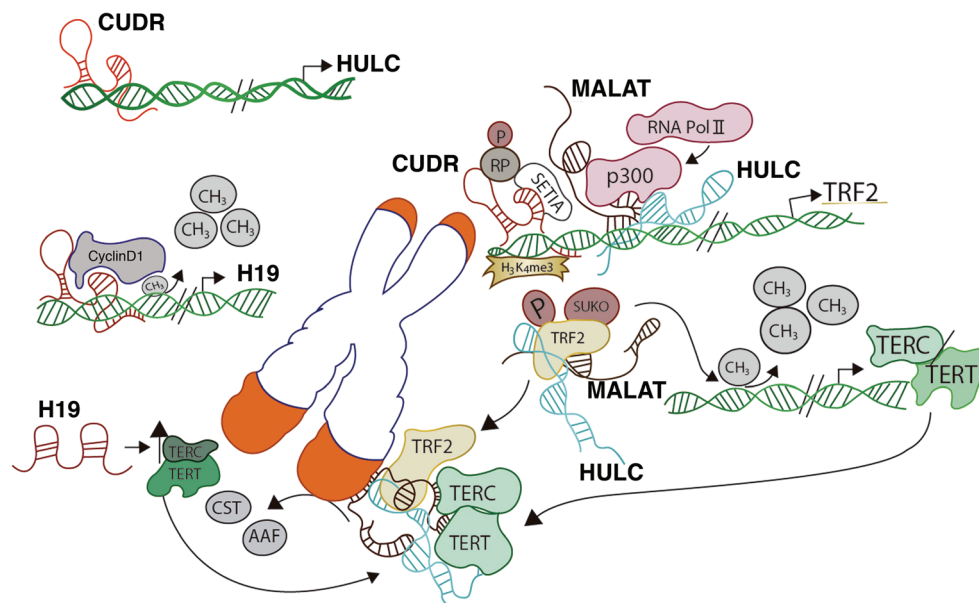


**Fig. 4 Role of lncRNAs in telomere elongation.** Role of different lncRNAs associated with telomeric DNA and proteins that promote telomere elongation. CUDR, MALAT and HULC promote the transcription of TRF2 through different mechanisms. MALAT and HULC may form a complex with TRF2 to demethylate the promoters

of TERC and TERT, thereby provoking CST and AAF proteins to be displaced from the telomeres and favoring telomeric elongation. CUDR may also promote the transcription of lncRNA H19 to promote the expression of TERC and TERT

that protects the ends of chromosomes. Excessive TRF2 binds to telomeric repeats, thereby prolonging their lengths and accelerating the malignant transformation of hepatocyte stem cells and their subsequent cancerous growth [116].

It has been reported that CUDR expression also plays an important role in the occurrence of hepatocellular carcinomas and is associated with their TNM stage and metastatic potential, as well as with postoperative patient survival [117]. Recent evidence shows that CUDR can also act on liver CSCs and promote CSC growth through TERT and c-Myc upregulation. CUDR binds to Cyclin D1, forming a complex that loads onto the H19 lncRNA promoter region to reduce its methylation and to provoke its overexpression (Fig. 4). Excessive H19 increases the binding of TERT to TERC and reduces the interplay between TERT and TERRA, thus enhancing telomerase activity and telomere length (Fig. 4c). CUDR may also mediate c-Myc overexpression through the CUDR-CyclinD1-CTCF complex (Fig. 4). Both TERT and c-Myc expression can lead to liver CSC proliferation [118].

Taken together, these findings indicate that CUDR can interact with other lncRNAs (H19, HULC and MALAT-1) and with proteins (Cyclin D1, TRF2 and SETA1) to enhance telomere elongation, disrupt genomic stability and induce malignant transformation and proliferation of (hepatic) stem cells (Fig. 4).

**lnc-DILC** lncRNA downregulated in liver cancer (lnc-DILC) was recently identified through high-throughput screening in liver tissues. lnc-DILC was found to be downregulated in liver cancer stem cells (LCSC) and to be restored during their

differentiation. The lnc-DILC expression level was found to be related to the proportion of CSCs, since the number of LCSC increased after lnc-DILC silencing and decreased after lnc-DILC overexpression. Loss and gain function analyses revealed that lnc-DILC can modulate the clonogenic and tumorigenic abilities of LCSCs. Lack of expression of this lncRNA facilitates the expansion of LCSCs and favors the progression of hepatocellular cancer. Conversely, it has been found that lnc-DILC expression exhibits a suppressive role in LCSC expansion. lnc-DILC binds to the IL6 promoter and inhibits its transcription, thereby blocking the IL-6/STAT3 signaling cascade. These findings indicate that lnc-DILC may mediate crosstalk between TNF/NF- $\kappa$ B signaling and autocrine IL6/STAT3 signaling to regulate LCSC expansion. Additional clinical data revealed that a low lnc-DILC expression predicts early recurrence and a short survival of hepatocellular carcinoma patients, thereby highlighting its clinical significance [119].

## 6 Therapeutic implications of CSC-associated lncRNAs

CSCs are key players in tumor initiation, maintenance, progression, metastasis and recurrence [120]. In addition, CSCs have intrinsic mechanisms allowing them to resist conventional drug treatments [121, 122]. Since CSCs are molecularly and functionally distinct from the bulk of tumor cells, therapeutic alternatives may be developed to eliminate CSCs that

otherwise may cause disease progression and/or recurrence. The putative advantage of such selective therapies is that they may have fewer side effects and exhibit less toxicity to non-cancer stem cells. This approach requires a clear understanding of the molecular mechanisms that directly regulate stem cell features. It has amply been shown that lncRNAs exhibit important capacities for inducing the self-renewal, migration, invasion, drug resistance and differentiation of CSCs [123–126]. lncRNAs are attractive treatment targets since they commonly exhibit restricted tissue-specific expression patterns. Their levels are frequently indicative for the severity of the disease [127]. lncRNAs are also ideal candidates for cancer screening, since they are readily detectable in body fluids such as blood, plasma, saliva and urine [16, 128, 129]. These features render lncRNAs into ideal targets to noninvasively detect or predict cancer behavior before, during and after therapy. An additional advantage of using lncRNAs as therapeutic targets is the feasibility to induce their degradation, modulate their transcription and/or block their interaction with other regulatory factors. Although a wide range of lncRNAs has been found to be deregulated in CSCs, its consequences are known for only a few of them. Accumulating data now provide insight into the functional implications of lncRNAs in controlling cell division, determining cell fate, conferring differential drug-resistance, protecting telomere ends, maintaining genomic architecture, interacting with key signaling pathways and regulating the transcription or translation of stem cell-related genes [58, 109, 123, 127, 130–132].

Several lines of evidence suggest that CSCs of advanced stage tumors utilize a symmetric division strategy to give rise daughter cells able to self-renew and, thus, to rapidly increase the pool of CSCs within a tumor [133]. This finding suggests that controlling or avoiding symmetrical CSC divisions in advanced tumors could be clinically beneficial. Since lncRNAs may play unique roles in regulating the balance between asymmetry and symmetry in CSCs [58, 134], altering their function may perturb the division machinery that establishes the unequal partitioning of cell fate-determining factors between daughter cells. As such, lncRNAs that control the manner in which CSCs divide could be considered as putative targets for the treatment of advanced cancers. It has been shown, for instance, that asymmetric distribution of lnc34a during cell division leads to asymmetric daughter cell fate, but that high lnc34a levels lead to CSC expansion via symmetric self-renewal [58]. Interestingly, this lncRNA is commonly upregulated in late-stage colorectal cancers, so its suppression could lead to asymmetric cell division and differentiation. It has been reported that lnc34a directly targets miR-34a and balances the cell division mode by a differential Notch1 distribution mediated by this miRNA [58]. Recently, a miR-34a mimic (MRX34) has been proposed to restore miR-34a function and, thus, to prevent CSC proliferation and expansion. Currently, phase II clinical trials are being

conducted to test the efficacy of MRX34 in advanced solid tumors [135], although the delivery efficiency into the tumors still remains a challenge. Also lnc34a could be considered as a target for therapeutic intervention of advanced tumors since it is feasible to develop small molecule inhibitors that block its function or disrupt its structure.

It is well documented that lncRNAs may also participate in the acquisition and maintenance of drug-resistance in CSCs. These lncRNAs may activate several mechanisms to promote this drug resistance, including modulation of drug transporter expression levels, regulation of survival signaling pathways, avoidance of apoptosis and induction of DNA repair. lncPVT1 and H19 are known to promote drug resistance in some types of cancer by modulating the expression of drug transporters such as MDR1 and MRP1 [130, 136, 137], whereas HOTAIR is known to modulate the DNA damage response pathway through suppression of p21 and p53 [46]. lncRNA CUDR has been found to increase drug-mediated resistance by regulating the Wnt signaling pathway [111] or by inducing Bcl2 expression mediated by miR-204-5p inhibition [138]. lncATB and lncROR have been found to reduce chemotherapy-induced cell death by modulating the expression levels of TGF $\beta$  [80, 139]. Since these lncRNAs play crucial roles in drug resistance, they might be used as therapeutic targets to overcome this resistance. Recent work has shown that lncRNAs that induce drug resistance can be disseminated to sensitive cells by vesicles (exosomes) that transmit regulatory lncRNAs. Once inside these cells, they have the ability to induce drug resistance and stem cell phenotypes [130]. lncARSR can, for example, be encapsulated by exosomes that are released into the extracellular environment and transferred to neighboring cells, thereby conferring drug resistance to sensitive cells [93]. lncROR is another lncRNA involved in the modulation of cellular responses to chemotherapy that can be transferred to other cells via extracellular vesicles [139]. The targeting lncRNAs transmitted by vesicles may be a useful approach to improve the responses to conventional therapeutic agents used for the treatment of cancer.

lncRNAs modulating other stem cell features may also be considered for therapeutic intervention. HOTAIR and MALAT-1 are, for example, well-known lncRNAs playing a role in maintaining stem cell features through the modulation of pluripotency stem cell factors [46, 47, 106]. Interestingly, these lncRNAs have been found in the plasma of cancer patients and are considered useful tools for primary cancer and metastasis detection [140]. Mohamed-Moustafa et al. [141] set out to find clinically relevant cancer-associated lncRNA by characterizing temporally expressed lncRNAs during S-phase. They found that most of these lncRNAs appeared to be strongly associated with cancer development. In addition, they found that a large proportion of these lncRNAs may act as independent prognostic indicators in some types of cancer. Subsequent modulation of these lncRNAs resulted in



alterations in cell cycle progression, proliferation, apoptosis, migration and senescence [141]. Hua-Sheng et al. [142] inferred lncRNAs with relevant functions in cancer by predicting their targets using molecular profiles of TCGA primary tumors. They linked lncRNAs with the deregulation of cancer genes and pathways known to influence tumor biology and found that a large number of these lncRNAs regulates hundreds of genes, many of which modulate cancer pathways across multiple tumor types [142]. These latter findings indicate that large-scale screening may result in the identification of potential oncogenic drivers and, thus, potential therapeutic targets.

## 7 Conclusions and perspectives

The large orchestra of molecular and cellular processes in which lncRNAs participate leads to the activation and/or disruption of a plethora of normal and abnormal biological processes such as cancer. CSCs have been extensively studied since they can drive tumor initiation and progression. CSCs are of particular significance due to their metastatic capacity and their ability to escape from common therapeutic agents, which renders them into the primary cause of tumor relapse. Despite their essential role in tumor development, the regulation of this subpopulation of cells is not completely deciphered yet and, therefore, more in-depth studies are required. Here, we have provided an overview of lncRNAs involved in the self-renewal, maintenance and differentiation of CSCs, as well as some of the underlying molecular mechanisms. lncRNAs can exert their functions at different levels and in different ways. In the nucleus they can act as scaffold, guide or capture, as exemplified by SOX4, HOTAIR and HOTTIP. In the cytoplasm they can function as endogenous competitors or sponges of miRNAs, as exemplified by ATB or DYNC2H1. Some lncRNAs, such as CTCF7 and H19, may act in both cellular compartments in order to maintain the self-renewal of the CSCs. There are also many lncRNAs, such as MALAT-1, H19 and CUDR, that work together to prolong telomeres and, by doing so, expand CSC subpopulations. As yet, only a few lncRNAs have been identified to be involved in CSC stemness, warranting further studies on the mechanisms involved in this feature.

lncRNAs are highly abundant within the genomes of our cells where they regulate multiple processes at the transcriptional, translational and post-translational level. We consider that it is essential to understand the molecular mechanisms whereby lncRNAs exert their functions and to uncover the roles that lncRNAs play in specific tissues. Such information will provide a basis for considering lncRNAs as diagnostic or prognostic markers, or even as targets for future therapies. Further studies are needed to establish which lncRNAs may serve as the best candidates for future therapeutic strategies

through hampering the self-renewal and proliferation capacities of CSCs. Since CSCs exhibit intrinsic mechanisms allowing them to overcome conventional therapeutic treatment regimens, specific methods are needed to ensure the eradication of CSCs and, thus, to avoid tumor recurrence. Extensive efforts have yielded ample information on the functional implications of specific lncRNAs in conferring drug resistance, controlling cell division, determining cell-fate and regulating the transcription or translation of stem cell-related genes. Blockage of these lncRNAs may be used to treat specific types of cancer. The fact that lncRNAs can readily be detected in serum, saliva, urine, blood or tissue biopsies, renders them highly attractive for clinical (diagnostic/prognostic) purposes. In addition, different approaches to target lncRNAs for therapeutic purposes can be considered, such as the use of siRNAs or locked nucleic acid molecules to induce lncRNA degradation, and CRISPR/Cas9 mediated gene editing or exosome delivery to modulate their expression. Currently, the major challenge of these approaches is to specifically deliver the respective molecules into their pre-selected tissues/cells. Without any doubt, lncRNAs are emerging as valuable tools for future clinical applications. In fact, some of them are already being tested in clinical trials to determine their putative therapeutic efficacy.

**Acknowledgments** We thank graphic designer Cristina Oropeza Ramírez for her excellent contribution.

## References

1. S. Djebali, C.A. Davis, A. Merkel, A. Dobin, T. Lassmann, A. Mortazavi, A. Tanzer, J. Lagarde, W. Lin, F. Schlesinger, C. Xue, G.K. Marinov, J. Khatun, B.A. Williams, C. Zaleski, J. Rozowsky, M. Roder, F. Kokocinski, R.F. Abdelhamid, T. Alioto, I. Antoshechkin, M.T. Baer, N.S. Bar, P. Batut, K. Bell, I. Bell, S. Chakraborty, X. Chen, J. Chrast, J. Curado, T. Derrien, J. Drenkow, E. Dumais, J. Dumais, R. Duttagupta, E. Falconnet, M. Fastuca, K. Fejes-Toth, P. Ferreira, S. Foissac, M.J. Fullwood, H. Gao, D. Gonzalez, A. Gordon, H. Gunawardena, C. Howald, S. Jha, R. Johnson, P. Kapranov, B. King, C. Kingswood, O.J. Luo, E. Park, K. Persaud, J.B. Preall, P. Ribeca, B. Risk, D. Robyr, M. Sammeth, L. Schaffer, L.H. See, A. Shahab, J. Skancke, A.M. Suzuki, H. Takahashi, H. Tilgner, D. Trout, N. Walters, H. Wang, J. Wrobel, Y. Yu, X. Ruan, Y. Hayashizaki, J. Harrow, M. Gerstein, T. Hubbard, A. Reymond, S.E. Antonarakis, G. Hannon, M.C. Giddings, Y. Ruan, B. Wold, P. Caminci, R. Guigo, T.R. Gingeras, Landscape of transcription in human cells. *Nature* **489**, 101–108 (2012)
2. V. Taucher, H. Mangge, J. Haybaeck, Non-coding RNAs in pancreatic cancer: Challenges and opportunities for clinical application. *Cell Oncol* **39**, 295–318 (2016)
3. S. Jalali, S. Gandhi, V. Scaria, Navigating the dynamic landscape of long noncoding RNA and protein-coding gene annotations in GENCODE. *Hum Genomics* **10**, 35 (2016)
4. J.L. Rinn, H.Y. Chang, Genome regulation by long noncoding RNAs. *Annu Rev Biochem* **81**, 145–166 (2012)

5. G. Bohmdorfer, S. Sethuraman, M.J. Rowley, M. Krzysztos, M.H. Rothi, L. Bouzit, A.T. Wierzbicki, Long non-coding RNA produced by RNA polymerase V determines boundaries of heterochromatin. *elife* **5**, e19092 (2016)
6. A. Barski, I. Chepelev, D. Liko, S. Cuddapah, A.B. Fleming, J. Birch, K. Cui, R.J. White, K. Zhao, Pol II and its associated epigenetic marks are present at pol III-transcribed noncoding RNA genes. *Nat Struct Mol Biol* **17**, 629–634 (2010)
7. K.W. Vance, C.P. Ponting, Transcriptional regulatory functions of nuclear long noncoding RNAs. *Trends Genet* **30**, 348–355 (2014)
8. L.L. Chen, Linking long noncoding RNA localization and function. *Trends Biochem Sci* **41**, 761–772 (2016)
9. J. Cao, The functional role of long non-coding RNAs and epigenetics. *Biol Proced Online* **16**, 11 (2014)
10. T.R. Mercer, J.S. Mattick, Structure and function of long noncoding RNAs in epigenetic regulation. *Nat Struct Mol Biol* **20**, 300–307 (2013)
11. M. Guttman, J.L. Rinn, Modular regulatory principles of large non-coding RNAs. *Nature* **482**, 339–346 (2012)
12. X. Wang, S. Arai, X. Song, D. Reichart, K. Du, G. Pascual, P. Tempst, M.G. Rosenfeld, C.K. Glass, R. Kurokawa, Induced ncRNAs allosterically modify RNA-binding proteins in cis to inhibit transcription. *Nature* **454**, 126–130 (2008)
13. K.C. Wang, H.Y. Chang, Molecular mechanisms of long noncoding RNAs. *Mol Cell* **43**, 904–914 (2011)
14. P.O. Angrand, C. Vennin, X. Le Bourhis, E. Adriaenssens, The role of long non-coding RNAs in genome formatting and expression. *Front Genet* **6**, 165 (2015)
15. A. Ferraro, Altered primary chromatin structures and their implications in cancer development. *Cell Oncol* **39**, 195–210 (2016)
16. J.R. Prensner, A.M. Chinnaiyan, The emergence of lncRNAs in cancer biology. *Cancer Discov* **1**, 391–407 (2011)
17. R.B. Perry, I. Ulitsky, The functions of long noncoding RNAs in development and stem cells. *Development* **143**, 3882–3894 (2016)
18. G. Eades, Y.S. Zhang, Q.L. Li, J.X. Xia, Y. Yao, Q. Zhou, Long non-coding RNAs in stem cells and cancer. *World J Clin Oncol* **5**, 134–141 (2014)
19. D. Hanahan, R.A. Weinberg, Hallmarks of cancer: The next generation. *Cell* **144**, 646–674 (2011)
20. S.L. Floor, J.E. Dumont, C. Maenhaut, E. Raspe, Hallmarks of cancer: Of all cancer cells, all the time? *Trends Mol Med* **18**, 509–515 (2012)
21. D. Hanahan, L.M. Coussens, Accessories to the crime: Functions of cells recruited to the tumor microenvironment. *Cancer Cell* **21**, 309–322 (2012)
22. A. Cicalese, G. Bonizzi, C.E. Pasi, M. Faretta, S. Ronzoni, B. Giulini, C. Brisken, S. Minucci, P.P. Di Fiore, P.G. Pelicci, The tumor suppressor p53 regulates polarity of self-renewing divisions in mammary stem cells. *Cell* **138**, 1083–1095 (2009)
23. M.F. Clarke, M. Fuller, Stem cells and cancer: Two faces of eve. *Cell* **124**, 1111–1115 (2006)
24. Y. Welte, J. Adjaye, H.R. Lehrach, C.R. Regenbrecht, Cancer stem cells in solid tumors: Elusive or illusive? *Cell Commun Signal* **8**, 6 (2010)
25. S. Bugide, V.K. Gonugunta, V. Penugurti, V.L. Malisetty, R.K. Vadlamudi, B. Manavathi, HPIP promotes epithelial-mesenchymal transition and cisplatin resistance in ovarian cancer cells through PI3K/AKT pathway activation. *Cell Oncol* **40**, 133–144 (2017)
26. M.R. Sam, P. Ahangar, V. Nejati, R. Habibian, Treatment of LS174T colorectal cancer stem-like cells with n-3 PUFAs induces growth suppression through inhibition of survivin expression and induction of caspase-3 activation. *Cell Oncol* **39**, 69–77 (2016)
27. M. Munz, P.A. Baeuerle, O. Gires, The emerging role of EpCAM in cancer and stem cell signaling. *Cancer Res* **69**, 5627–5629 (2009)
28. K. Vazquez-Santillan, J. Melendez-Zajgla, L. Jimenez-Hernandez, G. Martinez-Ruiz, V. Maldonado, NF-kappaB signaling in cancer stem cells: A promising therapeutic target? *Cell Oncol* **38**, 327–339 (2015)
29. A. Sathyanarayanan, K.S. Chandrasekaran, D. Karunakaran, microRNA-145 modulates epithelial-mesenchymal transition and suppresses proliferation, migration and invasion by targeting SIP1 in human cervical cancer cells. *Cell Oncol* **40**, 119–131 (2017)
30. Q. Zhang, K. Matsuura, D.E. Kleiner, F. Zamboni, H.J. Alter, P. Farci, Analysis of long noncoding RNA expression in hepatocellular carcinoma of different viral etiology. *J Transl Med* **14**, 328 (2016)
31. F. Wang, J.H. Yuan, S.B. Wang, F. Yang, S.X. Yuan, C. Ye, N. Yang, W.P. Zhou, W.L. Li, W. Li, S.H. Sun, Oncofetal long non-coding RNA PVT1 promotes proliferation and stem cell-like property of hepatocellular carcinoma cells by stabilizing NOP2. *Hepatology* **60**, 1278–1290 (2014)
32. M.A. Parasramka, T. Patel, Long non-coding RNA regulation of liver cancer stem cell self-renewal offers new therapeutic targeting opportunities. *Stem Cell Investig* **3**, 1 (2016)
33. H. Li, L. Zhu, L. Xu, K. Qin, C. Liu, Y. Yu, D. Su, K. Wu, Y. Sheng, Long noncoding RNA linc00617 exhibits oncogenic activity in breast cancer. *Mol Carcinog* **56**, 3–17 (2017)
34. J. Yao, J. Li, P. Geng, Y. Li, H. Chen, Y. Zhu, Knockdown of a HIF-2alpha promoter upstream long noncoding RNA impairs colorectal cancer stem cell properties in vitro through HIF-2alpha downregulation. *Onco Targets Ther* **8**, 3467–3474 (2015)
35. W. Li, X. He, R. Xue, Y. Zhang, X. Zhang, J. Lu, Z. Zhang, L. Xue, Combined over-expression of the hypoxia-inducible factor 2alpha gene and its long non-coding RNA predicts unfavorable prognosis of patients with osteosarcoma. *Pathol Res Pract* **212**, 861–866 (2016)
36. Y. Wang, J. Yao, H. Meng, Z. Yu, Z. Wang, X. Yuan, H. Chen, A. Wang, A novel long non-coding RNA, hypoxia-inducible factor-2alpha promoter upstream transcript, functions as an inhibitor of osteosarcoma stem cells in vitro. *Mol Med Rep* **11**, 2534–2540 (2015)
37. A. Shahryari, M.R. Rafiee, Y. Fouani, N.A. Olliae, N.M. Samaei, M. Shafiee, S. Semnani, M. Vasei, S.J. Mowla, Two novel splice variants of SOX2OT, SOX2OT-S1, and SOX2OT-S2 are coexpressed with SOX2 and OCT4 in esophageal squamous cell carcinoma. *Stem Cells* **32**, 126–134 (2014)
38. M.E. Askarian-Amiri, V. Seyfoddin, C.E. Smart, J. Wang, J.E. Kim, H. Hansji, B.C. Baguley, G.J. Finlay, E.Y. Leung, Emerging role of long non-coding RNA SOX2OT in SOX2 regulation in breast cancer. *PLoS One* **9**, e102140 (2014)
39. Z. Hou, W. Zhao, J. Zhou, L. Shen, P. Zhan, C. Xu, C. Chang, H. Bi, J. Zou, X. Yao, R. Huang, L. Yu, J. Yan, A long noncoding RNA Sox2ot regulates lung cancer cell proliferation and is a prognostic indicator of poor survival. *Int J Biochem Cell Biol* **53**, 380–388 (2014)
40. P.P. Amaral, C. Neyt, S.J. Wilkins, M.E. Askarian-Amiri, S.M. Sunkin, A.C. Perkins, J.S. Mattick, Complex architecture and regulated expression of the Sox2ot locus during vertebrate development. *RNA* **15**, 2013–2027 (2009)
41. M. Saghaeian Jazi, N.M. Samaei, M. Ghanei, M.B. Shadmehr, S.J. Mowla, Identification of new SOX2OT transcript variants highly expressed in human cancer cell lines and down regulated in stem cell differentiation. *Mol Biol Rep* **43**, 65–72 (2016)
42. S.S. Saha, R. Roy Chowdhury, N.R. Mondal, B. Chakravarty, T. Chatterjee, S. Roy, S. Sengupta., Identification of genetic variation

- in the lncRNA HOTAIR associated with HPV16-related cervical cancer pathogenesis. *Cell Oncol* **39**, 559–572 (2016)
43. S. Sharma Saha, R. Roy Chowdhury, N.R. Mondal, B. Chakravarty, T. Chatterjee, S. Roy, S. Sengupta, Identification of genetic variation in the lncRNA HOTAIR associated with HPV16-related cervical cancer pathogenesis. *Cell Oncol* **39**, 559–572 (2016)
  44. Y.N. Jun Dou, X. He, M.L. Di Wu, S. Wu, R. Zhang, M. Guo, Fengsu, I. Zhao, Decreasing lncRNA HOTAIR expression inhibits human colorectal cancer stem cells. *Am J Transl Res* **8**, 98–108 (2016)
  45. C. Padua Alves, A.S. Fonseca, B.R. Muys, E.L.B.R. de Barros, M.C. Burger, J.E. de Souza, V. Valente, M.A. Zago, W.A. Silva Jr., Brief report: The lincRNA Hotair is required for epithelial-to-mesenchymal transition and stemness maintenance of cancer cell lines. *Stem Cells* **31**, 2827–2832 (2013)
  46. J. Deng, M. Yang, R. Jiang, N. An, X. Wang, B. Liu, Long non-coding RNA HOTAIR regulates the proliferation, self-renewal capacity, tumor formation and migration of the Cancer stem-like cell (CSC) subpopulation enriched from breast Cancer cells. *PLoS One* **12**, e0170860 (2017)
  47. J.A. Haiyan Li, M. Wu, Q. Zheng, X. Gui, T. Li, P. Hu, D. Lu, LncRNA HOTAIR promotes human liver cancer stem cell malignant growth through downregulation of SETD2. *Oncotarget* **6**, 27847–27864 (2015)
  48. K. Fang, P. Liu, S. Dong, Y. Guo, X. Cui, X. Zhu, X. Li, L. Jiang, T. Liu, Y. Wu, Magnetofection based on superparamagnetic iron oxide nanoparticle-mediated low lncRNA HOTAIR expression decreases the proliferation and invasion of glioma stem cells. *Int J Oncol* **49**, 509–518 (2016)
  49. S.N. Min, T. Wei, X.T. Wang, L.L. Wu, G.Y. Yu, Clinicopathological and prognostic significance of homeobox transcript antisense RNA expression in various cancers: A meta-analysis. *Medicine* **96**, e7084 (2017)
  50. Y.-W.L. Ming-Yi Lu, P.-Y. Chen, P.-L. Hsieh, C.-Y. Fang, C.-Y. Wu, M.-L. Yen, B.-Y. Peng, D.P. Wang, H.-C. Cheng, C.-Z. Wu, Y.-H. Shih, D.-J. Wang, C.-c. Yu, L.-L. Tsai, Targeting lncRNA HOTAIR suppresses cancer stemness and metastasis in oral carcinomas stem cells through modulation of EMT. *Oncotarget* **8**, 98542–98552 (2017)
  51. P.D. Marco Galasso, M. Previati, S. Sandhu, J. Palatini, V. Coppola, S. Warner, M.E. Sana, R. Zanella, R. Abujarour, C. Despots, M.A. Teitell, R. Garzon, G. Calin, C.M. Croce, S. Volinia, A large scale expression study associates uc.283-plus lncRNA with pluripotent stem cells and human glioma. *Genome Medicine* **6**, 76 (2014)
  52. G.S. Markopoulos, E. Roupakia, M. Tokamani, E. Chavdoula, M. Hatzia Apostolou, C. Polyarchou, K.B. Marcu, A.G. Papavassiliou, R. Sandaltzopoulos, E. Kolettas, A step-by-step microRNA guide to cancer development and metastasis. *Cell Oncol* **40**, 303–339 (2017)
  53. Y. Li, T. Mine, C.G. Ioannides, Short GC-rich RNA similar to miR 1909 and 1915 folds in silico with the 5'-UTR and ORF of notch and responders: Potential for the elimination of cancer stem cells. *Oncol Rep* **24**, 1443–1453 (2010)
  54. A. Lujambio, A. Portela, J. Liz, S.A. Melo, S. Rossi, R. Spizzo, C.M. Croce, G.A. Calin, M. Esteller, CpG island hypermethylation-associated silencing of non-coding RNAs transcribed from ultraconserved regions in human cancer. *Oncogene* **29**, 6390–6401 (2010)
  55. S.-Y.L. Wei-Yu Chen, Y.-S. Chang, J.J. Yin, Hsiu-lien, T.H. Yeh, O.H. Mouhieddine, W. Abou-Kheir, Y.-N. Liu, MicroRNA-34a regulates WNT/TCF7 signaling and inhibits bone metastasis in Ras activated prostate cancer. *Oncotarget* **6**, 441–457 (2014)
  56. P. Bu, K.Y. Chen, J.H. Chen, L. Wang, J. Walters, Y.J. Shin, J.P. Goerger, J. Sun, M. Witherspoon, N. Rakhilin, J. Li, H. Yang, J. Milsom, S. Lee, W. Zipfel, M.M. Jin, Z.H. Gumus, S.M. Lipkin, X. Shen, A microRNA miR-34a-regulated bimodal switch targets notch in colon cancer stem cells. *Cell Stem Cell* **12**, 602–615 (2013)
  57. U.S.B. Sumithra, A.B. Das, Alternative splicing within the Wnt signaling pathway: Role in cancer development. *Cell Oncol* **39**, 1–13 (2016)
  58. L. Wang, P. Bu, Y. Ai, T. Srinivasan, H.J. Chen, K. Xiang, S.M. Lipkin, X. Shen, A long non-coding RNA targets microRNA miR-34a to regulate colon cancer stem cell asymmetric division. *elife* **5**, e14620 (2016)
  59. J. Wu, J. Zhang, B. Shen, K. Yin, J. Xu, W. Gao, L. Zhang, Long noncoding RNA lncTCF7, induced by IL-6/STAT3 transactivation, promotes hepatocellular carcinoma aggressiveness through epithelial-mesenchymal transition. *J Exp Clin Cancer Res* **34**, 116 (2015)
  60. S. Wan, E. Zhao, I. Kryczek, L. Vatan, A. Sadovskaya, G. Ludema, D.M. Simeone, W. Zou, T.H. Welling, Tumor-associated macrophages produce interleukin 6 and signal via STAT3 to promote expansion of human hepatocellular carcinoma stem cells. *Gastroenterology* **147**, 1393–1404 (2014)
  61. R. Bharti, G. Dey, M. Mandal, Cancer development, chemoresistance, epithelial to mesenchymal transition and stem cells: A snapshot of IL-6 mediated involvement. *Cancer Lett* **375**, 51–61 (2016)
  62. Y. Wang, L. He, Y. Du, P. Zhu, G. Huang, J. Luo, X. Yan, B. Ye, C. Li, P. Xia, G. Zhang, Y. Tian, R. Chen, Z. Fan, The long noncoding RNA lncTCF7 promotes self-renewal of human liver cancer stem cells through activation of Wnt signaling. *Cell Stem Cell* **16**, 413–425 (2015)
  63. J. Wu, D. Wang, Long noncoding RNA TCF7 promotes invasiveness and self-renewal of human non-small cell lung cancer cells. *Hum Cell* **30**, 23–29 (2017)
  64. P. Massoner, T. Thomm, B. Mack, G. Untergasser, A. Martowicz, K. Bobowski, H. Klocker, O. Gires, M. Puhr, EpCAM is overexpressed in local and metastatic prostate cancer, suppressed by chemotherapy and modulated by MET-associated miRNA-200c/205. *Br J Cancer* **111**, 955–964 (2014)
  65. C.C. Poirier F, P.M. Timmons, E.J. Robertson, M.J. Evans, P.W. Rigby, The murine H19 gene is activated during embryonic stem cell differentiation in vitro and at the time of implantation in the developing embryo. *Development* **113**, 1105–1114 (1991)
  66. F. Peng, T.T. Li, K.L. Wang, G.Q. Xiao, J.H. Wang, H.D. Zhao, Z.J. Kang, W.J. Fan, L.L. Zhu, M. Li, B. Cui, F.M. Zheng, H.J. Wang, E.W. Lam, B. Wang, J. Xu, Q. Liu, H19/let-7/LIN28 reciprocal negative regulatory circuit promotes breast cancer stem cell maintenance. *Cell Death Dis* **8**, e2569 (2017)
  67. H. Bauderlique-Le Roy, C. Vennin, G. Brocqueville, N. Spruyt, E. Adriaenssens, R.P. Bourette, Enrichment of human stem-like prostate cells with s-SHIP promoter activity uncovers a role in Stemness for the long noncoding RNA H19. *Stem Cells Dev* **24**, 1252–1262 (2015)
  68. X. Jiang, Y. Yan, M. Hu, X. Chen, Y. Wang, Y. Dai, D. Wu, Y. Wang, Z. Zhuang, H. Xia, Increased level of H19 long noncoding RNA promotes invasion, angiogenesis, and stemness of glioblastoma cells. *J Neurosurg* **124**, 129–136 (2016)
  69. S.R. Viswanathan, G.Q. Daley, Lin28: A microRNA regulator with a macro role. *Cell* **140**, 445–449 (2010)
  70. X. Cai, B.R. Cullen, The imprinted H19 noncoding RNA is a primary microRNA precursor. *RNA* **13**, 313–316 (2007)
  71. Y. Zheng, X. Lu, L. Xu, Z. Chen, Q. Li, J. Yuan, MicroRNA-675 promotes glioma cell proliferation and motility by negatively regulating retinoblastoma 1. *Hum Pathol* **69**, 63–71 (2017)
  72. A. Farzi-Molan, S. Babashah, B. Bakhshinejad, A. Atashi, M. Fakhr Taha, Down-regulation of the non-coding RNA H19 and its derived miR-675 is concomitant with up-regulation of insulin-



- like growth factor receptor type 1 during neural-like differentiation of human bone marrow mesenchymal stem cells. *Cell Biol Int* **42**, 940–948 (2018)
73. B.K. Dey, K. Pfeifer, A. Dutta, The H19 long noncoding RNA gives rise to microRNAs miR-675-3p and miR-675-5p to promote skeletal muscle differentiation and regeneration. *Genes Dev* **28**, 491–501 (2014)
  74. A. Keniry, D. Oxley, P. Monnier, M. Kyba, L. Dandolo, G. Smits, W. Reik, The H19 lincRNA is a developmental reservoir of miR-675 that suppresses growth and Igf1r. *Nat Cell Biol* **14**, 659–665 (2012)
  75. N. Liu, L. Zhong, J. Zeng, X. Zhang, Q. Yang, D. Liao, Y. Wang, G. Chen, Y. Wang, Upregulation of microRNA-200a associates with tumor proliferation, CSCs phenotype and chemosensitivity in ovarian cancer. *Neoplasma* **62**, 550–559 (2015)
  76. C. Liu, R. Liu, D. Zhang, Q. Deng, B. Liu, H.P. Chao, K. Rycaj, Y. Takata, K. Lin, Y. Lu, Y. Zhong, J. Krolewski, J. Shen, D.G. Tang, MicroRNA-141 suppresses prostate cancer stem cells and metastasis by targeting a cohort of pro-metastasis genes. *Nat Commun* **8**, 14270 (2017)
  77. Q. Yang, X. Wang, C. Tang, X. Chen, J. He, H19 promotes the migration and invasion of colon cancer by sponging miR-138 to upregulate the expression of HMGA1. *Int J Oncol* **50**, 1801–1809 (2017)
  78. W.-M.F. Wei-Cheng Liang, C.-W. Wong, Y. Wang, G.-X.H.W. Wei-Mao, L. Zhang, L.-J. Xiao, D.C.-C. Wan, Jin-Fang, M.M.-Y.W. Zhang, The lncRNA H19 promotes epithelial to mesenchymal transition by functioning as miRNA sponges in colorectal cancer. *Oncotarget* **6**, 22513–22525 (2015)
  79. S. Cufi, A. Vazquez-Martin, C. Oliveras-Ferreros, B. Martin-Castillo, J. Joven, J.A. Menendez, Metformin against TGFbeta-induced epithelial-to-mesenchymal transition (EMT): From cancer stem cells to aging-associated fibrosis. *Cell Cycle* **9**, 4461–4468 (2010)
  80. J.H. Yuan, F. Yang, F. Wang, J.Z. Ma, Y.J. Guo, Q.F. Tao, F. Liu, W. Pan, T.T. Wang, C.C. Zhou, S.B. Wang, Y.Z. Wang, Y. Yang, N. Yang, W.P. Zhou, G.S. Yang, S.H. Sun, A long noncoding RNA activated by TGF-beta promotes the invasion-metastasis cascade in hepatocellular carcinoma. *Cancer Cell* **25**, 666–681 (2014)
  81. W. Li, Y. Kang, A new lnc in metastasis: Long noncoding RNA mediates the prometastatic functions of TGF-beta. *Cancer Cell* **25**, 557–559 (2014)
  82. E. Karamitopoulou, Tumor budding cells, cancer stem cells and epithelial-mesenchymal transition-type cells in pancreatic cancer. *Front Oncol* **2**, 209 (2012)
  83. U. Wellner, J. Schubert, U.C. Burk, O. Schmalhofer, F. Zhu, A. Sonntag, B. Waldvogel, C. Vannier, D. Darling, A. zur Hausen, V.G. Brunton, J. Morton, O. Sansom, J. Schuler, M.P. Stemmler, C. Herzberger, U. Hopt, T. Keck, S. Brabletz, T. Brabletz, The EMT-activator ZEB1 promotes tumorigenicity by repressing stemness-inhibiting microRNAs. *Nat Cell Biol* **11**, 1487–1495 (2009)
  84. L.-J.W. Sheng-Jia Shi, B. Yu, Y.-H. Li, Y. Jin, X.-Z. Bai, LncRNA-ATB promotes trastuzumab resistance and invasion metastasis cascade in breast cancer. *Oncotarget* **6**, 11652–11663 (2015)
  85. C. Mehner, E. Miller, D. Khauv, A. Nassar, A.L. Oberg, W.R. Bamlet, L. Zhang, J. Waldmann, E.S. Radisky, H.C. Crawford, D.C. Radisky, Tumor cell-derived MMP3 orchestrates Rac1b and tissue alterations that promote pancreatic adenocarcinoma. *Mol Cancer Res* **12**, 1430–1439 (2014)
  86. Y. Gao, Z. Zhang, K. Li, L. Gong, Q. Yang, X. Huang, C. Hong, M. Ding, H. Yang, Linc-DYNC2H1-4 promotes EMT and CSC phenotypes by acting as a sponge of miR-145 in pancreatic cancer cells. *Cell Death Dis* **8**, e2924 (2017)
  87. T. Han, X.P. Yi, B. Liu, M.J. Ke, Y.X. Li, MicroRNA-145 suppresses cell proliferation, invasion and migration in pancreatic cancer cells by targeting NEDD9. *Mol Med Rep* **11**, 4115–4120 (2015)
  88. Z. Li, X. Zhao, Y. Zhou, Y. Liu, Q. Zhou, H. Ye, Y. Wang, J. Zeng, Y. Song, W. Gao, S. Zheng, B. Zhuang, H. Chen, W. Li, H. Li, H. Li, Z. Fu, R. Chen, The long non-coding RNA HOTTIP promotes progression and gemcitabine resistance by regulating HOXA13 in pancreatic cancer. *J Transl Med* **13**, 84 (2015)
  89. Z. Fu, C. Chen, Q. Zhou, Y. Wang, Y. Zhao, X. Zhao, W. Li, S. Zheng, H. Ye, L. Wang, Z. He, Q. Lin, Z. Li, R. Chen, LncRNA HOTTIP modulates cancer stem cell properties in human pancreatic cancer by regulating HOXA9. *Cancer Lett* **410**, 68–81 (2017)
  90. L. Quagliata, M.S. Matter, S. Piscuoglio, L. Arabi, C. Ruiz, A. Procono, M. Kovac, F. Moretti, Z. Makowska, T. Boldanova, J.B. Andersen, M. Hammerle, L. Tomillo, M.H. Heim, S. Diederichs, C. Cillo, L.M. Terracciano, Long noncoding RNA HOTTIP/HOXA13 expression is associated with disease progression and predicts outcome in hepatocellular carcinoma patients. *Hepatology* **59**, 911–923 (2014)
  91. C.R. Cochrane, A. Szczepny, D.N. Watkins, J.E. Cain, Hedgehog signaling in the maintenance of Cancer stem cells. *Cancers (Basel)* **7**, 1554–1585 (2015)
  92. M. Zhou, Y. Hou, G. Yang, H. Zhang, G. Tu, Y.E. Du, S. Wen, L. Xu, X. Tang, S. Tang, L. Yang, X. Cui, M. Liu, LncRNA-Hh strengthen Cancer stem cells generation in Twist-positive breast Cancer via activation of hedgehog signaling pathway. *Stem Cells* **34**, 55–66 (2016)
  93. L. Qu, J. Ding, C. Chen, Z. J. Wu, B. Liu, Y. Gao, W. Chen, F. Liu, W. Sun, X.F. Li, X. Wang, Y. Wang, Z.Y. Xu, L. Gao, Q. Yang, B. Xu, Y.M. Li, Z.Y. Fang, Z.P. Xu, Y. Bao, D.S. Wu, X. Miao, H.Y. Sun, Y.H. Sun, H.Y. Wang and L.H. Wang, Exosome-transmitted lncARSR promotes Sunitinib resistance in renal Cancer by acting as a competing endogenous RNA. *Cancer Cell* **29**, 653–668 (2016)
  94. Y. Li, Y. Ye, B. Feng, Y. Qi, Long Noncoding RNA lncARSR promotes doxorubicin resistance in hepatocellular carcinoma via modulating PTEN-PI3K/Akt pathway. *J Cell Biochem* **118**, 4498–4507 (2017)
  95. L. Qu, Z. Wu, Y. Li, Z. Xu, B. Liu, F. Liu, Y. Bao, D. Wu, J. Liu, A. Wang, X. Chu, Y. Sun, C. Chen, Z. Zhang, L. Wang, A feed-forward loop between lncARSR and YAP activity promotes expansion of renal tumour-initiating cells. *Nat Commun* **7**, 12692 (2016)
  96. C.M. Loewer, M. Guttman, Y.H. Loh, K. Thomas, I.H. Park, M. Garber, M. Curran, T. Onder, S. Agarwal, P.D. Manos, S. Datta, E.S. Lander, T.M. Schlaeger, G.Q. Daley, J.L. Rinn, Large intergenic non-coding RNA-ROR modulates reprogramming of human induced pluripotent stem cells. *Nat Genet* **42**, 1113–1117 (2010)
  97. Y. Pan, C. Li, J. Chen, K. Zhang, X. Chu, R. Wang, L. Chen, The emerging roles of long noncoding RNA ROR (lincRNA-ROR) and its possible mechanisms in human cancers. *Cell Physiol Biochem* **40**, 219–229 (2016)
  98. P. Hou, Y. Zhao, Z. Li, R. Yao, M. Ma, Y. Gao, L. Zhao, Y. Zhang, B. Huang, J. Lu, LincRNA-ROR induces epithelial-to-mesenchymal transition and contributes to breast cancer tumorigenesis and metastasis. *Cell Death Dis* **5**, e1287 (2014)
  99. Y. Pan, et al., Long noncoding RNA ROR regulates chemoresistance in docetaxel-resistant lung adenocarcinoma cells via epithelial mesenchymal transition pathway. *Oncotarget* **20**, 33144–33158 (2017)
  100. Y. Lou, H. Jiang, Z. Cui, L. Wang, X. Wang, T. Tian, Linc-ROR induces epithelial-to-mesenchymal transition in ovarian cancer by increasing Wnt/β-catenin signaling. *Oncotarget* **8**, 69983–69994 (2017)

101. F. Xia, Y. Xiong, Q. Li, Interaction of lincRNA ROR and p53/miR-145 correlates with lung cancer stem cell signatures. *J Cell Biochem* **1** (2017)
102. Z. Fu, G. Li, Z. Li, Y. Wang, Y. Zhao, S. Zheng, H. Ye, Y. Luo, X. Zhao, L. Wei, Y. Liu, Q. Lin, Q. Zhou, R. Chen, Endogenous miRNA sponge LincRNA-ROR promotes proliferation, invasion and stem cell-like phenotype of pancreatic cancer cells. *Cell Death Discov* **3**, 17004 (2017)
103. S. Wang, F. Liu, J. Deng, X. Cai, J. Han, Q. Liu, Long noncoding RNA ROR regulates proliferation, invasion, and Stemness of gastric Cancer stem cell. *Cell Reprogram* **18**, 319–326 (2016)
104. X. Zhou, Q. Gao, J. Wang, X. Zhang, K. Liu, Z. Duan, Linc-RNA-RoR acts as "sponge" against mediation of the differentiation of endometrial cancer stem cells by microRNA-145. *Gynecol Oncol* **133**, 333–339 (2014)
105. S. Chen, S. Nagel, B. Schneider, H. Dai, R. Geffers, M. Kaufmann, C. Meyer, C. Pommerenke, K.S. Thress, J. Li, H. Quentmeier, H.G. Drexler, R.A.F. MacLeod, A new ETV6-NTRK3 cell line model reveals MALAT1 as a novel therapeutic target - a short report. *Cell Oncol* **41**, 93–101 (2018)
106. F. Jiao, H. Hu, T. Han, C. Yuan, L. Wang, Z. Jin, Z. Guo, L. Wang, Long noncoding RNA MALAT-1 enhances stem cell-like phenotypes in pancreatic cancer cells. *Int J Mol Sci* **16**, 6677–6693 (2015)
107. L. Zeng, Y. Cen, J. Chen, Long non-coding RNA MALAT-1 contributes to maintenance of stem cell-like phenotypes in breast cancer cells. *Oncol Lett* **15**, 2117–2122 (2017)
108. Y. Han, L. Zhou, T. Wu, Y. Huang, Z. Cheng, X. Li, T. Sun, Y. Zhou, Z. Du, Downregulation of lincRNA-MALAT1 affects proliferation and the expression of Stemness markers in glioma stem cell line SHG139S. *Cell Mol Neurobiol* **36**, 1097–1107 (2016)
109. M. Wu, Z. Lin, X. Li, X. Xin, J. An, Q. Zheng, Y. Yang, D. Lu, HULC cooperates with MALAT1 to aggravate liver cancer stem cells growth through telomere repeat-binding factor 2. *Sci Rep* **6**, 36045 (2016)
110. F. Jiao, H. Hu, C. Yuan, L. Wang, W. Jiang, Z. Jin, Z. Guo, L. Wang, Elevated expression level of long noncoding RNA MALAT-1 facilitates cell growth, migration and invasion in pancreatic cancer. *Oncol Rep* **32**, 2485–2492 (2014)
111. Y. Fan, B. Shen, M. Tan, X. Mu, Y. Qin, F. Zhang, Y. Liu, Long non-coding RNA UCA1 increases chemoresistance of bladder cancer cells by regulating Wnt signaling. *FEBS J* **281**, 1750–1758 (2014)
112. M. Jiang, O. Huang, Z. Xie, S. Wu, X. Zhang, A. Shen, H. Liu, X. Chen, J. Wu, Y. Lou, Y. Mao, K. Sun, S. Hu, M. Geng, K. Shen, A novel long non-coding RNA-ARA: Adriamycin resistance-associated. *Biochem Pharmacol* **87**, 254–283 (2014)
113. W.P. Tsang, T.W. Wong, A.H. Cheung, C.N. Co, T.T. Kwok, Induction of drug resistance and transformation in human cancer cells by the noncoding RNA CUDR. *RNA* **13**, 890–898 (2007)
114. Q. Zheng, Z. Lin, X. Li, X. Xin, M. Wu, J. An, X. Gui, T. Li, H. Pu, H. Li, D. Lu, Inflammatory cytokine IL6 cooperates with CUDR to aggravate hepatocyte-like stem cells malignant transformation through NF-kappaB signaling. *Sci Rep* **6**, 36843 (2016)
115. X. Gui, H. Li, T. Li, H. Pu, D. Lu, Long noncoding RNA CUDR regulates HULC and beta-catenin to govern human liver stem cell malignant differentiation. *Mol Ther* **23**, 1843–1853 (2015)
116. T. Li, Q. Zheng, J. An, M. Wu, H. Li, X. Gui, H. Pu, D. Lu, SET1A cooperates with CUDR to promote liver Cancer growth and hepatocyte-like stem cell malignant transformation epigenetically. *Mol Ther* **24**, 261–275 (2016)
117. F. Wang, H.-Q. Ying, B.-S. He, Y.-Q. Pan, Q.-W. Deng, H.-L. Sun, J. Chen, X. Liu, S.-K. Wang, Upregulated lincRNA-UCA1 contributes to progression of hepatocellular carcinoma through inhibition of miR-216b and activation of FGFR1/ERK signaling pathway. *Oncotarget* **6**, 7899–7917 (2015)
118. Q.Z.H. Pu, H. Li, M. Wu, J. An, X. Gui, T. Li, D. Lu, CUDR promotes liver cancer stem cell growth through upregulating TERT and C-Myc. *Oncotarget* **6**, 40775–40798 (2015)
119. X. Wang, W. Sun, W. Shen, M. Xia, C. Chen, D. Xiang, B. Ning, X. Cui, H. Li, X. Li, J. Ding, H. Wang, Long non-coding RNA DILC regulates liver cancer stem cells via IL-6/STAT3 axis. *J Hepatol* **64**, 1283–1294 (2016)
120. V. Plaks, N. Kong, Z. Werb, The cancer stem cell niche: How essential is the niche in regulating stemness of tumor cells? *Cell Stem Cell* **16**, 225–238 (2015)
121. M. Prieto-Vila, R.U. Takahashi, W. Usuba, I. Kohama, T. Ochiya, Drug resistance driven by Cancer stem cells and their niche. *Int J Mol Sci* **18**, e2574 (2017)
122. L.T.H. Phi, I.N. Sari, Y.G. Yang, S.H. Lee, N. Jun, K.S. Kim, Y.K. Lee, H.Y. Kwon, Cancer stem cells (CSCs) in drug resistance and their therapeutic implications in Cancer treatment. *Stem Cells Int* **5416923**, 2018 (2018)
123. S. Lee, H.H. Seo, C.Y. Lee, J. Lee, S. Shin, S.W. Kim, S. Lim, K.C. Hwang, Human long noncoding RNA regulation of stem cell potency and differentiation. *Stem Cells Int* **6374504**, 2017 (2017)
124. A.M. Schmitt, H.Y. Chang, Long noncoding RNAs in Cancer pathways. *Cancer Cell* **29**, 452–463 (2016)
125. A.C.P. Ioannis Grammatikakis, K. Abdelmohsen, M. Gorospe, Long noncoding RNAs (lncRNAs) and the molecular hallmarks of aging. *Aging* **6**, 992–1009 (2014)
126. Y.T. Liting Yang, F. Xiong, H. Yi, F. Wei, S. Zhang, B.X. Can Guo, M. Zhou, N. Xie, X. Li, Y. Li, G. Li, W.X.Z. Zeng, LncRNAs regulate cancer metastasis via binding to functional proteins. *Oncotarget* **9**, 1426–1443 (2018)
127. A. Bhan, M. Soleimani, S.S. Mandal, Long noncoding RNA and Cancer: A new paradigm. *Cancer Res* **77**, 3965–3981 (2017)
128. A. Sahu, U. Singhal, A.M. Chinnaiyan, Long noncoding RNAs in cancer: From function to translation. *Trends Cancer* **1**, 93–109 (2015)
129. T. Shi, G. Gao, Y. Cao, Long noncoding RNAs as novel biomarkers have a promising future in Cancer diagnostics. *Dis Markers* **2016**, 9085195 (2016)
130. e.a. Qin-nan Chen, Long non-coding RNAs in anti-cancer drug resistance. *Oncotarget* **8**, 1925–1936 (2017)
131. J.R. Evans, F.Y. Feng, A.M. Chinnaiyan, The bright side of dark matter: lncRNAs in cancer. *J Clin Invest* **126**, 2775–2782 (2016)
132. L. Cheng, H. Ming, M. Zhu, B. Wen, Long noncoding RNAs as organizers of nuclear architecture. *Sci China Life Sci* **59**, 236–244 (2016)
133. B.M. Boman, M.S. Wicha, J.Z. Fields, O.A. Runquist, Symmetric division of cancer stem cells—a key mechanism in tumor growth that should be targeted in future therapeutic approaches. *Clin Pharmacol Ther* **81**, 893–898 (2007)
134. L. Landskron, V. Steinmann, F. Bonnay, T.R. Burkard, J. Steinmann, I. Reichardt, H. Harzer, A.S. Laurenson, H. Reichert, J.A. Knoblich, The asymmetrically segregating lncRNA cherub is required for transforming stem cells into malignant cells. *elife* **7** (2018)
135. M.S. Beg, A.J. Brenner, J. Sachdev, M. Borad, Y.K. Kang, J. Stoudemire, S. Smith, A.G. Bader, S. Kim, D.S. Hong, Phase I study of MRX34, a liposomal miR-34a mimic, administered twice weekly in patients with advanced solid tumors. *Investig New Drugs* **35**, 180–188 (2017)
136. M. Al-Hajj, M.S. Wicha, A. Benito-Hernandez, S.J. Morrison, M.F. Clarke, Prospective identification of tumorigenic breast cancer cells. *Proc Natl Acad Sci U S A* **100**, 3983–3988 (2003)
137. H. Fan, J.H. Zhu, X.Q. Yao, Knockdown of long noncoding RNA PVT1 reverses multidrug resistance in colorectal cancer cells. *Mol Med Rep* **17**, 8309–8315 (2018)
138. Z. Bian, L. Jin, J. Zhang, Y. Yin, C. Quan, Y. Hu, Y. Feng, H. Liu, B. Fei, Y. Mao, L. Zhou, X. Qi, S. Huang, D. Hua, C. Xing, Z.

- Huang, LncRNA-UCA1 enhances cell proliferation and 5-fluorouracil resistance in colorectal cancer by inhibiting miR-204-5p. *Sci Rep* **6**, 23892 (2016)
139. K. Takahashi, I.K. Yan, T. Kogure, H. Haga, T. Patel, Extracellular vesicle-mediated transfer of long non-coding RNA ROR modulates chemosensitivity in human hepatocellular cancer. *FEBS Open Bio* **4**, 458–467 (2014)
140. M. Rasool, A. Malik, S. Zahid, M.A. Basit Ashraf, M.H. Qazi, M. Asif, A. Zaheer, M. Arshad, A. Raza, M.S. Jamal, Non-coding RNAs in cancer diagnosis and therapy. *Non-coding RNA Research* **1**, 69–76 (2016)
141. M.M. Ali, V.S. Akhade, S.T. Kosalai, S. Subhash, L. Statello, M. Meryet-Figuere, J. Abrahamsson, T. Mondal, C. Kanduri, PAN-cancer analysis of S-phase enriched lncRNAs identifies oncogenic drivers and biomarkers. *Nat Commun* **9**, 883 (2018)
142. H.S. Chiu, S. Somvanshi, E. Patel, T.W. Chen, V.P. Singh, B. Zorman, S.L. Patil, Y. Pan, S.S. Chatterjee, N. Cancer Genome Atlas Research, A.K. Sood, P.H. Gunaratne, P. Sumazin, Pan-Cancer analysis of lncRNA regulation supports their targeting of Cancer genes in each tumor context. *Cell Rep* **e212**, 297–312 (2018)